

LEXSEE 20 uspq2d 1746

CONTINENTAL CAN COMPANY USA, INC. and CONTINENTAL PET
TECHNOLOGIES, INC., Plaintiffs-Appellants, v. MONSANTO COMPANY,
HOOVER UNIVERSAL, INC. and JOHNSON CONTROLS, INC., Defendants-
Appellees

No. 90-1328

UNITED STATES COURT OF APPEALS FOR THE FEDERAL CIRCUIT

948 F.2d 1264; 1991 U.S. App. LEXIS 26994; 20 U.S.P.Q.2D (BNA) 1746

November 13, 1991, Decided

SUBSEQUENT HISTORY:

Rehearing Denied December 26, 1991, Reported at:
1991 U.S. App. LEXIS 29979.

PRIOR HISTORY:

[**1] Appealed from: U.S. District Court for the
Southern District of Ohio; Judge Spiegel.

DISPOSITION:

Reversed in Part, Vacated in Part, and Remanded.

CASE SUMMARY

PROCEDURAL POSTURE: Plaintiff appealed an order of United States District Court for the Southern District of Ohio that granted partial summary judgment in favor of defendant, in an action alleging patent infringement for the use of a plastic bottle bottom.

OVERVIEW: Plaintiff filed suit alleging patent infringement for defendant's use of a plastic bottle bottom structure. Plaintiff appealed the trial court's order of partial summary judgment for defendant. The court reversed and remanded. The court held summary judgment was not proper in light of 35 U.S.C.S. § 103, which required analysis of not whether the differences in the structure were simple enhancements, but whether it would have been obvious to make the claimed structure. The court found that there existed material issues of disputed facts, which precluded summary judgment, on the production of hollow ribs using a blow molding process. The court also held that the trial court erred in determining that the patented bottle was on sale more than one year prior to application for patent, thereby barring patent entitlement. The court held that a product

is not considered on sale until the availability of the product to the public.

OUTCOME: The court reversed an order granting defendant partial summary judgment and remanded because the trial court failed to determine whether it would have been obvious to make the claimed structure, and erred in determining that the patented bottle was on sale even though it was not available to the public.

CORE CONCEPTS

Civil Procedure : Summary Judgment or Summary Adjudication : Summary Judgment Standard

An issue may be decided on motion for summary judgment when there is no genuine issue of material fact, and the movant is entitled to judgment as a matter of law.

Civil Procedure : Summary Judgment or Summary Adjudication : Summary Judgment Standard

The movant's burden in a summary judgment motion is to show that no fact material to the issue is in dispute, that even if all material factual inferences are drawn in favor of the non-movant the movant is entitled to judgment as a matter of law.

Patent Law : Infringement : Summary Judgment

Summary judgment is as available in patent cases as in other areas of litigation.

Patent Law : Novelty & Anticipation

See 35 U.S.C.S. § 102(a).

Patent Law : Novelty & Anticipation

Anticipation under 35 U.S.C.S. § 102(a) requires that the identical invention that is claimed was previously known to others and thus is not new.

Patent Law : Novelty & Anticipation

When more than one reference is required to establish unpatentability of the claimed invention anticipation under 35 U.S.C.S. § 102 can not be found, and validity is determined in terms of 35 U.S.C.S. § 103.

Patent Law : Novelty & Anticipation

To serve as an anticipation when the reference is silent about the asserted inherent characteristic, such gap in the reference may be filled with recourse to extrinsic evidence. Such evidence must make clear that the missing descriptive matter is necessarily present in the thing described in the reference, and that it would be so recognized by persons of ordinary skill.

Patent Law : Statutory Bars : On Sale

See 35 U.S.C.S. § 102(b).

Patent Law : Statutory Bars : On Sale

The on sale bar of 35 U.S.C.S. § 102(b) does not arise simply because the intended customer was participating in development and testing.

Patent Law : Statutory Bars : On Sale

Various factors pertinent to the on sale bar when there is an issue concerning the relationship between the patentee and the customer are: whether there was a need for testing by other than the patentee; the amount of control exercised; the stage of development of the invention; whether payments were made and the basis thereof; and whether confidentiality was required; and whether technological changes were made. All of the circumstances attending the relationship must be considered in light of the public policy underlying 35 U.S.C.S. § 102(b).

Patent Law : Statutory Bars : On Sale

The on sale bar is measured by the time the public came into possession of the invention. What starts the period running is the availability of the invention to the public through the categories of disclosure enumerated in 35 U.S.C.S. § 102(b).

Patent Law : Nonobviousness : Tests & Proof of Obviousness

Obviousness, 35 U.S.C.S. § 103, is reviewed as a legal conclusion based upon underlying facts of four general categories: the scope and content of the prior art, the differences between the prior art and the claimed invention, the level of ordinary skill at the time the

invention was made, and any objective considerations that may be present.

Patent Law : Nonobviousness : Tests & Proof of Obviousness

When differences that may appear technologically minor nonetheless have a practical impact, particularly in a crowded field, the court must consider the obviousness of the new structure in this light. Such objective indicia as commercial success, or filling an existing need, illuminate the technological and commercial environment of the inventor, and aid in understanding the state of the art at the time the invention was made.

Patent Law : Nonobviousness : Tests & Proof of Obviousness

It is not necessary that the patented invention be solely responsible for the commercial success in order for this factor to be given weight appropriate to the evidence, along with other pertinent factors, in determining obviousness.

COUNSEL:

Eugene F. Friedman, Eugene F. Friedman, Ltd., of Chicago, Illinois, argued for Plaintiffs-Appellants. With him on the brief were Edwin C. Thomas, III and David M. Novak, Bell, Boyd & Lloyd, of Chicago, Illinois. Also on the brief was Kurt L. Grossman, Wood, Herron & Evans, of Cincinnati, Ohio.

Henry J. Renk, Fitzpatrick, Cella, Harper & Scinto, of New York, New York, argued for Defendants-Appellees. With him on the brief were Lawrence F. Scinto and Bruce C. Haas. Also on the brief were Jacob K. Stein, Deborah DeLong, Thompson, Hine & Flory, of Cincinnati, Ohio, Lawrence L. Limpus, Monsanto Company, of St. Louis, Missouri and Edward L. Levine, Johnson Controls, Inc., of Milwaukee, Wisconsin.

JUDGES:

Newman, Archer, and Rader, Circuit Judges.

OPINIONBY:

NEWMAN

OPINION:

[*1265] NEWMAN, Circuit Judge

Continental Can Company USA and Continental PET Technologies (collectively "Continental") appeal the partial summary judgment of the United States District Court for the Southern District of Ohio, holding that United States Patent No. 4,108,324 (the Conobase or '324 [*2] patent) is invalid. n1 Final judgment was entered on this issue, for the purpose of appeal.

nl Continental Can Co. USA v. Monsanto Co., 1989 U.S. Dist. LEXIS 13417, 11 U.S.P.Q.2d (BNA) 1761 (S.D. Ohio 1989), reconsid. denied, No. C-1-86-1213 (S.D. Ohio Nov. 9, 1989).

Summary Judgment

An issue may be decided on motion for summary judgment when there is no genuine issue of material fact, and the movant is entitled to judgment as a matter of law. Fed. R. Civ. P. 56(c); *Anderson v. Liberty Lobby, Inc.*, 477 U.S. 242, 91 L. Ed. 2d 202, 106 S. Ct. 2505 (1986); *Celotex Corp. v. Catrett*, 477 U.S. 317, 325-26, 91 L. Ed. 2d 265, 106 S. Ct. 2548 (1986); *Scripps Clinic & Research Foundation v. Genentech, Inc.*, 927 F.2d 1565, 1571, 18 U.S.P.Q.2d (BNA) 1001, 1005 (Fed. Cir. 1991). The movant's burden is to show that no fact material to the issue is in dispute, that even if all material factual inferences are drawn in favor of the non-movant the movant is entitled to judgment as a matter of law. *Id.* Summary judgment is as available in patent cases [**3] as in other areas of litigation. *Chore-Time Equipment, Inc. v. Cumberland Corp.*, 713 F.2d 774, 778-79, 218 U.S.P.Q. (BNA) 673, 675 (Fed. Cir. 1983).

The purpose of the summary process is to avoid a clearly unnecessary trial, *Matsushita Elec. Industrial Co. v. Zenith Radio Corp.*, 475 U.S. 574, 587, 89 L. Ed. 2d 538, 106 S. Ct. 1348 (1986); it is not designed to substitute lawyers' advocacy for evidence, or affidavits for examination before the fact-finder, when there is a genuine issue for trial. As stated in *Adickes v. S.H. Kress & Co.*, 398 U.S. 144, 176, 26 L. Ed. 2d 142, 90 S. Ct. 1598 (1970) (Black, J., concurring), "the right to confront, cross-examine and impeach adverse witnesses is one of the most fundamental rights sought to be preserved by the Seventh Amendment". See also *Poller v. Columbia Broadcasting System, Inc.*, 368 U.S. 464, 473, 7 L. Ed. 2d 458, 82 S. Ct. 486 (1962).

While facilitating the disposition of legally meritless suits, when summary judgment [*1266] is improvidently granted the effect is to prolong litigation and increase its burdens. This is of particular concern in patent disputes, where the patent property is a wasting asset, and justice is ill served by delay in final resolution. [**4] In the case at bar, although some issues could be resolved on the law and undisputed facts, other issues require trial.

The Patented Invention

The '324 patent, entitled "Ribbed Bottom Structure for Plastic Container", inventors Suppayan M.

Krishnakumar, Siegfried S. Roy, John F. E. Pocock, Salil K. Das, and Gautam K. Mahajan, is directed to a plastic bottle whose bottom structure has sufficient flexibility to impart improved impact resistance, combined with sufficient rigidity to resist deformation under internal pressure. The patented bottle is said to provide a superior combination of these properties. The bottom structure is illustrated as follows:

[SEE FIG 2 IN ORIGINAL]

Claim 1 is the broadest claim of the '324 patent:

1. A container having a sidewall and a bottom structure closing the container at an end portion of the sidewall,

the outer surface of the bottom structure comprising a central concavity,

a convex heel surrounding the concavity and merging therewith and with the sidewall end portion, the lowermost points of the heel lying in a common plane,

and a plurality of ribs interrupting the outer surface of the concavity and distributed in a symmetrical [**5] array,

each rib extending longitudinally in the direction of the heel and downwardly from an inner portion of the concavity, whereby the outer end portion of each rib is lower than the inner end portion thereof,

characterized by the feature that the ribs are hollow.

Claims 2 through 5 include additional limitations, described as contributing to the structure's rigidity, flexibility, or both. Claim 2 specifies the ratios of thickness of the walls of the bottom structure to the thickness of the sidewall end portions. Claim 3 specifies that the margins of each rib merge smoothly with adjacent portions of the bottom structure. Claim 4 specifies that each rib is convex relative to the bottom structure. Claim 5 specifies that each rib is of fusiform (a gently tapered shape at the ends) configuration. Each claim carries an independent presumption of validity, [*1267] 35 U.S.C. § 282, and stands or falls independent of the other claims. *Altoona Publix Theatres, Inc. v. American Tri-Ergon Corp.*, 294 U.S. 477, 487, 79 L. Ed. 1005, 55 S. Ct. 455 (1935).

Continental brought suit for patent infringement against Monsanto Company and Monsanto's successor in this business, Hoover Universal, Inc. and Hoover's parent [**6] company, Johnson Controls (collectively "Monsanto"). Monsanto moved for partial summary judgment based on issues of validity under 35 U.S.C. §§ 102 and 103.

I

35 U.S.C. § 102(a)

The statutory requirement that a patented invention be "new" is tested in accordance with 35 U.S.C. § 102(a), which provides that:

§ 102. A person shall be entitled to a patent unless-

(a) the invention was known or used by others in this country, or patented or described in a printed publication in this or a foreign country, before the invention thereof by the applicant for patent. ...

The district court found that all the claims of the '324 patent were anticipated by U.S. Patent No. 3,468,443 (the Marcus patent). We conclude that the district court erred in claim interpretation, and also found disputed facts adversely to the nonmovant, thus inappropriately deciding the issue summarily.

Anticipation under § 102(a) requires that the identical invention that is claimed was previously known to others and thus is not new. *Scripps Clinic*, 927 F.2d at 1576, 18 U.S.P.Q.2d at 1010; *Titanium Metals Corp. of Am. v. Banner*, 778 F.2d 775, 780, 227 U.S.P.Q. (BNA) 773, 777-78 (Fed. Cir. 1985); [**7] *Lindemann Maschinenfabrik GmbH v. American Hoist and Derrick Co.*, 730 F.2d 1452, 1458, 221 U.S.P.Q. (BNA) 481, 485 (Fed. Cir. 1984). When more than one reference is required to establish unpatentability of the claimed invention anticipation under § 102 can not be found, and validity is determined in terms of § 103.

It was Monsanto's burden to show that every element of the several claims of the '324 patent was identically described in the asserted anticipating reference, the Marcus patent. The district court focused on the term "characterized by the feature that the ribs are hollow", which limits all of the '324 patent claims. Continental argues that the district court incorrectly construed this term, as a matter of law, and that the Marcus patent shows ribs that are not hollow, as that term is used in the '324 patent. Continental also points to other differences between the '324 claims and the description in the Marcus patent.

The Marcus patent rib structure is illustrated in Figure 5 and in cross-section in Figure 6:

[SEE FIG.5 IN ORIGINAL]

[SEE FIG.6 IN ORIGINAL]

[*1268] The Marcus patent does not state that its ribs are "hollow", or use a similar term. Continental's witnesses [**8] testified by deposition that the Marcus patent shows solid, not hollow, ribs. A witness (Adomaitis) had stated in an internal memorandum written at Continental in 1969, well before this litigation arose, that "the ribs of their [Marcus'] web can be made of solid beams only." Another witness, '324 co-inventor Pocock, testified that:

It seems evident to me that he [Marcus] was trying to produce some kind of container integrity by the production of essentially solid ribs on the bottom of the bottle. It seems to go to great length here to illustrate them as such.

Krishnakumar, another co-inventor, testified that it "is very obvious the ribs are shown solid", and that Figures 5 and 6 as well as Figures 7 through 12 of the Marcus patent all show solid ribs. However, Marcus, testifying for Monsanto, testified that his ribs were hollow, and that conventional blow molding would inherently produce hollow ribs.

The district court defined "hollow" as meaning that "the inside contour of the ribs generally follows the outside contour thereof", a definition on which the parties agreed. *Continental*, 11 U.S.P.Q.2d at 1764. See the court's opinion, 11 U.S.P.Q.2d at 1764-68, [**9] for various sketches made by the witnesses. Continental states that the district court erred in construing "hollow", and that the phrase "characterized by the feature that the ribs are hollow" must be construed in terms of the patent in which it appears. See, e.g., *Tandon Corp. v. United States Int'l Trade Comm'n*, 831 F.2d 1017, 1021, 4 U.S.P.Q.2d (BNA) 1283, 1286 (Fed. Cir. 1987). The '324 patent explicitly distinguished the Marcus patent teachings, stating that the '324 ribs are, unlike Marcus, not filled with plastic. The '324 specification uses the term "hollow", as do the prosecution history and the claims, for this purpose. The '324 patent's usage of "hollow" is illustrated in the rib cross-section in Figure 5A:

[SEE FIG 5A IN ORIGINAL]

The Marcus patent's rib structure thus was explicitly differentiated by the term "hollow" as used in the '324 specification, drawings, and prosecution history. Since the claim term must be construed as used by the patentee, the district court erred in its construction of the '324 claim term "hollow". On correct claim construction, the factual question of anticipation must be decided.

Monsanto's argument is that hollow [**10] ribs were inherently produced by Marcus. Monsanto thus argues that anticipation lies because the Marcus patent's ribs are "inherently" hollow, regardless of how they are shown in the Marcus patent. Monsanto argues that because the Marcus ribs are formed by injection blow molding, which is the same process described for the Conobase '324 ribs, hollow ribs are inherently disclosed in the Marcus patent.

To serve as an anticipation when the reference is silent about the asserted inherent characteristic, such gap in the reference may be filled with recourse to extrinsic evidence. Such evidence must make clear that the missing descriptive matter is necessarily present in the thing described in the reference, and that it would be so recognized by persons of ordinary skill. *In re Oelrich*, 666 F.2d 578, 581, 212 U.S.P.Q. (BNA) 323, 326 (CCPA 1981) (quoting *Hansgirk v. Kemmer*, 26 C.C.P.A. 937, 102 F.2d 212, 214, 40 U.S.P.Q. (BNA) 665, 667 (CCPA 1939)) provides:

[*1269] Inherency, however, may not be established by probabilities or possibilities. The mere fact that a certain thing *may* result from a given set of circumstances is not sufficient. [Citations omitted.] If, [**11] however, the disclosure is sufficient to show that the natural result flowing from the operation as taught would result in the performance of the questioned function, it seems to be well settled that the disclosure should be regarded as sufficient.

This modest flexibility in the rule that "anticipation" requires that every element of the claims appear in a single reference accommodates situations where the common knowledge of technologists is not recorded in the reference; that is, where technological facts are known to those in the field of the invention, albeit not known to judges. It is not, however, a substitute for determination of patentability in terms of § 103.

Continental does not dispute the applicability of the injection blow molding process. However, Continental disputes the material fact of whether this process necessarily produced "hollow" ribs in the Marcus base structure, as the term "hollow" is used in the '324 patent. Resolution of this disputed fact adversely to Continental was improper on summary judgment. The grant of summary judgment of anticipation under § 102(a) is vacated. The issue requires trial.

II

35 U.S.C. § 102(b)

The district court also held that [**12] the Marcus bottle was on sale, 35 U.S.C. § 102(b). Section 102(b) bars entitlement to a patent when:

(b) the invention was ... in public use or on sale in this country, more than one year prior to the date of the application for patent in the United States. ...

The Marcus bottle was developed some ten years before the filing date of the '324 patent, during a project wherein Marcus' employer, Admiral Plastics or APL Corporation, entered into agreements with the Coca-Cola Company for the development of a suitable plastic bottle. The agreements provided that Admiral Plastics would make and Coca-Cola would test the bottles, and that if a satisfactory bottle was developed it would be manufactured by Admiral and purchased by Coca-Cola. Minimum commercial quantities and maximum commercial prices were stated in an agreement, and costs were a matter of discussion. Admiral produced a variety of bottle shapes, including the Marcus bottle. The project was terminated after about two years, because the "mechanical performance" requirements were not met, as Coca-Cola wrote at the time.

The district court reasoned that this project "called for the eventual marketing of the Marcus bottles once [**13] all technical difficulties were resolved", *Continental*, 11 U.S.P.Q.2d at 1766, and on this basis held that the Marcus bottles were on sale. This holding was in error, for the "on sale" bar of § 102(b) does not arise simply because the intended customer was participating in development and testing. See *Great Northern Corp. v. Davis Core & Pad Co.*, 782 F.2d 159, 164-65, 228 U.S.P.Q. (BNA) 356, 358 (Fed. Cir. 1986). In *Baker Oil Tools, Inc. v. Geo Vann, Inc.*, 828 F.2d 1558, 1563-65, 4 U.S.P.Q.2d (BNA) 1210, 1213-15 (Fed. Cir. 1987), this court summarized various factors pertinent to the "on sale" bar when there is an issue concerning the relationship between the patentee and the customer: for example, whether there was a need for testing by other than the patentee; the amount of control exercised; the stage of development of the invention; whether payments were made and the basis thereof; whether confidentiality was required; and whether technological changes were made. All of the circumstances attending the relationship must be considered in light of the public policy underlying § 102(b). *UMC Electronics Co. v. United States*, 816 F.2d 647, 656, 2 U.S.P.Q.2d (BNA) 1465, 1471-72 (Fed. Cir. 1987), [**14] cert. denied, 484 U.S. 1025, 98 L. Ed. 2d 761, 108 S. Ct. 748 (1988).

The district court acknowledged that all technical difficulties were not resolved and that no sales were ever

made. [*1270] Although Admiral Plastics' hope was surely commercial sales, and the record shows that prices and quantities were discussed, this does not of itself place the subject matter "on sale" in the sense of § 102(b). The Marcus bottle was part of a terminated development project that never bore commercial fruit and was cloaked in confidentiality. While the line is not always bright between development and being on sale, see generally *UMC Electronics, supra*, in this case the line was not crossed. The "on sale" bar is measured by "the time the public came into possession of the invention", *id.* at 655, 2 U.S.P.Q. 2d at 1471 (quoting *In re Foster*, 52 C.C.P.A. 1808, 343 F.2d 980, 987-88, 145 U.S.P.Q. (BNA) 166, 173 (CCPA 1965), *cert. denied*, 383 U.S. 966, 16 L. Ed. 2d 307, 86 S. Ct. 1270, 149 U.S.P.Q. (BNA) 906 (1966) ("What starts the period running is clearly the availability of the invention to the public through the categories of disclosure enumerated in 102(b)...." (emphasis in original))). [*15] We conclude that the district court erred in holding that the circumstances that here existed placed the Marcus bottles "on sale" in terms of § 102(b). We therefore reverse and direct that on remand judgment on this issue shall be entered in favor of Continental, as a matter of law.

III

35 U.S.C. § 103

Obviousness, 35 U.S.C. § 103, is reviewed as a legal conclusion based upon underlying facts of four general categories, *viz.* the scope and content of the prior art, the differences between the prior art and the claimed invention, the level of ordinary skill at the time the invention was made, and any objective considerations that may be present. *Graham v. John Deere Co.*, 383 U.S. 1, 17, 15 L. Ed. 2d 545, 86 S. Ct. 684, 148 U.S.P.Q. (BNA) 459 (1966); *Interconnect Planning Corp. v. Feil*, 774 F.2d 1132, 1137-38, 227 U.S.P.Q. (BNA) 543, 547 (F.C. Cir. 1985).

The parties agreed that the scope and content of the prior art was adequately represented by four references: the Marcus patent discussed in Part I *ante*, a patent to Colombo (U.S. Patent No. 3,403,804), and two patents owned by Continental, U.S. Patent No. 3,598,270 (the Petaloid patent), and No. 3,935,955 (the Decaloid patent). They agreed [*16] on little else. In granting summary judgment of invalidity for obviousness, the district court found certain disputed material facts and misapplied certain precepts of law. We conclude that the issue was not amenable to summary resolution. Although it is not entirely clear how the references were combined by the court, we shall review the references briefly, in order to explain our conclusion.

The Petaloid Patent

The district court referred to the deposition testimony of Siegfried Roy, one of the co-inventors of the '324 patent, that the Petaloid base, inverted, was similar to the Conobase. Continental points out that neither Roy nor any other deponent suggested that the Petaloid base could be or should be inverted, or that inversion would provide an improved base structure. In *In re Gordon*, 733 F.2d 900, 902, 221 U.S.P.Q. (BNA) 1125, 1127 (Fed. Cir. 1984) this court held that although a prior art device could have been turned upside down, that did not make the modification obvious unless the prior art fairly suggested the desirability of turning the device upside down.

Continental points out that the Petaloid description differs in several other ways from [*17] the '324 invention. In the '324 structure the outer end of each rib is lower than the inner end, whereas in the Petaloid structure the outer ends of the ribs are higher than the inner ends; that is, the ribs in the Petaloid base extend upward from the center to the sidewall. The Petaloid bottle is supported on feet extending between the ribs, such feet being the locations for stress concentrations. The following drawing is from the Petaloid patent:

[*1271] [SEE FIG 3 IN ORIGINAL]

Continental states that the '324 Conobase is not only different, but avoids the stress concentrations of the Petaloid device, thus enhancing impact resistance. Monsanto argues that Continental simply used the Petaloid hollow ribs in combination with the Marcus patent. This requires determination of whether there was something in the prior art as a whole to suggest the desirability, and thus the obviousness, of making the combination, in a way that would produce the '324 structure. *See, e.g., Uniroyal, Inc. v. Rudkin-Wiley Corp.*, 837 F.2d 1044, 1051, 5 U.S.P.Q.2d (BNA) 1434, 1438 (Fed. Cir.), *cert. denied*, 488 U.S. 825, 102 L. Ed. 2d 51, 109 S. Ct. 75 (1988). Continental argues that it is not apparent, [*18] even with hindsight, how any combination of the Petaloid and Marcus patents or other references lead to the '324 base. The Petaloid patent shows concave ribs that extend all the way to the sidewall, while the Marcus ribs extend "from the heel" toward an annular central ring. The Petaloid base has wide, petal-like, open ribs, while Marcus shows narrow, beam-like ribs. The deposition testimony was in conflict as to the inferences drawn from the references.

On this disputed issue, drawing reasonable inferences in favor of the non-movant, it has not been established that one skilled in the art would be motivated to select and combine features from each source in order to make the '324 base. *Interconnect Planning*, 774 F.2d at 1143, 227 U.S.P.Q. at 551 ("When prior art references

require selective combination by the court to render obvious a subsequent invention, there must be some reason for the combination other than the hindsight gleaned from the invention itself").

The Decaloid Patent

The district court also referred to combination of the Decaloid base with the Marcus base. The Decaloid base has ten hollow ribs that extend to the sidewall, and ten feet [**19] between the ribs:

[*1272] [SEE FIG 2 IN ORIGINAL]

Monsanto does not explain, and we can not discern, how the combination with Marcus would have led a person of ordinary skill to the '324 base. The court's summary holding of obviousness based on these references, separately or in combination, can not be sustained.

The Colombo Patent

The Colombo base, like the Petaloid and Decaloid bases, has hollow ribs that extend to the sidewall, in a still different structure from that of Marcus and also from that of the '324 patent. Colombo describes his ribs as inverted U-shapes, concave, located on the outer surface of the central concavity:

[SEE FIG. 4 IN ORIGINAL]

Again, drawing reasonable factual inferences in favor of Continental, and in the absence of any suggestion or motivation in the prior art as a whole to make a selective combination of the Colombo and Marcus [*1273] structures along with other changes needed to obtain the '324 structure, summary judgment of obviousness was inappropriate.

The district court found that there was no substantial difference between the '324 invention and the combined teachings of the prior art:

As obviousness can be established on the basis of the combined [**20] teachings of references, we think it is clear that simple enhancements of existing prior art, i.e. inverting the '270 petaloid base, do not constitute a substantial difference between the subject matter claimed in the '324 patent and that of the prior art. Thus, the facts of this case reveal no substantial difference between '324 and the prior art.

Continental, 11 U.S.P.Q.2d at 1769 (citation omitted). However, as we have discussed, the criterion of § 103 is not whether the differences from the prior art are "simple

enhancements", but whether it would have been obvious to make the claimed structure.

Objective Indicia

The district court concluded that the structure in suit is simply a variation on known themes. It is in such circumstance that the objective indicia -- the so-called secondary considerations -- are most useful to the decision-maker. The significance of a new structure is often better measured in the marketplace than in the courtroom.

Thus when differences that may appear technologically minor nonetheless have a practical impact, particularly in a crowded field, the decision-maker must consider the obviousness of the new structure in this light. Such [**21] objective indicia as commercial success, or filling an existing need, illuminate the technological and commercial environment of the inventor, and aid in understanding the state of the art at the time the invention was made. *See In re Piasecki*, 745 F.2d 1468, 1475, 223 U.S.P.Q. (BNA) 785, 790 (Fed. Cir. 1984) (secondary considerations "often establish that an invention appearing to have been obvious in light of the prior art was not" (quoting *Stratoflex, Inc. v. Aeroquip Corp.*, 713 F.2d 1530, 1538-39, 218 U.S.P.Q. (BNA) 871, 879 (Fed. Cir. 1983))).

Continental licensed the '324 counterpart Japanese patent to a Japanese company, Yoshino, that we are told had been unable to develop a plastic bottle for hot-fill applications. A witness for Toyo Seikan, another Japanese licensee, testified that the Conobase "sustains itself in higher temperatures, and it does not cause buckling after you fill [the bottle]", as compared with previously available plastic bottles. Continental asserts that Monsanto had been unable to develop a satisfactory bottle for hot-fill applications, and had therefore obtained this technology from Yoshino.

The district court [**22] acknowledged the commercial success of the Conobase, but stated that "we are not convinced that the Conobase *alone* accounts for any of the success." 11 U.S.P.Q.2d at 1770 (emphasis in original). The court suggested that the commercial success in Japan was due to the market strength of the Japanese licensees, and held that there is no nexus between the merits of the product and its commercial success. It is not necessary, however, that the patented invention be solely responsible for the commercial success, in order for this factor to be given weight appropriate to the evidence, along with other pertinent factors. *See generally Demaco Corp. v. F. Von Langsdorff Licensing Ltd.*, 851 F.2d 1387, 1392-94, 7 U.S.P.Q.2d (BNA) 1222, 1226-28 (Fed. Cir.), cert. denied, 488 U.S. 956, 102 L. Ed. 2d 383, 109 S. Ct. 395 (1988); *Rosemount, Inc. v. Beckman Instruments, Inc.*,

727 F.2d 1540, 1546, 221 U.S.P.Q. (BNA) 1, 7 (Fed. Cir. 1984). Monsanto also states that the Conobase is different from the '324 invention, so that even were the Conobase successful, this does not inure to the benefit of the '324 patent. It is apparent that the factual issues surrounding [**23] the objective indicia were disputed, and material.

In view of the material facts requiring resolution, the issue of obviousness was not properly decided on motion

for summary [*1274] judgment. We vacate the grant based on 35 U.S.C. § 103, and remand for trial of this issue and the other issues remaining in the case.

Costs

Costs in favor of Continental.

REVERSED IN PART, VACATED IN PART, and
REMANDED.

LEXSEE 666 F2D 578, AT 581

IN RE JOHN A. OELRICH ET AL.

Appeal No. 81-564.

UNITED STATES COURT OF CUSTOMS AND PATENT APPEALS

666 F.2d 578; 1981 CCPA LEXIS 153; 212 U.S.P.Q. (BNA) 323

Oral argument on October 9, 1981

December 10, 1981

PRIOR HISTORY:

[**1]

Serial No. 452,050.

CASE SUMMARY

PROCEDURAL POSTURE: Appellant sought review of the decision of the United States Patent and Trademark Office Board of Appeals sustaining the patent examiner's rejection under 35 U.S.C.S. § 102 of a claim in appellant's application for an apparatus specially adapted for moving low inertia steering fins on guided missiles.

OVERVIEW: Appellant's claim for an apparatus specially adapted for moving low inertia steering fins on guided missiles was rejected by the patent examiner. The United States Patent and Trademark Office Board of Appeals affirmed the rejection concluding that under 35 U.S.C.S. § 102, the claim was anticipated by a patent previously issued to appellant. Appellant sought review, and the appellate court reversed. The appellate court concluded that the determinative issue was a question of inherency. The board contended that the apparatus of the previously issued patent inherently performed the function of the apparatus of the rejected claim. The appellate court stated the principle that mere recitation of a newly discovered function or property, inherently possessed by things in the prior art, does not distinguish a claim drawn to those things from the prior art. However, the court determined that in this case the rejected claim did not merely recite a newly discovered function of the old device. The appellate court concluded

that there was no inherency, because the rejected claim contained a limitation that was not inherently present in the device of the previously issued patent.

OUTCOME: The rejection of appellant's claim was reversed, because the claim did not merely recite a newly discovered function of the device in a previously issued patent and contained a limitation that was not inherently present in the device in the previously issued patent.

CORE CONCEPTS

Civil Procedure : Preclusion & Effect of Judgments : Res Judicata

Civil Procedure : Preclusion & Effect of Judgments : Collateral Estoppel

Patent Law : Collateral Estoppel

Res judicata does not have its usual impact when considering ex parte patent appeals; the public interest in granting valid patents outweighs the public interest underlying collateral estoppel and res judicata, particularly where the issue presented is not substantially identical to that previously decided.

Patent Law : Novelty & Anticipation

It is true that mere recitation of a newly discovered function or property, inherently possessed by things in the prior art, does not distinguish a claim drawn to those things from the prior art.

Patent Law : Novelty & Anticipation

Inherency may not be established by probabilities or possibilities. The mere fact that a certain thing may result from a given set of circumstances is not sufficient. If,

however, the disclosure is sufficient to show that the natural result flowing from the operation as taught would result in the performance of the questioned function, it seems to be well settled that the disclosure should be regarded as sufficient.

COUNSEL:

Roger A. VanKirk, attorney for appellant.

Joseph F. Nakamura, Solicitor, and *Thomas E. Lynch*, Associate Solicitor, for the Patent and Trademark Office.

OPINIONBY:

RICH

OPINION:

[*579]

Before MARKEY, Chief Judge, RICH, BALDWIN, MILLER, and NIES, Associate Judges.

RICH, Judge.

This appeal is from the decision of the United States Patent and Trademark Office (PTO) Board of Appeals (board) sustaining the examiner's rejection of claim 1 in application serial No. 452,050, filed March 18, 1974, entitled "Sub-Critical Time Modulated Control Mechanism," under 35 USC 102 as anticipated by appellant Oelrich's U.S. patent No. 3,430,536 for "Time Modulated Pneumatically Actuated Control Mechanism," issued March 4, 1969. We reverse.

Background

This application was the subject of *In re Oelrich*, 579 F.2d 86, 198 USPQ 210 (CCPA 1978), in which a rejection of claims 1-5 under 35 USC 103 was reversed. Appellant's method claims 2-5 now stand allowed.

The invention of claim 1 is directed to an apparatus specially adapted for moving low inertia steering fins on guided missiles. The prior art apparatus and the theory upon which it operates are fully [**2] discussed in our above prior opinion and will, therefore, not be repeated here. Generally, the claimed device responds to an electric signal from a missile guidance system, the magnitude of which is proportional to the desired amount of course-correcting fin movement, and converts the signal into a pneumatic pressure of appropriate magnitude which acts on a piston to move the missile guiding fin. The device which is the subject of the Oelrich patent "was employed only with the then available steering fins which they characterize as 'high inertia' loads." n1 The frequency at which this "high inertia" load system is operated is stated to be above the

critical (resonant) frequency of the system. 579 F.2d at 87-89, 198 USPQ at 212-13. The allowed method claims and apparatus claim 1 direct use of a carrier frequency below the critical frequency of the system.

n1 While the solicitor equates "low-inertia" with a "relatively light load" and "high-inertia" with a "relatively heavy load," appellants are not as unequivocal. They refer to "small inertia" and "low inertia" loads, but, for example, the Divigard affidavit refers to "Fin Inertia" in terms of "in-1b sec²/rad," a unit of measure applicable only in referencing moment of inertia, not inertia. The difference is significant because inertia, measured in terms of mass, is closely related to weight, while moment of inertia is affected by the distribution of the mass. Because of this ambiguity, we cannot and do not use the terms "weight" and "inertia" interchangeably. [**3]

Claim 1 reads (emphasis ours):

1. A time modulated fluid actuated control apparatus comprising:

housing means, said housing means defining a cylinder;

actuator piston means disposed in said housing means cylinder, said piston means including an output member adapted to be connected to a movable load, said load and control apparatus defining a system having a range of resonant frequencies;

solenoid operated valve means mounted on said housing means, said valve means being selectively operable to deliver pressurized fluid to and to vent fluid from said housing means cylinder at one side of said piston means;

means of generating variable input command signals commensurate with the desired position of the load, said command signals being characterized by a dynamic frequency range below said range of said resonant frequencies;

means for generating a signal at a carrier frequency, said carrier frequency being greater than the maximum dynamic command signal frequency and less than the minimum system resonant frequency; [*580]

means for modulating said carrier frequency signal by said command signals; and

means responsive to said modulated carrier frequency signal for [**4] controlling energization of said solenoid operated valve means.

In sustaining the examiner's rejection under § 102, the board expressed agreement with his reasoning, which is here summarized. Stating that "the issue is identical to that decided in *In re Ludtke*, 58 CCPA 1159, 441 F.2d 660, 169 USPQ 563 (1971)," the examiner noted that, for purposes of determining inherency, "the question is, does Oelrich [the reference patent] disclose a signal generator that necessarily must supply the carrier frequencies that appellants use?" The examiner turned to Exhibit A of coapplicant Divigard's affidavit, which states as an assumption in a "Linearized Simulation" of a "high inertia" load system that the critical resonance frequency must be kept below 80 Hz to avoid interaction with the carrier frequency which is between 100 and 150 Hz. Thus, the examiner concluded, "Exhibit A establishes Oelrich's carrier frequency range, which may now be compared with the carrier frequency range of applicants' low-inertia system." It was then asserted that the Oelrich and Kolk affidavits establish that good low inertia system design practice dictates a carrier frequency range of 95-190 Hz. Since the [**5] carrier frequency range for the high inertia system lies within the range for the low inertia system, and since the critical frequency of the low inertia system is near the solenoid limit of 175 Hz, the examiner posited that the Oelrich carrier frequencies would be sub-critical in the low inertia system, saying, "Thus Oelrich's signal generator does in fact inherently produce frequencies which would be sub-critical when used with a low-inertia system, and therefore, inherently supplies a carrier frequency range which is usable in applicants' system since this conclusion was deduced from specific data presented in the patent and in the affidavits supplied by appellants." The appellants also asserted our prior decision was res judicata.

OPINION

Although appellants' arguments on appeal are directed primarily to a discussion of res judicata n2 and whether a "product which is unwittingly produced is anticipation," resolution of this case is properly had by comparison of the reference patent to the limitations of claim 1. As will appear, the determinative issue is a question of inherency.

n2 The doctrine of res judicata, argued in view of our decision in *In re Oelrich*, 579 F.2d 86, 198 USPQ 210 (CCPA 1978), is not applicable to the instant rejection. The issue in the former case was obviousness; here it is anticipation. A new rejection is before us. Furthermore, res judicata does not have its usual impact when considering ex parte patent appeals; the public interest in granting valid patents outweighs the public interest underlying collateral estoppel and res judicata, particularly where the issue presented is not substantially

identical to that previously decided. *In re Russell*, 58 CCPA 1081, 1083, 439 F.2d 1228, 1230, 169 USPQ 426, 428 (1971); *In re Craig*, 56 CCPA 1438, 1441-42, 411 F.2d 1333, 1335-36, 162 USPQ 157, 159 (1969). [**6]

The distinguishing feature of claim 1 is defined in the paragraph which states that the apparatus contains a

means for generating a *** carrier frequency *** greater than the maximum dynamic command signal frequency and less than the minimum system resonant frequency. n3

n3 Emphasis is ours. Portions of the claim unnecessary to this discussion have been omitted for clarity.

Given that the carrier frequency which can be used in a low inertia system may fall within the range of carrier frequencies usable in a high inertia system (appellants admit as much), the PTO urges that the apparatus of the Oelrich patent inherently performs the function of the apparatus of claim 1, and that finding a new use for an old device does not entitle one to an apparatus claim for that device, citing *In re Wiseman*, 596 F.2d 1019, 201 USPQ 658 (CCPA 1979). Appellants in that case argued, however, that a structure suggested [**581] by the prior art was patentable to them because it also possessed an inherent but unknown function which they claimed to have discovered. This court stated that a "patent on such a structure would remove from the public that which is in the public domain by [**7] virtue of its inclusion in, or obviousness from, the prior art." *Id.* at 1023, 201 USPQ at 661.

Appellants here countered the PTO inherency contention at oral argument (no reply brief was filed) by urging that there is no "inherency" because there is no "inevitability," that is, the previously quoted "means plus function" limitation of claim 1 is not inherently (always) present in the device of the Oelrich patent.

It is true that mere recitation of a newly discovered function or property, inherently possessed by things in the prior art, does not distinguish a claim drawn to those things from the prior art. *In re Swinehart*, 58 CCPA 1027, 1031, 439 F.2d 210, 212-13, 169 USPQ 226, 229 (1971). In this case, however, claim 1 does not merely recite a newly discovered function of an old device. *In re Chandler*, 45 CCPA 911, 254 F.2d 396, 117 USPQ 361 (1958), a case not cited by either party to this appeal, is most pertinent to the instant controversy.

The claim in *Chandler*, *id.* at 912-13, 254 F.2d at 397, 117 USPQ at 361-62, drawn to an automatic control for a jet engine, included a "means responsive to said movement for regulating the propulsive power of said engine, in accordance [**8] with said movement, so that

said aircraft is propelled at a definite, selected speed, corresponding to the position of said engine relative to said aircraft, throughout the speed range of said aircraft." (Emphasis added.) In refuting the examiner's argument that the words beginning with "so that" were merely functional, and thus did not distinguish the device from that claimed in a patent to Goddard, this court stated:

*** the expression beginning with "so that" is not merely functional, but constitutes a part of the definition of the "means responsive to said movement." Thus that means is defined as being responsive to the movement of the engine in such a way that the aircraft will be propelled at a definite speed in the manner specified. Such a definition conforms to the provision of 35 U.S.C. 112 that an element in a claim for a combination "may be expressed as a means or step for performing a specified function without the recital of structure, material or acts in support thereof. n4

n4 For a similar case, see *In re Wilson*, 53 CCPA 1141, 1148-49, 359 F.2d 456, 461, 149 USPQ 523, 527 (1966). The provision of § 112 referred to is, of course, the sixth paragraph, formerly, at the times of Chandler and Wilson, the third paragraph. The change occurred January 24, 1978. [**9]

Likewise, the words after "means for generating a *** carrier frequency" in the claim on appeal constitute a limiting definition of the means. The PTO does not contend that this limitation, a carrier frequency which is

"less than the minimum *mum system resonant frequency," is expressly disclosed in the Oelrich patent. Neither, however, is this limitation inherent therein. In *Hansgirk v. Kemmer*, 26 CCPA 937, 940, 102 F.2d 212, 214, 40 USPQ 665, 667 (1939), the court said:

Inherency, however, may not be established by probabilities or possibilities. The mere fact that a certain thing may result from a given set of circumstances is not sufficient. [Citations omitted.] If, however, the disclosure is sufficient to show that the natural result flowing from the operation as taught would result in the performance of the questioned function, it seems to be well settled that the disclosure should be regarded as sufficient.

The relationship between the carrier frequency and the system critical frequency -- the former below the latter (and expressly made a claim limitation by use of "means plus function" language) -- cannot be said to be "the natural result flowing from the operation [**10] as taught." The Oelrich patent instructs that the device is "adapted to receive a carrier frequency substantially in [*582] excess of the particular system critical or resonant frequency * * *." Given this express teaching, a "means for generating a *** carrier frequency *** less than the minimum system resonant frequency" is not inevitably present.

The decision of the board is reversed.

REVERSED

LEXSEE 26 CCPA 937

HANS GIRG v. KEMMER

No. 4077

UNITED STATES COURT OF CUSTOMS AND PATENT APPEALS

26 C.C.P.A. 937; 102 F.2d 212; 1939 CCPA LEXIS 107; 40 U.S.P.Q. (BNA) 665

January 11, 1939, Oral argument by Mr. Flick and Mr. Bierman

February 27, 1939, Decided

DISPOSITION:
[**1] Reversed.

CASE SUMMARY

PROCEDURAL POSTURE: Appellant sought review of a decision of the Board of Appeals of the United States Patent Office affirming the award by the Examiner of Interferences of priority of invention in two counts of an interference, which counts defined an invention relating to a process of producing substantially pure magnesium.

OVERVIEW: Appellant contested the award of priority of invention to appellee in two counts of interference that defined an invention relating to a process of producing substantially pure magnesium. Appellant argued that neither in specification nor claims in appellee's application under consideration was there any mention of dust or its removal, which was the heart of the invention involved, until after he became advised of the disclosure in a foreign patent. Appellee contended that he disclosed a manner of heating the magnesium in such a way as to leave the dust behind. The court noted that where one copies a claim from an inadvertently issued patent, it should clearly appear that his application disclosed the invention either expressly or inherently. The court ruled that the mere fact that a certain thing may result from a given set of circumstances was not sufficient and that it would be wholly unjustified in holding that such an alleged disclosure of vital elements of the counts was sufficiently clear so as to enable appellee to make claims corresponding to the counts.

OUTCOME: Decision awarding priority of invention to appellee was reversed where an alleged disclosure of the

vital elements of the counts was not sufficiently clear so as to enable appellee to make claims corresponding to the counts.

CORE CONCEPTS

Patent Law : U.S. Patent & Trademark Office Prosecution Procedures : Filing Requirements

Where one copies a claim from an inadvertently issued patent it should clearly appear that his application disclosed the invention either expressly or inherently. The mere fact that a certain thing may result from a given set of circumstances is not sufficient. If, however, the disclosure is sufficient to show that the natural result flowing from the operation as taught would result in the performance of the questioned function, it seems to be well settled that the disclosure should be regarded as sufficient.

COUNSEL:

Brown, Critchlow & Flick (Jo. Baily Brown and Fulton B. Flick of counsel) for appellant.

H. C. Bierman for appellee.

JUDGES:

Before GARRETT, Presiding Judge, and BLAND, HATFIELD, LENROOT, and JACKSON, Associate Judges.

OPINION BY:

BLAND

OPINION:

[*937] APPEAL from Patent Office, Interference No. 73,230

[*938] BLAND, Judge, delivered the opinion of the court:

This is an appeal by the junior party Hansgirk from a decision of the Board of Appeals of the United States Patent Office, affirming that of the Examiner of Interferences awarding priority of invention in two counts of an interference, which counts define an invention relating to a process of producing substantially pure magnesium.

The interference involves Kemmer's application, serial No. 542,104, filed June 4, 1931, and Hansgirk's patent, No. 2,003,487, issued June 4, 1935, on an application filed February 3, 1933. Both counts were taken from the Hansgirk patent. Since Hansgirk's dates were all subsequent to those of Kemmer, the sole issue raised in the interference related to the right of Kemmer to make claims corresponding to the counts.

The invention as defined by the counts is particularly concerned with [*2] a process of producing magnesium which involves the removal of dust from magnesium vapor before it is condensed, the dust removal step being regarded as the novel feature of the invention. It was old in the art, prior to the entrance of either party into the field, to distill magnesium vapor from magnesium powder whether in powdered form or in the form of briquettes, and then to subsequently condense the same into metallic magnesium.

The record shows that the Primary Examiner, when Kemmer attempted to claim the invention of these counts in his said application ruled that Kemmer's disclosure did not warrant the allowance of the claims. He held that Kemmer's disclosure did not show the sequence of steps required by the claims and that the matter which he inserted in his amended application, which was to afford a basis for said claims, was new matter.

Thereafter, Kemmer filed a motion in another interference between himself and Hansgirk, involving a different application and patent, and sought to add for interference purposes the claims of the Hansgirk patent which are the present counts. The Primary Examiner ruled that Kemmer did not disclose the invention. Upon appeal to the Board [*3] of Appeals, the decision of the Primary Examiner, holding that Kemmer could not make the proposed counts, was reversed, one member of the board dissenting. The present interference was then declared, and on account of the respective dates as is above shown, Hansgirk was ordered to show cause why judgment on the record should not be entered against him. Hansgirk filed answer [*939] which amounted to a motion to dissolve, claiming that Kemmer's application

did not disclose the invention. The Examiner of Interferences, in view of the ruling of the board heretofore referred to, overruled Hansgirk's motion and, on the record, awarded priority to Kemmer. Hansgirk appealed to the Board of Appeals, which was the same board that had rendered the decision on the appeal from the Primary Examiner in the other interference. It again, by a majority opinion, one member dissenting, held that Kemmer could make the counts and affirmed the action of the Examiner of Interferences in awarding priority to him. Hansgirk then took an appeal to this court and the sole question presented is the right of Kemmer to make the claims corresponding to the counts.

Count 2 is similar in all respects to count [*4] 1, except that it contains the provision that the heating of the material containing the metallic magnesium in order to liberate the magnesium vapor is done *under reduced pressure*. For the purpose of this appeal, both counts may be regarded as identical. Count 1 reads as follows:

1. The process for producing substantially pure magnesium which comprises heating material containing metallic magnesium, to liberate magnesium vapor therefrom, removing the resulting vapor by a nonoxidizing gas from the heated zone, separating out dust from said vapor, and thereafter passing it into a condensation zone, and cooling it to condensation point.

It will be noticed that method count 1 contains the following five steps:

1. Heating the material containing metallic magnesium.
2. Removing the resulting vapor by a non-oxidizing gas from the heated zone.
3. Separating dust from the vapor.
4. Thereafter passing it into a condensation zone.
5. Cooling it to a condensation point.

Hansgirk argues here that neither in specification nor claims in the Kemmer application under consideration is there any mention of dust or its removal; that Kemmer never attempted to claim the subject matter, which [*5] is the heart of the invention involved, until after he had become advised of the Hansgirk disclosure in a Canadian patent; that the third stage of separating dust from vapor is a distinct and separate step from the other steps of the process, which follows the removal of the magnesium vapor from the heated zone, and that the counts must be so construed, if the same is to be regarded as valid, in view of the prior art; that since the counts are taken from the Hansgirk patent, they must be construed in the light of the teachings of the patent and that Hansgirk shows a separate step with a screen for removing the dust interposed between the vaporizing material and the

condensation chamber; that in the Kemmer application the dust problem was not considered and no mention of screening [*940] the dust from the vapor either in the heating zone or elsewhere is disclosed.

Kemmer relies for disclosure of the subject matter of the counts on the following language in his application:

In order to obtain highly refined magnesium metal I subject the metal obtained as above described to a distillation operation in a non-oxidizing atmosphere or in a vacuum and condense the vapors of magnesium [**6] to pure metal. Similarly the *quickly cooled powder mentioned above either as such or formed into briquets with or without a binder* may be directly subjected to this distillation operation for a more direct recovery of pure metal. [Italics ours.]

Kemmer contends, and a majority of the board agreed with him, that since he disclosed that his vaporizing heat was applied to the magnesium powder "formed into briquets with or without a binder," the vaporized magnesium in the briquette would find its way through the binder in such a way as to leave the dust behind. The binder of the briquettes is relied upon as supplying the disclosure of the portion of the counts which relates to the separation of the dust from the vapor.

We are not in agreement with the conclusion of the board in this respect and in deciding the issue involved it will not be necessary for us to discuss the question which Hansgirk seeks to present to the effect that the counts must be given the construction he argues for in order to make them valid, nor will it be necessary for us to consider the question discussed and argued at such great length by both parties as to whether or not the dust separation referred to [**7] in the counts must be regarded as occurring outside the heated chamber. We think that the decision of the issue may rest upon a ground concerning which there should be little dispute.

Where one copies a claim from an inadvertently issued patent it should clearly appear that his application disclosed the invention either expressly or inherently. (See *McKee v. Noonan*, 24 C.C.P.A. 784, 86 F.2d 986; *Lindley v. Shepherd*, 58 App. D.C. 31, 24 F.2d 606. He may disclose the invention by drawings, by the use of language, or he may disclose it by reciting and teaching such subject matter as will inherently do the thing or possess the quality which is claimed for it. So it is not enough to say that Kemmer said nothing about dust removal or about a screen which would remove it if the process defined by Kemmer would inherently perform the function in the manner prescribed by the count. Inherency, however, may not be established by probabilities or possibilities. The mere fact that a certain thing *may* result from a given set of circumstances is not

sufficient. See *Parker v. Ballantine*, 26 C.C.P.A. 799, 101 F.2d 220 (Patent Appeal [**8] No. 4026, decided January 23, 1939); *In re Ball*, 23 C.C.P.A. 830, 81 F.2d 242; *Brand v. Thomas*, 25 C.C.P.A. 1053, 96 F.2d 301. If, however, [*941] the disclosure is sufficient to show that the natural result flowing from the operation as taught would result in the performance of the questioned function, it seems to be well settled that the disclosure should be regarded as sufficient.

Now, when we view Kemmer's disclosure in the light of these principles, does it clearly show that his process inherently separates the dust from the vapor? We think not. Nothing is disclosed in his application that he sought to separate dust from vapor or that it was any part of the problem he was attempting to solve. He was attempting and did show a method of vaporizing magnesium from the magnesium material whether it was in the form of powder or in a briquette, either bound or unbound. There is no contention here, as we understand it, unless it be by inference, that there was any screening or separation of the vapor when vaporized, by heating the unbound powder, nor do we think there is any serious contention that there was any separation of dust from the vapor [**9] involved where the unbound briquette was used. It is contended by Kemmer, and found by the board, that the binding around the briquette acted as a screen through which the vapors passed during the process of vaporizing and that the critical element of the counts was, therefore, disclosed in the meagre sentence relating to the possible use of a bound briquette. Regardless of the question raised by Hansgirk as to the dust screening occurring after leaving the heating chamber, this interpretation of the counts is certainly not the meaning which the patentee gave in his application. In both forms of the invention shown by the drawings in his application he shows a screen in the form of loose, granular material, separate and apart from the material being heated.

Kemmer argues that binders are usually made up of bituminous substances which are porous and that the passage of the vapor through the porous material would screen out the dust. There is no disclosure in Kemmer's application that the binder was to be made of a material of a porous character, or that it would be made of any particular kind of material which would perform the function of screening. It is remotely possible that some [**10] kind of screen or binding might be placed around the briquette which would, to some extent, perform the function that Kemmer and the board now claim for it, but it is not sufficient, under the above-stated, well-settled principles, to say that a binder *might* be selected which *might* do a certain thing. It would seem to us that we would be wholly unjustified in holding that such an alleged disclosure of the vital elements of the counts was

sufficiently clear so as to enable Kemmer to make claims corresponding to the counts.

In view of the ambiguity in the counts as to the meaning of the step relating to the separation of the vapor, we think the counts [*942] should be construed in the light of the patent from which they were taken. *Hausman v. Hochman*, 23 C.C.P.A. 1162, 83 F.2d 703; *Neumair v. Malocsay*, 22 C.C.P.A. 1349, 77 F.2d 622. To construe them as Kemmer wishes them construed, it is necessary to hold that *the material itself which is being heated constitutes the separating means*. There is no hint in the patent of such teaching. The counts do not call for separation of the dust from the mass to be heated but call for "separating [*11] dust from said vapor." In both forms of disclosure in Hansgirk's patent, the vapor is first removed from the material and then, in passing through screening material, which is not a part of the material from which the vapor is derived, the dust is left behind. We think the counts should be construed to mean that the removing of the dust is brought about by some means other than by the heated material itself.

However, it is our view that if the board's interpretation of the count was the proper one, we are of the opinion that it was not warranted in concluding that the vapor in passing through a briquette binding, the nature of which was not disclosed, would inherently leave the dust behind. In our view of the case it makes no difference whether the briquettes retained their form or not or whether by the heat they would be reduced to

powder as was suggested by the minority member of the board. We may not conjecture, under the circumstances, that the binder, under the teachings of Kemmer, would be selected of such material as would possess such porosity or other characteristic as would bring about the desired results. If it be assumed that the binding of the briquette prevents the dust [*12] from leaving its original position in the mass of the material being heated, no separation such as is called for by the counts has taken place. This reasoning would presuppose that the process only involved separating the dust from the material. The counts call for *separating the dust from the vapor* and, obviously, the fair meaning of the phrase would require that the vapor, at some point before the dust was separated from it, would have an existence separate from that of the material.

For reasons stated, it is our view that the Kemmer disclosure was not sufficient to form the basis for making the counts and that the interference should have been dissolved on the ground that Kemmer could not make the claims corresponding to the counts.

In this court, Hansgirk moved to strike certain portions of Kemmer's brief. On December 27, 1938, this court ordered certain portions of the same to be stricken and reserved decision as to items 2 and 3 pending argument on appeal. The motion of Hansgirk to strike said items 2 and 3 is denied.

The decision of the Board of Appeals is *reversed*.

Use of a Prenylation Inhibitor as a Novel Antiviral Agent

JEFFREY S. GLENN,^{1*} JAMES C. MARSTERS, JR.,² AND HARRY B. GREENBERG^{1,3}

Division of Gastroenterology,¹ and Department of Microbiology and Immunology,³ Stanford University School of Medicine and Veterans Administration Medical Center, Palo Alto, California 94305-5487, and Bioorganic Chemistry, Genentech Inc., South San Francisco, California 94080²

Received 3 March 1998/Accepted 24 July 1998

No specific therapy exists for hepatitis delta virus (HDV), which can cause severe liver disease. Molecular genetic studies have implicated the prenylation site of large delta antigen as a critical determinant of HDV particle assembly. We have established a cell culture model which produces HDV-like particles, and we show that delta antigen prenylation can be pharmacologically inhibited by the prenylation inhibitor BZA-5B. Furthermore, BZA-5B specifically abolishes particle production in a dose-dependent manner. These results demonstrate that the use of such a prenylation inhibitor-based antiviral therapy may be feasible and identify a novel class of potential antiviral agents.

Hepatitis delta virus (HDV) is a novel viral pathogen that is an important cause of acute and chronic liver disease in various parts of the world (4, 14, 16, 18, 24, 29). There is currently no effective treatment for HDV infections. Recent advances in our understanding of the viral life cycle have revealed new targets for antiviral therapy.

The HDV particle's core contains the 1.7-kb single-stranded circular genomic RNA (32) and the virally encoded small and large delta antigens. The particle core is encapsulated by a lipid envelope embedded with hepatitis B virus (HBV) surface antigen (HBsAg) proteins (2). HBsAg is provided by HBV, which accounts for the occurrence of HDV infections only in the presence of an HBV infection.

Infectious HDV particles can be produced in vitro by cells transfected with cloned DNAs containing portions of the HBV and HDV genomes (28, 33). Virus-like particles can also be produced in the absence of genome replication. Indeed, cotransfection into cultured cells of plasmids encoding only large delta antigen and HBsAg is sufficient for the production and release of particles (5, 31). Essential to large delta antigen's requisite role in HDV assembly are the last four amino acids at the carboxyl terminus (Cys-Arg-Pro-Gln-COOH), which together form a "CXXX box," a motif recognized by prenyltransferase enzymes as a substrate for covalent addition of a prenyl lipid to the CXXX box cysteine (13, 21, 26, 34). Prenyl lipid addition to delta antigen may help target the protein to cellular membranes containing HBsAg and may help trigger virus assembly (7, 10).

When the large delta antigen's CXXX box is destroyed by genetic mutation, prenylation is prevented and particle production is abolished (11, 19). While these studies demonstrated the critical role of prenylation in HDV virion morphogenesis, a strategy that uses mutagenesis to disrupt delta antigen prenylation in natural infections would be impractical. Therefore, we investigated whether virion assembly is similarly inhibited when delta antigen prenylation is prevented by pharmacologic means—by using a drug that specifically inhibits the enzyme responsible for the transfer of the prenyl lipid to delta antigen.

Construction and characterization of a particle-producing cell line. We constructed a permanent cell line capable of continuously producing HDV-like particles. Briefly, a clone of NIH 3T3 cells stably transfected with pSVL-large, which expresses large delta antigen (11), and pHygro, which encodes hygromycin resistance, was further cotransfected with SV24H, which expresses HBsAg (3), and pRCCMV (Invitrogen), which encodes G418 resistance. Cells were transfected with Lipofectamine (Gibco BRL) according to the manufacturer's directions and selected with hygromycin B and G418. One of the resulting clones, termed LH, was selected for further characterization.

Confluent LH cells were washed twice with phosphate-buffered saline, harvested in cell lysis buffer (50 mM Tris [pH 8.8], 2% sodium dodecyl sulfate [SDS]), and analyzed for the presence of large delta antigen. Briefly, samples were subjected to SDS-polyacrylamide gel electrophoresis (PAGE) with 12% resolving gels, followed by transfer to Immobilon polyvinylidene difluoride membranes (Millipore), essentially as described previously (11). The blots were treated with a human antibody against delta antigen (11) and with alkaline phosphatase-conjugated rabbit antibody to human immunoglobulin G (Promega), followed by chemifluorescence development (with a kit from Amersham) and detection (STORM 840; Molecular Dynamics). The results (Fig. 1, lanes 2) confirm the presence of large delta antigen in LH cells. In addition, similar to other cell lines stably transfected with cDNA encoding HBsAg (17, 20, 27), LH cells abundantly express and constitutively secrete HBsAg into the media, as measured by a commercial assay (Auszyme; Abbott Laboratories). Finally, LH cells also produce and release HDV-like particles that contain both HBsAg and delta antigen. The particles can be isolated from clarified medium supernatants by either immunoprecipitation with a monoclonal antibody to HBsAg (Abbott Laboratories) (Fig. 1A, lane 1) or ultracentrifugation through a 20% sucrose cushion and collection of the pellet (25) (Fig. 1B, lane 1). The LH cell line is thus well suited to pharmacologic studies dependent on precise reproducibility and aimed at measuring the effect of various inhibitors on particle production.

Effect of BZA-5B on large delta antigen prenylation. We next wished to identify a compound capable of inhibiting large delta antigen prenylation. For this purpose, we chose to test BZA-5B, a drug originally synthesized as a specific prenyltransferase inhibitor and known to inhibit prenylation of the oncoprotein H-Ras^{V12} (22). BZA-5B can abrogate the prenylation-

* Corresponding author. Mailing address: Department of Medicine, Division of Gastroenterology, MC 5487, Stanford University School of Medicine, MSLS, P-304, 1201 Welch Rd., Palo Alto, CA 94305-5487. Phone: (650) 723-6661. Fax: (650) 723-5488. E-mail: Jeffrey.glenn@stanford.edu.

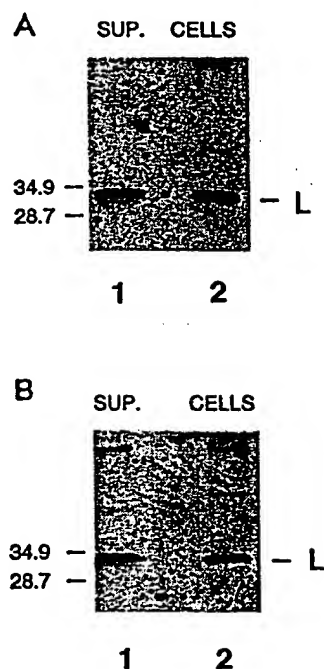


FIG. 1. LH cells produce HDV-like particles. (A) HDV-like particles (lane 1) were immunoprecipitated from clarified medium supernatants (Sup.) of LH cells with a monoclonal antibody to HBsAg and subjected to immunoblot analysis for the presence of large delta antigen. LH cells remaining on the dish were harvested in cell lysis buffer and an aliquot (lane 2) was included in the immunoblot analysis. (B) Particles (lane 1) were isolated by ultracentrifugation of clarified medium supernatants of LH cells and an aliquot was subjected to immunoblot analysis, along with a sample of LH cell lysate (lane 2). L, large delta antigen. The locations of prestained molecular mass markers are shown at the left (in kilodaltons).

dependent, H-Ras^{V12}-mediated transformation of Rat-1 cells without observed gross cellular toxicity (15).

To determine the effect of BZA-5B on large delta antigen prenylation, we performed *in vitro* translation-prenylation reactions, essentially as described previously (11), with the addition of BZA-5B. Briefly, combined *in vitro* transcription-translation reactions with rabbit reticulocyte lysates (Promega) were programmed with a plasmid encoding large delta antigen in the presence of [³H]mevalonate (60 Ci/mmol [R, S]; American Radio-labeled Chemicals), a metabolic precursor of prenyl lipids. A carrier (final concentrations of 0.5 mM dithiothreitol [DTT] and 0.05% dimethyl sulfoxide [DMSO]) or various concentrations of BZA-5B dissolved in the carrier were included in the reactions. Aliquots of each reaction mixture were then subjected to SDS-PAGE and either fluorography (11) (Fig. 2A) or immunoblot analysis for delta antigen as described above (Fig. 2B).

In the absence of BZA-5B, [³H]mevalonate was incorporated into large delta antigen (Fig. 2A, lane 3), indicating that it undergoes prenylation, as previously shown (11). BZA-5B had no apparent effect on the translation of large delta antigen (Fig. 2B), whereas profound inhibition of posttranslational prenyl lipid modification was observed at 5 μ M BZA-5B. No prenylation was detectable at concentrations of 25 μ M and above (Fig. 2A, lanes 4 to 7). Thus, BZA-5B appears to be a potent inhibitor of large delta antigen prenylation. These results are in good agreement with recent data showing that large delta antigen is prenylated by farnesyltransferase (23), the prenyltransferase most sensitive to BZA-5B (15). Our results also suggested that BZA-5B would be a good candidate for inhibiting HDV particle production.

Effect of BZA-5B on particle production. To test the hypothesis that an inhibitor of delta antigen prenylation can prevent virus-like-particle production, the effect of BZA-5B on LH-cell particle production was studied (Fig. 3). LH cells were seeded at low confluency in 100-mm-diameter dishes (15). Duplicate dishes were grown in media containing a carrier (0.5 mM DTT and 0.05% DMSO—to minimize oxidation and enhance cellular penetration of the compound) alone or a carrier plus various concentrations of BZA-5B. After four medium changes, made every other day, portions (2.5 ml) of the respective final clarified medium supernatants were quantitatively analyzed for the presence of HDV-like particles with the centrifugation-over-sucrose-cushion and immunoblot procedures described above (Fig. 3A). The large delta antigen bands were quantitated with the ImageQuant (Molecular Dynamics) software package. All quantitations were performed within the linear range of the chemifluorescence detection, as determined by serial dilutions of large delta antigen standards. As a control for nonspecific inhibition of protein synthesis and secretion, HBsAg was quantitated in duplicate aliquots (10 μ l) of each medium supernatant sample with a commercial assay (Auszyme; Abbott Laboratories). After the medium supernatants were collected, the underlying LH cells were harvested and counted, and a fraction of them were subjected to immunoblot analysis (Fig. 3B). The percentage of control particles per cell and of HBsAg per cell was then calculated for each concentration of BZA-5B and plotted as a function of drug concentration (Fig. 3C).

As shown in Fig. 3A, a significant inhibition of particle production was observed with 10 μ M BZA-5B compared to that in the control with the carrier alone (lane 2 versus lane 1). At 50 μ M BZA-5B, particle production is reduced to below the level of detection (Fig. 3A, lane 4). The inhibition of particle formation was not due to a decrease in the cellular pool of delta antigen (Fig. 3B). To assess whether BZA-5B's inhibition of particle production was secondary to a more general effect on secretion or cell metabolism, rather than direct prenylation inhibition, we measured the HBsAg contained in the collected medium supernatants. HBsAg does not harbor a CXXX box and it is therefore not subject to prenylation, although the known constitutive secretion of HBsAg alone into the media could be

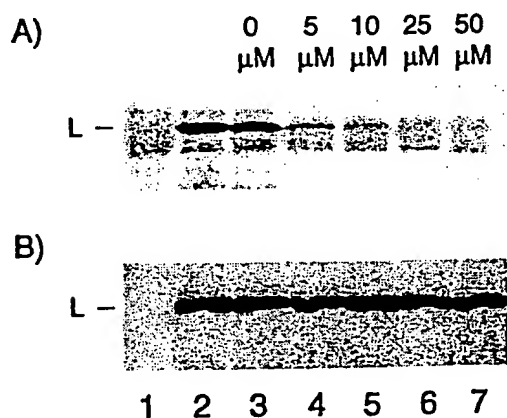


FIG. 2. BZA-5B inhibits prenylation of large delta antigen. Combined *in vitro* transcription-translation reactions were performed with rabbit reticulocyte lysates programmed with water (lanes 1) or a plasmid encoding large delta antigen (lanes 2 to 7) in the presence of [³H]mevalonate and either water (lanes 2), a carrier (0.5 mM DTT and 0.05% DMSO) (lanes 3), or a carrier with 5, 10, 25, or 50 μ M BZA-5B, as indicated. Aliquots (1 μ l) were subjected to SDS-PAGE and either fluorography (A) or immunoblot analysis (B). L, large delta antigen.

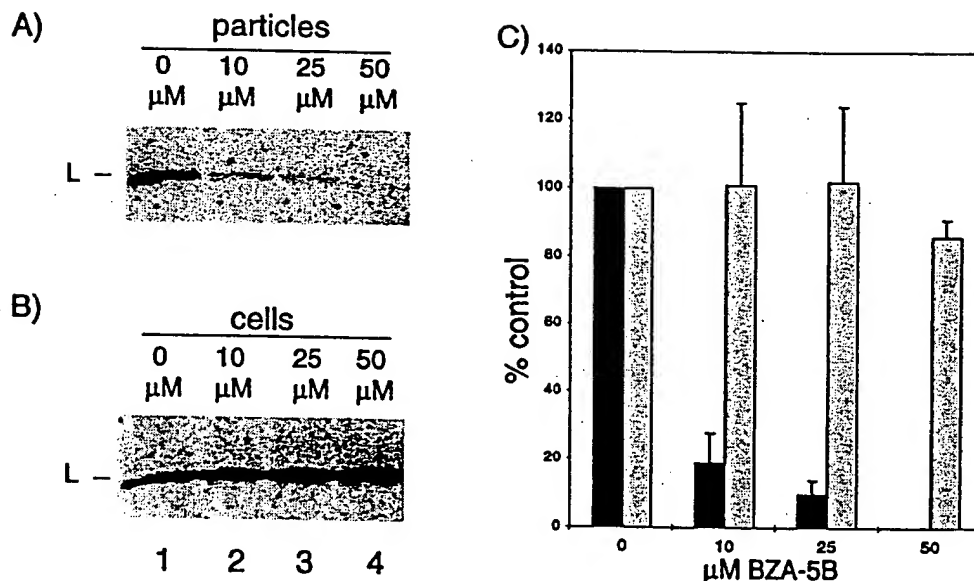


FIG. 3. BZA-5B inhibits HDV-like-particle production. Duplicate dishes of LH cells were grown in media containing a carrier (0.5 mM DTT and 0.05% DMSO) alone (lanes 1) or a carrier with either 10, 25, or 50 μM BZA-5B. Clarified medium supernatants were analyzed for the presence of HDV-like particles by quantitative immunoblot analysis (A). The underlying cells were harvested and counted, and the presence of large delta antigen was analyzed by immunoblotting (B). Only one of the duplicate set of blots is shown. (C) HBsAg was quantitated in duplicate aliquots of each medium supernatant sample, and the percentage of control HBsAg per cell (light bars) and of control particles per cell (dark bars), determined from the experiment whose results are shown in panel A, at each concentration of BZA-5B is plotted. Error bars represent the average deviations.

affected by nonspecific toxicity. As indicated in Fig. 3C, however, BZA-5B selectively abolished prenylation-dependent HDV-like particle release while exerting no such effect on the constitutive secretion of HBsAg.

As with most pharmacologic inhibitor experiments, it is possible that the inhibition of particle formation is unrelated to BZA-5B's effect on delta antigen prenylation. Since particle formation, however, can be similarly abolished when delta antigen prenylation is specifically prevented by a completely different and nonpharmacologic means—namely, genetic mutation of the prenylation site on delta antigen (11)—our data suggests that it is indeed the specific ability of BZA-5B to inhibit delta antigen prenylation (Fig. 2) that is responsible for preventing particle formation (Fig. 3).

These results have obvious implications for a new type of antiviral therapy based on prenylation inhibition. Such an antiviral strategy may be able to be applied to other viruses found to have similarly prenylated proteins. While delta antigen was the first viral protein shown to undergo prenylation, analysis of sequence data banks reveals the presence of CXXX box-containing proteins in numerous other viruses, including herpes simplex virus, cytomegalovirus, and hepatitis A virus (10).

As an initial viral target, HDV is particularly attractive because preventing prenylation of large delta antigen might have two antiviral consequences. First, as we show here, particle assembly could be blocked. Second, as a result of not being released in the form of viral particles, the large delta antigen concentration within infected cells may increase. Because large delta antigen is a potent *trans*-dominant inhibitor of HDV genome replication (6, 12), the antiviral effect of prenylation inhibition on assembly could thus be amplified by an additional suppression of viral genome replication.

Strategies designed to inhibit viral prenylation could affect host cell prenylation as well. Several factors, however, may help limit the potential for intolerable side effects. Normal cellular prenylation is accomplished by a family of prenyltransferases (34). Thus, selective inhibition of the prenyltransferase

that modifies delta antigen may not affect host cell functions which depend on other prenyltransferases. Some substrates can be prenylated by more than one prenyltransferase (1, 30). Such potential cross-specificity may help mitigate unwanted prenylation inhibition of critical cellular proteins by BZA-5B. Indeed, BZA-5B is surprisingly well tolerated in a variety of experimental systems (9, 22); in our experiments, we observed no gross cellular toxicity and a mild (30 to 50%) inhibition of growth rate at the highest BZA-5B concentrations. In addition, viral assembly may be more sensitive than key host cell functions to the effects of prenylation inhibitors. It is possible that inhibiting the prenylation of only a fraction of the large delta antigen in a nascent virus particle may be sufficient for abrogating normal assembly of the entire particle. Ultimately, the true benefit-to-risk ratio will need to be determined for each clinical application. In the case of HDV, there are established animal models (8) which may now be suitable for further evaluating the proposed antiviral strategy.

We thank Bruno Bordier, Anson Lowe, Thomas Merigan, and Edward Mocarski for helpful discussions and critical reading of the manuscript.

This work was supported by grants from the Stanford Digestive Disease Center and the Veterans Administration. J.S.G. is also the recipient of a Howard Hughes Medical Institute Physician Postdoctoral Fellowship.

REFERENCES

1. Armstrong, S. A., V. C. Hannah, J. L. Goldstein, and M. S. Brown. 1995. CAAX geranylgeranyl transferase transfers farnesyl as efficiently as geranyl to Rho B. *J. Biol. Chem.* 270:7864-7868.
2. Bonino, F., B. Hoyer, J. W.-K. Shih, M. Rizzetto, R. H. Purcell, and J. L. Gerin. 1984. Delta hepatitis agent: structural and antigenic properties of the delta-associated particle. *Infect. Immun.* 43:1000-1005.
3. Bruss, V., and D. Ganem. 1991. Mutational analysis of hepatitis B surface antigen particle assembly and secretion. *J. Virol.* 65:3813-3820.
4. Casey, J. L. 1996. Hepatitis delta virus. *Genetics and pathogenesis. Clin. Lab. Med.* 16:451-464.
5. Chang, F.-L., P.-J. Chen, S.-J. Tu, C.-J. Wang, and D.-S. Chen. 1991. The large form of hepatitis delta antigen is crucial for assembly of hepatitis delta virus.

Photoreactive Analogues of Prenyl Diphosphates as Inhibitors and Probes of Human Protein Farnesyltransferase and Geranylgeranyltransferase Type I*

(Received for publication, April 7, 1995, and in revised form, May 26, 1995)

Yuri E. Bukhtiyarov†, Charles A. Omer‡, and Charles M. Allen†¶

From the †Department of Biochemistry and Molecular Biology, J. Hillis Miller Health Center, University of Florida, Gainesville, Florida 32610 and the ‡Department of Cancer Research, Merck Research Labs., West Point, Pennsylvania 19486

Photoreactive analogues of prenyl diphosphates have been useful in studying prenyltransferases. The effectiveness of analogues with different chain lengths as probes of recombinant human protein prenyltransferases is established here. A putative geranylgeranyl diphosphate analogue, 2-diazo-3,3,3-trifluoropropionyloxy-farnesyl diphosphate (DATFP-FPP), was the best inhibitor of both protein farnesyltransferase (PFT) and protein geranylgeranyltransferase-I (PGGT-I). Shorter photoreactive isoprenyl diphosphate analogues with geranyl and dimethylallyl moieties and the DATFP-derivative of farnesyl monophosphate were much poorer inhibitors. DATFP-FPP was a competitive inhibitor of both PFT and PGGT-I with K_i values of 100 and 18 nM, respectively. [32 P]DATFP-FPP specifically photoradiolabeled the β -subunits of both PFT and PGGT-I. Potoradiolabeling of PGGT-I was inhibited more effectively by geranylgeranyl diphosphate than farnesyl diphosphate, whereas photoradiolabeling of PFT was inhibited better by farnesyl diphosphate than geranylgeranyl diphosphate. These results lead to the conclusions that DATFP-FPP is an effective probe of the prenyl diphosphate binding domains of PFT and PGGT-I. Furthermore, the β -subunits of protein prenyltransferases must contribute significantly to the recognition and binding of the isoprenoid substrate.

Prenylated proteins have an important role in cellular regulation, therefore, a description of their structure/function relationships and post-translational processing has been of great interest (1-3). Among the post-translational events is the modification of cysteine residues in carboxyl termini with either a farnesyl or geranylgeranyl moiety by sequence specific protein prenyltransferases. Protein farnesyltransferase (PFT)¹ is a $\alpha\beta$ -heterodimer (4, 5), which transfers the C_{15} isoprenoid from farnesyl diphosphate (FPP) to a Cys residue in the sequence

-Cys- A_1 - A_2 -Ser(Met, Gln), where A_1 and A_2 represent aliphatic amino acids (1-3, 6, 7). Protein geranylgeranyltransferase-I (GGGT-I) is also a $\alpha\beta$ -heterodimer (4), but it transfers the C_{20} moiety from geranylgeranyl diphosphate (GGPP) to a Cys residue in proteins terminating in Leu (-Cys- A_1 - A_2 -Leu) (8-11). A different class of geranylgeranyltransferases, PGGT-II or rab prenyltransferases (12), modify proteins ending in -Cys-Cys, -Cys-X-Cys, and -Cys-Cys-X-X (8, 13-15).

Although, the substrate specificity of prenyltransferases which recognize the -C- A_1 - A_2 -X motif has been well established and many inhibitors of these enzymes have been described (16-20), the full extent of involvement of the protein subunits or their respective amino acid residues in the prenylation reaction has not yet been elucidated for any of these prenyltransferases. A detailed description of the "active sites" of these enzymes would aid in the development of more specific enzyme inhibitors based on rational design. One means of investigating the structure of a substrate binding domain is to probe it with photoreactive substrate analogues. Earlier studies have shown photoinhibition and photolabeling of bacterial prenyltransferases with a photoreactive analogue of FPP, diazotrifluoropropionyloxy-geranyl diphosphate, DATFP-GPP (1, $n = 1$), (21, 22). DATFP-GPP was subsequently shown to be an inhibitor of protein prenyltransferase activity in cytosolic extracts of cultured human lymphocytes (23). DATFP-GPP and the GGPP analogue, DATFP-FPP (1, $n = 2$), have now been used to probe protein prenyltransferase function.

Since PFT and PGGT-I show specificity toward both the protein and prenyl diphosphate substrates, the common α -subunit is not likely to be the sole determinant for substrate specificity. Accordingly, Omer *et al.* (5) showed that [3 H]DATFP-GPP, the radiolabeled putative FPP analogue, specifically labeled the β -subunit of recombinant human PFT (hPFT). Recently Yokoyama *et al.* (24) have synthesized [3 H]DATFP-FPP and also shown that it photoradiolabeled the β -subunit of bovine brain PGGT-I. Although, the radioactive photoreactive prenyl diphosphate probes labeled only the β -subunits of these prenyltransferases and the labeling could be inhibited by the natural substrate for each enzyme, no evidence was presented to unequivocally demonstrate that the photoprobe binds to the active site. More specifically, demonstration that these probes inhibit the prenyltransferases competitively, with K_i values similar to the K_m of the natural substrates, was not established. In addition, neither demonstration of chain length specificity of the photoprobes for inhibition of activity was established nor was the specificity of the prenyl diphosphates in their protection of the labeling of the β -subunits determined.

We present here an improved synthesis and characterization of DATFP-FPP. DATFP-FPP was shown to competitively in-

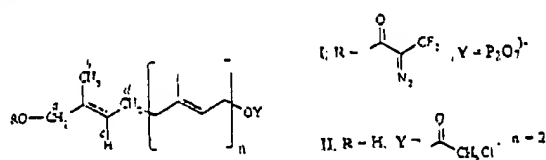
* This work was supported in part by Grant F93UF-2 from the American Cancer Society, Florida Division, and The Cancer Center, University of Florida. The costs of publication of this article were defrayed in part by the payment of page charges. This article must therefore be hereby marked "advertisement" in accordance with 18 U.S.C. Section 1734 solely to indicate this fact.

† To whom correspondence should be addressed.

¶ The abbreviations used are: PFT, protein farnesyltransferase; Bt, biotinylated; DATFP, diazotrifluoropropionyloxy; GPP, geranyl diphosphate; DMAPP, dimethylallyl diphosphate; FMP, farnesyl monophosphate; FPP, farnesyl diphosphate; GGPP, geranylgeranyl diphosphate; PGGT-I, protein geranylgeranyltransferase type I; NOESY, nuclear Overhauser effect spectroscopy; DQF-COSY, double quantum filtered correlation spectroscopy; MALDI-MS, matrix assisted laser desorption ionization mass spectrometry; HPLC, high performance liquid chromatography; Tricine, N-(2-hydroxy-1,1-bis(hydroxymethyl)ethyl)glycine.

19036

Photoaffinity Labeling of Prenyltransferases



STRUCTURE 1.

hibit both hPFT and hPGGT-I and demonstrated better inhibition than the shorter DATFP-isoprenyl homologues. Furthermore, whereas [^{32}P]DATFP-FPP (Structure 1) photolabeled the β -subunits of both human recombinant enzymes, inhibition of rsdiolabeling showed preference for the enzyme's prenyl diphosphate substrate.

EXPERIMENTAL PROCEDURES

Materials—E.E-(³H)FPP (15–20 Ci/mmol) and E.E-(1-³H)GGPP (15–20 Ci/mmol) were purchased from American Radiolabeled Chemicals and DuPont NEN. Biotinylated (Bt) KTKCVIS was prepared by the Protein Chemistry Core Facility, Interdisciplinary Center for Biotechnology Research, University of Florida. Bt-KKFFCAIL was generously provided by Dr. Alison Joly, University of California Los Angeles. FPP and GGPP were prepared as described previously (25). DATFP-GPP, (³H)DATFP-GPP (4.3 mCi/mmol), and DATFP-dimethylallyl diphosphate (DATFP-DMAPP) were prepared previously (21, 22). All other reagents were purchased from Sigma unless otherwise indicated. Recombinant hPFT, having a truncated α -subunit (hPFT₁₋₄₅₅), and hPGGT-I were prepared as described previously (5, 26).

Synthesis of DATFP-FPP and DATFP-FMP—The chemical synthesis of the photoreactive analogues, DATFP-FPP ($n = 2$) was accomplished by modifying the procedures described earlier (21). A similar synthesis has recently been accomplished by Yokoyama *et al.* (24). The principal feature of these syntheses was the oxidation of the monochloroacetyl ester of farnesol to the ω -hydroxypropenyl chloroacetate. The esterification of this dihydroxy monoester with diazotriisopropenyl chloride gave the ω -DATFP-farnesyl chloroacetate. Then selective removal of the chloroacetyl group to give DATFP-farnesol was achieved with methanolic ammonium and phosphorylation gave the final product, DATFP-FPP.

A critical step for this scheme is the selective oxidation of (*E,E*)-3,7,11-trimethyl-1-(chloroacetoxy)-2,6,10-dodecatriene (farnesyl chloroacetate) to (*E,E*)-3,7,11-trimethyl-1-(chloroacetoxy)-2,6,10-dodecatrien-12-ol (*ω*-hydroxyfarnesyl chloroacetate, II). Farnesyl chloroacetate, in contrast to geranyl chloroacetate (21) was more reactive with selenious acid/*t*-butyl hydroperoxide. As a result, the oxidation of *trans* *ω*-terminal methyl group of the farnesyl group was accompanied by the oxidation of methylene groups as well. Increasing the extent of the reaction only led to the formation of the over-oxidation products with more than one hydroxy or carbonyl group in the molecule. Therefore, the conditions were optimized for the oxidation by limiting consumption of the starting material and minimizing the formation of over-oxidation products. This was achieved by treatment for a shorter period of time and at a lower temperature than previously reported (21, 27). Farnesyl chloroacetate (4.6 g, 15.5 mmol) was oxidized with *t*-butyl hydroperoxide (3.45 ml, 31 mmol) and H_2SeO_3 (1 g, 7.8 mmol) in 25 ml of CH_2Cl_2 for 2 h at 0 °C. The *ω*-hydroxyfarnesyl chloroacetate was obtained in 24% yield (1.18 g, 3.8 mmol) after purification by silica gel chromatography with stepwise gradient elution from petroleum ether/benzene (3:2, v/v) to benzene/ethyl acetate (35:65, v/v). The alcohol eluted with 5–10% ethyl acetate in benzene. Its R_F was 0.32 in benzene/ethyl acetate (9:1, v/v). This yield represents a 6-fold increase over the other reported synthesis (24). Limited consumption of the starting material also permitted its recovery for subsequent utilization.

Standard one-pulse DQF-COSY and NOESY experiments using a Varian Unity 600 nmr system were carried out to establish that the presumed structure (II) was correct. ¹H nmr shifts δ (ppm) (C⁶HCl₅) (600 MHz) were: 1.59 (3H, s), 1.65 (3H, s), 1.71 (3H, s), 1.95 (2H, tr), 2.03 (2H, tr), 2.09 (4H, overlapping triplets), 3.96 (2H, s), 4.04 (2H, s), 4.69 (2H, d), 5.05 (1H, tr), 5.34 (1H, tr), 5.36 (1H, tr). The DQF-COSY and NOESY analyses show that monohydroxylation of the terminal *trans*-methyl group was achieved. The presence of three methyl peaks and four methylene signals in the spectrum rule out the possibility that II was a secondary alcohol. The alcoholic group obviously resides on the terminal carbon because the symmetrized DQF-COSY spectrum showed that the methylene protons α (δ , 3.9 ppm), assigned to the oxidized carbon, and the vinyl proton ϵ (δ , 5.36 ppm) were scalar coupled. The α protons were

coupled long range to the methylene protons *d* (δ , 2.09 ppm) and the methyl group *b* (δ , 1.65 ppm). The *trans*-orientation of the ω -hydroxyl moiety was expected by analogy to the work of others, who have established that farnesylacetate (28) and other *gem*-dimethyl allylic compounds (29) are oxidized by selenium dioxide with the formation of the *trans*-hydroxy derivatives. This result was confirmed here by noting that the chemical shifts of the vinyl proton *c* (δ , 5.36) and the terminal methyl group *h* (δ , 1.65) are the values expected for a *trans*-allylic alcohol and are in contrast to the shifts (δ , 5.25 (vinyl) and δ , 1.76 (methyl)) expected for the corresponding *cis* alcohol (30).

Other intermediates of the synthetic pathway were pure as assessed by TLC using Kieselgel 60 F₂₅₄ plates (E. Merck) and were analyzed by ¹H nmr analysis using a Varian EM-390 (90 MHz) spectrometer. Their proton nmr spectral results were consistent with expected products.

DATFP-farnesol was phosphorylated by a previously described method (31). The products of phosphorylation, DATFP-FMP and DATFP-FPP, were separated by DE52 cellulose (Whatman) column chromatography with a linear gradient from 25 to 500 mM ammonium acetate in 50% (v/v) aqueous methanol. DATFP-FPP was isolated in 10% yield (0.02 mmol) after further purification by chromatography on CF-11 cellulose in tetrahydrofuran, 100 mM NH_4HCO_3 (85:15, v/v) (25). $R_F = 0.30$ in 2-propanol/ NH_4OH / H_2O (6:3:1, v/v/v). $\epsilon_{233} = 11,600 \text{ L mol}^{-1} \text{ cm}^{-1}$ (in 1 mM NH_4OH).

Fractions containing DATFP-FMP were lyophilized and applied to an Amberlite XAD-2 column in 1 mM aqueous ammonia. The pure monophosphate was eluted with 90% methanol. $R_F = 0.61$ in 2-propanol/ $\text{NH}_4\text{OH}/\text{H}_2\text{O}$ (6:3:1, v/v/v). $\epsilon_{240} = 9,700 \text{ L}\cdot\text{mol}^{-1}\cdot\text{cm}^{-1}$ (in 1 mM NH_4OH).

Synthesis of [32 P]DATFP-FPP—DATFP-farnesol was also converted to its [32 P]diphosphate derivative by reaction with [32 P]bis-(triethylammonium)hydrogen phosphate in the presence of a large excess of CCl_3CN . In a typical procedure, 2–5 mCi of carrier free $\text{H}_2\text{^{32}PO}_4$ were mixed with aqueous H_2PO_4 to achieve the desired specific activity (40–500 mCi/mmol). The solution was lyophilized over P_2O_5 and the calculated amount of Et_3N in dry acetonitrile was added to prepare [32 P]bis-(triethylammonium)hydrogen phosphate. DATFP-farnesol (50 mM) in a 20–50% solution of CCl_3CN in acetonitrile was added to achieve a 2 molar excess of inorganic phosphate over DATFP-farnesol. The reaction was allowed to proceed at room temperature under a blanket of inert gas for 1–2 h. The solvent and the excess CCl_3CN were removed in a stream of argon, and the residue was taken up with the buffer for ion-exchange chromatography (20 mM ammonium acetate in 50% MeOH). The sample was loaded onto a $1 \times 17\text{-cm}$ column of Whatman DE52 cellulose equilibrated with the same buffer. After washing the column with the buffer, radioactive mono- and diphosphates of DATFP-farnesol were eluted consecutively with 100 mM ammonium acetate in 50% MeOH. Fractions were analyzed by TLC. Those containing [32 P]DATFP-FPP were combined, evaporated, and lyophilized. In some cases the product was further purified by chromatography on Kieselgel 60 plates (250 μm , E. Merck) in 2-propanol/ NH_4OH / H_2O (6:3:1, v/v/v). Radiochemical purity of the product was at least 70% as assessed by thin-layer radiochromatography.

Protein Prenyltransferase Assay—hPFT and hPGGT-I were assayed with Bt-peptide and the appropriate [^3H]prenyl diphosphate (32, 33). hPFT incubation mixtures (100 μl) contained 69 mM potassium phosphate buffer, pH 7.0, 55 μM ZnCl_2 , 5.5 mM MgCl_2 , and 10 mM dithiothreitol. hPGGT-I incubation mixtures (180–200 μl) were modified after those described by Zhang *et al.* (34) with the addition of 0.2% polyvinyl alcohol (5). The specific concentrations of Bt-KTKCVIS, Bt-KKFFCALL, [^3H]FPP, and [^3H]GGPP and enzyme are given in the legends to the figures. Control assay mixtures omitted the biotinylated peptide. Incubations were carried out at 37 $^\circ\text{C}$ for 30 min followed by the addition of a suspension of 0.86–0.61 units of avidin-agarose beads in a solution containing 26 mM EDTA, 0.5 M NaCl, and either 2 mM FPP or GGPP for the hPFT and hPGGT-I assays, respectively. After incubation for another 10 min at 37 $^\circ\text{C}$, the beads were washed as described previously (11), collected analytically on GN-6 Metrical (Gelman) membrane filters, and analyzed for radioactivity.

Inhibition Experiments.—Photoprobes to be tested as inhibitors were added from stock solutions (made basic with aqueous ammonia) to reaction mixtures containing the enzyme with either [^3H]FPP or [^3H]GGPP and the appropriate Bt-peptide. Prenyltransferase assays were carried out in the dark. K_m values were determined from the intercept ($-1/S$) of Lineweaver-Burke plots at $1/V = 0$. K_i value was estimated from the slopes of the double reciprocal plots in the presence of inhibitor. All kinetic analyses were conducted with saturating levels of the appropriate Bt-peptide. The data reported in Table I and all figures represent the average of duplicate determinations. The standard error

of the enzymatic activity determinations did not exceed 10%. The mean values for two repeats were taken for calculation of kinetic parameters using the Enzfitter program (44).

Photolabeling Experiments. Recombinant hPFT or hPGGT-I (2–7 μ g) were pre-equilibrated with [32 P]DATFP-FPP for 5 min at room temperature in 25 mM potassium phosphate buffer, pH 7.0, containing 2 mM $MgCl_2$ and 20 μ M $ZnCl_2$ in a total volume of 30–80 μ l. Open microcentrifuge tubes containing the samples were placed under a bactericidal lamp, cooled to 4 $^{\circ}C$, and irradiated for 8–10 min. Electrophoresis sample buffer was then added to each tube and the samples were analyzed by SDS-polyacrylamide gel electrophoresis on a 10% Tris-Tricine gel (35). The gel was silver stained (36), dried, and autoradiographed using Fuji RX x-ray film. In some cases the radioactive bands corresponding to the α - and β -subunits were excised, transferred to scintillation vials, and counted for radioactivity.

HPLC and MALDI-MS Analyses. Incubation mixtures for HPLC analysis of hPFT reaction products contained in a final volume of 410 μ l: 6.1 mM potassium phosphate buffer, pH 7.0, 0.5 mM $MgCl_2$, 5 μ M $ZnCl_2$, 9.8 mM dithiothreitol, 61 μ M KTKCVIS, 122 μ M allylic diphosphate, and 29 pmol of recombinant hPFT. Reactions proceeded at 37 $^{\circ}C$ for up to 6 h. At different times, the reaction was stopped by freezing the samples at $-18^{\circ}C$. Aliquots (50 μ l) from these samples were then analyzed by HPLC using a Perkin-Elmer Series 4 liquid chromatograph equipped with a Perkin-Elmer analytical C_{18} column (4.6 \times 250 mm) and an LC-75 spectrophotometric detector preset to 215 nm. Mixtures of solvent A (0.1% trifluoroacetic acid in water) and solvent B (0.1% trifluoroacetic acid in acetonitrile) were used for gradient elution. The column was equilibrated for 1 min with 2% B and then eluted with a concave gradient to 60% B (19 min) followed by a linear gradient to 80% B (10 min).

Matrix-assisted Laser Desorption Ionization Mass Spectrometry (MALDI-MS) of the isolated farnesylated peptide was performed on a Voyager RP MALDI time-of-flight mass spectrometer (PerSeptive Biosystems) in a positive ion analysis mode using α -cyano-4-hydroxycinnamic acid as a matrix.

RESULTS

Inhibition of Recombinant Human PFT and PGGT-I by Various DATFP-Derivatives. Four DATFP-derivatives were tested as inhibitors of hPFT and hPGGT-I. DATFP-FPP showed distinctly better inhibition of hPFT than the shorter chain analogues (DATFP-GPP and DATFP-DMAPP) (Fig. 1A). The monophosphate of DATFP-farnesol (DATFP-FMP) was a much poorer inhibitor than the corresponding diphosphate with inhibitory properties similar to DATFP-GPP. The effectiveness of these inhibitors on hPGGT-I was similar to that exhibited with hPFT, except that DATFP-GPP was no better an inhibitor than the shorter analogue DATFP-DMAPP (Fig. 1B).

Inhibition of Recombinant hPFT and hPGGT-I by DATFP-FPP. Double reciprocal plots of the activities of hPFT in the presence of two different concentrations of DATFP-FPP showed competitive inhibition (Fig. 2A) with a K_i of 100 nM. This K_i value was only slightly higher than the estimated K_m of 20 nM for FPP, which was determined in the same experiment. Similarly, hPGGT-I was competitively inhibited by DATFP-FPP with a K_i value of 18 nM, whereas the estimated K_m value of 16 nM was observed for its isoprenoid substrate, GGPP (Fig. 2B).

The inhibition kinetics could also be a manifestation of the function of the DATFP-derivatives as alternative substrates. Product formation from the reaction of the DATFP-derivatives and peptide with hPFT was assessed by two independent methods. No detectable product appearance (or loss of KTKCVIS) was observed by HPLC analysis (see "Experimental Procedures" for details) when DATFP-FPP, DATFP-GPP, or DATFP-DMAPP was used as an alternative prenyl donor. At least 5 nmol of a prenylated peptide could have been detected by this method of analysis. As a positive control, FPP and 25 nmol of unbiotinylated KTKCVIS were incubated with hPFT over a 6-h period. A time dependent loss of KTKCVIS (elution time = 17 min) and appearance of a product peak (elution time = 27 min) were observed. At the end of the incubation, the starting peptide was completely consumed. The nature of the HPLC puri-

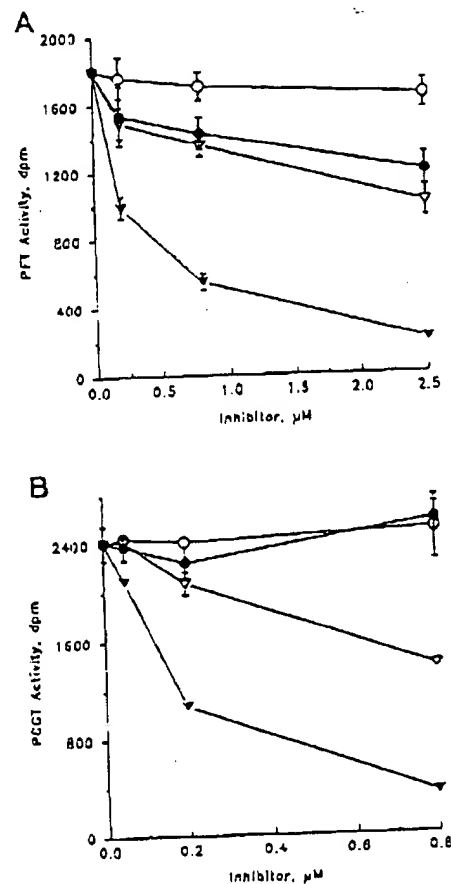


FIG. 1. Inhibition of hPFT and hPGGT-I by various DATFP-prenyl diphosphates. Assays were carried out as described under "Experimental Procedures" using (A) hPFT, 2 ng/ml, with 50 nM [32 H]FPP and 10 μ M Bt-KTKCVIS or (B) hPGGT-I, 1 ng/ml, with 45 nM [32 H]GGPP, 1.5 μ M Bt-KKFFCAIL, and different amounts of DATFP-FPP (●), DATFP-GPP (○), DATFP-DMAPP (○), and DATFP-FMP (▽).

fied product was established by MALDI-MS analysis. A parent molecular ion $[M + H]^+$ of 983 mass units, which corresponds to the expected mass for a farnesylated peptide, was obtained. MALDI-MS analysis of a whole incubation mixture without subsequent HPLC purification also showed the appearance of farnesylated peptide. These experiments show that DATFP-FPP cannot serve as a substrate in the reaction catalyzed by hPFT, despite a low K_i value of hPFT for DATFP-FPP. One concludes then that DATFP-FPP behaved as a dead end inhibitor in the kinetic experiments shown on Fig. 2A. An alternative and more sensitive method of analysis was used to test [32 H]DATFP-GPP as a potential substrate for hPFT. Incubation of hPFT with [32 H]DATFP-GPP and Bt-KTKCVIS showed no detectable radiolabeled product using the standard enzymatic assay. The conclusions from this experiment support the findings from HPLC analysis, but are tempered by the fact that DATFP-GPP was not as good an inhibitor of hPFT as DATFP-FPP.

Covalent Labeling of the β -Subunits of hPFT and hPGGT-I with [32 P]DATFP-FPP. Photolysis of [32 P]DATFP-FPP in the presence of recombinant human protein prenyltransferases led to specific radiolabeling of the β -subunits of both enzymes (Fig. 3). In the absence of irradiation, no radioactive bands were observed (data not shown). The photolabeling was not affected by the absence of a peptide substrate (Fig. 3, lanes 2'), which is consistent with the random order of substrate binding previously postulated for hPFT (37) and bovine brain PGGT-I (24).

Selective Inhibition of Photolabeling of hPFT and hPGGT-I

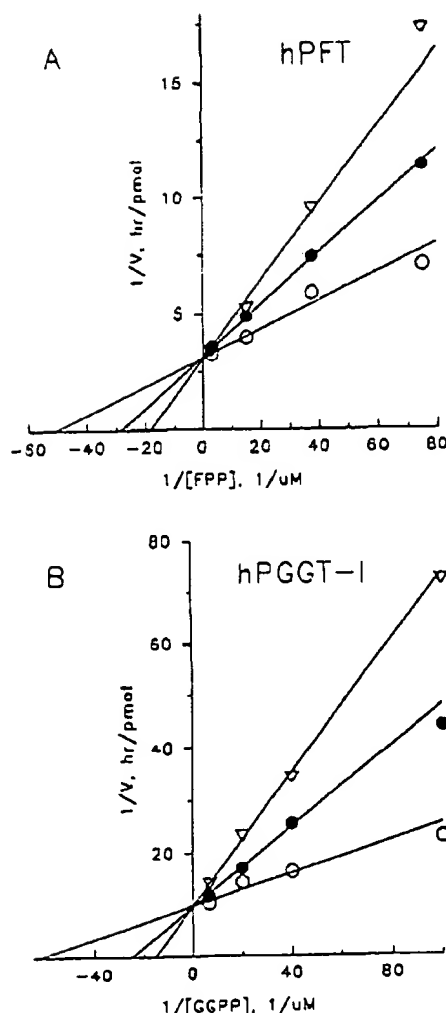


FIG. 2. Double reciprocal plots of the activity of hPFT and hPGGT-I in the presence of inhibitor DATFP-FPP. hPFT and hPGGT-I were assayed as described under "Experimental Procedures" using (A) 2 ng/ml recombinant hPFT, 10 μ M Bt-KTKCVIS, variable [3 H]FPP, and 0 nM (○), 66.7 nM (●), and 200 nM (▽) DATFP-FPP, and (B) 1.7 ng/ml of recombinant hPGGT-I, 2 μ M KKFFCAIL, variable [3 H]GGPP, and 0 nM (○), 22.2 nM (●), and 66.7 nM (▽) DATFP-FPP.

by Prenyl Diphosphate Substrates—Preincubation of hPFT and hPGGT-I with the appropriate prenyl diphosphate substrate resulted in almost complete inhibition of photolabeling (Fig. 3). The protective effect of the natural substrate (FPP in the case of hPFT, lane 3', or GGPP for hPGGT, lane 4') was substantially stronger than that of the alternative prenyl diphosphate. The inhibitory results described in Fig. 3 were obtained with relatively high concentrations of FPP and GGPP. Therefore, a more quantitative comparison of the relative effectiveness of FPP and GGPP as inhibitors of the cross-linking was evaluated at about 10 times lower concentrations of prenyl diphosphates and radiolabeled probe (Fig. 4). Photolabeling of the β -subunits of hPFT and hPGGT was strongly inhibited with 1.67 μ M FPP and GGPP, respectively, while 6.7 μ M GGPP and FPP in the corresponding cases had markedly less effect. The natural prenyl diphosphate substrates were clearly much better inhibitors for their respective protein prenyltransferases. This suggests that the photoprobe binds specifically to the prenyl diphosphate substrate binding domain of each enzyme.

Weak but noticeable nonspecific radiolabeling of the α -subunits of the enzymes was also observed (see Figs. 3 and 4),

although the level of nonspecific labeling varied from preparation to preparation of the photoprobe. The level of α -subunit labeling was not affected by the presence of isoprenoid substrates in photolysis incubations and it appeared to be similar to that observed for the β -subunits under conditions where the concentrations of inhibiting isoprenoid substrate were very high.

The level of photolabeling of the β -subunits of both hPFT and hPGGT-I increased with increasing concentrations of [32 P]DATFP-FPP and was saturable (data not shown). The apparent relative affinities of the prenyltransferases for DATFP-FPP versus their natural prenyl diphosphate substrates were also estimated indirectly by determining the dependence of inhibition of the radiolabeling of the β -subunits on the concentrations of FPP and GGPP. Prenyl diphosphate concentrations which gave 50% inhibition of β -subunit photolabeling at 2.2 μ M [32 P]DATFP-FPP were 0.4 μ M FPP and 1.1 μ M GGPP, respectively, for hPFT and hPGGT-I (data not shown). Therefore, the photoprobe binds well to both enzymes but with an affinity which is poorer compared to FPP (for hPFT) and comparable to GGPP (for hPGGT-I).

DISCUSSION

The application of photoaffinity labeling to the study of prenyltransferases offers the possibility of exploring the active sites of these enzymes. This points to the need to develop photoreactive isoprenoid analogues which react specifically with different prenyl diphosphate binding domains. Brems and Rilling (38) showed the potential of using photoreactive isoprenoid analogues as probes of prenyltransferases by demonstrating that [3 H]-azidophenylethyl diphosphate labeled the isopentenyl diphosphate binding site of avian liver FPP synthase. Our approach has been to synthesize analogues of the allylic prenyl diphosphate substrate where the ω -isoprene residue was replaced by the photoreactive DATFP group. Previous work described the synthesis of diazotrifluoropropionyloxy derivatives of dimethylallyl and geranyl diphosphate (I, $n = 0, 1$) as analogues of GPP and FPP, respectively (21). The planar configuration of the diazoacyl group was expected to mimic an isoprene unit having a rigid arrangement of substituents around the double bond. The effectiveness of DATFP-GPP as an inhibitory analogue of FPP has been described for several prenyltransferases (21–23, 39). Recently, [3 H]DATFP-GPP and [3 H]DATFP-FPP have been used to photolabel the β -subunits of recombinant hPFT (5) and purified bovine brain PGGT-I (24), respectively.

We have now shown that both hPFT and hPGGT-I were strongly inhibited by DATFP-FPP, whereas the shorter chain analogues DATFP-GPP and DATFP-DMAPP were much poorer inhibitors. Furthermore, the monophosphate ester of the geranylgeranyl analogue, DATFP-FMP, was also a poor inhibitor. One would conclude then that the diphosphate moiety and a lipid moiety, at least as long as the DATFP-farnesyl group, are necessary for exhibiting strong inhibitory properties. Surprisingly, DATFP-FPP, the putative GGPP analogue, was a better inhibitor of hPFT than the FPP analogue DATFP-GPP. This might suggest that hPFT recognizes the farnesyl moiety of DATFP-FPP and binds it more tightly than the DATFP-geranyl moiety of DATFP-GPP.

The apparent binding affinities of DATFP-FPP for hPFT and hPGGT-I were estimated by two methods: 1) kinetic analysis of inhibition of prenyltransferase activity by the photoprobe and 2) analysis of the concentration-dependent inhibition of enzyme photolabeling by the natural substrates FPP and GGPP. DATFP-FPP was a competitive inhibitor of both hPFT and hPGGT-I. The K_i (100 nM) of hPFT for DATFP-FPP, determined kinetically, was 5 times higher than the K_m for FPP.

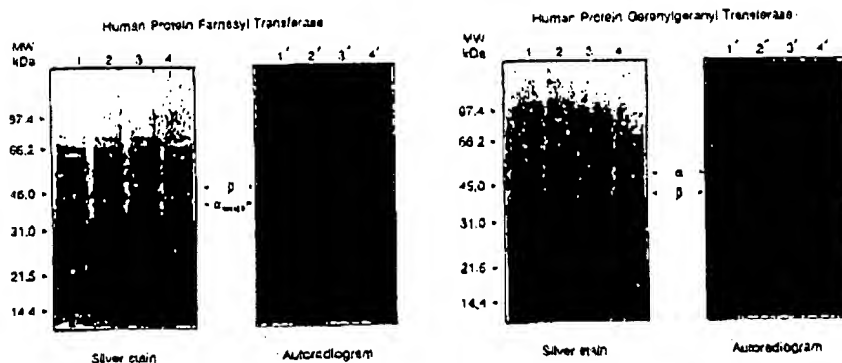


FIG. 3. Photolabeling of human PFT and PGGT-I with [32 P]DATFP-FPP. hPFT (4 μ g) or hPGGT-I (7 μ g) were irradiated with 33.3 μ M [32 P]DATFP-FPP (80 mCi/mmol) in 42 mM potassium phosphate buffer, pH 7.0, 3 mM $MgCl_2$, 33 μ M $ZnCl_2$ for 10 min at 4 $^{\circ}C$ with or without Bt-peptide, FPP, or GGPP. Proteins were separated by SDS-polyacrylamide gel electrophoresis in 10% Tris-Tricine gels and silver stained (lanes 1-4). Labeled protein was detected by autoradiography (12 h; lanes 1'-4'). Gels with hPFT are in the left panels and those with hPGGT-I are in the right panels. Irradiation conditions: lanes 1 and 1', with 33 μ M Bt-KTKCVIS and Bt-ICKFFCAIL, respectively; lanes 2 and 2', without the peptides; lanes 3 and 3', with 67 μ M FPP; lanes 4 and 4', with 67 μ M GGPP.

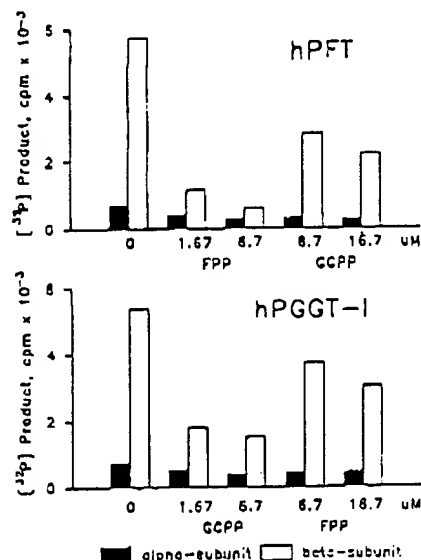


FIG. 4. Comparison of the inhibitory effect of C_{15} - and C_{30} -allylic diphosphates on the photolabeling of the hPFT and hPGGT-I by [32 P]DATFP-FPP. hPFT (top) and hPGGT-I (bottom), 2 μ g each, were irradiated for 16 min at 4 $^{\circ}C$ with 3.8 μ M [32 P]DATFP-FPP (1 Ci/mmol) in a 42 mM potassium phosphate buffer containing 3 mM $MgCl_2$, 33 μ M $ZnCl_2$, and different concentrations of FPP and GGPP. The concentration of FPP or GGPP is shown below the graph. The α - (filled bars) and β -subunits (open bars) were separated on a 10% Tris-Tricine polyacrylamide gel and counted for radioactivity.

whereas, the K_i (18 nM) of hPGGT-I for DATFP-FPP was about the same as the K_m for GGPP (Table I). The K_m values observed here are comparable to those previously reported for these enzymes (5, 34). Analyses of probe affinity for the enzymes by the indirect method, where inhibition of photolabeling of hPFT and hPGGT-I by FPP and GGPP was assessed, also showed that relative differences in affinity between DATFP-FPP and the natural substrates were similar to the ratios of K_i/K_m for these compounds. Therefore, the affinities of DATFP-FPP for hPFT and hPGGT-I were somewhat less than either of the natural substrates. Nevertheless, DATFP-FPP binds competitively and tightly to both enzymes.

The mode of involvement of protein subunits or their respective amino acids residues in the active sites of prenyltransferases in general has not been established, although the first crystal structure for a prenyltransferase, FPP synthase, has now been reported (40). Radiolabeled photoanalogues of pre-

TABLE I
Kinetic constants

Substrate (inhibitor)	K_i	K_m	
	DATFP-FPP	FPP	GGPP
hPFT	0.10 μ M	0.02 μ M	
hPGGT-I	0.018 μ M		
			0.016 μ M

nyltransferase substrates have the potential to identify key features of the protein structure of prenyltransferases. The FPP analogue, [3H]DATFP-GPP, has already been shown to photolabel two other prenyltransferases (22, 41) in addition to the β -subunits of hPFT (5) and hPGGT-I (24). The synthesis of the GGPP analogues, [3H]- and [^{32}P]DATFP-FPP, has now made it possible to also photolabel purified bovine brain (24) and recombinant human PGGT-I. Heavy labeling of the β -subunits of these enzymes, in contrast to the weaker nonspecific labeling of the α -subunits, points to the specificity of the cross-linking procedure. Effective inhibition of labeling of the respective prenyltransferases by their prenyl diphosphate substrates and poor inhibition by the prenyl diphosphate substrate of the other protein prenyltransferase clearly shows that the photoprobe is directed toward the active site or "substrate binding site" and not some other hydrophobic environment on the β -subunit. Therefore, demonstrating that DATFP-FPP is a competitive inhibitor of the natural allylic diphosphate substrates for the protein prenyltransferases and showing that inhibition of labeling of the β -subunits of both hPFT and hPGGT-I is specific for the prenyl diphosphate substrate leads to the conclusion that the β -subunits of these protein prenyltransferases are involved in the specific recognition and binding of the prenyl diphosphate substrate. The mode of association of the prenyl diphosphate with subunits of rab PGGT still remains to be established.

The labeling of the β -subunit with the isoprenoid related probes is consistent with previous photo-cross-linking results which showed that both peptide and protein substrates can interact with the β -subunit of PFT (42, 43). These probes now offer the opportunity to identify specific amino acid residues in the isoprenoid and peptide binding domains of these enzymes. The ^{32}P -labeled photoprobes offer some advantages over the 3H -labeled probes for peptide localization and analysis because they are more readily detectable. In addition, the ^{32}P -labeled probes can be easily prepared because phosphorylation is the last step in the synthesis. Identification of cross-linked amino acid residues would provide potential targets for a variety of

approaches to precisely define critical residues which are involved in catalysis and determining the specificity of isoprenoid substrate binding. Such approaches might include site-directed mutagenesis and the design of other reactive prenyl diphosphate analogues. Since both hPFT and hPGGT-I show a tolerance for alterations in the structure of the ω -isoprene unit when binding prenyl diphosphate analogues, new isoprenoid based analogues might be designed with more effective and site-specific functional groups attached at the ω -terminus. One approach could be to incorporate substituents which are chemically reactive with specific amino acid residues. One can also envision the use of such photoprobes to map the binding sites of other prenyltransferases and enzymes that metabolize prenyl diphosphates. The synthesis of appropriate isoprenoid analogues could bring new perspective to studies on proteins involved in prenylated protein biosynthesis and function, such as COOH-terminal proteases, methyl transferases, and prenylated protein binding proteins.

Acknowledgements—600 MHz nmr DQF-COSY and NOESY experiments were carried out by John West at the Center for Structural Biology, University of Florida. MADLI-MS analysis was done by Huang P. Nguyen. Protein Chemistry Core of ICBR, University of Florida.

REFERENCES

- Casey, P. J., Soleki, P. A., Der, C. J., and Buss, J. E. (1999) *Proc. Natl. Acad. Sci. U. S. A.* 86, 8323-8327
- Finagold, A. A., Schafer, W. R., Rine, J., Whiteway, M., and Tamanoi, F. (1990) *Science* 249, 165-169
- Clarke, S. (1992) *Annu. Rev. Biochem.* 61, 355-386
- Seabra, M. C., Reiss, Y., Casey, P. J., Brown, M. S., and Goldstein, J. L. (1991) *Cell* 65, 429-434
- Omer, C. A., Kral, A. M., Diehl, R. E., Prendergast, G. C., Powers, S., Allen, C. M., Gibbs, J. B., and Kohl, N. E. (1993) *Biochemistry* 32, 5167-5176
- Hancock, J. F., Magee, A. I., Childs, J. E., and Marshall, C. J. (1989) *Cell* 57, 1167-1177
- Maltose, W. A., and Erdman, R. A. (1983) *J. Biol. Chem.* 258, 16168-16172
- Moore, S. L., Schaber, M. D., Mosser, S. D., Rande, E., O'Hara, M. B., Garaky, V. M., Marshall, M. S., Pompilano, D. L., and Gibbs, J. B. (1991) *J. Biol. Chem.* 266, 14603-14610
- Casey, P. J., Thissen, J. A., and Moomaw, J. F. (1991) *Proc. Natl. Acad. Sci. U. S. A.* 88, 3631-3635
- Yokoyama, K., and Gelb, M. H. (1993) *J. Biol. Chem.* 268, 4055-4060
- Yokoyama, K., Goodwin, G. W., Ghomashchi, F., Glomset, J. A., and Gelb, M. H. (1991) *Proc. Natl. Acad. Sci. U. S. A.* 88, 5302-5306
- Andres, D. A., Seabra, M. C., Brown, M. S., Armstrong, S. A., Smeland, T. E., Cremer, F. P. M., and Goldstein, J. L. (1993) *Cell* 73, 1091-1099
- Yamane, H. K., Farnsworth, C. C., Xie, H., Howald, W., Fung, E. K.-K., Clarke, S., Gelb, M. H., and Glomset, J. A. (1990) *Proc. Natl. Acad. Sci. U. S. A.* 87, 5568-5572
- Munby, S. M., Casey, P. J., Gilman, A. G., Gutawski, S., and Sternweis, P. C. (1990) *Proc. Natl. Acad. Sci. U. S. A.* 87, 5873-5877
- Farnsworth, C. C., Kawata, M., Yoshida, Y., Takai, Y., Gelb, M. H., and Glomset, J. A. (1991) *Proc. Natl. Acad. Sci. U. S. A.* 88, 6196-6200
- Jamca, G. L., Goldstein, J. L., Brown, M. S., Rawson, T. E., Somers, T. C., McDowell, R. S., Crowley, C. W., Lucas, E. K., Levinson, A. D., and Marsters, J. C., Jr (1993) *Science* 260, 1937-1942
- Graham, S. L., deSolms, S. J., Giuliani, E. A., Kohl, N. E., Mosser, S. D., Oliff, A. I., Pompilano, D. L., Rande, E., Breslin, M. J., Deana, A. A., Garaky, V. M., Scholz, T. H., Gibbs, J. B., and Smith, R. L. (1994) *J. Med. Chem.* 37, 725-732
- Qian, Y., Blazkovich, A., Saleem, M., Seong, C. M., Wathen, S. P., Hamilton, A. D., and Seba, S. M. (1994) *J. Biol. Chem.* 269, 12410-12413
- Hancock, J. F. (1993) *Curr. Biol.* 3, 770-772
- Tamanoi, F. (1993) *Trends Biol. Sci.* 18, 349-353
- Baba, T., and Allen, C. M. (1988) *Biochemistry* 23, 1312-1322
- Baba, T., Muth, J., and Allen, C. M. (1985) *J. Biol. Chem.* 260, 10467-10475
- Des, N. P., and Allen, C. M. (1991) *Biochem. Biophys. Res. Commun.* 179, 729-735
- Yokoyama, K., McGeary, P., and Gelb, M. H. (1995) *Biochemistry* 34, 1344-1354
- Davieson, V. J., Woodside, A. B., Neal, T. A., Strameler, K. E., Muehlbacher, M., and Poulter, C. D. (1996) *J. Org. Chem.* 61, 4768-4779
- Zhang, F. L., Diehl, R. E., Kohl, N. E., Gibbs, J. B., Giroa, E., Casey, P. J., and Omer, C. A. (1994) *J. Biol. Chem.* 269, 3175-3180
- Umbreit, M., and Sharpless, K. B. (1977) *J. Am. Chem. Soc.* 99, 5526-5528
- Marshall, J. A., Jensen, T. M., and DeHoff, E. S. (1986) *J. Org. Chem.* 51, 4315-4319
- Bhalerao, U. T., and Rapoport, H. (1971) *J. Am. Chem. Soc.* 93, 4835-4840
- Chan, K. C., Jewell, R. A., Nurtung, W. H., and Rapoport, H. (1968) *J. Org. Chem.* 33, 3382-3385
- Holloway, P. W., and Popjak, G. (1967) *Biochem. J.* 104, 57-70
- Farnsworth, C. C., Wolda, S. L., Gelb, M. H., and Glomset, J. A. (1989) *J. Biol. Chem.* 264, 20422-20429
- Joly, A., Popjak, G., and Edwards, P. A. (1991) *J. Biol. Chem.* 266, 13495-13498
- Zhang, F. L., Moomaw, J. F., and Casey, P. J. (1994) *J. Biol. Chem.* 269, 23465-23470
- Schägger, H., and von Jagow, G. (1987) *Anal. Biochem.* 165, 368-379
- Wray, W., Boulakas, T., Wray, V. P., and Hancock, R. (1981) *Anal. Biochem.* 118, 197-203
- Pompilano, D. L., Rande, E., Schaber, M., Mosser, S., Anthony, N., and Gibbs, J. B. (1992) *Biochemistry* 31, 3800-3807
- Brems, D. N., and Rilling, H. C. (1978) *Biochemistry* 18, 860-864
- Allen, C. M. (1985) *Methods Enzymol.* 111, 281-299
- Tareh, L. C., Yan, M., Poulter, C. D., and Sacchettini, J. C. (1994) *Biochemistry* 33, 10671-10677
- Dogdo, O., and Camera, B. (1987) *Biochim. Biophys. Acta* 920, 140-148
- Reiss, Y., Seabra, M. C., Armstrong, S. A., Slaughter, C. A., Goldstein, J. L., and Brown, M. S. (1991) *J. Biol. Chem.* 266, 10672-10677
- Ying, W., Sepp-Lorenzino, L., Cai, K., Aloise, P., and Coleman, P. S. (1994) *J. Biol. Chem.* 269, 470-477
- Leatherbarrow, R. J. (1987) *Enzfleur*. Elsevier-Biosoft, Amsterdam, Holland



α -Cyanocinnamide Derivatives: A New Family of Non-Peptide, Non-Sulfhydryl Inhibitors of Ras Farnesylation

Enrique Poradosu,^a Aviv Gazit,^b Hadas Reuveni^a and Alexander Levitzki^{a,*}

^aDepartment of Biological Chemistry, The Institute of Life Sciences, The Hebrew University of Jerusalem, Jerusalem 91904, Israel

^bDepartment of Organic Chemistry, The Institute of Chemistry, The Hebrew University of Jerusalem, Jerusalem 91904, Israel

Received 2 March 1998; accepted 2 April 1999

Abstract—Farnesylation of Ras and other proteins is required for their membrane attachment and normal function. Here we report on the synthesis of α -cyanocinnamide derivatives, a new family of farnesyltransferase inhibitors. These compounds are nonpeptidic and do not contain sulfhydryl groups. The most potent compound is a pure competitive inhibitor with respect to the Ras protein and mixed competitive with respect to farnesyl diphosphate. Selectivity studies against geranylgeranyltransferase and biological activities of selected compounds are described. © 1999 Published by Elsevier Science Ltd. All rights reserved.

Introduction

The Ras proteins are a class of plasma membrane associated G-proteins that act as a molecular switch in normal and pathogenic mitogenic signalling pathways across the cell membrane. Point mutations in the ras oncogenes which lock the Ras switch in its active GTP-bound state are found in 40% of all cancers.^{1,2} The Ras protein is localized to the inner leaflet of the plasma membrane. Anchoring to the membrane is achieved through a series of post-translational modifications directed by its carboxy terminal CAAX motif (C-cysteine, A-aliphatic, X-methionine or serine), which is farnesylated at the cysteine residue by the protein Ras farnesyl transferase (FT). After a subsequent proteolytic removal of the three C-terminal amino acids the farnesylated cysteine residue is methyl esterified.^{3,4} The initial farnesylation is a prerequisite for all subsequent covalent modifications.⁵

The biological role of Ras prenylation has been extensively studied; the modification of Ras with a specific isoprenoid is required for hSOS promoted guanine nucleotide exchange,⁶ and the activation of Raf-1,⁷ B-Raf,⁸ and ERK.⁹ Moreover, membrane localization of Ras is essential for its normal function and the transforming activity of its oncogenic version.¹⁰ Thus, interfering with the Ras pathway by inhibiting Ras farnesylation and membrane localization was

hypothesized to be a potentially specific chemotherapeutic strategy.

Although biological effects exerted by FT inhibitors were correlated with their ability to abolish Ras membrane anchorage, several lines of evidence suggest that the biological effects of FT inhibitors are mediated by the inhibition of farnesylation of proteins other than Ras, like Rho B.¹¹⁻¹³

Despite the open questions concerning the mechanism of action of FT inhibitors, experimental data obtained in the past four years has clearly demonstrated their biological activity. FT inhibitors cause reversal of Ras induced transformation in intact cells,¹⁴⁻¹⁸ inhibition of Ras tumor growth in nude mice¹⁹⁻²² and tumor regression in Ha-Ras transgenic animals,²³ with minimal toxic effects. These findings strongly support the use of FT inhibitors as potential anticancer drugs.

Analysis of the crystal structure of FT shows that it possesses a bound zinc ion within an open coordination sphere that includes a water molecule, suggesting a catalytic function as opposed to the closed spheres characteristic of structural metal ions. The crystallographic data also indicates that the sulfhydryl group in the CAAX motif is localized in close proximity to the zinc atom and adjacent to the farnesylpyrophosphate α phosphate.²⁴ Accordingly, in CAAX motif peptidic analogues the cysteine residue confers improved potency to the inhibitor.²⁵⁻²⁶ However, the sulfhydryl moiety has been replaced with various degrees of success in various

* Corresponding author.

peptidic derivatives^{16,17,29–34} and is not present in some non-peptide inhibitors.^{35–37}

In this study we report on the synthesis and evaluation of a new class of non-peptide, non-sulphydryl FT inhibitors based on the α -cyano-cinnamide structure. These compounds exhibit FT inhibition activity in vitro and in intact cells. The structure–activity relationship of α -cyano-cinnamide derivatives, selectivity studies of FT versus geranyl–geranyl transferase type I (GGT I) inhibition,^{38,39} and their biological activities are described.

Results and Discussion

α -Cyano-cinnamide derivatives design

With the aim to design non-peptide FT inhibitors lacking a sulphydryl group we first synthesized a series of CAAX peptides in which the cysteine residue was replaced by various groups with different affinities towards Zn^{+2} (data not shown). A direct correlation was observed between the chelating capability to the inhibitory activity towards FT. The best inhibitor of this series was HVFM with an IC_{50} of 12 μM , in agreement with published results in which the cysteine residue in CAAX peptidic analogues was replaced by histidine.²⁹

Since tyrosine kinase inhibitors from the tyrphostin family which are hydroxy derivatives of α -cyanocinnamide were shown to be tyrosine mimics,⁴⁰ we chose as a non-peptidic scaffold the α -cyanocinnamide structure with the assumption that it will potentially mimic the phenylalanine residue in the potent CVFM peptide inhibitor.

α -Cyanocinnamide derivatives were prepared by a straight-forward synthesis (Fig. 1); phenolic aldehydes were reacted with excess α,ω -dibromoalkanes and the monobromo product purified by chromatography. The various thio-analogues were prepared from these bromo compounds and the corresponding mercapto-heterocycles, which were then condensed in the Knoevenagel reaction with aryl cyano-acetamides⁴¹ or benzyl cyano-acetamides (prepared analogously). Yields were not optimized.

The inhibitory activity of a series of compounds based on the α -cyanocinnamide structure substituted with

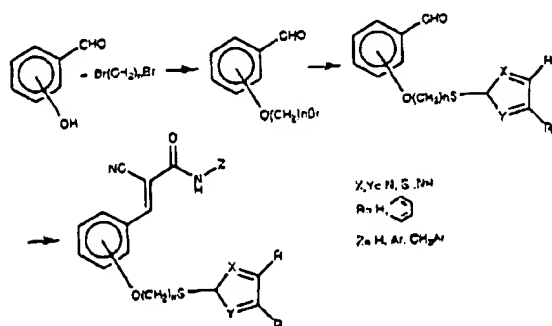


Figure 1. A general scheme for the synthesis of α -cyanocinnamide derivatives.

imidazole and related heterocyclic groups is shown in Table 1. The most effective compound was the imidazole substituted α -cyanocinnamide (3) with an IC_{50} of 11.5 μM .

Next we examined the optimal length of the alkyl linker between the pharmacophore and the cinnamide ring and the optimal position on that ring (Table 2). The most effective analogues had linkers in position *ortho* and *meta* with an optimal length of 3 and 4 methylenes. These inhibitors showed an IC_{50} of 17.5 and 11.5 μM for the imidazole derivatives (compounds 10 and 3, respectively) and 36.6 and 33.3 μM for the benzimidazole analogues (compounds 5 and 2, respectively).

In order to further explore the binding pocket of the inhibitors a phenyl (14) and benzyl (29) derivatives of compound 10 were prepared. While the benzyl ring improved the inhibitory activity twofold (IC_{50} of 10.3 μM) the phenyl ring has a deleterious effect compared to the parental compound (IC_{50} of 162 μM). Further examination of phenyl and benzyl amide derivatives yielded two different families in which the rings were systematically substituted with chemically different groups (Table 3). The most potent compound from this series was 26, which inhibited FT with an IC_{50} of 1.8 μM .

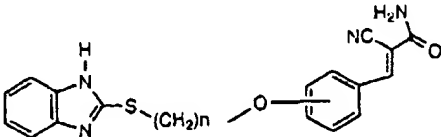
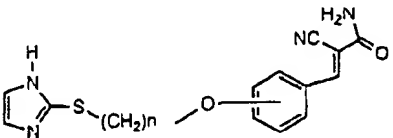
Interestingly, substitutions of different chemical nature in the phenyl ring at position R2 like the polar carboxyl in compound 13 (IC_{50} 12.1 μM) or Cl in compound 12 (IC_{50} 7 μM) gave analogues with similar inhibitory activities (Table 3). Free rotation of the phenyl ring in space suggests the possibility that these substituents are oriented to opposite sites in the same pocket. A similar result was obtained in CAAX non-peptidic analogues.^{42,43}

As a preliminary test of this hypothesis we prepared the phenyl imidazole derivatives with the double substitution

Table 1. Imidazole and related substitutions of α -cyanocinnamide. In vitro IC_{50} s against FT are reported for each compound. Each result represents results of two to four tests. Assays were conducted as described in Experimental

Compound no.	AGR	R	FT IC_{50} (μM)
1	109		500
2	71		33.3
3	124		11.5

Table 2. Optimization of linker positioning and length in benzimidazole and imidazole derivatives of α -cyanocinnamide. In vitro IC_{50} s against FT are reported for each compound. Each result represents results of two to four tests. Assays were conducted as described in Experimental

			
Compound no.	AGR	n (ortho)	FT IC_{50} (μ M)
4	93	2	153.1
5	85	3	36.6
6	94	4	115.1
Compound no.	AGR	n (meta)	FT IC_{50} (μ M)
7	87	2	112.3
8	79	3	31.6
2	71	4	33.3
9	74	5	100
			
Compound no.	AGR	n (ortho)	FT IC_{50} (μ M)
10	123	3	17.5
Compound no.	AGR	n (meta)	FT IC_{50} (μ M)
3	124	4	11.5

3,4 and 3,5-chloro,carboxy. These compounds inhibited the FT reaction with an IC_{50} of 50.6 and 40 μ M (18 and 25, respectively) (Table 3). This negative result implies that the geometry of the hydrophobic and carboxylic subpockets within this cleft requires a much more flexible structure than the phenyl ring to reach both sites simultaneously. Further work is in progress to examine this hypothesis.

Although compound 10, which is the core of the inhibitors described, was designed to mimic the HVF portion of the HVFM peptide, the molecular structure of the FT inhibitors developed differ markedly from the CAAX motif. Therefore we studied the kinetics of the FT inhibition by the most potent in vitro inhibitor, 26. Inhibition modalities other than Ras competition would indicate a binding site different from the catalytic pocket to which the inhibitors were targeted based on theoretical considerations. Compound 26 is a pure competitive inhibitor of FT with respect to the Ras protein and mixed competitive with respect to farnesyl pyrophosphate, as shown by the double reciprocal plots ($1/v$ versus $1/[S]$) and the slope replots (slope versus $[I]$) (Fig. 2). The intersection of the reciprocal plots below the $1/FPP$ axis means that the constant affecting K_i and K_{FPP} resulting from the mutual influence between FPP

and the inhibitor is <1 . The inhibition pattern of CAAX alternative substrates was found to be pure competitive with respect to Ras and non-competitive with respect to FPP.⁴⁴ Although the mechanism of inhibition of compound 26 implies a different space orientation within the active site than CAAX alternative substrates it indicates that the inhibitor binds to the catalytic pocket as expected.

Inhibition of FT versus GGT I

Early studies showed that the closely FT related prenyl transferase GGT I transfers a geranyl-geranyl group to CAAX containing sequences where X is preferably leucine or phenylalanine.^{45–47} Since geranyl-geranylation of normal proteins is 5–10 times more common than farnesylation,^{25,48,49} the common assumption was that a compound displaying a strong selectivity towards FT will have the advantage of reduced side effects than a more general prenylation inhibitor. However, the discovery that in cells resistant to FT inhibitors the K- and N-Ras isoforms become geranyl-geranylated by GGT I,^{50,51} and the ability of geranyl-geranylation inhibitors to block platelet-derived and epidermal growth factor dependent tyrosine phosphorylation,⁵² and to block cells at G0/G1^{53,54} has aroused new interest in this more ubiquitous prenyl transferase reaction.

A selectivity study of some FT inhibitors described here was performed by testing their inhibitory activity towards GGT I (Table 4). Most of the compounds tested inhibit both enzymes in vitro at comparable concentrations, (0.2–5 selectivity factor), with the highest factor of selectivity towards FT (selectivity factor = 33) observed for compound 26. Similar to other series of FT inhibitors^{35,55,56} selectivity was achieved despite the lack of a structural element clearly corresponding to the specificity determining X residue in the CAAX motif.

Biological results

Compounds 13, 26, and 29 were tested for their ability to inhibit protein prenylation in intact cells. Compounds 13 and 26 completely inhibit Ras farnesylation at a concentration of 120 μ M, Rap-1 geranyl-geranylation was not affected at the same concentrations (Fig. 3). The effect of these compounds on cell growth was assessed on a LIM1899 colon carcinoma cell line expressing a mutant K-Ras(Gly¹²→Cys¹²), NIH3T3 and v-H-Ras transformed NIH3T3 cell lines (Table 5). The IC_{50} s obtained (70–180 μ M) are in correlation with the concentrations required for FT inhibition in whole cells. Previously it was reported that in K-Ras transformed cells resistance to FT inhibitors could be attributed to K-Ras geranyl-geranylation,⁵⁰ however, LIM1899 cells which express a mutated K-Ras were inhibited to the same extent as NIH3T3 cells transformed with v-H-Ras and normal NIH3T3 cells (Table 5). Compound 26 (AGR129) also inhibited colony formation in soft agar of v-H-Ras transformed NIH3T3 cells (Fig. 4). At 100 μ M, the concentration required for complete inhibition of FT in whole cells, a 75% inhibition of colony formation was observed.

Conclusions

Imidazole derivatives of α -cyano-cinnamide constitute a novel class of non-peptidic, non-sulphydryl FT inhibitors. The most potent inhibitors of this class inhibit FT with IC_{50} values at the low micromolar range and are targeted to the catalytic site of the FT enzyme. These compounds inhibit both the farnesylation of Ras in intact cells and the cell growth of cells harboring mutated v-H-Ras and K-Ras(Gly¹²→Cys¹²).

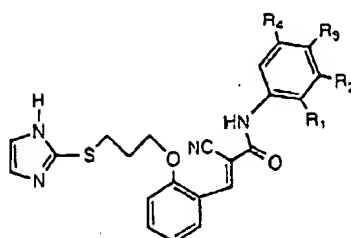
Experimental

General chemical procedures

All starting materials were purchased from Aldrich. NMR spectra were recorded on a Bruker 300 pulsed FT spectrometer. Chemical shifts are in ppm relative to TMS internal standard. Mass spectra were recorded with a MAT311 instrument. Combustion analyses for all new compounds were within 0.4% of the theoretical value. Work up means adding to water, extracting with

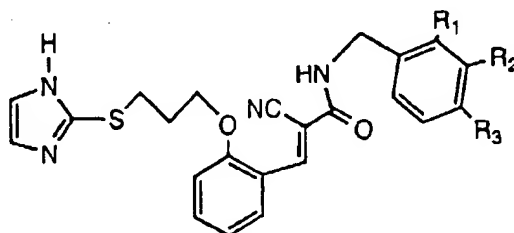
Table 3. In vitro FT inhibition by phenyl (A) and benzyl (B) derivatives of AGR128 (compound 10). In vitro IC_{50} s against FT are reported for each compound. Each result represents results of two to four tests. Assays were conducted as described in Experimental

(A)



Compound no.	AGR	R1	R2	R3	R4	FT IC_{50} (μ M)
11	139	H	CH ₃	H	H	72.6
12	141	H	Cl	H	H	7
13	142	H	COOH	H	H	12.1
14	144	H	H	H	H	162
15	154	H	H	COOCH ₂ CH ₃	H	> 300
16	158	H	H	COOH	H	16.3
17	163	H	Cl	COOCH ₃	H	58.4
18	169	H	Cl	COOH	H	50.5
19	173	H	COOCH ₃	H	COOCH ₃	> 64
20	180			H	H	13.6
21	182	pH	H	H	H	26
22	189	H	NH ₂	H	COOCH ₃	> 128
23	190	H	COOCH ₃	OH	H	> 128
24	196	H	Cl	H	COOCH ₃	> 64
25	197	H	Cl	H	COOH	40

(B)



Compound no.	AGR	R1	R2	R3	FT IC_{50} (μ M)
26	129	H	Cl	H	1.8
27	130	H	H	Cl	12.8
28	137	Cl	H	H	4.3
29	143	H	H	H	10.6
30	146	H	OCH ₃	OCH ₃	21.5
31	147	H	Cl	Cl	23.6
32	148	OCH ₃	H	OCH ₃	20.5

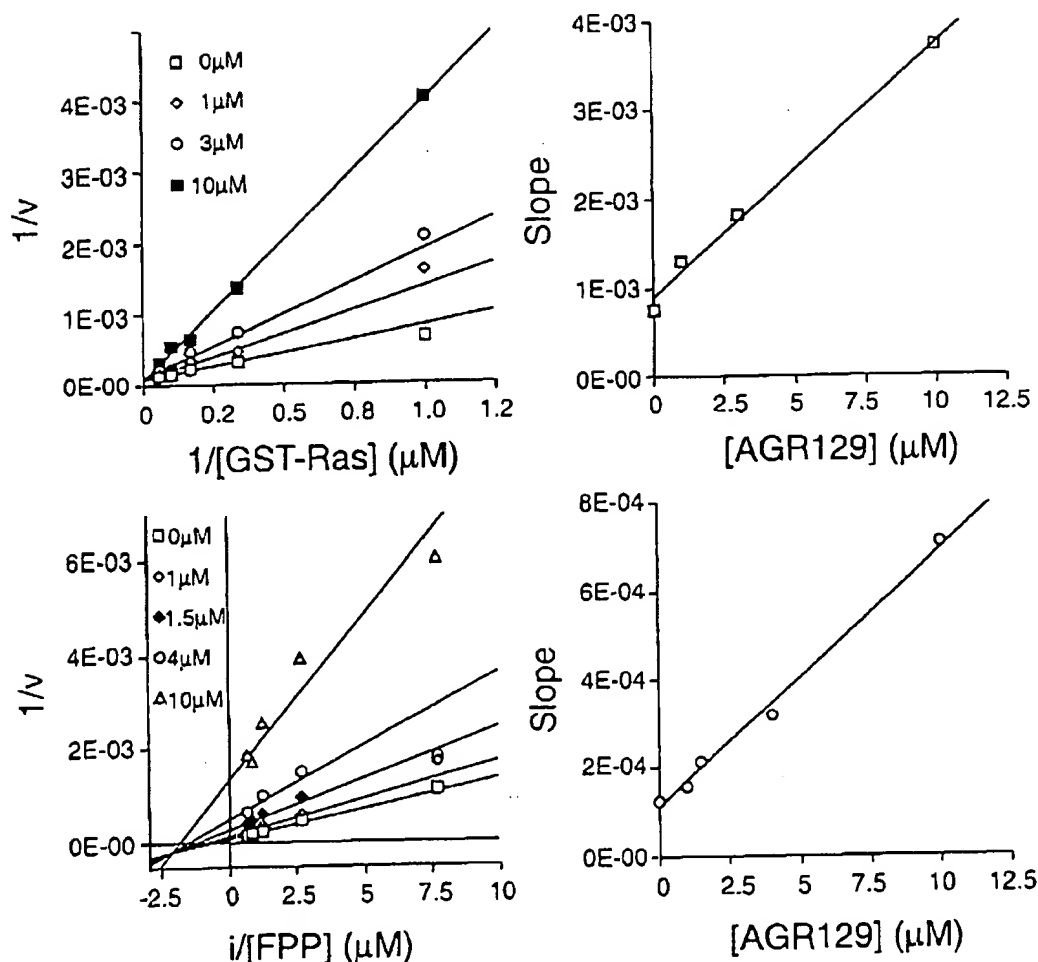


Figure 2. Kinetics of inhibition of the FT reaction by AGR129. The activity of FT was determined as described in Experimental except that the reaction was performed in the presence of 1, 3, 6, 10, and 18 μM of GST-Ras, and a fixed concentration of 0.5 μM FPP, or in the presence of 0.1, 0.3, 0.5, 1, and 1.8 μM of FPP and a fixed concentration of 5 μM GST-Ras. Initial reaction velocity (v) is expressed as pmol of farnesylated GST-Ras/h/mg enzyme. Families of double reciprocal plots and their respective slope replots are shown. AGR129 concentrations were as indicated in the figure.

dichloromethane (or with ethyl acetate when indicated), drying the organic phase and evaporating to dryness.

Compound 1. (a). Bromo aldehyde. 25 g, 0.2 M, 3-hydroxy benzaldehyde, 70 g, 0.32 M, 1,4-dibromo butane, and 17 g KOH in 150 mL ethanol were refluxed 18 h. Work up and chromatography (silica gel, 70–230 mesh, elution with CH_2Cl_2) gave 10.3 g, 20% yield, white oil. NMR (CDCl_3) δ 9.97 (1H, s, CHO), 7.40 (3H, m), 7.18 (1H, m), 4.06 (2H, t, $J=6.0$ Hz), 3.50 (2H, t, $J=6.0$ Hz), 2.0 (4H, m). (b) Benzothiazole aldehyde. 0.5 g, 2.2 mM, of the above bromo aldehyde, 0.38 g, 2.3 mM, 2-mercapto benzothiazole, and 0.2 g KOH in 50 mL ethanol were stirred 19 h at room temperature. Work up (HCl and EtAc) and chromatography gave after titration with benzene-hexane 0.11 g, 37% yield, white solid, mp 104°C. NMR (CDCl_3) δ 9.95 (1H, s, CHO), 7.60 (4H, m), 7.40 (3H, m), 7.22 (1H, m), 4.03 (2H, t, $J=6.0$ Hz), 3.53 (2H, t, $J=6.0$ Hz), 2.10 (4H, m). (c) 170 mg, 0.5 mM, 1b, 50 mg, 0.6 mM, cyano acetamide, and 15 mg β -alanine in 15 mL ethanol were refluxed 4 h.

Table 4. A comparison of FT and GGT I in vitro inhibitory activity by selected inhibitors. Selectivity factor is expressed as the ratio of the GGT I to FT inhibitory activities

Compound no.	FT IC_{50} (μM)	GGT I IC_{50} (μM)	Selectivity factor
3	11.5	53.6	4.7
12	7	9.2	1.3
13	12.1	42.6	3.5
16	16.3	7.2	0.4
21	26	6.7	0.3
25	40	7.5	0.2
26	1.8	59.3	33
27	12.8	19.5	1.5
28	4.3	15.8	3.7
29	10.6	19.3	1.8

Evaporation and recrystallization from benzene gave 125 mg, 61% yield, white solid, mp 175°C. NMR ($\text{DMSO}-d_6$) δ 8.22 (1H, s, vinyl), 7.65 (4H, m), 7.30 (4H, m), 4.10 (2H, t, $J=5.8$ Hz), 3.68 (2H, t, $J=5.8$ Hz), 2.12 (4H, m).

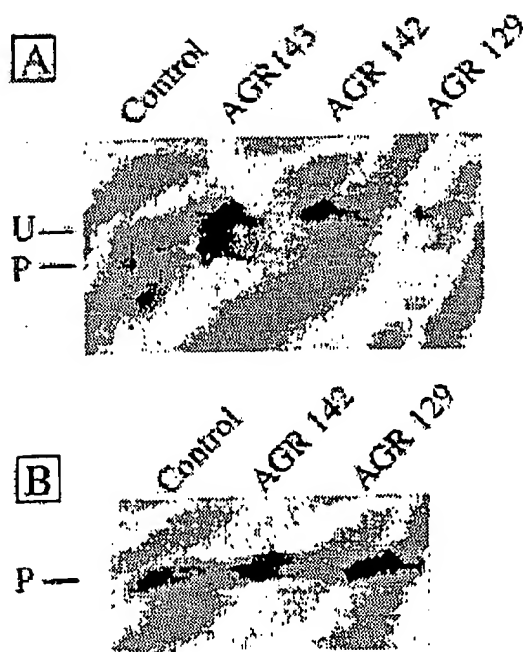


Figure 3. Effect of α -cyanocinnamide derivatives on post-translational processing of Ras and Rap1A/K-Rev. v-H-Ras transformed NIH3T3 cells were treated with the indicated compounds at a concentration of 120 μ M for 48 h or vehicle alone (control). Cell extracts were separated by SDS-Page (40 μ g of protein/lane) and visualized by western blot. (A) v-H-Ras; (B) Rap1A. P, phosphorylated proteins; U, unphosphorylated protein. Compound 13 = AGR142, compound 29 = AGR142, compound 26 = AGR129.

Table 5. Cell growth inhibition. Inhibitions are expressed as IC_{50} s in μ M. (3T3 = NIH3T3, vRas = v-H-Ras transformed NIH3T3, LIM = LIM1899)

Compound no.	3T3	vRas	LIM
13	98	80	73
26	186	152	100

Compound 2. (a). 1.6 g, 6.2 mM, bromo aldehyde 1a, 1 g, 6.5 mM, 2-mercapto benzimidazole, and 1 g, 10 mM, Et_3N in 30 mL ethanol were stirred 26 h at room temperature. Work up and recrystallization from benzene gave 0.6 g, 30% yield, viscous solid. NMR (acetone- d_6) δ 10.0 (1H, s, CHO), 7.50 (4H, m), 7.25 (4H, m), 4.18 (2H, t, $J=6.0$ Hz), 3.86 (2H, t, $J=6.0$ Hz), 2.2 (4H, m). (b) 310 mg, 0.95 mM, 2a, 84 mg, 1 mM cyano acetamide, and 15 mg β -alanine in 20 mL ethanol were refluxed 8 h. Evaporation and trituration in acetone-hexane gave 200 mg light-yellow solid, 54% yield, mp 154°C. NMR (acetone- d_6) δ 8.28 (1H, s, vinyl), 7.63 (4H, m), 7.30 (4H, m), 4.15 (2H, t, $J=6.0$ Hz), 3.72 (2H, t, $J=6.0$ Hz), 2.10 (4H, m).

Compound 3. (a). 1.6 g, 6.2 mM, 1a, 0.67 g, 6.7 mM, 2-mercapto imidazole, and 0.5 KOH in 30 mL ethanol were stirred 20 h at ambient temperature. Work up and chromatography gave after trituration from acetone-hexane 540 mg, 32% yield, white solid, mp 165°C. NMR ($CDCl_3$) δ 11.17 (1H, br.s, NH), 9.93 (1H, s, CHO), 7.4 (3H, m), 7.15 (2H, s, imidazole), 7.10 (1H,

m), 3.93 (2H, t, $J=5.7$ Hz), 3.05 (2H, t, $J=5.7$ Hz), 1.60 (4H, m). (b) 260 mg, 0.93 mM, 3a, 84 mg, 1 mM, cyano acetamide, and 18 mg β -alanine in 20 mL ethanol were refluxed 3 h. Work up and trituration with acetone-hexane gave 150 mg, 47% yield, white solid, mp 162°C. NMR (acetone- d_6) δ 8.18 (1H, s, vinyl), 7.45 (3H, m), 7.12 (2H, s), 7.08 (1H, m), 3.90 (2H, t, $J=5.8$ Hz), 3.10 (2H, t, $J=5.8$ Hz), 1.70 (4H, m).

Compound 4. (a). Bromo aldehyde, 7 g, 57 mM, salicyl aldehyde, 15 g, 80 mM, dibromo ethane, and 7 g KOH in 30 mL water and 50 mL ethanol were refluxed 20 h. Work up and chromatography gave 0.83 g, 6% yield, white oil. NMR ($CDCl_3$) δ 9.95 (1H, s, CHO), 7.40 (4H, m), 4.33 (2H, t, $J=6.0$ Hz), 3.62 (2H, t, $J=6.0$ Hz). (b) 0.8 g, 3.5 mM, 4a, 0.5 g, 3.3 mM, 2-mercapto benzimidazole, and 0.2 g KOH in 30 mL ethanol were stirred at room temperature 14 h. Work up and trituration in CH_2Cl_2 -hexane gave 0.45 g, 44% yield, oily solid. NMR (acetone- d_6) δ 9.93 (1H, s, CHO), 7.53 (4H, m), 7.30 (4H, m), 4.45 (2H, t, $J=6.0$ Hz), 3.72 (2H, t, $J=6.0$ Hz). (c) 400 mg, 1.3 mM, 4b, 130 mg, 1.5 mM, cyano acetamide, and 18 mg β -alanine in 20 mL ethanol were refluxed 3 h. Work up and trituration with acetone-hexane gave 120 mg, 25% yield, white solid, mp 212°C. NMR (acetone- d_6) δ 8.26 (1H, s, vinyl), 7.45 (4H, m), 7.30 (4H, m), 4.40 (2H, t, $J=5.8$ Hz), 3.60 (2H, t, $J=5.8$ Hz).

Compound 5. (a). Bromo aldehyde, 7 g, 57 mM, salicyl aldehyde, 16 g, 79 mM, 1,3-dibromo propane, and 7 g KOH in 30 mL water and 50 mL ethanol were refluxed 24 h. Work up and chromatography gave 1.3 g, 9% yield, white oil. NMR ($CDCl_3$) δ 9.95 (1H, s, CHO), 7.83 (1H, m), 7.55 (1H, m), 7.06 (2H, m), 4.24 (2H, t, $J=6.0$ Hz), 3.62 (2H, t, $J=6.0$ Hz), 2.40 (2H, quint, $J=6.0$ Hz). (b) 0.45 g, 1.8 mM, 5a, 0.2 g, 1.5 mM, 2-mercapto benzimidazole, and 0.2 g KOH in 30 mL ethanol were stirred at room temperature 30 h. Work up and trituration in CH_2Cl_2 -hexane gave 0.29 g, 61% yield, white solid, mp 168°C. NMR (acetone- d_6) δ 9.95 (1H, s, CHO), 7.53 (4H, m), 7.30 (4H, m), 4.45 (2H, t, $J=6.0$ Hz), 3.72 (2H, t, $J=6.0$ Hz), 2.30 (2H, quint., $J=6.0$ Hz). (c) 160 mg, 0.5 mM, 5b, 45 mg, 0.5 mM, cyano acetamide and 5 mg β -alanine in 20 mL ethanol were refluxed 3 h. Work up and chromatography gave 40 mg, 21% yield, white solid, mp 77°C. NMR (acetone- d_6) δ 8.24 (1H, s, vinyl), 7.48 (4H, m), 7.36 (4H, m), 4.40 (2H, t, $J=5.8$ Hz), 3.60 (2H, t, $J=5.8$ Hz), 2.30 (2H, quint., $J=6.0$ Hz).

Compound 6. (a). Bromo aldehyde, 7 g, 57 mM, salicyl aldehyde, 15 g, 70 mM, 1,4-dibromo butane, and 7 g KOH in 30 mL water and 40 mL ethanol were refluxed 24 h. Work up and chromatography gave 0.76 g, 5% yield, white oil. NMR ($CDCl_3$) δ 9.95 (1H, s, CHO), 7.42 (4H, m), 4.06 (2H, t, $J=6.0$ Hz), 3.52 (2H, t, $J=6.0$ Hz), 2.0 (4H, m). (b) 0.73 g, 2.8 mM, 6a, 0.4 g, 2.7 mM, 2-mercapto benzimidazole, and 0.2 g KOH in 30 mL ethanol were stirred at room temperature 14 h. Work up and trituration in CH_2Cl_2 -hexane gave 0.6 g, 65% yield, white solid, mp 68°C. NMR (acetone- d_6) δ 9.95 (1H, s, CHO), 7.53 (4H, m), 7.31 (4H, m), 4.44 (2H, t, $J=6.0$ Hz), 3.70 (2H, t, $J=6.0$ Hz), 2.30 (2H, m).

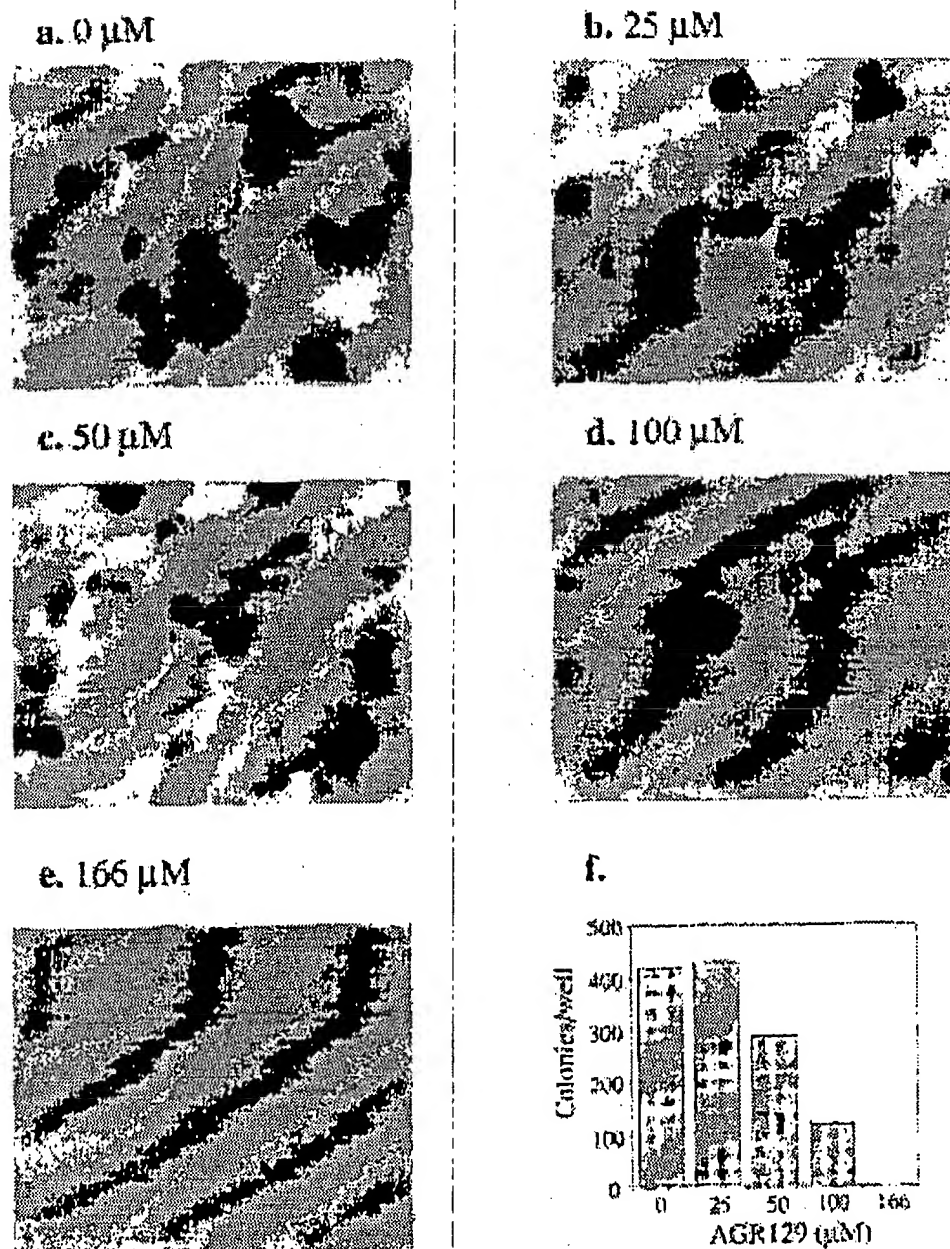


Figure 4. Inhibition of colony formation in soft agar by AGR129 (compound 26). v-H-Ras transformed NIH3T3 cells were seeded on a 96-well plate (3500 cells/well) in soft agar (see Materials and Methods). Serial dilutions of the inhibitor were applied in the growth medium from the top. After 12 days the colonies were stained with MTT, counted in the microscope and photographed. (a) 0 μM, (b) 25 μM, (c) 50 μM, (d) 100 μM, (e) 166 μM, (f) number of colonies per well plotted against the concentration of the inhibitor.

(c) 400 mg, 1.2 mM, 6b, 130 mg, 1.5 mM, cyano acetamide, and 10 mg β-alanine in 20 mL ethanol were refluxed 3 h. Work up and chromatography gave 120 mg, 25% yield, white solid, mp 138°C. NMR (acetone- d_6) δ 8.28 (1H, s, vinyl), 7.48 (4H, m), 7.36 (4H, m), 4.40 (2H, t, J = 5.8 Hz), 3.60 (2H, t, J = 5.8 Hz), 2.34 (2H, m)

Compound 7. (a). Bromo aldehyde, 4.9 g, 40 mM, 3-hydroxy benzaldehyde, 12.2 g, 65 mM, 1,2-dibromo ethane, and 5 g KOH in 40 mL water and 40 mL ethanol were refluxed 24 h. Work up and chromatography gave 1.05 g, 11% yield, white oil. NMR ($CDCl_3$) δ 9.97 (1H, s,

CHO), 7.42 (3H, m), 7.20 (1H, m), 4.35 (2H, t, J = 6.0 Hz), 3.66 (2H, t, J = 6.0 Hz). (b) 0.43 g, 2.0 mM, 7a, 0.25 g, 1.6 mM, 2-mercapto benzimidazole, and 0.2 g KOH in 30 mL ethanol were stirred at room temperature 30 h. Work up and trituration in CH_2Cl_2 -hexane gave 0.115 g, 24% yield, white solid, mp 164°C. NMR (acetone- d_6) δ 9.95 (1H, s, CHO), 7.53 (3H, m), 7.31 (4H, m), 7.15 (1H, m), 4.44 (2H, t, J = 6.0 Hz), 3.70 (2H, t, J = 6.0 Hz). (c) 105 mg, 0.35 mM, 7b, 30 mg, 1.5 mM, cyano acetamide, and 5 mg β-alanine in 20 mL ethanol were refluxed 6 h. Work up and chromatography gave 40 mg, 31% yield, white solid, mp 121°C. NMR

(acetone- d_6) δ 8.28 (1H, s, vinyl), 7.50 (3H, m), 7.38 (4H, m), 7.20 (1H, m), 4.40 (2H, t, $J=5.9$ Hz), 3.61 (2H, t, $J=5.9$ Hz).

Compound 8. (a). Bromo aldehyde, 5.1 g, 42 mM, 3-hydroxy benzaldehyde, 14 g, 69 mM, 1,3-dibromo propane, and 5 g KOH in 60 mL water and 50 mL ethanol were refluxed 18 h. Work up and chromatography gave 4.3 g, 33% yield, white oil. NMR ($CDCl_3$) δ 9.97 (1H, s, CHO), 7.45 (3H, m), 7.18 (1H, m), 4.16 (2H, t, $J=6.0$ Hz), 3.62 (2H, t, $J=6.0$ Hz), 2.34 (2H, quint., $J=6.0$ Hz). (b) 1.5 g, 6.2 mM, 8a, 0.9 g, 6.0 mM, 2-mercapto benzimidazole, and 0.2 g KOH in 30 mL ethanol were stirred at room temperature 26 h. Work up and chromatography gave 0.29 g, 24% yield, viscous oil. NMR (acetone- d_6) δ 9.95 (1H, s, CHO), 7.53 (3H, m), 7.30 (4H, m), 7.25 (1H, m), 4.43 (2H, t, $J=6.0$ Hz), 3.74 (2H, t, $J=6.0$ Hz), 2.30 (2H, quint., $J=6.0$ Hz). (c) 300 mg, 0.96 mM, 8b, 90 mg, 1.07 mM, cyano acetamide, and 5 mg β -alanine in 20 mL ethanol were refluxed 3 h. Workup and trituration in CH_2Cl_2 -hexane gave 160 mg, 44% yield, white solid, mp 132°C. NMR (acetone- d_6) δ 8.20 (1H, s, vinyl), 7.48 (3H, m), 7.36 (4H, m), 7.19 (1H, m), 4.40 (2H, t, $J=5.8$ Hz), 3.60 (2H, t, $J=5.8$ Hz), 2.30 (2H, quint., $J=5.8$ Hz).

Compound 9. (a). Bromo aldehyde, 4.9 g, 40 mM, 3-hydroxy benzaldehyde, 12.6 g, 55 mM, 1,5-dibromo pentane, and 5 g KOH in 40 mL water and 40 mL ethanol were refluxed 20 h. Workup and chromatography gave 2.7 g, 25% yield, white oil. NMR ($CDCl_3$) δ 9.97 (1H, s, CHO), 7.40 (3H, m), 7.18 (1H, m), 4.03 (2H, t, $J=6.0$ Hz), 3.44 (2H, t, $J=6.0$ Hz), 2.0 (4H, m), 1.7 (2H, m). (b) 1.3 g, 5.0 mM, 9a, 0.6 g, 4.0 mM, 2-mercapto benzimidazole, and 0.3 g KOH in 30 mL ethanol were stirred at room temperature 23 h. Workup and chromatography gave 0.5 g, 29% yield, viscous oil. NMR (acetone- d_6) δ 9.95 (1H, s, CHO), 7.47 (3H, m), 7.30 (4H, m), 7.20 (1H, m), 4.43 (2H, t, $J=6.0$ Hz), 3.54 (2H, t, $J=6.0$ Hz), 2.20 (4H, m), 1.85 (2H, m). (c) 250 mg, 0.73 mM, 9b, 67 mg, 0.8 mM, cyano acetamide, and 5 mg β -alanine in 20 mL ethanol were refluxed 8 h. Work up and trituration in CH_2Cl_2 -hexane gave 195 mg, 65% yield, white solid, mp 82°C. NMR (acetone- d_6) δ 8.25 (1H, s, vinyl), 7.48 (3H, m), 7.36 (4H, m), 7.19 (1H, m), 4.40 (2H, t, $J=5.8$ Hz), 3.60 (2H, t, $J=5.8$ Hz), 2.20 (4H, m), 1.90 (2H, m).

Compound 10. (a). 0.8 g, 3.3 mM, 5a, 0.32 g, 3.2 mM, 2-mercapto imidazole, and 0.2 KOH in 30 mL ethanol were stirred 20 h at ambient temperature. Work up and chromatography gave after trituration from acetone hexane 356 mg, 43% yield, white solid, mp 88°C. NMR ($CDCl_3$) δ 10.4 (1H, s, CHO), 7.80 (1H, d, $J=7.8$ Hz), 7.54 (1H, t), 7.10 (2H, s, imidazole), 7.04 (1H, t, $J=7.5$ Hz), 6.96 (1H, d, $J=8.4$ Hz), 4.22 (2H, t, $J=6.0$ Hz), 3.24 (2H, t, $J=6.0$ Hz), 2.22 (2H, quint., $J=6.0$ Hz). (b) 45 mg, 0.17 mM, 3a, 20 mg, 0.24 mM, cyano acetamide, and 4 mg β -alanine in 20 mL ethanol were refluxed 4 h. Workup and trituration with acetone-hexane gave 44 mg, 80% yield, white solid, mp 164°C. NMR (acetone- d_6) δ 9.0 (1H, s, vinyl), 8.4 (1H, d, $J=8.2$ Hz), 7.50 (1H, t, $J=7.8$ Hz), 7.10 (1H, m), 7.07 (2H, s, imidazole), 6.93

(1H, m), 4.16 (2H, t, $J=6.0$ Hz) 3.28 (2H, t, $J=6.0$ Hz), 2.19 (2H, quint., $J=6.0$ Hz).

Compounds 11–32. These compounds were prepared from the imidazole aldehyde 5a and the appropriate aryl or benzyl cyano acetamide. One illustrating example is given to each followed by data to the analogues of its group.

Aryl analogues 11–25

Compound 12. (a). 4 g, 31 mM, 3-Cl aniline, and 4.7 g, 47 mM, methyl cyanoacetate were heated at 120°C without solvent at open flask, for 15 h, the cooled reaction was chromatographed directly (silica gel, 70–230 mesh, elution with dichloromethane) to give 0.92 g, 15% yield, white solid, mp 132°C. NMR (acetone- d_6) δ 7.84 (1H, m), 7.40 (2H, m), 7.16 (1H, m), 3.85 (2H, s). (b) 41 mg, 0.156 mM, 5a, 31 mg, 0.16 mM, 12a, and 6 mg β -alanine in 20 mL ethanol were refluxed 4 h. Evaporation and trituration in CH_2Cl_2 -hexane gave 60 mg, 87% yield, light-yellow solid, mp 152°C. NMR (acetone- d_6) δ 9.06 (1H, s, vinyl), 8.25 (1H, m), 7.82 (1H, m), 7.5–7.0 (7H, m), 7.10 (2H, s, imidazole), 4.19 (2H, t, $J=6.0$ Hz), 3.30 (2H, t, $J=6.0$ Hz), 2.22 (2H, quint., $J=6.0$ Hz). MS m/e 438, 440 (M^+ , 12, 4%), 312 ($M-NHAr$, 14), 193 (20), 127 (100).

N-Aryl cyano acetamides. Compound, yield (%), mp (°C). 11, 19, 127, 13, 25, 256, 14, 17, 193, 15, 17, 138, 16, 30, 254, 17, 25, 178, 18, 30, 222, 19, 47, 132, 20, 6, 138, 21, 7, 158, 22, 7, 112, 23, 5, 127, 24, 30, 187, 25, 13, 236.

Compounds 11–25. Compound, yield (%), mp (°C). 11, 44, 148, 13, 60, 214, 14, 90, 182, 15, 92, 117, 16, 55, 215, 17, 66, 158, 18, 44, 148, 19, 97, 173, 20, 95, 197, 21, 84, 159, 22, 43, 133, 23, 50, 145, 24, 38, 170, 25, 42, 192.

Benzyl analogues 26–32

Compound 29. (a). 15 mL, 0.14 M, benzyl amine, and 13 mL, 0.14 M, methyl cyanoacetate were heated at 120°C without solvent at open flask, for 16 h, the cooled reaction was chromatographed directly (silica gel, 70–230 mesh, elution with dichloromethane) to give 9.4 g, 38 yield, white solid, mp 132°C. NMR ($CDCl_3$) δ 7.4 (5H, m), 4.47 (2H, d, $J=6.0$ Hz), 3.38 (2H, s). (b) 63 mg, 0.24 mM, 5a, 46 mg, 0.26 mM, 29a, and 6 mg β -alanine in 20 mL ethanol were refluxed 4 h. Evaporation and trituration in CH_2Cl_2 -hexane gave 36 mg, 37% yield, light-yellow solid, mp 132°C. NMR (acetone- d_6) δ 9.00 (1H, s, vinyl), 8.15 (1H, m), 7.82 (1H, m), 7.5–7.0 (7H, m), 7.12 (2H, s, imidazole), 4.52 (2H, d, $J=5.8$ Hz), 4.24 (2H, t, $J=6.0$ Hz), 3.32 (2H, t, $J=6.0$ Hz), 2.26 (2H, quint., $J=6.0$ Hz).

N-Benzyl cyano acetamides. Compound, yield (%), mp (°C). 26, 80, 96, 27, 90, 115, 28, 51, 98, 30, 96, 133, 31, 85, 126, 32, 81, 134.

Compounds 26–32. Compound, yield (%), mp (°C). 26, 43, 172, 27, 57, 147, 28, 53, oil, 30, 47, 141, 31, 41, 89, 32, 58, 111.

Biological assays

FT and GGT I inhibition assays and protein processing assay in intact cells were conducted as described.⁵⁷ Kinetic assays were performed in the same way as the inhibition assays except for adding serial dilutions of the substrates as indicated in the figure legend.

Cell growth inhibition assay. NIH3T3, v-H-Ras transformed NIH3T3 and LIM1899⁵⁸ were seeded in 96-well plates (2000 cells/well), after incubation overnight serial dilutions of the inhibitors were added. Medium and inhibitor solution were replaced every 24 h. After growing the cells for 3 days they were fixed by adding glutaraldehyde to a final concentration of 0.5%. Plates were washed with DDW, 200 L/well³ and borate buffer, pH 8.5, 0.1 M, 200 L/well. Plates were incubated for 60 min at room temperatures with methylene blue 1%, 100 mL/well, in borate buffer (pH 8.5, 0.1 M) and washed in DDW until background was cleared. After drying the dye was dissolved with 200 mL HCl 0.1 M and the OD was measured in a plate reader at 620 nm.

Soft agar assay. Each well of a 96-well tissue culture plate was coated with 100 μ L of bottom agar mixture (DMEM, 10% FCS and 1% agarose). v-H-Ras transformed NIH3T3 cells were suspended in top agar mixture (DMEM, 10% FCS, 0.3% agarose, 70,000 cells/mL), and seeded in 96-well plates (3500 cells/well) on top of the base layer. Serial dilutions of the inhibitors were added in 50 μ L medium (DMEM, 10% FCS) on top. Plates were incubated for 12 days in a humidified 37°C incubator. At the end point 25 μ L MTT (5 mg/mL in PBS) was added and the plates were incubated at 37°C for an additional 4 h. The upper solution was washed with PBS and colored colonies were counted under a light microscope, magnification $\times 100$. Colonies from four fields of 2.5 \times 2 mm from each duplicate well were counted and the average number of colonies per well was calculated. Subsequently 100 μ L of solubilization solution (20% SDS, 2% acetic acid, 25 mM HCl, 50% dimethylformamide) was added and the plate was incubated in a sealed container overnight, absorbance was read at 570 nm with a reference wavelength of 630 nm using a ELISA plate reader to account for possible effects on colony size.

References

1. Boss, J. L. *Cancer Res.* 1989, 49, 4682.
2. Barbacid, M. *Annu. Rev. Biochem.* 1987, 56, 779.
3. Clarke, S. *Annu. Rev. Biochem.* 1992, 61, 355.
4. Casey, P. J. *Curr. Opin. Cell Biol.* 1994, 6, 219.
5. Hancock, J. F. *Curr. Biol.* 1993, 3, 770.
6. Porfiri, E.; Evans, T.; Chardin, P.; Hancock, J. F. *J. Biol. Chem.* 1994, 269, 22672.
7. Kikuchi, A.; Williams, L. T. *J. Biol. Chem.* 1994, 269, 20054.
8. Okada, T.; Masuda, T.; Shinkai, M.; Kariya, K.-I.; Kataoka, T. *J. Biol. Chem.* 1996, 271, 4671.
9. Itoh, T.; Kaibuchi, K.; Masuda, T.; Yamamoto, T.; Matsuura, Y.; Mueda, A.; Shimizu, K.; Takai, Y. *J. Biol. Chem.* 1993, 268, 3025.
10. Kato, K.; Cox, A. D.; Hisaka, M. M.; Graham, S. M.; Buss, J. E.; Der, C. J. *Proc. Natl. Acad. Sci. USA* 1992, 89, 6403.
11. Prendergast, G. C.; Davide, J. P.; deSolms, S. J.; Giuliani, E. A.; Graham, S. L.; Gibbs, J. B.; Oliff, A.; Kohl, N. E. *Mol. Cell. Biol.* 1994, 14, 4193.
12. Lebowitz, P. F.; Davide, J. P.; Prendergast, G. C. *Mol. Cell. Biol.* 1995, 15, 6613.
13. Lebowitz, P. F.; Sakamuro, D.; Prendergast, G. C. *Cancer Res.* 1997, 57, 708.
14. Kohl, N. E.; Mosser, S. D.; deSolms, S. J.; Giuliani, E. A.; Pompliano, D. L.; Graham, S. L.; Smith, R. L.; Scolnick, E. M.; Oliff, A.; Gibbs, J. B. *Science* 1993, 260, 1934.
15. James, G. L.; Goldstein, J. L.; Brown, M. S.; Rawson, T. E.; Somers, T. C.; McDowell, R. S.; Crowley, C. W.; Lucas, B. K.; Levinson, A. D.; Marsters, J. C., Jr. *Science* 1993, 260, 1937.
16. Manne, V.; Yan, N.; Carboni, J. M.; Tuomari, A. V.; Ricca, C. S.; Brown, J. G.; Andahazy, M. L.; Schmidt, R. J.; Patel, D.; Zahler, R.; Weinmann, R.; Der, C. J.; Cox, A. D.; Hunt, J. T.; Gordon, E. M.; Babacid, M.; Seizinger, B. R. *Oncogene* 1995, 10, 1763.
17. Patel, D.; Gordon, E. M.; Schmidt, R. J.; Weller, H. N.; Young, M. G.; Zahler, R.; Babacid, M.; Carboni, J. M.; Gullo-Brown, J. L.; Hunihan, L.; Ricca, C.; Robinson, S.; Seizinger, B. R.; Tuomari, A. V.; Manne, V. *J. Med. Chem.* 1995, 38, 435.
18. Cox, A. D.; Garcia, A. M.; Westwick, J. K.; Kowalczyk, J. J.; Lewis, M. D.; Brenner, D. A.; Der, C. J. *J. Biol. Chem.* 1994, 269, 19203.
19. Kohl, N. E.; Wilson, F. R.; Mosser, S. D.; Giuliani, E. A.; deSolms, S. J.; Conner, M. W.; Anthony, N. J.; Holtz, W. J.; Gomez, R. P.; Lee, T. J.; Smith, R. L.; Graham, S. L.; Hartman, J. D.; Koblan, K. S.; Kral, A. M.; Miller, P. J.; O'Neill, T. J.; Rands, E.; Schaber, M. D.; Gibbs, J. B.; Oliff, A. *Proc. Natl. Acad. Sci. USA* 1994, 91, 9141.
20. Nagasu, T.; Yoshimatsu, K.; Rowell, C.; Lewis, M. D.; Garcia, A. M. *Cancer Res.* 1995, 55, 5310.
21. Williams, T. M.; Ciccarone, T. M.; MacTough, S. C.; Bock, R. L.; Conner, M. W.; Davide, J. P.; Hamilton, K.; Koblan, K. S.; Kohl, N. E.; Kral, M. A.; Mosser, S. D.; Omer, C. A.; Pompliano, D. L.; Rands, E.; Schaber, M. D.; Shah, D.; Wilson, F. R.; Gibbs, J. B.; Graham, S. L.; Hartman, G. D.; Oliff, A. J.; Smith, R. L. *J. Med. Chem.* 1996, 39, 1345.
22. Leftheris, K.; Kline, T.; Vite, G. D.; Cho, Y. H.; Bhide, R. S.; Patel, D. V.; Patel, M. M.; Schmidt, R. J.; Weller, H. N.; Andahazy, M. L.; Carboni, J. M.; Gullo-Brown, J. L.; Lee, F. Y.; Ricca, C.; Rose, W. C.; Yan, N.; Barbacid, M.; Hunt, J. T.; Meyers, C. A.; Seizinger, B. R.; Zahler, R.; Manne, V. *J. Med. Chem.* 1996, 39, 224.
23. Kohl, N. E.; Omer, C. A.; Conner, M. W.; Anthony, N. J.; Davide, J. P.; deSolms, S. J.; Giuliani, E. A.; Gomez, R. P.; Graham, S. L.; Hamilton, K.; Handt, L. K.; Hartman, J. D.; Koblan, K. S.; Kral, A. M.; Miller, P. J.; Mosser, S. D.; O'Neill, T. J.; Rands, E.; Schaber, M. D.; Gibbs, J. B.; Oliff, A. *Nature Medicine* 1995, 1, 792.
24. Park, H.-W.; Boduluri, S. R.; Moomaw, J. F.; Casey, P. J.; Beese, L. S. *Science* 1997, 275, 1800.
25. Gibbs, J. B.; Oliff, A.; Kohl, N. E. *Cell* 1994, 77, 175.
26. Goldstein, J. L.; Brown, M. S.; Stradley, S. J.; Reiss, Y.; Gierasch, L. M. *J. Biol. Chem.* 1991, 266, 15575.
27. Reiss, Y.; Stradley, S. J.; Gierasch, L. M.; Brown, M. S.; Goldstein, J. L. *Proc. Natl. Acad. Sci. USA* 1991, 88, 732.
28. Brown, M. S.; Goldstein, J. L.; Paris, K. J.; Burnier, J. P.; Marsters, J. C., Jr. *Proc. Natl. Acad. Sci. USA* 1992, 89, 8313.
29. Leftheris, K.; Kline, T.; Natarajan, S.; DeVirgilio, M. K.; Cho, Y. H.; Pluscec, J.; Ricca, C.; Robinson, S.; Seizinger, B. R.; Manne, V.; Meyers, C. A. *Bioorg. Med. Chem. Lett.* 1994, 4, 887.
30. Leonard, D. M.; Schuler, K. R.; Poulter, C. J.; Eaton, S. R.;

- Sawyer, T. K.; Hodges, J. C.; Su, T.-Z.; Scholten, J. D.; Gowan, R. C.; Sebti-Leopold, J. S.; Doherty, A. M. *J. Med. Chem.* 1997, 40, 192.
31. Patel, D. V.; Patel, M. M.; Robinson, S. S.; Gordon, E. M. *Bioorg. Med. Chem. Lett.* 1994, 4, 1883.
32. Hall, C. C.; Watkins, J. D.; Ferguson, S. B.; Foley, L. H.; Georgopapadakou, N. H. *Bio. Res. Com.* 1995, 217, 728.
33. Hunt, J. T.; Lee, V. G.; Leftheris, K.; Seizinger, B.; Carboni, J.; Mabius, J.; Ricca, C.; Yan, N.; Manne, V. *J. Med. Chem.* 1996, 39, 353.
34. Kowalczyk, J. J.; Ackermann, K.; Garcia, A. M.; Lewis, M. D. *Bioorg. Med. Chem. Lett.* 1995, 5, 3073.
35. Bishop, W. R.; Bond, R.; Petrin, J.; Wang, L.; Patton, R.; Doll, R.; Njoroge, G.; Catino, J.; Schwartz, J.; Windsor, W.; Syto, R.; Schwartz, J.; Carr, D.; James, L.; Kirschmeier, P. *J. Biol. Chem.* 1995, 270, 30611.
36. Mallanis, A. K.; Njoroge, F. G.; Doll, R. J.; Snow, M. E.; Kaminski, J. J.; Rossman, R. R.; Vibulbhan, B.; Bishop, W. R.; Kirschmeier, P.; Liu, M.; Bryant, M. S.; Alvarez, C.; Carr, D.; James, L.; King, I.; Li, Z.; Lin, C. C.; Nardo, C.; Petrin, J.; Remiszewski, S. W.; Taveras, A. G.; Wang, S.; Wong, J.; Catino, J.; Girijavallabhan, V.; Ganguly, A. K. *Bioorg. Med. Chem.* 1997, 5, 93.
37. Njoroge, F. G.; Doll, R. J.; Vibulbhan, B.; Alvarez, C. S.; Bishop, W. R.; Petrin, J.; Kirschmeier, P.; Carruthers, N. I.; Wong, J. K.; Albanese, M. M.; Piwinski, J. J.; Catino, J.; Girijavallabhan, V.; Ganguly, A. K. *Bioorg. Med. Chem.* 1997, 5, 101.
38. Moomaw, J. F.; Casey, P. J. *J. Biol. Chem.* 1992, 267, 17438.
39. Casey, P. J. *Lipid Res.* 1992, 33, 1731.
40. Posner, I.; Engel, M.; Gazit, A.; Levitzki, A. *Mol. Pharmacol.* 1994, 45, 673.
41. Gazit, A.; Oshero, N.; Posner, I.; Jaish, P.; Poradosu, E.; Gilon, C.; Levitzki, A. *J. Med. Chem.* 1991, 34, 1897.
42. Qian, Y.; Vogt, A.; Sebti, S. M.; Hamilton, A. D. *J. Med. Chem.* 1996, 39, 217.
43. Vogt, A.; Qian, Y.; Blaskovich, M. A.; Fossum, R. D.; Hamilton, A. D.; Sebti, S. M. *J. Biol. Chem.* 1995, 270, 660.
44. Pompliano, D. L.; Rands, E.; Schaber, M. D.; Mosser, S. D.; Anthony, N. J.; Gibbs, J. B. *Biochemistry* 1992, 31, 3800.
45. Yokoyama, K.; Goodwin, G. W.; Ghomashchi, F.; Glomset, J. A.; Gelb, M. H. *Proc. Natl. Acad. Sci. USA* 1991, 88, 5302.
46. Moores, S. L.; Schaber, M. D.; Mosser, S. D.; Rands, E.; O'Hara, M. B.; Garsky, V. M.; Marshall, M. S.; Pompliano, D. L.; Gibbs, J. B. *J. Biol. Chem.* 1991, 266, 14603.
47. Casey, P. J.; Thissen, J. A.; Moomaw, J. F. *Proc. Natl. Acad. Sci. USA* 1991, 88, 8631.
48. Gibbs, J. B. Patent no. 0-461-869-A2, 1991.
49. Maltese, W. A. *FASEB J.* 1990, 4, 3319.
50. Rowell, C. A.; Kowalczyk, J. J.; Lewis, M. D.; Garcia, A. M. *J. Biol. Chem.* 1997, 272, 14093.
51. Whyte, D. B.; Kirschmeier, P.; Hockenberry, T. N.; Nunczoliva, I.; James, L.; Catino, J. J.; Bishop, W. R.; Pai, J. K. *J. Biol. Chem.* 1997, 272, 14459.
52. McGuire, T.; Qian, Y.; Hamilton, A. D.; Sebti, S. M. *J. Biol. Chem.* 1996, 271, 27402.
53. Miguel, K.; Pradines, A.; Sun, J.; Qian, Y.; Hamilton, A. D.; Sebti, S. M.; Favre, G. *Cancer Res.* 1997, 57, 1846.
54. Vogt, A.; Qian, Y.; McGuire, T. F.; Hamilton, A. D.; Sebti, S. M. *Oncogene* 1996, 13, 1991.
55. Sebti, S. M.; Vogt, A.; Qian, Y.; Blaskovich, M. A.; Fossum, R. D.; Hamilton, A. D. *J. Biol. Chem.* 1995, 270, 660.
56. deSolms, S. J.; Deana, A. A.; Giuliani, E. A.; Graham, S. L.; Kohl, N. E.; Mosser, S. D.; Oliff, A. I.; Pompliano, D. L.; Rands, E.; Scholtz, T. H.; Wiggins, J. M.; Gibbs, J. B.; Smith, R. L. *J. Med. Chem.* 1995, 38, 3967.
57. Reuveni, H.; Gitler, A.; Poradosu, E.; Gilon, C.; Levitzki, A. *Bioorg. Med. Chem.* 1997, 5, 85.
58. Whitehead, R. H.; Zang, H. H.; Hayward, I. P. *Immun. Cell Biol.* 1992, 70, 227.

Synergy between Anions and Farnesyl diphosphate Competitive Inhibitors of Farnesyl:Protein Transferase*

(Received for publication, April 7, 1997)

Jeffrey D. Scholten^{‡§}, Karen K. Zimmermann[‡], Maritza G. Oxender[‡], Daniele Leonard[‡], Judith Sebolt-Leopold[‡], Richard Gowan[‡], and Donald J. Hupe[‡]From the Departments of [‡]Biochemistry and [§]Chemistry, Parke-Davis Pharmaceutical Research, Division of Warner-Lambert Company, Ann Arbor, Michigan 48105

Investigation of the comparative activities of various inhibitors of farnesyl:protein transferase (FPTase) has led to the observation that the presence of phosphate or pyrophosphate ions in the assay buffer increases the potency of farnesyl diphosphate (FPP) competitive inhibitors. In addition to exploring the phenomenon of phosphate synergy, we report here the effects of various other ions including sulfate, bicarbonate, and chloride on the inhibitory ability of three FPP competitive compounds: Cbz-His-Tyr-Ser(OBn)TrpNH₂ (2), Cbz-His-Tyr-(OPO₃²⁻)-Ser(OBn)TrpNH₂ (3), and α -hydroxyfarnesyl phosphonic acid (4). Detailed kinetic analysis of FPTase inhibition revealed a high degree of synergy for compound 2 and each of these ions. Phosphorylation of 2 to give 3 completely eliminated any ionic synergistic effect. Moreover, these ions have an antagonistic effect on the inhibitory potency of compound 4. The anions in the absence of inhibitor exhibit non-competitive inhibition with respect to FPP. These results suggest that phosphate, pyrophosphate, bicarbonate, sulfate, and chloride ions may be binding at the active site of both free enzyme and product-bound enzyme with normal substrates. These bound complexes increase the potency of FPP competitive inhibitors and mimic an enzyme:product form of the enzyme. None of the anions studied here proved to be synergistic with respect to inhibition of geranylgeranyl transferase I. These findings provide insight into the mechanism of action of FPP competitive inhibitors for FPTase and point to enzymatic differences between FPTase and geranylgeranyl transferase I that may facilitate the design of more potent and specific inhibitors for these therapeutically relevant target enzymes.

Since mutations rendering the Ras protein (p21) oncogene are prevalent in many human cancers (1) and farnesylation of the C-terminal region of the Ras protein is essential for activation of Ras function *in vivo* (2, 3), a potential therapeutic approach to tumor regression would be to inhibit the farnesylation reaction. Farnesyl:protein transferase (FPTase)¹ catalyzes the transfer of a 15-carbon group to several cellular proteins containing the requisite C-terminal CAAX recognition sequence. The specificity for transfer of farnesyl relies on the CAAX motif comprised of a cysteine followed by two aliphatic

amino acids and ending mainly with a methionine or serine. FPTase isolated from rat brain is a 97-kDa $\alpha\beta$ heterodimeric protein requiring both zinc and magnesium metal ions (4, 5). The reaction mechanism for this enzyme is shown in Fig. 1 where a thioether bond is formed upon transfer of the farnesyl moiety of farnesyl diphosphate (FPP) to the thiol of the cysteine residue. The kinetic mechanism for the two-substrate reaction is functionally ordered where FPP binds first onto FPTase (6, 7).

Several classes of compounds have been identified as potent inhibitors of FPTase. These include peptide mimetic structures based on the tetrapeptide CVFM (5, 8–11), bisubstrate analog structures (12), and farnesyl pyrophosphate competitive compounds (13–15). These inhibitors show a wide range of specificity with respect to other prenylating enzymes including geranylgeranyl transferase. Geranylgeranyl transferase I transfers a 20-carbon geranylgeranyl group to proteins characterized by a CAAX motif, generally with a terminal leucine. The α subunit is identical for both rat FPTase and rat geranylgeranyl transferase I while the β subunit has 30% sequence identity (16).

Recently, the pentapeptide (1) was identified as a potent inhibitor of FPTase (17, 18). This compound was shown to be competitive with respect to FPP and was also demonstrated to be more potent in phosphate buffer than in a Hepes buffered system under otherwise identical conditions (19). In this study, the mechanism by which phosphate enhances inhibition of the tetrapeptide (2) was studied kinetically. We also wished to determine whether other anions (in particular product pyrophosphate) would cause this same enhancement, and whether other known FPP analog inhibitors share this anion requirement. Furthermore, we wanted to determine whether the phosphate enhancement of binding could be accomplished by covalently linking the phosphate to the inhibitor on an available tyrosine hydroxyl, and whether this abolished the enhancement by exogenous phosphate ion. Finally, we wanted to determine whether the phosphate enhancement of inhibitor binding was specific for FPTase compared with geranylgeranyl transferase I since distinguishing inhibition characteristics for these two similar enzymes may be critical in generating selective agents with distinctive cellular activities and further delineating the specificity by which these enzymes operate.

EXPERIMENTAL PROCEDURES

Materials—Tritiated farnesyl pyrophosphate and geranylgeranyl pyrophosphate were obtained from American Radiolabeled Chemicals (St. Louis, MO). Thr-Lys-Cys-Val-Ile-Met and biotin-Aha-Thr-Lys-Cys-Val-Ile-Met were synthesized according to solid phase peptide chemistry techniques (21, 22). α -Hydroxyfarnesyl phosphonic acid was synthesized as described (13). Compounds 1, 2, and 3 were synthesized as described (20). Potassium phosphate and sodium sulfate were obtained from Fisher and were the highest grade available. Sodium pyrophosphate and potassium chloride were obtained from Sigma. Potassium bicarbonate was obtained from Mallinckrodt and Hepes buffer was obtained from Life Technologies, Inc. Geranylgeranyl transferase I was

* The costs of publication of this article were defrayed in part by the payment of page charges. This article must therefore be hereby marked "advertisement" in accordance with 18 U.S.C. Section 1734 solely to indicate this fact.

§ To whom correspondence should be addressed. Tel.: 313-998-5955; Fax: 313-996-1356; E-mail: scholtj@as.wl.com.

¹ The abbreviations used are: FPTase, farnesyl:protein transferase; FPP, farnesyl diphosphate; DTT, dithiothreitol; HPLC, high performance liquid chromatography.

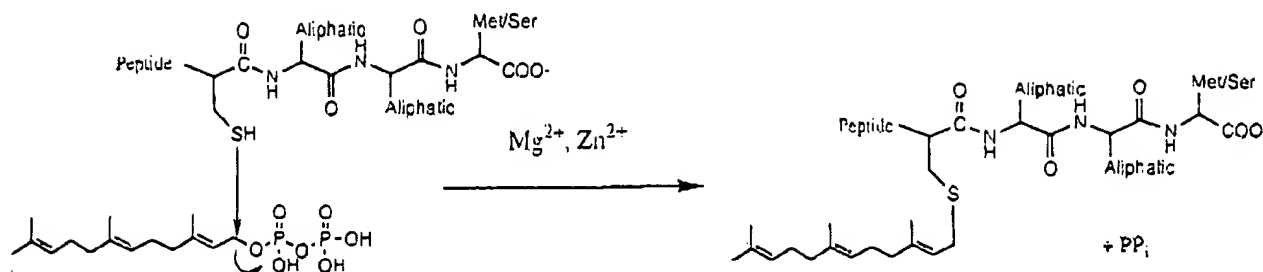


FIG. 1. Reaction catalyzed by farnesyl:protein transferase.

a gift from Dr. Michael Gelb, University of Washington, Seattle, WA. FPTase was expressed by baculovirus in SF9 cells and purified according to the following procedure adapted from Reiss *et al.* (4).

Purification of Farnesyl:Protein Transferase—SF9 cell pellets from 1.5 liters of suspension growth were resuspended in buffer containing 20 mM Tris chloride (pH 7.5), 50 mM NaCl, 20 μ M ZnCl₂, and 1 mM DTT (Buffer A) and homogenized by French Press at 700 kpsi. Homogenates were centrifuged at 100,000 $\times g$ for 45 min and supernatants adjusted to 55% saturation with ammonium sulfate. Precipitated material was collected by spinning at 20,000 $\times g$ for 20 min and resuspended in Buffer A. Samples were then dialyzed against 4 liters of Buffer A for 2 h and then 4 liters of fresh Buffer A for 16 h. Dialyzed samples were then filtered (0.4 μ m) and loaded onto a Q-Sepharose column (HiLoad 26/10) using an fast protein liquid chromatography system (Pharmacia Biotech Inc.). The column was washed with 220 ml of Buffer A followed by 60 ml of Buffer B (20 mM Tris chloride (pH 7.5), 160 mM NaCl, 20 μ M ZnCl₂, and 1 mM DTT). The enzyme was eluted with a linear gradient (440 ml) of buffer containing 150 mM to 1 M NaCl at a flow rate of 4 ml/min. Fractions containing FPTase activity were pooled, brought to 10% glycerol, and stored at -80°C for later affinity purification.

The affinity column for FPTase purification was prepared by mixing 12.8 mg of CNBr-activated CH-Sepharose with 26 mg of the peptide Thr-Lys-Cys-Val-Ile-Met in 43 ml of coupling buffer (100 mM NaHCO₃ and 500 mM NaCl (pH 8.2)) for 4 h with constant stirring at room temperature. The resin was then washed with 300 ml of Buffer C (50 mM Tris chloride, 100 mM NaCl, and 1 mM DTT) and poured into a column. The column was stored in 20 mM Tris chloride (pH 7.5), 0.02% sodium azide at 4°C .

Prior to FPTase purification, the affinity column (2.5 \times 12 cm) was washed with 300 ml of cold Buffer C. Thawed, active fast protein liquid chromatography fractions (80–100 ml) were then loaded onto the column and cycled through 3 times. The column was washed with 300 ml of Buffer D (50 mM Tris chloride, 100 mM NaCl, 1 mM DTT, and 0.2% PEG 8000) and the enzyme eluted with 300 ml of elution buffer (50 mM Tris succinate, 1 mM DTT, 500 mM NaCl, 0.2% PEG 8000, and 10% glycerol (pH 5)). The eluent was concentrated in an Amicon concentrator with a YM10 membrane to 5–10 ml, washed twice with 10 ml of Buffer E (50 mM Tris, 100 mM NaCl, 1 mM DTT, 0.2% PEG 8000, and 10% glycerol), and quick frozen in a dry ice-ethanol bath. The enzyme was a single band for each subunit by Coomassie Blue stain on a Novex 4–20% Tris glycine SDS-polyacrylamide electrophoresis gel.

Peptide Synthesis, Purification, and Characterization—The peptide analogs were synthesized by solid phase peptide synthetic methodologies (21, 22). The peptide analogs were prepared using an *N*-Fmoc protecting group strategy on a Rink-amide resin (4,2',4'-dimethoxyphenyl-Fmoc-aminomethyl)-phenoxy resin) (23).

The *N*-Fmoc group was removed with 20% piperidine in *N*-methylpyrrolidone prior to coupling with the next protected amino acid. All amino acids were double coupled as their *N*-hydroxybenzotriazole (HOBt) activated esters or as their PyBOP-activated esters unless incomplete coupling was indicated by the Kaiser test (24). The peptides were simultaneously deprotected and cleaved from the resin by treatments with 25–70% trifluoroacetic acid in methylene chloride, depending on the side chain protecting groups, at room temperature for 2–3 h.

Crude peptides were then purified to homogeneity by preparative reversed-phase high performance liquid chromatography (HPLC) eluting with a linear gradient of 0.1% aqueous trifluoroacetic acid with increasing concentrations of 0.1% trifluoroacetic acid in acetonitrile (CH₃CN). Peptide fractions found to be homogeneous by analytical reversed-phase HPLC were combined, concentrated, and lyophilized. All the peptides were analyzed for homogeneity by analytical HPLC, and characterized by amino acid analysis, elemental analysis, fast atom bombardment or electrospray mass spectrometry, and proton nuclear

magnetic resonance (¹H NMR) spectroscopy.

Phosphorylation of the tyrosine residue was carried out while the peptide was still linked to the resin using an excess of di-*t*-butyl-*N,N*-diethylphosphoramidite and tetrazole, followed by oxidation with 70% *t*-butylperoxide in methylene chloride. The *t*-butyl groups were removed simultaneously under the cleavage conditions (60% trifluoroacetic acid in methylene chloride).

In Vitro FPTase Enzyme Assay—Enzyme activity was monitored using scintillation proximity assay technology from Amersham. Standard reactions were carried out in a 100- μ l volume containing 50 mM Hepes (pH 7.4), 5 mM MgCl₂, 20 μ M ZnCl₂, 1 mM DTT, 0.1% PEG 8000, 200 nM peptide (biotin-Aha-Thr-Lys-Cys-Val-Ile-Met), 134 nM tritiated farnesylpyrophosphate, and 0.3–0.5 nM affinity purified farnesyl:protein transferase. Inhibitors were assayed at a final concentration of 5% dimethyl sulfoxide. When the effect of various ions were studied, buffered potassium phosphate, Na₂P₂O₇, Na₂SO₄, KCl, or KHCO₃ were added to the assay buffer at the indicated concentrations. All reactions were initiated with the addition of enzyme followed by incubation at 37°C for 30 min. The reactions were terminated with the addition of 150 μ l of stop reagent (prepared by diluting 20 mg/ml scintillation proximity assay beads (resuspended in phosphate-buffered saline + 0.05% NaN₃) 1:10 with buffer containing 1.5 M magnesium acetate, 200 mM H₃PO₄, and 0.5% bovine serum albumin). Radioactive product was then counted on a Wallac Microbeta 1450 scintillation counter.

Data Analysis—Initial velocity data were obtained from the counts obtained from radiolabeled product using the scintillation proximity assay technology and analyzed using the kinetics software package KinetAsyst II (IntelleKinetics, Princeton, NJ) on a Macintosh computer. The data for the double inhibition experiments were fitted to Equation 1 where one inhibitor is noncompetitive for FPP, and the other inhibitor is competitive for FPP, and the inhibitors are not mutually exclusive (25).

$$v/v_{max} = \frac{[S]}{K_i(1 + [IYK_i + [XYK_i + [I][XYBK_i] + [S](1 + [XYaK_i] - (Eq. 1)$$

In Equation 1, β is the interaction factor for the two inhibitors and α is the factor by which K_i changes when inhibitor (I) occupies the enzyme active site. Individual K_i constants were derived by nonlinear least squares fit to Equation 2 in the case of competitive kinetics or to Equation 3 in the case of noncompetitive kinetics.

$$v = V_{max}[SYK_m(1 + [IYK_i] + [S] (Eq. 2)$$

$$v = V_{max}SYK_m(1 + [IYK_i] + [S](1 + [IYK_i] (Eq. 3)$$

RESULTS

Peptidic Inhibitors of Farnesyl:Protein Transferase Are Competitive with Respect to Farnesyl Diphosphate—We have previously seen an effect of phosphate anion on the inhibitory potency of the FPP competitive pentapeptide (1). Truncation of this compound yielded Cbz-His-Tyr-Ser(OBn)-Trp-NH₂ (compound 2, Fig. 2) which is equally potent and also competitive for FPP. As shown in Table I, compound 2 has a K_i of 984 nM when assayed in Hepes buffer in the absence of phosphate. However, when 5 mM potassium phosphate is added to this buffer system, the inhibition becomes 53-fold more potent showing a K_i of 18 nM. Because of these large differences in inhibitory potency against the enzyme, we wished to analyze kinetically this phenomenon using compound 2 and several different anions.

Several Anions Inhibit FPTase and Are Synergistic with Cbz-

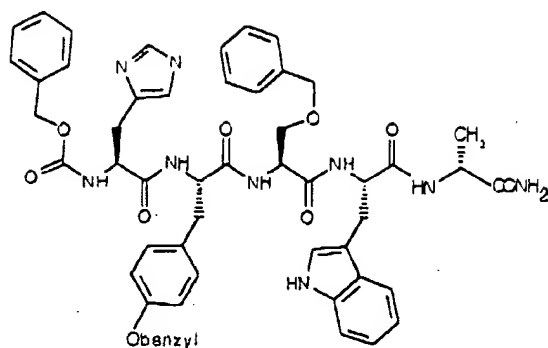
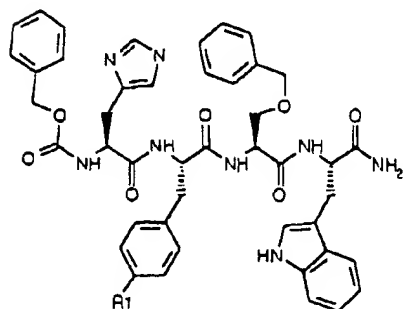
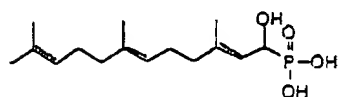
Cbz-His-Tyr(OBn)-Ser(OBn)-Trp-DAla-NH₂ (1)R1 = OH Cbz-His-Tyr-Ser(OBn)-Trp-NH₂ (2)R1 = PO₄²⁻ Cbz-His-Tyr(OPO₃H₂)-Ser(OBn)-Trp-NH₂ (3) α -Hydroxyfarnesyl phosphonic acid (4)

FIG. 2. Inhibitors of farnesyl:protein transferase.

His-Tyr-Ser(OBn)-Trp-NH₂ (Compound 2)—Table II shows the inhibition constants of several anions against FPTase. Each ion shows noncompetitive kinetics with respect to FPP and an inhibition constant in the mM range. Pyrophosphate is the most potent inhibitor shown with a K_i of 1.4 mM due to the fact that pyrophosphate is also a product inhibitor (13). When inhibitor 2 is tested in the presence of these anions, a significant enhancement of inhibition is observed. By varying anion concentration and compound 2, a kinetic analysis can be made based on possible synergy of inhibition. The degree of synergy can be analyzed using Equation 1 in a system where a competitive inhibitor and a noncompetitive inhibitor may bind to the active site in combination favorable to binding and resulting in an enhancement of inhibition (25). A β value is derived that is a measure of cooperativity and can also be described as an interaction factor between the two molecules. If β is greater than 1, the binding of one inhibitor is hindering the binding of the other. If β is equal to 1, the binding of each species has no effect on the other, and if β is less than 1, then the binding of the two species are synergistic. In Fig. 3, a Dixon plot of compound 2 versus varying concentrations of phosphate anion show lines that intersect above the x axis indicative of a synergy of inhibition and gives a β value = 0.012. The β value actually represents the reciprocal of the maximal enhancement that can be

TABLE I
Inhibitors of farnesyl:protein transferase

Compound	IC ₅₀ ^a	K _i	IC ₅₀ ^b	K _i
	μ M	nM	μ M	nM
2	6,100	954 = 311	160	18.6 = 2.3
3	6	2.6 = 0.6	3	3.6 = 0.5
4		49 = 10		488 = 32

^a Hepes buffer system.^b Hepes plus 5 mM phosphate buffer system.TABLE II
Inhibition of farnesyl:protein transferase by anions

Compound	K _i	with Respect to FPP	
		K _i	Inhibitor type
	mM	mM	
HPO ₄ ²⁻	144	1000	NC
PP _i	1.4	1.4	NC
HSO ₄ ⁻	24	72	NC
HCO ₃ ⁻	160	327	NC
Cl ⁻	1160	3069	NC

observed, for the case of phosphate and compound 2, this increase is over 80-fold. The β values for several anions tested and their possible fold enhancement of inhibition with compound 2 are listed in Table III and all show synergy of inhibition.

Covalent Attachment of a Phosphate onto Compound 2 Disrupts the Synergism of Inhibition—Because of the large increase in inhibition by phosphate anion on compound 2, a synthetic strategy was devised to covalently link the phosphate group onto the tyrosine hydroxyl group of 2. This yielded a much more potent inhibitor (compound 3, Fig. 2) while retaining the characteristic of being competitive for FPP as shown in Fig. 4. In addition to being a low nanomolar inhibitor, this compound is unaffected by the presence of phosphate in the buffer. As shown in Table I, the K_i values of this compound are 2.6 and 3.6 nM in a Hepes buffer system with and without added phosphate. Comparing compound 2 and 3 where the only difference is the added phosphate group, their K_i values in a Hepes buffer system are 984 and 2.6 nM, respectively. However, in the presence of 5 mM phosphate, the K_i for compound 2 is 53-fold lower while the K_i for compound 3 remains relatively unchanged.

Inhibition of Farnesyl:Protein Transferase by (α -Hydroxyfarnesyl)phosphonic acid (4)—(α -Hydroxyfarnesyl)phosphonic acid (4) is shown in Fig. 2 and is competitive with respect to FPP exhibiting a K_i = 49 nM in a Hepes buffer system. This value is consistent with that reported in the literature (13). However, when 5 mM phosphate is added to the assay buffer, the K_i of this compound increases 10-fold to 488 nM (see Table I) yet remains competitive with respect to FPP. This result seems to imply that there is now mutual competition between compound 4 and phosphate anion.

Inhibition of Geranylgeranyl Transferase I—Compound 2 was also assayed against geranylgeranyl transferase I in the presence of the anions shown in this study. However, in this case, there was no increase in inhibition observed when any of the anions were included in the assay buffer.

DISCUSSION

As the ongoing search for potent inhibitors of FPTase continues, a better understanding of the enzyme mechanism of FPTase is necessary to provide insight into the design and synthesis of potent FPTase inhibitors. Employing a phosphate buffer system, we identified several compounds as very potent inhibitors of the farnesylation reaction. Subsequent examination of their inhibitory potency in a nonphosphate buffering system revealed significantly lower enzyme inhibition *in vitro*. Further investigation showed that the phosphate anion was

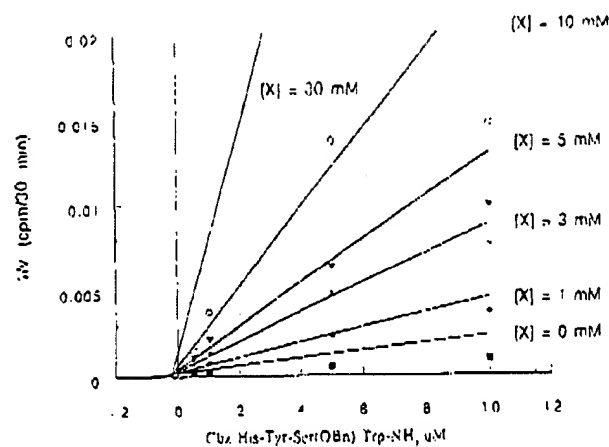


FIG. 3. Dixon plot of initial velocity versus inhibitor concentration for Cbz-His-Tyr-Ser(OBn)-Trp-NH₂ (2) at varying potassium phosphate concentrations (X).

TABLE III
Inhibitor synergy of compound 2 with various anions

Anion	β	Fold increase in inhibition ($1/\beta$)
HPO ₄ ²⁻	0.012	83
PP _i	0.92	1.2
HSO ₄ ⁻	0.31	3.2
HCO ₃ ⁻	0.043	23
Cl ⁻	0.007	146

acting in a synergistic way with certain inhibitors. Moreover, this synergism was observed only for inhibitors that were competitive with respect to farnesyl diphosphate. Using compound 2 we have kinetically analyzed the synergistic role played by several anions. Not all FPP competitive inhibitors, however, were synergistic with phosphate anion as evidenced by the behavior of α -hydroxyfarnesyl phosphonic acid (4).

Kinetic Analysis of Synergy of Inhibition of FPTase—In a Hepes buffer system compound 2 is competitive with respect to FPP having a K_i of 984 nM. In the same buffer system plus 5 mM potassium phosphate, compound 2 is still competitive with respect to FPP but the K_i is reduced 53-fold to 18 nM. This effect could be indicative of synergy of inhibition between two molecules operating together at the active site. Similar inhibitory effects have been observed with phosphoenolpyruvate mutase (26) and with phosphoenolpyruvate carboxylase from *Zea mays* (27). Phosphoenolpyruvate carboxylase proceeds through a random sequential mechanism where a high level of synergism of binding of substrates is observed. Very high levels of synergistic inhibition was found between oxalate and carbamyl phosphate ($\beta = 0.0013$). In the case of phosphoenolpyruvate mutase, synergy of inhibition between oxalate and anions that alone were noncompetitive inhibitors suggested a "combined presence" in the enzyme active site as a bimolecular transition state analog. In both of these cases, the inhibitor oxalate was a very close mimetic of the original substrate phosphoenolpyruvate. In our case, the peptidic inhibitors bear little resemblance intuitively to the original substrates.

Using affinity purified FPTase from rat brain, phosphate was kinetically analyzed as an inhibitor. We found noncompetitive inhibition with respect to FPP in the high millimolar concentration range. In cases where one inhibitor is noncompetitive and the other is competitive, the amount of synergism between two compounds can be measured using a Dixon plot to arrive at an interaction β value. β is a measure of the amount of synergistic cooperativity between the two inhibitors. A Dixon

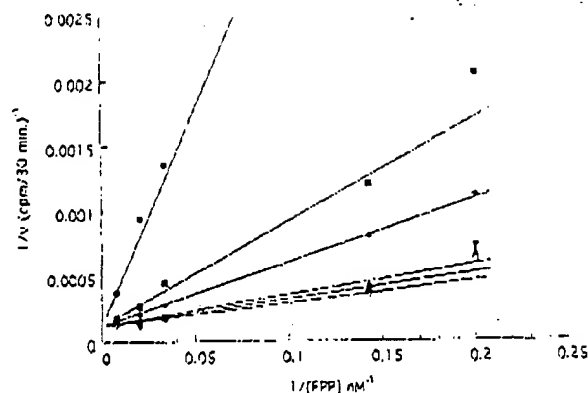


FIG. 4. Double-reciprocal plot of initial velocity versus varying farnesyl diphosphate concentration. Concentrations of inhibitor, Cbz-His-Tyr(OPO₃H₂)-Ser(OBn)-Trp-NH₂ (3), are as follows: ●, [I] = 50 nM; ■, [I] = 10 nM; ◆, [I] = 5 nM; ▲, [I] = 1 nM; ▼, [I] = 0.5 nM; ○, 0 nM. $K_m = 13.4 \pm 2.3$ nM; $V_{max} = 8160 \pm 409$ cpm/30 min; $K_i = 2.6 \pm 0.6$ nM.

plot is shown in Fig. 3 for the case of compound 2 and phosphate anion. Here, β is 0.012 showing that an increase of over 80-fold ($1/\beta$) in inhibition is possible.

Because an improvement of inhibition with phosphate anion was observed with a tetrapeptide based molecule, other anions were used to test whether synergism would also be found. The anions sulfate, carbonate, chloride, and pyrophosphate were found to retain a synergistic effect with compound 2, whereas nitrate and acetate showed little or no effect. When the anions were tested for direct inhibition of FPTase, all showed noncompetitive inhibition with respect to farnesyl diphosphate. This kinetic pattern is consistent with these anions binding to two different forms of the enzyme. One logical binding site for phosphate, for example, could be at the portion of the active site of FPTase that actively binds the pyrophosphate group of farnesyl diphosphate known as the pyrophosphate binding pocket.

Evidence for Synergy of Inhibition at the Active Site of FPTase—There are four pieces of supportive evidence that the anion contributing to synergy of inhibition is acting at the enzyme active site. First, noncompetitive kinetics for phosphate was observed with respect to FPP against farnesyl:protein transferase. Second, based on the effect of phosphate anion on inhibition of FPTase, a second inhibitor, compound 3, was synthesized which contained a covalently linked phosphate group. For this compound, the effect of phosphate anion to enhance inhibition was no longer found. The inhibition of compound 3 itself against FPTase was 3 nM making this compound one of the most potent inhibitors reported to date against FPTase (see Fig. 4). Third, when α -hydroxyfarnesyl phosphonate was studied, there appeared to be a direct competition for this binding pocket and antisyrnergy was observed. The K_i in Hepes buffer was 10-fold lower than that observed in the presence of 5 mM phosphate. Finally, when inhibitors that are competitive with respect to the peptide substrate were studied (CVFM for example), no phosphate effect was observed.

Kinetic analysis reveals that the anions are noncompetitive with respect to FPP. Therefore, the phosphate must bind to two different forms of the enzyme. Phosphate can bind to the free form of the enzyme because the pyrophosphate pocket is still unoccupied. In considering other forms of the enzyme to which phosphate could bind, the E:FPP form of the enzyme where the pyrophosphate pocket is already occupied seems unlikely. Furthermore, once the bulky peptide substrate binds at the active site, catalysis happens extremely fast and product release is thought to be rate-limiting (7). If there is an ordered mechanism of product release, the pyrophosphate would leave prior to

Synergism and Inhibition of FPTase

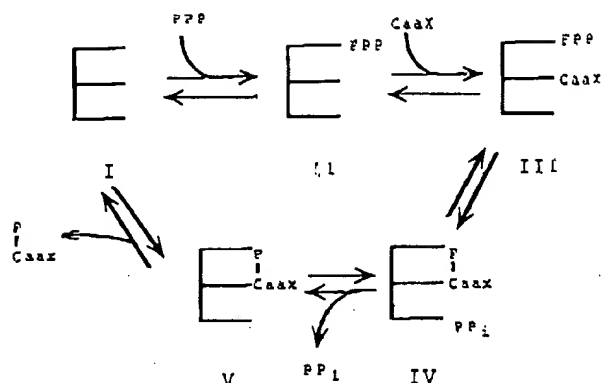


FIG. 5. Possible mechanism of action for farnesyl:protein transferase.

the farnesylated peptide providing a second form of the enzyme which would then be accessible to phosphate binding at the putative pyrophosphate binding pocket of the active site. Fig. 5 shows how phosphate anion could exhibit noncompetitive kinetics of inhibition with respect to FPP and bind to two different forms of the enzyme. In this mechanistic scheme, phosphate binds to the free form of the enzyme (I) because the pyrophosphate pocket is still unoccupied. In addition, after release of pyrophosphate from the E:farnesylated peptide:PP form of the enzyme, there would exist an E:farnesylated peptide form of the enzyme (V) that would have a pyrophosphate binding pocket now accessible to phosphate anion. If the inhibitor 2 was acting like a farnesylated product (F-CAAX), then phosphate could bind to the enzyme:inhibitor form of the enzyme. The consequence would presumably be a closely mimicked step of the enzyme catalytic mechanism. Since product release is rate-limiting, the E:F-CAAX species would be a considered a kinetically long lasting species. This may account for the synergy of inhibition observed.

There are several examples in the literature of such synergism like phosphoenolpyruvate mutase (26) where many anions were used as a close substrate analog and synergy of inhibition was observed. In addition, synergy of inhibition with anions and a substrate analog was observed for phosphoenolpyruvate carboxylase (27). In both cases, the data could be analyzed in terms of a transition state analog. But in this case, the inhibitor is not a structural analog of either substrate in the enzyme catalyzed reaction. Nevertheless, anions have a dramatic impact on the degree of inhibition with certain FPP competitive compounds and may be used to design more effective inhibitors against the enzyme possibly as transition state analogs.

Comparison of Synergy of Inhibition for FPTase and Geranylgeranyl Transferase I—Since FPTase and geranylgeranyl transferase I share a common subunit and undergo very similar reactions (the length of the prenyl chain differing by five carbon units) it was of interest to examine if there still existed the same synergy of inhibition. The IC_{50} for compound 2 against geranylgeranyl transferase I is $12 \mu M$ and no effect of phosphate or other anions was found. The lack of an anion effect may point out differences between these two enzymes that could be used to increase specificity of inhibition for each respective protein. Since the two enzymes share an identical α subunit, the differences in synergy of inhibition may lie elsewhere. One possibility may be that kinetically, geranylgeranyl transferase I does not release PP_i in an ordered fashion leaving no room for any anions to combine with a partial product form of an inhibitor. It would also be plausible that the specific inhibitor 2 does not mimic a product complex for geranylgeranyl transferase I.

It is interesting that phosphate has such an effect on

FPTase-I as opposed to geranylgeranyl transferase I. The amount of phosphate found *in vivo* at the cellular level is thought to be in the low millimolar range (28–30). This anion would then be present in high enough concentrations to see an observable effect in cellular assays and could be used advantageously to increase the specificity of inhibition between the two prenyl transferases. Finally, enzymatic differences between these two catalytic enzymes may become more apparent based on the phosphate synergy phenomenon.

Conclusion—We have shown that in the presence of various anions there is a large increase in potency of inhibition for compound (2). This effect has been analyzed kinetically to reveal a synergy of inhibition in the case of FPTase that does not exist for geranylgeranyl transferase I. Furthermore, an inhibitor (3) has been designed to use this effect to increase potency against FPTase.

REFERENCES

- Barbacid, M. (1987) *Annu. Rev. Biochem.* 56, 719–827
- Kato, K., Cox, A. D., Hisaka, M. M., Graham, S. M., Busch, J. E., and Der, C. J. (1992) *Proc. Natl. Acad. Sci. U. S. A.* 89, 5403–5407
- McGeady, P., Kurda, S., Shimizu, K., Takai, Y., and Gelb, M. H. (1995) *J. Biol. Chem.* 270, 26547–26551
- Reich, Y., Goldstein, J. L., Seabra, M. C., Casey, P. J., and Brown, M. S. (1990) *Cell* 62, 81–88
- Reich, Y., Brown, M. S., and Goldstein, J. L. (1992) *J. Biol. Chem.* 267, 8403–8408
- Pompliano, D. L., Schaber, M. D., Mosser, S. D., Omer, C. A., Shafer, J. A., and Gibbs, J. B. (1999) *Biochemistry* 32, 8341–8347
- Furline, E. S., Leean, J. J., Landavazo, A., Moomaw, J. F., and Casey, P. J. (1995) *Biochemistry* 34, 6557–6562
- Leftheris, K., Kline, T., Natarajan, S., DeVirgilio, M. K., Cho, Y. H., Pluscec, J., Ricca, C., Robinson, S., Seizinger, B. R., Manne, V., and Meyers, C. A. (1994) *Bioorg. & Med. Chem. Lett.* 4, 897–899
- Wai, J. S., Bamberger, D. L., Fisher, T. E., Graham, S. L., Smith, R. L., Gibbs, J. B., Mosser, S. D., Oliff, A. L., Pompliano, D. L., Rands, E., and Kohl, N. E. (1994) *Bioorg. & Med. Chem.* 2, 939–947
- Garcia, A. M., Rovell, C., Ackermann, K., Kowalczyk, J. J., and Lewis, M. D. (1993) *J. Biol. Chem.* 268, 18415–18418
- Vogt, A., Qian, Y., Blaskovich, M. A., Fossum, R. D., Hamilton, A. D., and Sebti, S. M. (1995) *J. Biol. Chem.* 270, 660–664
- Paul, D. V., Gordon, E. M., Schmidt, R. J., Weller, H. N., Young, M. G., Zahler, R., Barbacid, M., Carboni, J. M., Gullo-Brown, J. L., Hunihan, L., Ricca, C., Robinson, S., Seizinger, B. R., and Tuomari, A. V. (1995) *J. Med. Chem.* 38, 435–442
- Pompliano, D. L., Rands, E., Schaber, M. D., Mosser, N. J., Anthony, N. J., and Gibbs, J. B. (1992) *Biochemistry* 31, 3800–3807
- Singh, S. B., Zink, D. L., Leisch, J. M., Goetz, M. A., Jenkins, R. G., Nallin-Omar, M., Silverman, K. C., Bills, G. F., Mosley, R. T., Gibbs, J. B., Albers-Schonberg, G., and Lingham, R. B. (1993) *Tetrahedron* 49, 5917–5926
- Dolenc, J. M., and Poulter, C. D. (1995) *Proc. Natl. Acad. Sci. U. S. A.* 92, 5008–5011
- Armstrong, S. A., Seabra, M. G., Sudhoff, T. C., Colstein, J. L., and Brown, M. S. (1993) *J. Biol. Chem.* 268, 12221–12229
- Scholt-Leopold, J., Gowan, R., Su, T., and Leonard, D. (1994) *85th Annual Meeting of AACR, Toronto, Canada, April 10, 1994*
- Leonard, D., Eaton, S., Sawyer, T., and Bolton, G. (1994) *107th ACS National Meeting, San Diego, CA, March 13, 1994*
- Scholten, J. D., Zimmerman, K., Oxender, G. M., Sebolt-Leopold, J., Gowan, R., Leonard, D., and Hupe, D. J. (1996) *Bioorganic and Medicinal Chemistry* 4, 1537–1543
- Leonard, D. M., Shuler, K. R., Poulter, C. J., Eaton, S. R., Sawyer, T. K., Hodges, J. C., Scholten, J. D., Gowan, R. C., Sebolt-Leopold, J. S., and Doherty, A. M. (1997) *J. Med. Chem.* 40, 192–200
- Stewart, J. M., and Young, J. D. (1984) *Solid Phase Peptide Synthesis*, Pierce Chemical Co.
- Badanaky, M., and Badanaky, A. (eds) (1984) in *The Practice of Peptide Synthesis*, Springer-Verlag, Berlin, Heidelberg
- Rink, H. (1987) *Tetrahedron Lett.* 28, 3787–3790
- Kaiser, E., Coluccini, R. L., Boessinger, C. D., and Cook, P. I. (1970) *Anal. Biochem.* 34, 595–598
- Segal, I. H. (1976) *Enzyme Kinetics, Behavior and Analysis of Rapid Equilibrium and Steady-State Enzyme Systems*, pp. 423–436 John Wiley & Sons, Inc., New York
- Seidel, H. M., and Knowles, J. R. (1994) *Biochemistry* 33, 5641–5646
- James, W. J., O'Leary, M. H., and Cleland, W. W. (1992) *Biochemistry* 31, 6421–6428
- Amatrudo, T. T., Hollingworth, D. R., DeEsopo, N. D., Upton, G. V., and Rundy, P. K. (1980) *J. Clin. Endocrinol. Metab.* 20, 339–379
- Buchli, R., Martin, E., Boessinger, P., and Ruppel, H. (1994) *Pediatr. Res.* 35, 431–435
- Sieck, E. A., Kientsch-Engel, R. I., Ghimi, F. M., and Wieland, O. H. (1964) *Eur. J. Biochem.* 141, 543–548

F

Oreganic Acid, a Potent Inhibitor of Ras Farnesyl-Protein Transferase

Keith C. Silverman, Hiranthi Jayasuriya, Carmen Cascales,* Dolores Vilella,* Gerald F. Bills, Rosalind G. Jenkins, Sheo B. Singh, and Russell B. Lingham

Merck Research Laboratories, P.O. Box 2000, Rahway, New Jersey 07065; and *Merck Sharp & Dohme de España, S.A. Josefa Valcarcel 38, 28027 Madrid, Spain

Received February 6, 1997

A sulfated tricarboxylic acid fungal metabolite is an inhibitor of human farnesyl-protein transferase (FPTase). The compound, designated as oreganic acid, has a molecular weight of 494, an empirical formula of $C_{22}H_{38}O_{10}S$ and inhibits FPTase with an IC_{50} value of 14 nM. Oreganic acid is a selective inhibitor of FPTase because it does not inhibit human geranylgeranyl-protein transferase type I (GGPTase-I). It is not a time-dependent inhibitor, reversibly inhibits FPTase, is competitive with respect to farnesyl diphosphate and non-competitive with respect to the Ras acceptor peptide. The structure of oreganic acid resembles that of farnesyl diphosphate and most likely inhibits FPTase by mimicking farnesyl diphosphate at the active site of the enzyme. © 1997 Academic Press

Farnesylation of Ras by the hetero-dimeric farnesyl-protein transferase (FPTase) is the mechanism whereby Ras is directed towards and anchored in the cell membrane. Farnesylation occurs on the carboxyl terminal cysteine which is part of the CAAX motif. Membrane localization of Ras is an initial and essential step in ras-mediated oncogenesis. Inhibition of Ras farnesylation prevents Ras membrane localization and blocks Ras cell-transforming activity thereby validating FPTase as a target for anti-cancer chemotherapeutics (4, 5, 6). Several FPTase inhibitors have recently been reported which selectively inhibit Ras processing in certain cell lines, (2, 3, 7, 11, 14) prevent tumorigenesis in nude mice (12) and promote regression of mammary and salivary carcinomas in ras transgenic mice (13).

We recently described the isolation and inhibitory FPTase activity of chaetomelic acids (5, 15, 20), fusidienol (21), preussomerins and deoxypreussomerins (22), actinoplanic acids (19, 23, 24), barcelonic acid (9) and cylindrols (25) that are structurally diverse, selective and potent natural product inhibitors of FPTase. Our continued search for unique inhibitors of FPTase

from microbial sources has lead to the isolation of a novel, potent, specific, reversible inhibitor of FPTase that resembles farnesyl diphosphate. The compound contains a polar tricarboxylic acid head group and a long chain fatty tail terminating with a hydroxy group that is sulfated. The structure of oreganic acid was reported by Jayasuriya et al. (10). The details of the biological characterization of oreganic acid are described in this manuscript.

MATERIALS AND METHODS

Source and fermentation of the producing organism. The producing organism (MF 6046) was an endophytic fungus isolated from the leaves of *Berberis oregana* from Lord Ellis Summit, Humboldt Co., CA. The seed culture was prepared as described by Lingham et al. (15) and incubated at 25 °C for 6 days on a gyratory (220 rpm, 5.1 cm throw) prior to the inoculation of the production flasks. The production medium contained in grams/liter: sucrose, 75.0; tomato paste, 10.0; malt extract, 5.0; $(NH_4)_2SO_4$, 1.0; soy flour, 1.0; and KH_2PO_4 , 9.0. Production flasks were inoculated with 2.0 ml of vegetative seed growth and were incubated at 25 °C (with shaking) for 8 days.

Isolation of oreganic acid. The compound was isolated and the structure elucidated as described by Jayasuriya et al. (10).

Enzyme assays. Recombinant human FPTase and GGPTase-I were prepared as described by Omer et al. (16). FPTase and GGPTase-I assays were performed essentially as described (15) and contained the following: 2 nM FPTase, 50nM [3H]farnesyl diphosphate (FPP) and 100 nM Ras-CVIM or 400 nM Ras-CVLS; 2 nM GGPTase-I, 100 nM [3H]geranylgeranyl diphosphate (GGPP), and 500 nM Ras-CAIL. Kinetic constants were determined and reversibility studies were performed as previously described (5, 19). Fermentation extracts or pure compounds were dissolved in 100% DMSO and diluted twenty-fold into the assay to give a final solvent concentration of 5%.

RESULTS

Our continued search for novel FPTase inhibitors from microbial sources resulted in the isolation of ore-

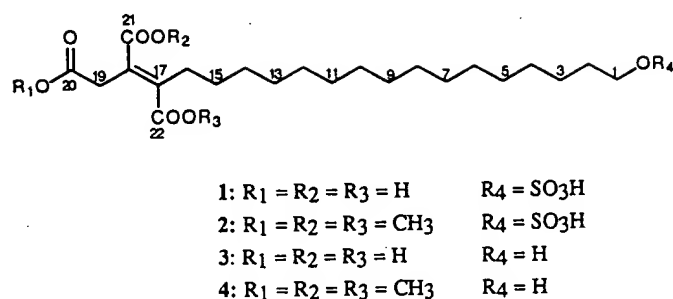


FIG. 1. Structure of Oreganic Acid and Analogs.

ganic acid (Figure 1). Also shown in Figure 1 are three analogs of oreganic acid. The producing culture was an endophytic fungus that did not sporulate under standard fermentation conditions and could not be identified taxonomically. Oreganic acid was isolated and the structure was elucidated as described by Jayasuriya et al. (10). It has a molecular weight of 494 and an empirical formula of $C_{22}H_{38}O_{10}S$.

The effect of oreganic acid on FPTase activity when either Ki-Ras-CVIM or Ha-Ras-CVLS is used as the acceptor peptide substrate is presented in Figure 2. Oreganic acid is a potent inhibitor of FPTase activity exhibiting an IC_{50} (concentration that elicits 50% inhibition) value of 14 nM (Figure 2). The activity of this compound is independent of which Ras peptide substrate is used, implying that oreganic acid does not interact with the Ras peptide binding site on the enzyme. To further examine the effects of the compound a kinetic analysis was performed and the results are presented in Figure 3. Oreganic acid is competitive

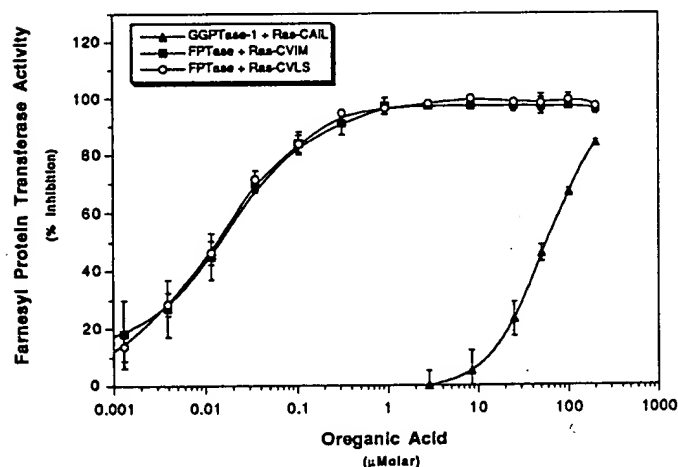


FIG. 2. Inhibition of Prenyl Protein Transferases by Oreganic Acid. Enzyme assays were performed as previously described (19) using 2 nM human recombinant prenyl protein transferase per assay. The FPTase and GGPTase-I activities in the absence of inhibitor were 329 ± 50 fmoles FPP hydrolyzed/ μ g/min. and 6663 ± 297 fmoles GGPP hydrolyzed/ μ g/min., respectively. All data were calculated relative to the DMSO control.

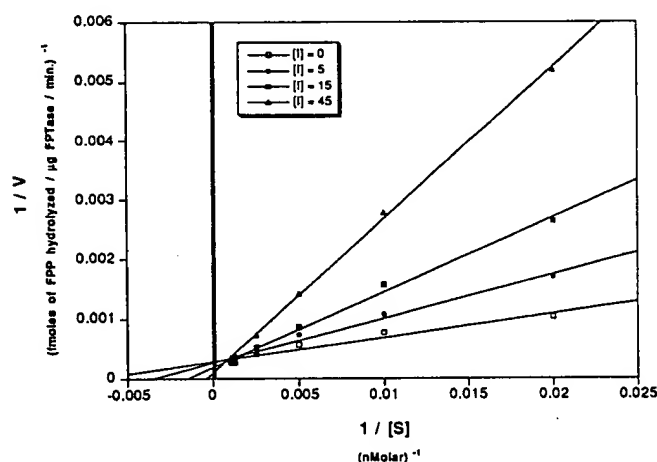


FIG. 3. Oreganic Acid competes with Farnesyl Pyrophosphate for binding to Farnesyl Protein-Transferase. Kinetic constants were determined as previously described by Gibbs et al. (5). The concentration of 3H -farnesyl pyrophosphate (3H -FPP) was varied as the concentrations of Ras-CVLS and hFPTase were held constant at 1 μ M and 2 nM, respectively. The concentrations of Oreganic Acid used were 0, 5, 15, and 45 nM. Kinetic analysis was performed using k-cat enzyme kinetics software from Biometallics, Inc., Princeton, NJ.

with respect to farnesyl diphosphate exhibiting an inhibition constant (K_i) of 4.5 nM (Figure 3) and displays a complex kinetic pattern of mixed non-competitive or un-competitive inhibition with respect to the Ki-Ras-CVIM peptide substrate (data not shown).

Oreganic acid is a poor inhibitor of GGPTase-I (Figure 2) ($IC_{50} \approx 60 \mu$ M) exhibiting an exquisite selectivity for FPTase over GGPTase-I. Oreganic acid is not a time-dependent inhibitor of FPTase (Figure 4) while it is a reversible inhibitor of the enzyme (Table I). When tested in an assay designed to evaluate the compound's effect on the posttranslational processing of Ras in in-

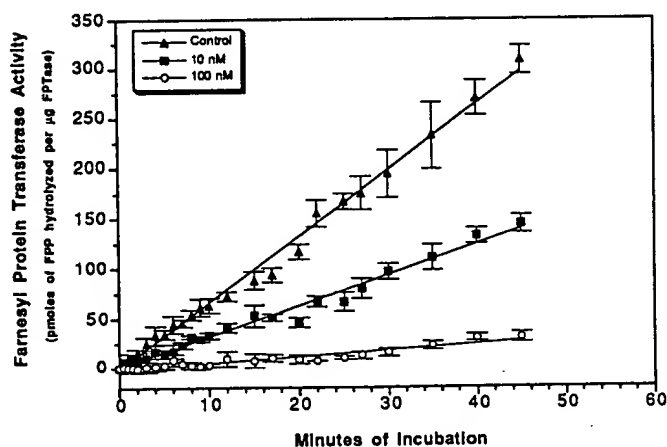


FIG. 4. Time Course of Inhibition of Farnesyl Protein-Transferase by Oreganic Acid. Enzyme assays were performed as previously described Lingham et al. (15) using 100 nM Ras-CVIM, 50 nM FPP and 2 nM human FPTase. The figure shows the inhibition over time for 1.) Control, 2.) 10 nM, and 3.) 100 nM Oreganic Acid.

TABLE I
Reversibility of Oreganic Acid

Conditions	FPTase activity (fmol/ μ g/min)	Percent inhibition (%)
I. Initial incubation and no centrifugation		
1. FPTase + 5% DMSO	5036	—
2. FPTase + 100 nM Oreganic acid	2883	43
II. Inhibitor + centrifugation		
3. FPTase + 5% DMSO + centrifugation + 5% DMSO added back in the assay	2900	—
4. FPTase + 5% DMSO + centrifugation + 100 nM Oreganic acid added back in the assay	1443	50
5. FPTase + 100 nM Oreganic acid + centrifugation + 5% DMSO added back in the assay	3118	—
6. FPTase + 100 nM Oreganic acid + centrifugation + 100 nM Oreganic acid added back in the assay	1290	56

Tubes containing 20 nM human FPTase were incubated with either: (i) DMSO or (ii) 100 nM oreganic acid for 20 minutes at 31°C. Aliquots (10 μ l) were removed and assayed directly (see Condition I of the table). The remaining volumes were gel-filtered through 2.2 ml Sephadex G-25 columns equilibrated with 100 mM HEPES, pH 7.5, 100 mM NaCl, 5 mM MgCl₂, 2 mM DTT and 0.2% (w/v) n-octyl- β -D-glucopyranoside. The column eluates (25 μ l), in column equilibration buffer, were tested for FPTase activity as previously described (15). DMSO or oreganic acid were added back to the assay tubes as shown above (see Condition II of the table). Data was calculated relative to the DMSO control.

tact cells, oreganic acid was inactive up to 10 μ M (data not shown).

Of the four compounds presented in Figure 1 the sulfated free acid form of oreganic acid was more active than the desulfated form (compound 3, IC₅₀ = 3.3 μ M). A trimethyl ester analog (compound 2) was significantly less active (IC₅₀ = 11 μ M) and the desulfated form of the trimethyl ester (compound 4) was completely inactive (up to 20 μ M).

DISCUSSION

The compound that forms the basis of this report is a potent specific inhibitor of FPTase activity. Structurally, it is a tricarboxylic alkyl sulfate that resembles farnesyl diphosphate. Oreganic acid has a complex head structure with an extended fatty acid chain that terminates with a sulfated hydroxy group. This is similar to chaetomelic acids A and B (15, 20) and actinoplanic acids A and B (19). These inhibitors inhibit FPTase activity by competing with farnesyl diphosphate. Oreganic acid differs from these previous compounds in having a sulfate group at one end of the molecule. Not surprisingly, oreganic acid is competitive with respect to farnesyl diphosphate (Figure 4) but not with the Ras peptide substrate. Like chaetomelic acids and actinoplanic acids, oreganic acid mimics farnesyl diphosphate by being able to utilize the carboxylic acids and fatty chain as substitutes for the polar phosphate head groups and the isoprene groups, respectively. Trimethylation of the carboxylic groups (Figure 1(2)) leads to a significant decrease in FPTase inhibitory activity. This is probably due to a change in the charge around the acidic groups that affects the way the compound fits within the farnesyl diphosphate binding pocket on the enzyme.

Furthermore, there are similarities between the tri-carboxylic acid head group of oreganic acid and the dicarboxylic acid head group of chaetomelic acid A. We have previously demonstrated that to maximally inhibit FPTase activity, the carboxyl groups in chaetomelic acid must be in a *cis* geometry (20). In contrast, the carboxylic acid groups of oreganic acid have a *trans* geometry centered around a double bond. The third carboxyl group plays a significant role as it renders itself in a *cisoid* conformation with respect to one or the other of the carboxyl groups around the double bond. The additional carboxyl group could explain why oreganic acid is significantly more potent than *trans* chaetomelic acid A. The arrangement of the carboxyl groups can account for some of the potency of oreganic acid, however, the geometry of the carboxyl groups is not responsible for all of the compound's potency.

Oreganic acid is unique in having a sulfate group at one end of the molecule which contributes to the overall negative charge of the compound. The desulfated analog of oreganic acid (Figure 1(3)) is considerably less active than the parent compound. This suggests that both the carboxyl and sulfate ends of oreganic acid contribute to the overall potency of the compound. One speculative possibility is that the sulfate group increases the affinity of the compound for the enzyme compared to that of the polar head group alone. The carboxyl and sulfate ends fill the polar end of the FPP binding pocket and have an additive effect. The effect of the sulfate group on the potency of oreganic acid is pronounced when one compares the activities of the trimethyl ester (Figure 1(2)) with the desulfated trimethyl ester (Figure 1(4)).

Oreganic acid is not a time-dependent inhibitor of the FPTase enzyme indicating that it associates readily and rapidly with the enzyme. Furthermore, oreganic

acid is equally active against FPTase when either Ki-Ras-CVIM or Ha-Ras-CVLS is used as the peptide acceptor substrates (Figure 2). It has been reported that FPTase has a 20-fold higher affinity for Ras-CVIM than Ras-CVLS (17, 18) and that mutations in Ki-ras-CVIM are by far the most frequent in human tumors (1). This raises the question of which Ras acceptor peptide to use in assays designed to screen for physiological relevant inhibitors of FPTase. Recently James et al. (8) reported that BZA-2B, a benzodiazepine peptidomimetic, was eight-fold more active when Ha-Ras-CVLS rather than Ki-Ras-CVIM was the peptide substrate. When BZA-2B was tested in cell-based assays of tumorigenicity it was less active than would have been predicted from the *in-vitro* FPTase data. It is encouraging to see that oreganic acid is equally active when either peptide substrate is used.

Kohl et al. (12) and others (2, 3, 7, 11, 14) have reported the development of compounds that are inhibitors of FPTase *in vitro*, inhibitors of ras-processing *in vivo* (in cell lines and nude mice) and enhance tumor regression in transgenic mice. Unfortunately, oreganic acid does not affect Ras processing in whole cell assays. This is probably due to the charged nature of the compound that precludes its entry into the cell. Masking of the charged groups by a pro-drug strategy may result in activity in whole cells. However, given the results with the methylated and desulfated compounds (Figure 1) it is unlikely that this will be a straight-forward process. The current challenge is to find microbial inhibitors of FPTase that exhibit *in vivo* activity.

REFERENCES

- Barbacid, M. (1987) *Annu. Rev. Biochem.* **56**, 779–827.
- Bishop, W. R., Bond, R., Petrin, J., Wang, L., Patton, R., Doll, R., Njoroge, G. C., Catino, J., Schwartz, J., Windsor, W., Syto, R., Schwartz, J., Carr, D., James, L., and Kirschmeier, P. (1995) *J. Biol. Chem.* **270**, 30611–30618.
- Garcia, A. M., Rowell, C., Ackermann, K., Kowalczyk, J. J., and Lewis, M. D. (1993) *J. Biol. Chem.* **268**, 18415–18418.
- Gibbs, J. B. (1992) *Semin. Cancer Biol.* **3**, 383–390.
- Gibbs, J. B., Pompilano, D. L., Mosser, S. D., Rands, E., Lingham, R. B., Singh, S. B., Scolnick, E. M., Kohl, N. E., and Oliff, A. (1993) *J. Biol. Chem.* **268**, 7617–7620.
- Gibbs, J. B., Oliff, A., and Kohl, N. E. (1994) *Cell* **77**, 175–178.
- James, G. L., Goldstein, J. L., Brown, M. S., Rawson, T. E., Somers, T. C., McDowell, R. S., Crowley, C. W., Lucas, B. K., Levinson, A. D., and Marsters, J. C. (1993) *Science* **260**, 1937–1942.
- James, G. L., Goldstein, J. L., and Brown, M. S. (1995) *J. Biol. Chem.* **270**, 6221–6226.
- Jayasuriya, H., Ball, R. G., Zink, D. L., Smith, J., Goetz, M. A., Jenkins, R. G., Nallin-Omstead, M., Silverman, K. C., Bills, G. F., Heck, J. V., Lingham, R. B., Cascales, C., Pelaez, F., and Singh, S. B. (1995) *J. Nat. Prod.* **58**, 986–991.
- Jayasuriya, H., Bills, G. F., Cascales, C., Zink, D. L., Goetz, M. A., Jenkins, R. G., Silverman, K. C., Lingham, R. B., and Singh, S. B. (1996) *Bioorg. Med. Chem. Lett.* **6**, 2081–2084.
- Kohl, N. E., Mosser, S. D., DeSolms, S. J., Giuliani, E. A., Pompilano, D. L., Graham, S. L., Smith, R. L., Scolnick, E. M., Oliff, A., Gibbs, J. B. (1993) *Science* **260**, 1934–1937.
- Kohl, N. E., Wilson, F. R., Mosser, S. D., Giuliani, E., DeSolms, S. J., Conner, M. W., Anthony, N. J., Holtz, W. J., Gomez, R. P., Lee, T. J., Smith, R. L., Graham, S. L., Hartman, G. D., Gibbs, J. B., and Oliff, A. (1994) *Proc. Natl. Acad. Sci.* **91**, 9141–9145.
- Kohl, N. E., Conner, M. W., Gibbs, J. B., Graham, S. L., Hartman, G. D., and Oliff, A. O. (1995) *Jour. Cell. Biochem.* **22**, 145–150.
- Lerner, E. C., Qian, Y., Hamilton, A. D., and Sebt, S. M. (1995) *J. Biol. Chem.* **270**, 26770–26773.
- Lingham, R. B., Silverman, K. C., Bills, G. F., Cascales, C., Sanchez, M., Jenkins, R. G., Gartner, S. E., Martin, I., Diez, M. T., Pelaez, F., Mochales, S., Kong, Y. L., Burg, R. W., Meinz, M. S., Huang, L., Nallin-Omstead, M., Mosser, S. D., Schaber, M. D., Omer, C. A., Pompilano, D. L., Gibbs, J. B., and Singh, S. B. (1993) *Appl. Microbiol. Biotechnol.* **40**, 370–374.
- Omer, C. A., Diehl, R. E., and Kral, A. M. (1995) *Meth. Enzymol.* **250**, 3–12.
- Omer, C. A., and Gibbs, J. B. (1994) *Mol. Micro.* **11**, 219–225.
- Reiss, Y., Stradley, S. J., Gierasch, L. M., Brown, M. S., and Goldstein, J. L. (1991) *Proc. Natl. Acad. Sci.* **88**, 732–736.
- Silverman, K. C., Cascales, C., Genilloud, O., Sigmund, J. M., Gartner, S. E., Koch, G. E., Gagliardi, M. M., Heimbuch, B. K., Nallin-Omstead, M., Sanchez, M., Diez, M. T., Martin, I., Garrity, G. M., Hirsch, C. F., Gibbs, J. B., Singh, S. S., and Lingham, R. B. (1995) *Appl. Microbiol. Biotechnol.* **43**, 610–616.
- Singh, S. B., Zink, D. L., Liesch, J. M., Goetz, M. A., Jenkins, R. G., Nallin-Omstead, M., Silverman, K. C., Bills, G. F., Mosley, R. T., Gibbs, J. B., Albers-Schonberg, G., and Lingham, R. B. (1993) *Tetrahedron* **49**, 5917–5926.
- Singh, S. B., Jones, E. T., Goetz, M. A., Bills, G. F., Nallin-Omstead, M., Jenkins, R. G., Lingham, R. B., Silverman, K. C., and Gibbs, J. B. (1994) *Tetrahedron Lett.* **27**, 4693–4696.
- Singh, S. B., Zink, D. L., Liesch, J. M., Ball, R. G., Goetz, M. A., Bolessa, E. A., Giacobbe, R. A., Silverman, K. C., Cascales, C., Gibbs, J. B., and Lingham, R. B. (1994a) *J. Org. Chem.* **59**, 6296–6302.
- Singh, S. B., Liesch, J. M., Lingham, R. B., Goetz, M. A., and Gibbs, J. B. (1994b) *J. Am. Chem. Soc.* **116**, 11606–11607.
- Singh, S. B., Liesch, J. M., Lingham, R. B., Silverman, K. C., Sigmund, J. M., and Goetz, M. A. (1995) *J. Org. Chem.* **60**, 7896–7901.
- Singh, S. B., Ball, R. G., Bills, G. F., Cascales, C., Gibbs, J. B., Goetz, M. A., Hoogsteen, K., Jenkins, R. G., Liesch, J. M., Lingham, R. B., Silverman, K. C., and Zink, D. L. (1996) *J. Org. Chem.* **61**, 7727–7737.

Yeast Protein Geranylgeranyltransferase Type-I: Steady-State Kinetics and Substrate Binding[†]

William G. Stirtan and C. Dale Poulter*

Department of Chemistry, University of Utah, Salt Lake City, Utah 84112

Received October 15, 1996; Revised Manuscript Received January 23, 1997[‡]

ABSTRACT: Protein geranylgeranyltransferase type-I (PGGTase-I) catalyzes alkylation of the cysteine residue in proteins containing a consensus C-terminal CaaX sequence ending in Leu or Phe by the C₂₀ hydrocarbon moiety in geranylgeranyl diphosphate (GGPP). A kinetic study of the alkylation reaction was conducted with a continuous assay based on the fluorescence enhancement that accompanies geranylgeranylation of dansyl-GCIII. The kinetic constants $k_{cat} = 0.34 \pm 0.01 \text{ s}^{-1}$, $K_M^G = 0.86 \pm 0.05 \mu\text{M}$ for GGPP, and $K_M^D = 1.6 \pm 0.1 \mu\text{M}$ for dansyl-GCIII were calculated from initial rates measured at varying concentrations of the substrates. Inhibitor studies were conducted with dead-end inhibitors for GGPP and the peptide substrate. Double reciprocal plots for the peptide mimic Cys-AMBA-Leu gave a competitive pattern when plotted against varying concentrations of dansyl-GCIII and an uncompetitive pattern against GGPP. Similar plots for 1-phosphono-(E,E,E)-geranylgeraniol, a dead-end inhibitor for GGPP, gave a competitive double reciprocal plot for varied concentrations of GGPP and induced potent substrate inhibition by dansyl-GCIII when dansyl-GCIII was the varied substrate. The dissociation constant (K_D) for the PGGTase-I-GGPP complex was $120 \pm 20 \text{ nM}$. These results are consistent with an ordered binding mechanism for PGGTase-I where GGPP adds before peptide.

The posttranslational modification of proteins in eukaryotic cells with hydrophobic C₁₅ farnesyl or C₂₀ geranylgeranyl isoprenoid units is a common phenomenon. The modification involves alkylation of a cysteine residue near the C-terminus of the proteins to form a stable thioether and confers lipophilic properties to the proteins essential for their biological activity. Prenylated proteins fulfill a variety of important roles, including those in signal transduction and regulation of vesicular traffic (for a recent review, see Zhang & Casey, 1996).

Three protein prenyltransferases, a protein farnesyltransferase (PFTase),¹ a protein geranylgeranyltransferase type-I (PGGTase-I), and a protein geranylgeranyltransferase type-II (PGGTase-II), catalyze the alkylation reactions. PFTase and PGGTase-I modify cysteine residues in carboxy-terminal CaaX motifs in which "a" is an aliphatic amino acid, and "X" is one of several possible residues. When "X" is Ala, Met, Ser, Cys, or Gln, the protein substrate is farnesylated, and when "X" is Leu or Phe, the protein is geranylgeranylated (Moores et al., 1991; Reiss et al., 1991; Yokoyama et al., 1991; Omer et al., 1993; Caplin et al., 1994). Protein substrates for PFTase include fungal mating factors, nuclear lamins, and Ras G-proteins (Maltese, 1990; Moores et al., 1991; Clark, 1992). Substrates for PGGTase-I include the γ subunit of neural G-proteins and several Ras-related

G-proteins (Maltese, 1990; Mumby et al., 1990; Kawata et al., 1990; Casey et al., 1991; Yamane et al., 1991). Following prenylation, the carboxy-terminal aaX tripeptide is removed, and the new carboxy-terminal cysteine is often methylated. PGGTase-II, often called Rab geranylgeranyltransferase, catalyzes alkylation of both cysteine residues in Rab proteins containing carboxy-terminal CC, CXCX, or CXC motifs (Seabra et al., 1992; Farnsworth et al., 1994).

All three protein prenyltransferases are α/β dimers, and each shares a high degree of similarity at the amino acid level. PFTase and PGGTase-I contain a common α subunit in combination with distinctive β subunits, which confer different selectivities for the two enzymes toward their isoprenoid and protein substrates. For PGGTase-II, an escort protein to bring the protein substrate to the catalytic heterodimer and to escort the geranylgeranylated product to membrane is required in addition to the catalytic heterodimer (Andres et al., 1993; Fujimura et al., 1994; Jiang & Ferro-Novick, 1994).

There is considerable interest in understanding how protein prenyltransferases bind their substrates because of the prominent roles modified proteins play in eukaryotic cells, including regulation of cell division and control of vesicle fusion (Gibbs et al., 1994). In kinetic studies with bovine PFTase, it was suggested that the enzyme binds substrates by a random mechanism (Pompliano et al., 1992), but with a preference for adding FPP before peptide (Pompliano et al., 1993). However, recent studies with the human (Furfine et al., 1995) and yeast (Dolence et al., 1995) forms of PFTase support an ordered addition of substrates.

PGGTase-I has been purified from bovine brain (Moomaw & Casey, 1992; Yokoyama & Gelb, 1993), and the yeast (Mayer et al., 1992; Stirtan & Poulter, 1995), rat, and human (Zhang et al., 1994a,b) enzymes have been purified from recombinant organisms. Steady-state kinetic studies with

[†] This work was supported by the National Institutes of Health Grant GM 21328.

* To whom correspondence should be addressed. Fax: (801) 581-4391. E-mail: Poulter@chemistry.chem.utah.edu.

[‡] Abstract published in *Advance ACS Abstracts*, April 1, 1997.

Abbreviations: PFTase, protein farnesyltransferase; PGGTase-I, protein geranylgeranyltransferase type-I; PGGTase-II, protein geranylgeranyltransferase type-II; FPP, farnesyl diphosphate; GGPP, geranylgeranyl diphosphate; 1-P-GGOH, 1-phosphono-(E,E,E)-geranylgeraniol; dansyl-GCIII, dansyl-Gly-Cys(S-geranylgeranyl)-Ile-Ile-Leu; AMBA, 3-(aminomethyl)benzoic acid; Tris, tris(hydroxymethyl)aminomethane; EDTA, ethylenediaminetetraacetic acid; DMSO, dimethyl sulfoxide; TLC, thin-layer chromatography; DTT, dithiothreitol.

mammalian PGGTase-I and reversible dead-end inhibitors suggested that the substrate binding mechanism was random (Zhang et al., 1994b; Yokoyama et al., 1995) but, like PFTase, appeared to be "functionally" ordered with geranylgeranyl diphosphate (GGPP) adding before the protein substrate (Yokoyama et al., 1995). Recently, we described the purification of recombinant yeast PGGTase-I and a continuous fluorescence assay to monitor enzyme activity (Stirtan & Poulter, 1995). We now present steady-state kinetic and inhibition studies which demonstrate that yeast PGGTase-I binds substrates to give a catalytically competent ternary complex by an ordered mechanism with no evidence of a random component.

MATERIALS AND METHODS

Materials. [^3H]GGPP (19.3 Ci mmol $^{-1}$) was purchased from DuPont New England Nuclear Research Products (Boston, MA). Unlabeled GGPP was synthesized from geranylgeranyl bromide and tris(tetrabutylammonium) pyrophosphate (Davisson et al., 1986). *n*-Dodecyl β -D-maltoside was purchased from Calbiochem, and dansylglycine was from Sigma (St. Louis, MO). Dansyl-GCIII was prepared by solid-phase synthesis methods on an ABI peptide synthesizer Model 431A. 1-Phosphono-(*E,E,E*)-geranylgeraniol (1-P-GGOH) was prepared as described previously (Yokoyama et al., 1995). Cys-AMBA-Leu (Nigam et al., 1993) was provided by Dr. Andrew Hamilton. Recombinant yeast PGGTase-I was expressed in *Escherichia coli* (JM101/pWGS-1-257B) and purified as described previously (Stirtan & Poulter, 1995). Fluorescence data were collected on a Spex FluoroMax spectrofluorimeter. Quartz cuvettes were purchased from NSG Precision Cells Inc.

Methods. Preparation of Solutions. Stock solutions of GGPP (10–15 mM) were prepared in 25 mM NH_4HCO_3 , and concentrations of GGPP were determined by phosphate analysis (Reed and Rilling, 1976). Stock solutions of dansyl-GCIII (~300 μM) were prepared by dissolving the dansylated peptide in peptide buffer (50 mM Tris-HCl, pH 7.5, 0.1 mM EDTA, 5 mM DTT, 0.020% *n*-Dodecyl β -D-maltoside) or with detergent-free peptide buffer for inhibition studies. The concentration of dansyl-GCIII was determined from a standard curve of A_{340} versus the concentration of dansylglycine, in the same buffer. Stock solutions of dansyl-GCIII, the geranylgeranylated product of the PGGTase-I reaction, were prepared and used in calibration studies exactly as described previously (Stirtan & Poulter, 1995).

Prenyltransferase Assay. PGGTase-I was assayed using a continuous fluorescence assay based on the large fluorescence enhancement which accompanies geranylgeranylation of a dansylated pentapeptide (Pickett et al., 1995; Stirtan & Poulter, 1995). Assays were carried out at 30 °C in prewarmed cuvettes (3 mm 2) using a thermostated cuvette holder. Buffer concentrations in the final assay volume (220 μL) for all kinetic studies were 50 mM Tris-HCl, pH 7.5, 5.0 mM DTT, 1.0 mM MgCl_2 , 10 μM ZnCl_2 , 0.020% *n*-dodecyl β -D-maltoside. Typically, solutions of dansyl-GCIII (10 μL) and GGPP (10 μL) were added to assay buffer (53 mM Tris-HCl, pH 7.5, 5.3 mM DTT, 1.1 mM MgCl_2 , 11 μM ZnCl_2 , 0.021% *n*-Dodecyl β -D-maltoside) (190 μL). The mixture was preincubated at 30 °C for 5 min before the reaction was initiated with enzyme (10 μL , ~180 ng) previously diluted with assay buffer to the appropriate concentration. The sample was vigorously mixed, a 200 μL -

portion of the reaction was immediately transferred to a prewarmed cuvette, and the fluorescence intensity was measured for 5 min. Excitation and emission wavelengths were 340 and 486 nm, respectively, with a bandpass of 5.1 nm for both excitation and emission monochromators, unless otherwise noted. The rate of change in fluorescence intensity (cps s $^{-1}$) was converted to units of velocity ($\mu\text{M s}^{-1}$) given the following conversion factor ($m = 3.6 \times 10^6$ cps μM^{-1}) and fluorescence enhancement ($E = 10$) (Stirtan & Poulter, 1995).

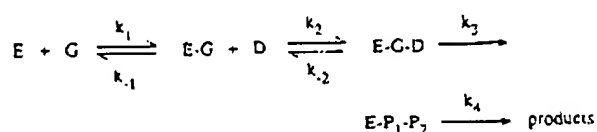
Inhibition Studies. Stock solutions of 1-P-GGOH were prepared in DMSO. Stock solutions of Cys-AMBA-Leu were prepared in H $_2$ O, and DTT was added to 5 mM. The concentration of Cys-AMBA-Leu was determined by thiol titration prior to the addition of DTT. For inhibition studies, GGPP solutions were prepared in 25 mM NH_4HCO_3 /0.44% *n*-Dodecyl β -D-maltoside to reduce variation in duplicate measurements at low GGPP concentrations which can arise from GGPP adsorption to pipette tips and microcentrifuge tubes (Zhang et al., 1994b). Typically, solutions of GGPP (10 μL), dansyl-GCIII (10 μL), and inhibitor (10 μL) were added to detergent-free assay buffer (180 μL), preincubated at 30 °C for 5 min, and initiated with PGGTase-I as described above. A bandpass of 6.4 or 7.6 nm was used in all inhibition studies. The conversion factor at each slit width was determined in separate calibration experiments as described previously (Stirtan & Poulter, 1995).

The ability of PGGTase-I to geranylgeranilate Cys-AMBA-Leu was examined using a TLC assay similar to that reported for PFTase (Goldstein et al., 1991). Cys-AMBA-Leu (230 μM) was incubated with [^3H]GGPP (110 mCi mmol $^{-1}$, 8.5 μM) and PGGTase-I (160 ng) in 50 mM Tris-HCl, pH 7.5, 5.0 mM DTT, 1.0 mM MgCl_2 , 10 μM ZnCl_2 , 0.020% *n*-Dodecyl β -D-maltoside (25 μL) for 30 min at 30 °C. The entire reaction mixture was spotted onto a 4 \times 18 cm analytical aluminum-backed silica TLC plate (Whatman) and allowed to dry. The plate was eluted with *n*-propyl alcohol/ammonium hydroxide/water (6:3:1 v/v/v), and cut into 1 cm strips. Scintillation fluid (CryoScint, ICN) (10 mL) was added, and the samples were counted for radioactivity.

Measurement of the Dissociation Constant for GGPP. The K_D for GGPP dissociating from the PGGTase-I-GGPP complex was determined at 30 °C using [^3H]GGPP (1 Ci mmol $^{-1}$) in buffer containing 50 mM Tris-HCl, pH 7.5, 5.0 mM DTT, 1.0 mM MgCl_2 , 10 μM ZnCl_2 , 0.020% *n*-Dodecyl β -D-maltoside. Solutions (100 μL) containing PGGTase-I (0.21 μM) and [^3H]GGPP (0.065–0.58 μM) were incubated at 30 °C for 30 min and then transferred to a Microcon-30 (Amicon). The sample was centrifuged (ca. 10 s), allowing a small volume (10–15 μL) to pass through the membrane. A portion (10 μL) was taken from the top compartment and counted to determine the total GGPP concentration. The free GGPP concentration was determined from the bottom compartment after correcting for membrane retention using a correction factor obtained in an identical experiment, except in the absence of enzyme. K_D was calculated by fitting the data to the following equation: $[\text{bound GGPP}] = [\text{E}]/([\text{free GGPP}]/(K_D + [\text{free GGPP}]))$.

Equations for Analysis of Kinetic Data. For the mechanism shown in Scheme 1, the dependence of the steady-state velocity on substrate concentration for PGGTase-I is shown in eq 1, where G and D are the concentrations of

Scheme 1: An Ordered Bireactant Mechanism



GGPP and dansyl-GCIIIL, respectively. K_M^G and K_M^D are the K_M values for GGPP and dansyl-GCIIIL at saturating second substrate concentration, respectively. K_s is the dissociation constant for GGPP, v is the velocity of product formation, and V is the maximal velocity of product formation.

$$v = \frac{VGD}{K_s K_M^D + K_M^D G + K_M^G D + GD} \quad (1)$$

A graphical analysis of double reciprocal plots was used to determine the mode of inhibition, and data were fit to the appropriate rate equation using a nonlinear regression analysis to obtain inhibition constants (Leatherbarrow, 1992). Equations 2 and 3 were used for competitive and uncompetitive inhibition. Data for substrate inhibition were fit to eq 4, where V , K , and K_i are apparent constants (Danenberg & Danenberg, 1978).

$$v = \frac{VA}{K(1 + I/K_i) + A} \quad (2)$$

$$v = \frac{VA}{K + A(1 + I/K_i)} \quad (3)$$

$$v = \frac{VA}{K + A + A^2/K_i} \quad (4)$$

RESULTS

Steady-State Kinetic Studies. Earlier kinetic studies with mammalian PGGTase-I suggested that the enzyme binds substrates by a mechanism which is formally random (Zhang et al., 1994b; Yokoyama et al., 1995) but has a kinetically preferred pathway in which GGPP binds before peptide (Yokoyama et al., 1995). Using dead-end reversible inhibitors, we found that yeast PGGTase-I bound GGPP before dansyl-GCIIIL by an ordered mechanism with no evidence for a random component. We examined the steady-state mechanism for recombinant yeast PGGTase-I using a continuous fluorescence assay based on the large fluorescence enhancement that accompanies geranylgeranylation of the dansylated pentapeptide substrate dansyl-GCIIIL (Stirtan & Poulter, 1995) to measure initial velocities. This assay is more precise than single point assays that measure incorporation of radioactivity into prenylated peptides. Steady-state kinetic constants were obtained by fitting hyperbolic plots of initial velocity versus GGPP (G) concentration, at several concentrations of dansyl-GCIIIL (D) (Figure 1), to eq 1: $K_M^G = 0.94 \pm 0.03 \mu\text{M}$, $K_M^D = 1.8 \pm 0.2 \mu\text{M}$, $k_{cat} = 0.35 \pm 0.01 \text{ s}^{-1}$, and $K_s = 14 \pm 80 \text{ nM}$. Double reciprocal plots of the initial velocities versus the concentration of GGPP, at different concentrations of dansyl-GCIIIL, were parallel over substrate concentrations between $0.5K_M$ and $6K_M$, consistent with $K_s \ll K_M^G$ (Segel, 1975).

Given the uncertainty in the calculated value for K_s , the dissociation constant for GGPP was determined in a separate

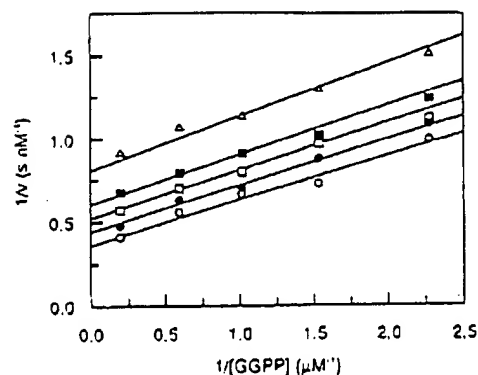
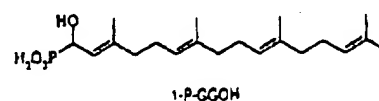
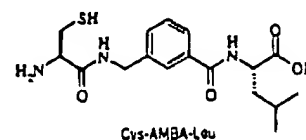


FIGURE 1: A double reciprocal plot of initial velocities versus GGPP concentrations at fixed concentrations of dansyl-GCIIIL. The concentration of GGPP was varied between 0.5 and 5 μM at several dansyl-GCIIIL concentrations: 9.5 (○), 3.8 (●), 2.3 (□), 1.7 (■), and 1.0 μM (Δ). Assays were carried out in duplicate under standard assay conditions and lines were calculated using the appropriate equation (see Materials and Methods).

experiment using a microfiltration assay. The measured value for $K_D = 120 \pm 20 \text{ nM}$ is similar to that reported previously for the yeast PFTase-FPP complex (Dolence et al., 1995) and is significantly larger than that observed for mammalian PGGTase-I (Yokoyama et al., 1995). If K_s in eq 1 is fixed at the experimentally determined K_D for GGPP (120 nM), a very modest change in the calculated steady-state kinetic constants is observed: $K_M^G = 0.86 \pm 0.05 \mu\text{M}$, $K_M^D = 1.6 \pm 0.1 \mu\text{M}$, and $k_{cat} = 0.34 \pm 0.01 \text{ s}^{-1}$.

Kinetic Studies with Dead-End Reversible Inhibitors. Compounds that are dead-end inhibitors for GGPP and dansyl-GCIIIL were used to distinguish between random and ordered binding mechanisms for addition of substrates to PGGTase-I. Since uncompetitive inhibition is not observed with substrate analogs possessing significant activity (Spector and Cleland, 1981), a thin-layer chromatographic assay was used to confirm that Cys-AMBA-Leu (Nigam et al., 1993) was completely inert towards geranylgeranylation by PGGTase-I (data not shown). Double reciprocal plots of initial velocities for varied dansyl-GCIIIL and GGPP concentrations at different fixed concentrations of Cys-AMBA-Leu are shown in Figure 2. When dansyl-GCIIIL was the varied substrate, in the presence of a fixed concentration of GGPP, Cys-AMBA-Leu gave a competitive inhibition profile ($K_i = 78 \pm 8 \mu\text{M}$) (Figure 2a). When the concentration of GGPP was varied at fixed concentrations of dansyl-GCIIIL, the data for inhibition by Cys-AMBA-Leu showed uncompetitive inhibition ($K_i = 140 \pm 10 \mu\text{M}$) (Figure 2b), consistent with an ordered kinetic mechanism.

A hydroxyphosphonic acid analog of GGPP, 1-P-GGOH, was a competitive inhibitor of yeast PGGTase-I when GGPP



was varied (Figure 3a). The inhibition constant for 1-P-GGOH ($K_i = 0.20 \pm 0.05 \mu\text{M}$) is similar to the value

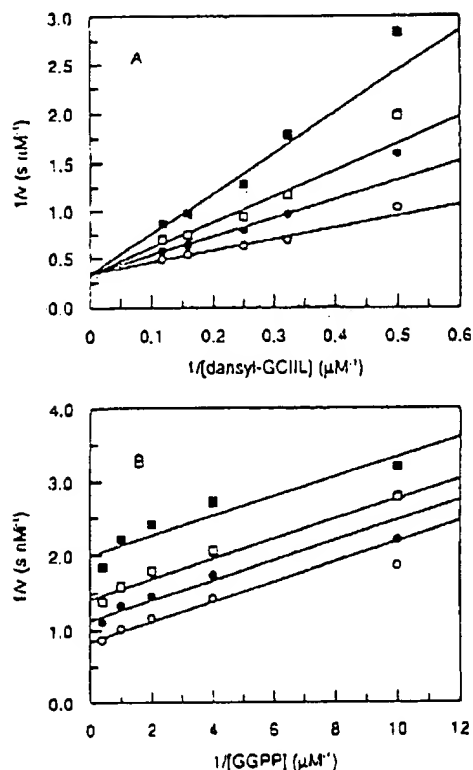


FIGURE 2: Inhibition of PGGTase-I by Cys-AMBA-Leu. (A) A double reciprocal plot of initial velocity versus dansyl-GCIII concentration at 0 (O), 50 (●), 100 (□), 200 μM (■) Cys-AMBA-Leu and a fixed unsaturating concentration of GGPP (1.2 μM). (B) A double reciprocal plot of initial velocity versus GGPP concentration at 0 (O), 50 (●), 100 (□), or 200 μM (■) Cys-AMBA-Leu and a fixed unsaturating concentration of dansyl-GCIII (2.9 μM). Each assay was performed in duplicate and the calculated lines were obtained using the appropriate equation (see Materials and Methods).

obtained for the mammalian enzyme (Yokoyama et al., 1995). Furthermore, in the presence of unsaturating concentrations of GGPP, 1-P-GGOH induced substrate inhibition by dansyl-GCIII (Figure 3b).

These results are consistent with an ordered mechanism, where the dead-end inhibitor that is competitive with the first substrate induces substrate inhibition by the second substrate (Fromm, 1967; Danenberg & Danenberg, 1978; Cleland, 1990). This scenario is illustrated for the ordered mechanism shown in Scheme 2, where dansyl-GCIII (D) binds to the enzyme-1-P-GGOH complex to form an inactive ternary E·I·D complex. An increase in the concentration of dansyl-GCIII (D) increases the concentration of the E·I·D complex. Since binding and, by the principle of microscopic reversibility, dissociation is ordered, the inhibitor is unable to dissociate prior to D. Thus, the amount of enzyme available to bind GGPP (G) is reduced. Conversely, in a random mechanism where the dissociation of each substrate is unaffected by the other substrate, induced substrate inhibition is not observed since the inhibitor would be free to dissociate from the inactive E·I·D complex to form the productive complex E·D. We were unable to extract individual inhibition constants from this data using the full rate expression describing the induced substrate inhibition (Danenberg & Danenberg, 1978; Cleland, 1990) shown in Scheme 2. Apparent Michaelis and inhibition constants for dansyl-GCIII (K_M^D and K_i^D), for different fixed concentrations of

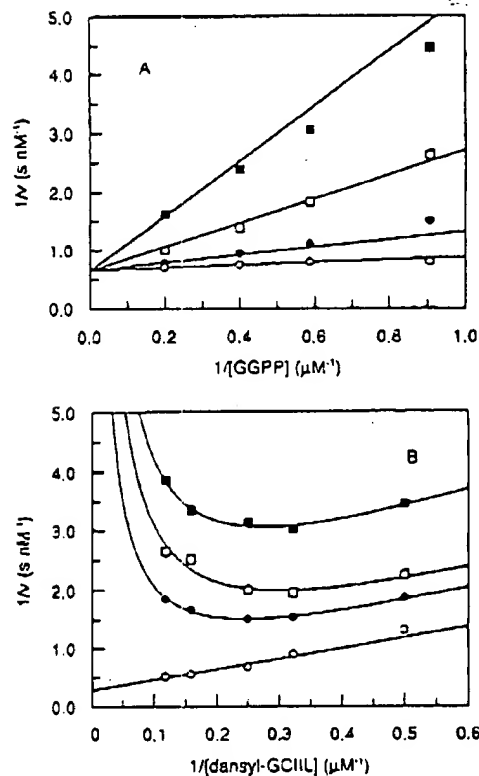
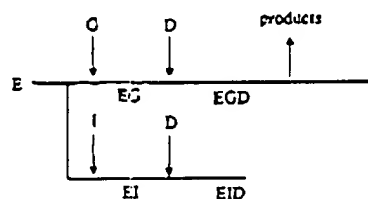


FIGURE 3: Inhibition of PGGTase-I by 1-P-GGOH. (A) A double reciprocal plot of initial velocity versus GGPP concentration at 0 (O), 0.40 (●), 1.6 (□), or 4.0 μM (■) 1-P-GGOH and a fixed unsaturating concentration of dansyl-GCIII (4.0 μM). (B) A double reciprocal plot of initial velocity versus dansyl-GCIII concentration at 0 (O), 7.7 (●), 15 (□), or 30 μM (■) 1-P-GGOH and a fixed unsaturating concentration of GGPP (1 μM). The apparent Michaelis and inhibition constants for dansyl-GCIII (K_M^D and K_i^D) at the various 1-P-GGOH concentrations, obtained from eq 4 are as follows: 0 μM 1-P-GGOH, K_M^D = 6.3 μM ; 7.7 μM 1-P-GGOH, K_M^D = 10 μM , K_i^D = 1.6 μM ; 15 μM 1-P-GGOH, K_M^D = 6.2 μM , K_i^D = 1.7 μM ; 30 μM 1-P-GGOH, K_M^D = 3.8 μM , K_i^D = 3.4 μM . Each assay was performed in duplicate and the calculated lines were obtained using the appropriate equation (see Materials and Methods).

Scheme 2: An Ordered Bireactant Mechanism with Induced Substrate Inhibition



1-P-GGOH, were obtained from fitting the data in Figure 3b to eq 4 and are given in the figure legend. A plot of $1/v$ versus the dansyl-GCIII concentration, in the region of the induced substrate inhibition (3–9 μM dansyl-GCIII) at 1 μM GGPP and 30 μM 1-P-GGOH is linear (data not shown), consistent with the prediction from Scheme 2 that there is a high degree of order in this reaction and that the rate for the reaction approaches zero as the concentration of dansyl-GCIII is raised. Conversely, a significant contribution from a random pathway would result in partial substrate inhibition and a hyperbolic plot of $1/v$ versus dansyl-GCIII (Danenberg & Cleland, 1975).

Induced substrate inhibition by dansyl-GCIIIL should be competitive with respect to GGPP (G), since at a saturating concentration of GGPP all enzyme should be in the E-G form. Conversely, a noncompetitive pattern is expected if the substrate inhibition resulted from a different mechanism, such as dansyl-GCIIIL binding to a secondary site on the enzyme. A double reciprocal plot in which GGPP was varied from 1 to 7 μM at three different inhibitory levels of dansyl-GCIIIL (2.9, 5.7, and 8.5 μM) in the presence of 14 μM 1-P-GGOH gave a competitive inhibition pattern consistent with the mechanism presented in Scheme 2, although a small deviation from the expected competitive pattern was observed for the lowest concentration of dansyl-GCIIIL, where substrate inhibition was weakest. Values of K_{1s} (5 μM) and K_M^P (4 μM) were determined from a slope replot.

DISCUSSION

Previous steady-state kinetic studies with the mammalian form of PGGTase-I indicated that the enzyme binds substrates by a random sequential mechanism (Zhang et al., 1994b; Yokoyama et al., 1995). Isotope trapping experiments, however, suggested that an ordered binding of substrates was required to produce a competent ternary complex. Enzyme-bound GGPP was trapped as product before dissociating from the enzyme upon addition of a peptide substrate; whereas, enzyme-bound peptide was not trapped by GGPP (Yokoyama et al., 1995). These results were interpreted to suggest that PGGTase-I adds substrates by a "formally random," mechanism, while possessing a kinetically preferred pathway where GGPP binds before peptide (Yokoyama et al., 1995). Similar results were reported for mammalian PFTases (Pompliano et al., 1993; Furfine et al., 1995). However, a steady-state kinetic analysis of the yeast enzyme with dead-end inhibitors for FPP and peptide gave classic double reciprocal plots for an ordered mechanism where FPP adds first (Dolence et al., 1995).

PFTases, from a variety of sources (Dolence et al., 1995) and mammalian PGGTase-I (Yokoyama et al., 1995) are inhibited by their peptide substrates. Dolence and co-workers (1995) concluded for the yeast enzymes that inhibition probably resulted from nonproductive binding of the peptide in a manner that blocked entry of FPP into the catalytic site. Our earlier studies with yeast PGGTase-I gave no indication of substrate inhibition over a range of peptide concentrations. $0.5 \leq K_M \leq 5$ (Stirtan & Poulter, 1995). Since the amino acid sequences of PFTases and PGGTases have substantial similarity, indeed they have a common subunit in their host organisms, one anticipates similar binding mechanisms for the two enzymes. The absence of substrate inhibition for yeast PGGTase-I presumably resulted from a higher dissociation constant for the enzyme-peptide complex. However, when the yeast enzyme was incubated with 1-P-GGOH, an unreactive analog of GGPP, the peptide substrate became a potent inhibitor. These results are consistent with an ordered addition of substrates where binding of the second substrate, in this case peptide, is enhanced substantially by binding of the first.

The Michaelis and dissociation constants for GGPP with yeast PGGTase-I are significantly higher than previously reported for its mammalian counterpart (Zhang et al., 1994b; Yokoyama et al., 1995). A similar trend was found for PFTases (Cassidy et al., 1995; Dolence et al., 1995). The

phenomenon has been reported for other prenyltransferases and may reflect intrinsic differences in the levels of intermediates in the isoprenoid pathways in yeast and mammals.

In contrast to mammalian PGGTase-I, the recombinant yeast enzyme gave double reciprocal plots with dead-end inhibitors that were fully consistent with an ordered mechanism. Cys-AMBA-Leu was competitive against dansyl-GCIIIL and uncompetitive against GGPP. 1-P-GGOH gave a classic competitive profile against GGPP and induced substrate inhibition by dansyl-GCIIIL in a manner consistent with the binding mechanism outlined in Scheme 2.

In summary, steady state kinetic studies of recombinant yeast PGGTase-I indicate that the enzyme binds substrates by an ordered mechanism with addition of GGPP before peptide. In contrast to other PFTases and PGGTases-I, the yeast enzyme is not inhibited by its peptide substrate at concentrations up to 5.0 K_M . However, strong substrate inhibition is seen in the presence of a dead-end inhibitor for GGPP, indicating a substantial synergistic effect in substrate binding. These results, taken together with the uncompetitive inhibition profile from our dead-end peptide substrate analog, firmly support an ordered mechanism.

ACKNOWLEDGMENTS

We would like to thank Dr. Andrew Hamilton for a generous gift of Cys-AMBA-Leu, and Dr. David Witter for providing 1-phosphono-(*E,E,E*)-geranylgeraniol. Dansylated peptides were synthesized and purified by Dr. R. Schackmann of the Utah Regional Cancer Center Protein/DNA Core Facility.

REFERENCES

- Andres, D. A., Seabra, M. C., Brown, M. S., Armstrong, S. A., Smeland, T. E., Cremers, F. P. M., & Goldstein, J. L. (1993) *Cell* 73, 1091-1099.
- Caplin, B. E., Hettich, L. A., & Marshall, M. S. (1994) *Biochim. Biophys. Acta* 1205, 39-48.
- Casey, P. J., Thissen, J. A., & Moomaw, J. F. (1991) *Proc. Natl. Acad. Sci. U.S.A.* 88, 8631-8635.
- Cassidy, P. B., Dolence, J. M., & Poulter, C. D. (1995) *Methods Enzymol.* 250, 30-43.
- Clark, S. (1992) *Annu. Rev. Biochem.* 61, 355-386.
- Cleland, W. W. (1990) *The Enzymes*, Chapter III, pp 119-120. Academic Press, San Diego, CA.
- Danenberg, P. V., & Cleland, W. W. (1975) *Biochemistry* 14, 28-39.
- Danenberg, P. V., & Danenberg, K. D. (1978) *Biochemistry* 17, 4018-4024.
- Davisson, V. J., Woodsides, A. B., Neal, T. R., Stremmer, K. E., Muchlbacher, M., & Poulter, C. D. (1996) *J. Org. Chem.* 61, 4768-4779.
- Dolence, J. M., Cassidy, P. B., Mathis, J. R., & Poulter, C. D. (1995) *Biochemistry* 34, 16687-16694.
- Farnsworth, C. C., Seabra, M. C., Ericsson, L. H., Gelb, M. H., & Glomset, J. A. (1994) *Proc. Natl. Acad. Sci. U.S.A.* 91, 11965-11967.
- Fromm, H. J. (1967) *Biochim. Biophys. Acta* 139, 221-230.
- Fujimura, K., Tanaka, K., Nakano, A., & Toe-e, A. (1994) *J. Biol. Chem.* 269, 9205-9212.
- Furfine, E. S., Leban, J. J., Landavano, A., Moomaw, J. F., & Casey, P. J. (1995) *Biochemistry* 34, 6857-6862.
- Gibbs, J. B., Oliff, A., & Kohl, N. E. (1994) *Cell* 77, 175-178.
- Goldstein, J. L., Brown, M. S., Sradley, S. J., Reiss, Y., & Gierusch, L. M. (1991) *J. Biol. Chem.* 266, 15575-15578.
- Jiang, Y., & Fermo-Novick, S. (1994) *Proc. Natl. Acad. Sci. U.S.A.* 91, 4377-4381.

- Kawata, M., Farnsworth, C. C., Yoshida, Y., Gelb, M. H., Glomset, J. A., & Takai, Y. (1990) *Proc. Natl. Acad. Sci. U.S.A.* 87, 8960-8964.
- Leatherbarrow, R. J. (1992) *GraFit Version 3.01*, Erithicus Software Ltd., Staines, U.K.
- Maltese, W. A. (1990) *FASEB J.* 4, 3319-3328.
- Mayer, M. L., Caplin, B. E., & Marshall, M. S. (1992) *J. Biol. Chem.* 267, 20589-20593.
- Moomaw, J. F., & Casey, P. J. (1992) *J. Biol. Chem.* 267, 17433-17443.
- Moore, S. L., Schaber, M. D., Mosser, S. D., Rands, E., O'Hara, M. B., Garsky, V. M., Marshall, M. S., Pompliano, D. L., & Gibbs, J. B. (1991) *J. Biol. Chem.* 266, 14603-14610.
- Mumby, S. M., Casey, P. J., Gilman, A. G., Gutowski, S., & Sternweis, P. C. (1990) *Proc. Natl. Acad. Sci. U.S.A.* 87, 5873-5877.
- Nigam, M., Seong, C.-M., Qian, Y., Hamilton, A. D., & Sefti, S. M. (1993) *J. Biol. Chem.* 268, 20695-20698.
- Omer, C. A., Kral, A. M., Diehl, R. E., Prendergast, G. C., Powers, S., Allen, C. M., Gibbs, J. B., & Kohl, N. E. (1993) *Biochemistry* 32, 5167-5176.
- Pickert, W. C., Zhang, F. L., Silverstrim, C., Schow, S. R., Wick, M. M., & Kerwar, S. S. (1995) *Anal. Biochem.* 225, 60-63.
- Pompliano, D. L., Rands, E., Schaber, M. D., Mosser, S. D., Anthony, N. J., & Gibbs, J. B. (1992) *Biochemistry* 31, 3800-3807.
- Pompliano, D. L., Schaber, M. D., Mosser, S. D., Omer, C. A., Shafer, J. A., & Gibbs, J. B. (1993) *Biochemistry* 32, 8341-8347.
- Reed, B. C., & Rilling, H. C. (1976) *Biochemistry* 15, 3739-3745.
- Reiss, Y., Stradley, S. J., Gierasch, L. M., Brown, M. S., & Goldstein, J. L. (1991) *Proc. Natl. Acad. Sci. U.S.A.* 88, 732-736.
- Scabra, M. C., Goldstein, J. L., Sudhof, T. C., & Brown, M. S. (1992) *J. Biol. Chem.* 267, 14497-14503.
- Segel, I. H. (1975) *Enzyme Kinetics*, pp 564-565, John Wiley, New York.
- Spector, T., & Cleland, W. W. (1981) *Biochem. Pharmacol.* 30, 1-7.
- Stirtan, W. G., & Poulter, C. D. (1995) *Arch. Biochem. Biophys.* 321, 182-190.
- Yamane, H. K., Farnsworth, C. C., Xie, H., Evans, T., Howald, W. N., Gelb, M. H., Glomset, J. A., Clark, S., & Fung, B. K.-K. (1991) *Proc. Natl. Acad. Sci. U.S.A.* 88, 286-290.
- Yokoyama, K., & Gelb, M. H. (1993) *J. Biol. Chem.* 268, 4055-4060.
- Yokoyama, K., Goodwin, G. W., Ghomashchi, F., Glomset, J. A., & Gelb, M. H. (1991) *Proc. Natl. Acad. Sci. U.S.A.* 88, 5302-5306.
- Yokoyama, K., McGeady, P., & Gelb, M. H. (1995) *Biochemistry* 34, 1344-1354.
- Zhang, F. L., Diehl, R. E., Kohl, N. E., Gibbs, J. B., Giros, B., Casey, P. J., & Omer, C. A. (1994a) *J. Biol. Chem.* 269, 3175-3180.
- Zhang, F. L., Moomaw, J. F., & Casey, P. J. (1994b) *J. Biol. Chem.* 269, 23465-23470.
- Zhang, F. L., & Casey, P. J. (1996) *Annu. Rev. Biochem.* 65, 241-269.

B1962579C

Phase I and Pharmacokinetic Study of the Oral Farnesyl Transferase Inhibitor SCH 66336 Given Twice Daily to Patients With Advanced Solid Tumors

By Ferry A.L.M. Eskens, Ahmad Awada, David L. Cutler, Maja J.A. de Jonge, Gré P.M. Luyten, Marije N. Faber, Paul Statkevich, Alex Sparreboom, Jaap Verweij, Axel-R. Hanauske, and Martine Piccart for the European Organization for Research and Treatment of Cancer Early Clinical Studies Group

Purpose: A single-agent dose-escalating phase I and pharmacokinetic study on the farnesyl transferase inhibitor SCH 66336 was performed to determine the safety profile, maximum-tolerated dose, and recommended dose for phase II studies. Plasma and urine pharmacokinetics were determined.

Patients and Methods: SCH 66336 was given orally bid without interruption to patients with histologically or cytologically confirmed solid tumors. Routine antiemetics were not prescribed.

Results: Twenty-four patients were enrolled onto the study. Dose levels studied were 25, 50, 100, 200, 400, and 300 mg bid. Pharmacokinetic sampling was performed on days 1 and 15. At 400 mg bid, the dose-limiting toxicity (DLT) consisted of grade 4 vomiting, grade 4 neutropenia and thrombocytopenia, and the combination of grade 3 anorexia and diarrhea with reversible grade 3 plasma creatinine elevation. After dose reduction, at 300 mg bid, the DLTs consisted of grade 4 neutropenia, grade 3 neurocortical toxicity,

and the combination of grade 3 fatigue with grade 2 nausea and diarrhea. The recommended dose for phase II studies is 200 mg bid, which was found feasible for prolonged periods of time. Pharmacokinetic analysis showed a greater than dose-proportional increase in drug exposure and peak plasma concentrations, with increased parameters at day 15 compared with day 1, indicating some accumulation on multiple dosing. Plasma half-life ranged from 4 to 11 hours and seemed to increase with increasing doses. Steady-state plasma concentrations were attained at days 7 through 14. A large volume of distribution at steady-state indicated extensive distribution outside the plasma compartment.

Conclusion: SCH 66336 can be administered safely using a continuous oral bid dosing regimen. The recommended dose for phase II studies using this regimen is 200 mg bid.

J Clin Oncol 19:1167-1175. © 2001 by American Society of Clinical Oncology.

IN MAMMALIAN CELLS, three functional *ras* genes are found. *K-ras*, *N-ras*, and *H-ras* genes encode for K-Ras, N-Ras, and H-Ras proteins, respectively. Ras is synthesized as a soluble and biologically inactive protein that undergoes several posttranslational modifications before being localized to the inner surface of the plasma membrane, where it exerts its activity as transducer of various extracellular growth-promoting stimuli. An essential step in the posttranslational processing of Ras is farnesylation, the addition of a farnesyl or C₁₅ isoprenoid moiety from farnesyl diphosphate to the cysteine residue at the C-terminal side of Ras. Farnesyl transferase is the crucial enzyme in this process.¹⁻¹⁰ Mutations in one or more *ras* genes are frequently found in various human tumor types in variable incidence.^{3,8,10} Mutated *ras* oncogenes encode for oncoproteins that are synthesized in a way completely comparable to the synthesis of normal Ras. However, Ras oncoproteins are insensitive to the inhibitory activity of GTPase activating protein. As a result, cells harboring these Ras oncoproteins will show autonomous proliferation and malignant transformation.

As farnesylation of Ras oncoproteins is the essential enzymatic step in the process of posttranslational activation, inhibiting this step could theoretically result in the inhibi-

tion of this autonomous and malignant growth and proliferation. Thus, specific inhibitors of farnesyl transferase could possibly lead the way toward a specifically targeted treatment of *ras* oncogene-dependent tumor. Recently, however, evidence has emerged that the antiproliferative effects of farnesyl transferase inhibitors do not depend solely on inhibition of Ras and that the gain of alternate prenylated (geranylgeranylated) forms of the *Rho* protein *Rho-B* mediate cell growth inhibition.¹¹ Besides, when inhibiting farnesylation, it has to be taken into account that

From the Department of Medical Oncology, Rotterdam Cancer Institute (Daniel den Hoed Kliniek), Rotterdam; Department of Ophthalmology, University Hospital, Rotterdam; and NDDO Oncology, Amsterdam, the Netherlands; Institut Jules Bordet and European Organization for Research and Treatment of Cancer Early Clinical Studies Group, Brussels, Belgium; and Schering-Plough Research Institute, Kenilworth, NJ.

Submitted April 27, 2000; accepted October 4, 2000.

Address reprint requests to Ferry A.L.M. Eskens, MD, Department of Medical Oncology, University Hospital Rotterdam, PO Box 2040, 3000 CA Rotterdam, the Netherlands; email: eskens@oncd.azr.nl.

© 2001 by American Society of Clinical Oncology.

0732-183X/01/1904-1167

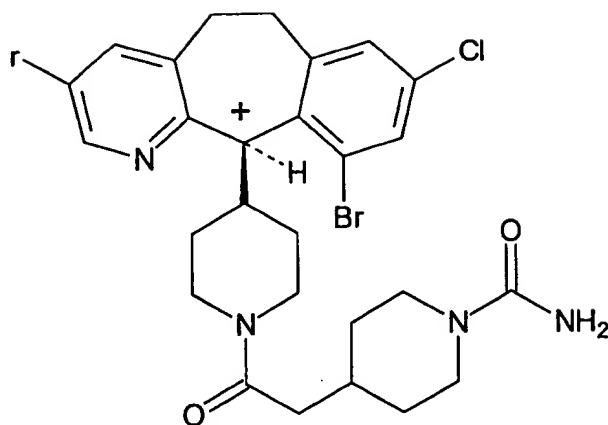


Fig 1. Chemical structure of SCH 66336.

this process is not restricted to Ras, as other cellular proteins also have to be farnesylated before exerting their activity.³

Several specific inhibitors of farnesyl transferase have been developed. SCH 66336 ((11R) 4[2[4-(3,10-dibromo-8-chloro-6,11-dihydro-5H-benzo[5,6] cyclohepta [1,2b]pyridin-11yl)-1-piperazinyl]-2-oxoethyl]-1-piperidinecarboxamide) (Fig 1) is a tricyclic nonpeptidyl, nonsulphydryl farnesyl transferase inhibitor. In vitro, it blocks farnesylation of H-Ras by purified human farnesyl protein transferase with an 50% inhibitory concentration (IC_{50}) of 1.9 nmol/L and farnesylation of K-Ras-4B with an IC_{50} of 5.2 nmol/L. SCH 66336 blocks anchorage-independent growth of K-Ras-transformed rodent fibroblasts with an IC_{50} of 0.4 μ mol/L and blocks the transformed growth properties (eg, anchorage-independent growth) of rodent fibroblasts that have been transformed with mutant *ras* and human tumor cell lines containing mutated *ras*.^{12,13} It does not inhibit geranylgeranyl protein transferase 1 in concentrations up to 50 μ mol/L. Anchorage-independent growth of various mutated K-*ras*-containing human tumor cell lines, such as HTB 177 lung carcinoma, A549 lung carcinoma, HCT 116 colon carcinoma, and HPAF II and MiaPaCa pancreatic carcinoma, is inhibited by SCH 66336 at concentrations of 0.5 μ mol/L, whereas the growth of the DLD-1 colon carcinoma cell line is inhibited at 3 μ mol/L. Interestingly, several human tumor cell lines that do not contain *ras* mutations, such as HTB 173 and HTB 175 lung carcinoma and MCF-7 breast carcinoma, are also sensitive to the growth-inhibitory effects of SCH 66336. This might be explained in part by the action of oncogenes or autocrine factors that lie upstream in the Ras signal transduction pathway. In in vivo studies, SCH 66336 showed growth-inhibitory effects in human tumor xenografts, including DLD-1 and HCT 16 colon carcinoma, A549 and HTB 177 lung carcinoma, AsPc-1, HPAF-II, HS 700T and MiaPaCa pancreas carcinoma, and DU 145 prostate carci-

noma. Additionally, in a WAP-H-*ras* transgenic mouse model developing tumors of the mammary and salivary gland, dose-dependent tumor regressions have been recorded.¹⁴ Preclinical chronic oral toxicity studies revealed dose-dependent myelosuppression, weight loss, diarrhea, and vomiting in rats and monkeys (Schering-Plough Research Institute, Kenilworth, NJ, data on file).

This phase I and pharmacokinetic study represents the first administration of SCH 66336 in patients with advanced solid tumors using a continuous twice daily oral dosing regimen.

PATIENTS AND METHODS

Eligibility Criteria

Patients with a cytologically or histologically confirmed diagnosis of a solid tumor refractory to standard treatment or for whom no standard therapy was available were eligible for this study. Patients with primary CNS neoplasm, known brain or leptomeningeal metastases, or known bone marrow involvement were excluded. Further eligibility criteria included the following: age \geq 18 years; World Health Organization performance status of \leq 2; life expectancy of \geq 12 weeks; no anticancer therapy in the previous 4 weeks (6 weeks for nitrosoureas or mitomycin); no prior bone marrow or stem-cell transplantation; no known human immunodeficiency virus positivity or AIDS-related illness; adequate function of bone marrow (hemoglobin \geq 6.2 mmol/L, absolute neutrophil count \geq 1.5×10^9 /L, platelet count \geq 100×10^9 /L), liver (bilirubin \leq 25 μ mol/L; AST and ALT within 2.5 times the normal upper limit), and kidney (serum creatinine \leq 140 μ mol/L); ability to take oral medication; and no more than two prior combination chemotherapy regimens or one prior combination regimen plus two single-agent regimens. Local ethics boards approved the protocol and informed-consent brochures. All patients gave written informed consent at study entry.

Pretreatment Assessment and Follow-Up Studies

Before therapy, a complete medical history was taken and a physical examination was performed. A complete blood count, including WBC differential, and serum chemistry, including sodium, potassium, calcium, magnesium, phosphorus, urea, uric acid, creatinine, total protein, albumin, glucose, alkaline phosphatase, bilirubin, AST, ALT, gamma-glutamyl transpeptidase, and lactate dehydrogenase, were performed, as were urine analysis, ECG, and chest x-ray. Because some visual proteins (ie, rhodopsin kinase and transducin gamma) are known to undergo farnesylation, patients were referred for ophthalmologic examination including retinal photography before treatment, after 4 and 8 weeks, and bimonthly thereafter. Weekly evaluations included history, physical examination, toxicity assessment according to National Cancer Institute common toxicity criteria (version date December 1994), complete blood count, serum chemistries, urine analysis, and ECG. Tumor measurements were performed before treatment, at 4 and 8 weeks, and bimonthly thereafter and were evaluated according to the World Health Organization criteria for response.¹⁵ In case of progressive disease, patients were taken off study.

Drug and Drug Administration

SCH 66336 ((11R) 4[2[4-(3,10-dibromo-8-chloro-6,11-dihydro-5H-benzo[5,6] cyclohepta[1,2b]pyridin-11yl)-1-piperazinyl]-2-oxoethyl]-

1-piperidinecarboxamide) is a crystalline solid containing one chiral center. It was supplied as 25-, 100-, and 200-mg blue opaque gelatin capsules by Schering-Plough Research Institute. The capsules were swallowed immediately after breakfast and after supper, with approximately 240 mL of noncarbonated water. On days of pharmacokinetic sampling, patients were administered standardized meals immediately before drug administration. SCH 66336 was taken for 28 consecutive days and was continued in case of stable disease or disease remission after this period for as long as no disease progression and/or no unacceptable drug-related toxicity was seen. Routine antiemetics were not prescribed. SCH 66336 administration was immediately interrupted at the occurrence of dose-limiting toxicity (DLT).

Dosage and Dose Escalation

The starting dose of SCH 66336 was 25 mg bid. This dose was based on the safety results of the 15-mg/kg/d dose in 3-month toxicology studies in monkeys. Although this was not a "no-effect dose," the only findings in monkeys were increased liver weight. At the first day of treatment, patients were given a single dose for pharmacokinetic purposes.

Dose escalation was performed according to a schedule of dose doublings. At each dose level, a minimum of three patients had to have 28 days of treatment before escalation was allowed. Once DLT was seen in one patient at a given dose level, at least six patients had to be treated at that dose level before further dose escalation was allowed. DLT was defined as any \geq grade 3 nonhematologic toxicity or a serum creatinine elevation of \geq three times the upper limit of normal. Grade 3 fever in absence of infection and grade 3 nausea or vomiting in patients not receiving adequate antiemetic treatment were not considered DLT. Neutropenia or thrombocytopenia \geq grade 3 or grade 4 anemia constituted hematologic DLT. The maximum-tolerated dose was defined as the highest dose to be administered to a group of six patients producing tolerable, manageable, and reversible but DLT in at least two out of six patients. At the proposed dose for phase II studies, a maximum of one out of six patients was allowed to experience DLT. No inpatient dose escalation was allowed.

Pharmacokinetic Studies

For pharmacokinetic analysis, 6-mL blood samples were taken on day 1 via an intravenous cannula before administration, at 30, 60, and 90 minutes, and at 2, 4, 6, 8, 12, 14, and 24 hours after dosing. On day 14, a blood sample was taken before the evening dose; on day 15, blood samples were taken before the morning dosing, at 30, 60, and 90 minutes, and at 2, 4, 6, 8, and 12 hours after dosing, with the last sample to be taken before the evening dose. On day 16, a sample was taken before the morning dose. If patients were on treatment after three 28-day cycles, optional pharmacokinetic blood samples were again obtained. Blood samples were collected in sodium heparin tubes and were immediately centrifuged at 3,000 rpm for 15 minutes at 10°C, after which plasma was divided into two aliquots of at least 1 mL and frozen at -70°C until analysis. Plasma samples were assayed by a specific and sensitive high-performance liquid chromatography assay.¹⁶ The lower limit of quantitation of the assay was 1.0 ng/mL. SCH 66336 excretion in urine was measured on day 15 in urine samples collected from 0 to 6 and 6 to 12 hours after dosing. Urine samples were analyzed using the same validated high-performance liquid chromatography assay. For urine analysis, the lower limit of quantitation was 2.0 ng/mL.

For each patient, the area under the plasma concentration-versus-time curve (AUC) was calculated by the trapezoidal rule and extrapolated

to infinity by linear regression analysis. The apparent total-body clearance/F (F denotes the oral bioavailability fraction) was calculated as dose/AUC. The apparent volume of distribution at steady state ($V_{d,ss}/F$) was calculated by a noncompartmental method based on the statistical moment theory.¹⁷ The terminal disposition half-life was calculated by dividing 0.693 by the fitted rate constant for drug elimination from the central compartment, estimated by linear regression analysis of the final data points of the log-linear concentration-time plot.

Statistical Analysis

Interpatient differences in pharmacokinetic parameters were assessed by the coefficient of variation, expressed as the ratio of the SD and the observed mean. Pharmacokinetic parameters were analyzed as a function of the SCH 66336 dose level using the Kruskal-Wallis one-way analysis of ranks followed by Dunn's multiple comparison test for identifying statistically different groups. Variability in pharmacokinetics between administration days was evaluated by either the paired Student's *t* test after testing for normality and heteroscedasticity or the Wilcoxon test for matched pairs. Statistical calculations were performed using the Number Cruncher Statistical System 5.X series (J.L. Hintze, East Kaysville, UT). Statistical significance was considered to be reached at $P < .05$, with a two-tailed distribution. All data are presented as mean \pm SD, except where indicated otherwise.

RESULTS

Twenty-four patients (14 men and 10 women) with a median age of 56 years (range, 28 to 77 years) were enrolled onto the study. Patient characteristics are listed in Table 1. The median duration of treatment was 40 days (range, 5 to 280 days; mean, 63.4 days). Dose levels studied were 25 ($n = 4$), 50 ($n = 5$), 100 ($n = 3$), 200 ($n = 6$), 400 ($n = 3$), and 300 ($n = 3$) mg bid.

Hematologic Toxicity

Hematologic toxicities observed in this trial are listed in Table 2. Transient grade 1 neutropenia reversible without treatment interruption was seen in the fourth week and in the fourth month of treatment in one patient at 50 mg bid and in the first week and the second month of treatment in one patient at 100 mg bid. At 400 mg bid, grade 4 neutropenia lasting from day 14 to 28 was seen in one patient. Granulocyte colony-stimulating factor was administered from day 26 to 29. This patient also developed transient grade 4 thrombocytopenia after withdrawal of the study drug. At 300 mg bid, grade 4 neutropenia lasting from day 17 to 35 was seen in one patient. No granulocyte colony-stimulating factor was administered. Transient grade 1 thrombocytopenia was recorded in the third week of treatment in one patient at 25 mg and 300 mg bid, respectively. One patient at 300 mg bid developed grade 2 thrombocytopenia lasting 5 days after treatment had been stopped because of other toxicities. One patient at 400 mg bid developed grade 3 anemia 6 days after treatment had been stopped.

Table 1. Patient Characteristics

Characteristic	No. of Patients
No. of patients entered	24
No. of patients assessable	24
Male/female	14/10
Age, years	
Median	56.5
Range	28-77
WHO performance status	
Median	1
Range	0-2
0	9
1	12
2	3
Prior therapy	
None	5
Chemotherapy	8
Radiotherapy	3
Chemo- and radiotherapy	8
Primary tumor site	
Colorectal	5
Lung	3
Breast	2
Cervix uteri	2
Unknown primary	2
Liver	2
Miscellaneous	8

Abbreviation: WHO, World Health Organization.

Nonhematologic Toxicity

Major nonhematologic side effects observed in this trial are listed in Table 3. Toxicity was mainly gastrointestinal and consisted of watery diarrhea, nausea, vomiting, and anorexia. In patients with diarrhea, loperamide administered on an as-needed basis resulted in prompt relief of symptoms. At lower doses, vomiting was usually mild and required no specific treatment. Anorexia occurred mainly at the highest dose levels, was mild, and required no specific therapy. Other toxicities consisted of grade 1 or 2 elevation of liver enzymes and reversible grade 1 or 2 elevated plasma creatinine levels recorded at all dose levels studied. In one patient at 400 mg bid, grade 3 anorexia and diarrhea,

together with grade 2 nausea and grade 1 vomiting, resulted in grade 3 creatinine due to dehydration, defining DLT. Grade 1 weight loss was recorded in three patients at 200 mg bid and one patient each at 300 and 400 mg bid. Almost all patients who experienced weight loss had various concurrent gastrointestinal toxicities. Transient grade 2 fever was recorded in one patient at 300 mg bid who also developed transient grade 2 oral mucositis after SCH 66336 administration was interrupted because of other side effects. Atrial flutter/fibrillation was recorded in the third month of therapy in a single patient at 100 mg bid. This patient had a prior history of atrial fibrillation. Asymptomatic sinus bradycardia (55 beats/min) was recorded in the third week of treatment in one patient at 300 mg bid. A 24-hour Holter monitoring following the day of onset revealed numerous episodes of bradycardia. Nineteen days after discontinuation of the study drug because of other toxicities, 24-hour Holter monitoring showed no further episodes of bradycardia. Serial ECGs showed no relevant changes in any of the patients. Ophthalmologic examinations revealed no retinal changes.

DLT

Since in the first three patients at 200 mg bid no toxicity greater than grade 1 was recorded, the dose was doubled to 400 mg bid. At this dose, DLT was seen in three consecutive patients. It consisted of grade 4 vomiting in the first week of treatment in one patient, grade 4 neutropenia lasting 14 days that coincided with grade 4 thrombocytopenia lasting 5 days which occurred after 2 weeks of treatment in a second patient, and the combination of grade 3 diarrhea, grade 3 anorexia, grade 2 nausea, and grade 1 vomiting leading to reversible grade 3 elevation of plasma creatinine that occurred after the first week in a third patient. Three additional patients were then treated at the next lower dose level of 200 mg bid, but as no additional DLTs were recorded, it was decided to escalate the dose to 300 mg bid. At this dose, DLT was again observed in three consecutive patients, consisting of grade 4 neutropenia lasting 10 days and occurring after 3 weeks of treatment, reversible grade 3

Table 2. Hematologic Toxicity (worst per patient)

Dose Level (bid, mg)	No. of Patients	Neutropenia (CTC grade)				Thrombocytopenia (CTC grade)			
		1	2	3	4	1	2	3	4
25	4	—	—	—	—	1	—	—	—
50	5	1	—	—	—	—	—	—	—
100	3	1	—	—	—	—	—	—	—
200	6	—	—	—	—	—	—	—	—
400	3	—	—	—	1	—	—	—	1
300	3	—	—	—	1	1	1	—	—

Abbreviation: CTC, common toxicity criteria.

Table 3. Nonhematologic Toxicity (worst per patient)

Dose Level (bid, mg)	No. of Patients	Nausea (CTC grade)			Anorexia (CTC grade)			Diarrhea (CTC grade)				Vomiting (CTC grade)				Fatigue (CTC grade)			Neurocortical (CTC grade)			Creatinine (CTC grade)		
		1	2	3	1	2	3	1	2	3	4	1	2	3	4	1	2	3	1	2	3	1	2	3
25	4	—	—	—	1	—	—	—	—	—	—	—	—	—	—	—	—	—	—	—	1	—	—	
50	5	1	—	—	—	—	—	2	—	—	—	1	—	—	—	1	—	—	—	—	3	—	—	
100	3	1	—	—	—	—	—	1	—	—	—	1	—	—	—	1	—	—	—	—	1	—	—	
200	6	5	—	1	4	—	1	1	1	2	1	2	2	—	—	3	1	—	—	—	5	—	—	
400	3	—	3	—	—	—	2	1	1	1	—	2	—	—	1	—	1	—	—	—	1	1	1	
300	3	2	1	—	1	1	—	2	1	—	—	2	—	—	—	1	1	1	—	—	1	1	—	

neurocortical toxicity consisting of disorientation and confusion in the first week of treatment, and the combination of grade 3 fatigue with grade 2 nausea and grade 2 diarrhea occurring in the third week of treatment. No patient at 400 mg bid or 300 mg bid was able to complete 28 days of treatment. The recommended dose for phase II trials was set at 200 mg bid. The six patients treated at this dose level received the drug for a median of 57 days (range, 52 to 280 days).

Pharmacokinetics

Pharmacokinetic studies were completed in all 24 patients. The plasma concentration-versus-time profiles of SCH 66336 were similar for all patients studied, with mean curves obtained at the tested SCH 66336 dose levels shown in Fig 2. The mean single-dose noncompartmental pharmacokinetic parameters of SCH 66336 after doses ranging from 25 to 400 mg are listed in Table 4. Significant interpatient variability in pharmacokinetic parameters was apparent at all dose levels. The absorption of the drug was relatively slow, and peak concentrations were reached between 2.7 and 8.0 hours after drug intake. Peak plasma concentrations as well as AUCs increased in a greater than dose-proportional manner (Fig 3A). A 16-fold increase in dose (from 25 to 400 mg) was associated with an increase in mean peak plasma concentration of approximately 56-fold and an increase in the AUC of approximately 200-fold. The apparent clearance of SCH 66336 decreased exponentially from $1,190 \pm 462$ mL/min at a dose of 25 mg to 101 ± 27.3 mL/min at 400 mg (Fig 3B), while the $V_{d,ss}/F$ decreased from 331 ± 27.0 L to 90.4 ± 22.4 L at the same dose levels. There was a trend to increasing plasma half-life with increasing dose that was statistically significant at the two highest dose levels ($P < .007$; Kruskal-Wallis test). The peak plasma concentrations (not shown) and AUC_{0-12} (Table 4) increased approximately two- to five-fold on repeated dosing in a dose-independent manner ($P = .103$; Kruskal-Wallis test), which is more than expected based on accumulation effects only ($P = .0016$; paired Student's *t* test). In contrast, the terminal disposition half-life (data not shown)

was comparable between days 1 and 15, although the mean difference reached borderline significance ($P = .04$; Wilcoxon test for matched pairs of 10 patients). This suggests that the dose dependency in apparent clearance does not arise primarily from factors associated with saturation of excretory routes. Steady-state concentrations of SCH 66336 were attained by days 7 to 14, with only minor inpatient variability in trough levels (median coefficient of variation, 15.5%; range, 6% to 60%). The cumulative urinary excretion of unchanged SCH 66336 was dose-independent and accounted for only less than 0.02% of the administered dose. The mean renal clearance, ie, the product of the dose-fraction excreted unchanged in urine and the apparent total body clearance, was estimated as 0.117 ± 0.0105 mL/min, suggesting that SCH 66336 is not cleared by renal processes.

Response

No partial or complete responses were seen. One patient with pseudomyxoma peritonei had stable disease for 9+ months, whereas one patient with metastatic follicular thyroid carcinoma had stable disease for 7 months with ongoing treatment.

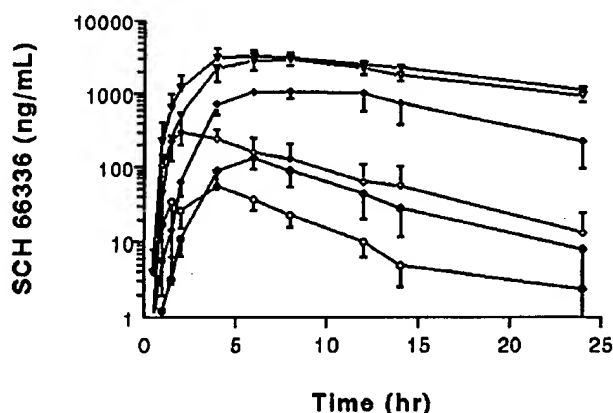


Fig 2. Plasma concentration-versus-time profiles of SCH 66336 in patients treated at a dose level of 25 mg (\circ), 50 mg (\bullet), 100 mg (\triangle), 200 mg (\diamond), 300 mg (∇), or 400 mg (\blacktriangledown). Mean values (symbols) and SE (bar) are shown for all patients treated on day 1 at the indicated SCH 66336 dose level.

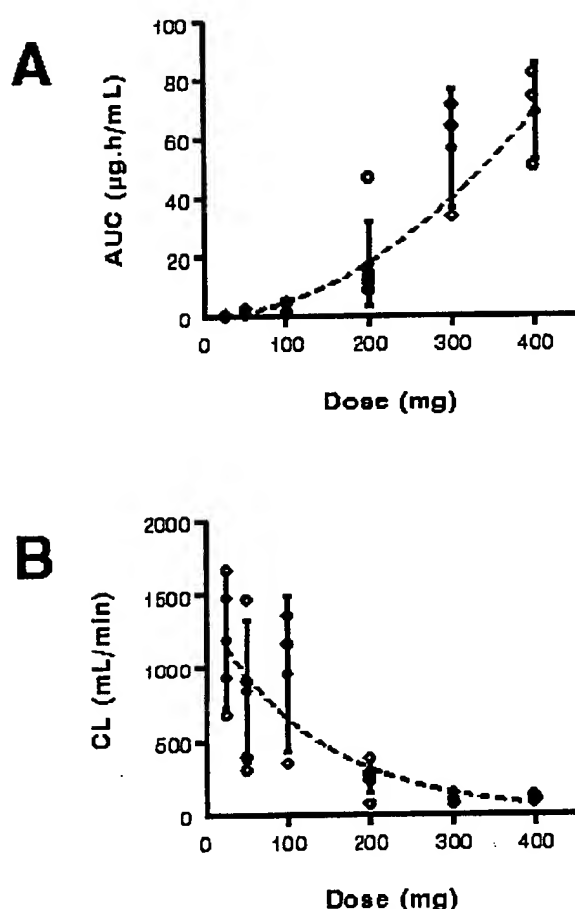


Fig 3. (A) Effect of dose on the AUC and (B) apparent clearance of SCH 66336 in 24 cancer patients. Closed symbols with error bars indicate mean values of the pharmacokinetic parameter at each of the tested dose levels and SD, respectively.

DISCUSSION

We performed a phase I and pharmacokinetic study to explore safety, tolerability, maximum-tolerated dose, and

pharmacokinetics of the oral farnesyl transferase inhibitor SCH 66336. In this study using continuous oral bid administration, side effects attributable to the study drug were hematologic and nonhematologic, whereas DLTs included neutropenia, thrombocytopenia, various gastrointestinal side effects, and neurocortical toxicity with reversible disorientation and confusion.

The hematologic toxicity of SCH 66336 in the current study consisted of dose-dependent, uncomplicated, and reversible neutropenia and thrombocytopenia occurring mainly at the two highest, nontolerable dose levels tested. At the dose level recommended for phase II studies, 200 mg bid, myelosuppression did not occur, even in the patient who was on treatment for up to 9+ months. This parallels the experience in three other studies using different dosing regimens of SCH 66336 in which hematologic toxicity was absent at these dose levels.¹⁸⁻²⁰ One of these studies also used a continuous treatment schedule.²⁰ This finding is in contrast to results obtained with other farnesyl transferase inhibitors. In two published reports on L-778,123, a peptidomimetic farnesyl transferase inhibitor given intravenously, myelosuppression comprised one of the DLTs and also occurred at dose levels recommended for further activity testing.^{21,22}

Out of three phase I studies²³⁻²⁵ that have been reported on the farnesyl transferase inhibitor R115777, myelosuppression comprised DLT in two,^{23,24} whereas in the third study, which used a 5 days on, 9 days off schedule, only minimal hematopoietic toxicity was observed.²⁵ In the only published phase I study with the novel farnesyl transferase inhibitor BMS-214662, exploring an intermittent treatment schedule, no myelosuppression was recorded.²⁶ Clearly, for farnesyl transferase inhibitors, myelosuppression is a class effect, with marked differences depending on agent and schedule of administration.

The nonhematologic side effects of SCH 66336 in our current study were predominantly gastrointestinal and con-

Table 4. Summary of SCH 66336 Pharmacokinetic Data

Dose Level (mg)	No. of Patients	C_{max} (ng/mL)	T_{max} (hour)	AUC ($\mu\text{g} \cdot \text{h/mL}$)	$T_{1/2}$ (hour)	CL/F (mL/min)	$V_{d,ss}$ /F (L)	AUC_{0-12}/AUC_{0-24} *
25	4	63.9 \pm 2.24	3.4 \pm 1.3	0.397 \pm 0.167	3.57 \pm 1.32	1,190 \pm 462	331 \pm 27.0	2.65 \pm 0.27
50	5	156 \pm 96.1	5.2 \pm 1.1	1.35 \pm 0.955	3.68 \pm 1.49	845 \pm 486	460 \pm 532	5.28 \pm 1.83
100	3	333 \pm 70.6	2.7 \pm 1.2	2.46 \pm 1.96	4.09 \pm 1.29	958 \pm 536	299 \pm 114	3.66 \pm 1.35
200	6	1,380 \pm 728	6.7 \pm 2.7	17.7 \pm 14.4	5.45 \pm 1.22	253 \pm 103	114 \pm 43.8	3.29 \pm 0.56
300	3	2,900 \pm 1,290	7.3 \pm 1.2	56.4 \pm 20.0	10.0 \pm 0.59†	98.7 \pm 42.9	85.4 \pm 35.9	3.38 \pm 1.60
400	3	3,610 \pm 1,290	8.0 \pm 5.3	69.1 \pm 16.5	10.4 \pm 0.25†	101 \pm 27.3	90.4 \pm 22.4	NA

NOTE. Data are expressed as mean values \pm SD.

Abbreviations: C_{max} , peak plasma concentration; T_{max} , time to peak concentration; $T_{1/2}$, terminal disposition half-life; CL/F, apparent clearance; $V_{d,ss}$, apparent volume of distribution at steady-state; AUC_{0-12}/AUC_{0-24} , ratio of AUC_{0-12} values measured on days 15 and 1, respectively.

*Dose-independent, $P = .103$ (Kruskal-Wallis test), but significantly different from 1, $P = .0016$ (paired Student's t test).

†Significantly different, $P < .006$ (Kruskal-Wallis test followed by Dunn's multiple comparison).

Table 5. Clinical Studies (single agent) of Farnesyltransferase Inhibitors; Schedule, DLT, Recommended Dose, Side Effects /

Drug (ref)	Schedule	DLT	Recommended Dose (mg)	Side Effects at Recommended Dose
SCH 66336 ¹⁸	PO/bid d 1-7 q 3 weeks	Diarrhea, fatigue	350 bid	ANC, plts, N/V, diarrhea, fatigue
SCH 66336 ¹⁹	PO/bid d 1-14 q 4 weeks	Gastrointestinal	200 bid	N/V, diarrhea, fatigue
SCH 66336 ²⁰	PO/od continuous	Diarrhea	300 od	Diarrhea, N/V, renal, fatigue
L-778,123 ²¹	IV d 1-7 q 3 weeks	Q-Tc, neutropenia	560 (m ²) od	ANC, plts, N/V, somnolence, fatigue
L-778,123 ²²	IV d 1-14 q 3 weeks	Neutropenia, Q-Tc	560 (m ²) od	?
L-778,123 ²²	IV d 1-28 q 5 weeks	?	?	?
R115777 ²³	PO/bid continuous	Skin, neutropenia, thrombocytopenia, neuromotor/sensory	300 bid	Skin, ANC, plts, fatigue, N/V, neuro, dizziness
R115777 ²⁴	PO/bid d 1-21 q 4 weeks	Neutropenia, thrombocytopenia, confusion, fatigue, bilirubin	240 (m ²) bid	ANC, plts, fatigue, confusion
R115777 ²⁵	PO/bid d 1-5 q 2 weeks	Neuropathy, fatigue	?	?
BMS-214662 ²⁶	IV course 1 PO course 2 d 1 q 3 weeks	Hepatotoxicity Gastrointestinal	?	Fatigue, somnolence, gastrointestinal

Abbreviations: PO, orally; bid, twice daily; od, once daily; IV, intravenously; d, day; q, every; Q-Tc, asymptomatic Q-Tc prolongation at ECG; ANC, absolute neutrophil count; plts, platelets; N/V, nausea and vomiting.

sisted of mild dose-dependent, noncumulative, and reversible diarrhea, vomiting, anorexia, and nausea. When diarrhea occurred at the recommended dose for phase II studies, treatment with loperamide always resulted in prompt and complete relief. Patients were advised to use loperamide on an on-demand basis, which always proved to be sufficient. At the recommended dose for phase II studies, vomiting was also usually mild and short-lasting and required no specific treatment. Anorexia and nausea occurred at virtually all dose levels and usually were mild. Gastrointestinal side effects were recorded in all studies of SCH 66336 and comprised DLT in all treatment schedules analyzed. This may suggest that gastrointestinal toxicity is not cumulative. Presumably partly related to these various gastrointestinal side effects, mild weight loss was noted in almost all patients. However, patients without gastrointestinal toxicity also experienced some weight loss that occurred mainly within the first 2 weeks of treatment. Remarkably, no additional weight loss was seen with ongoing treatment.

Nongastrointestinal side effects were diverse, infrequent, and usually mild. At the lower dose levels, noncumulative and reversible grade 1 creatinine increases were seen, but coinciding urine analysis never revealed any abnormality; therefore, we cannot rule out mild dehydration caused by various gastrointestinal side effects as the principal cause of these creatinine increases. In the patient at the nontolerable dose level 400 mg bid in whom grade 3 creatinine was recorded, urine analysis revealed no abnormalities and interruption of SCH 66336 dosing and intravenous rehydration resulted in a rapid and complete normalization of creatinine levels. In the present study, two episodes of

reversible atrial rhythm abnormalities (atrial fibrillation in a patient with previous cardiac history and asymptomatic sinus bradycardia) occurred, but serial ECGs did not show consistent changes in all other patients. This is in sharp contrast with the data from studies with L-778,123, in which prolongation of the Q-T time constituted DLT.^{21,22} In the current study, one episode of grade 3 rapidly reversible neurocortical toxicity consisting of disorientation and confusion was recorded, but no other episodes of either neurocortical toxicity or peripheral neuropathy were recorded in any of the other studies with SCH 66336. Reversible peripheral neurosensory and motor as well as central neurocortical toxicity have been described with oral R115777.²³⁻²⁵ No neuropathy was recorded with BMS-214662.²⁶

When considering which treatment schedule of SCH 66336 should preferably be used in future clinical trials, one should note that preclinical data demonstrate that SCH 66336 is a reversible competitive inhibitor of farnesyl transferase, and the biochemical effects are rapidly reversed on withdrawal of the compound. Because the compound thus is a competitive inhibitor, the schedule most likely to result in continuous inhibition of farnesyl transferase would be the continuous schedule. This schedule achieves the highest total dose and the longest exposure time.

When summarizing the results of the recorded toxicity profiles of the farnesyl transferase inhibitors that are currently being tested in clinical studies (SCH 66336, R115777 and L-778,123, and BMS-214662), one can conclude that myelosuppression is a common feature, whereas nonhematologic toxicities differ in essential ways. Table 5 lists the

results of the clinical studies with farnesyltransferase inhibitors presented to date.

This present study clearly demonstrates a dose dependency in SCH 66336 plasma pharmacokinetics in cancer patients, which contrasts with previous findings from pre-clinical dose-response studies. In the rat, peak plasma levels reached values of 3, 10, and 30 $\mu\text{mol/L}$ at oral doses of 10, 30, and 100 mg/kg, respectively.²⁷ In cancer patients, both the apparent clearance and the apparent $V_{d,ss}/F$ demonstrated a more than four- to 10-fold decrease at a dose of 400 mg, compared with 25 mg. The most likely explanation is an increase in F with multiple dose administration resulting in an apparent decrease in V_d and an apparent decrease in total-body clearance/ F . The opposing effects of these two processes on drug elimination leaves the apparent terminal disposition half-life almost dose-independent, except at the two highest dose levels. In addition, at repeated dosing, ie, when comparing the mean drug exposure and peak plasma concentrations of the various dose levels tested at day 15 with those of day 1, substantial increases were found that were greater than predicted based on accumulation processes alone. Clearly, this may have important clinical ramifications; if clinical outcomes are related to drug exposure, then a simple percentage increase in dose will have a much greater impact on total drug exposure than would be expected with a behavior based on linear pharmacokinetics. Trough plasma concentrations drawn around day 14 to 16 do not show trends suggesting that steady-state was reached. Most importantly, at the recommended dose for further clinical studies applying continuous dosing regimens with SCH 66336, trough plasma concentrations were shown to exceed 1.5 $\mu\text{mol/L}$, which is above concentrations required in vitro to induce significant growth inhibition in

colony assays against various primary human tumor specimens.²⁸

The general principles of dose dependency in pharmacokinetics have recently been reviewed.²⁹ The dose-dependent pharmacokinetic behavior of SCH 66336 in cancer patients most likely involves multiple nonlinear (absorption) mechanisms, including saturation of metabolic processes responsible for presystemic biotransformation (eg, the cytochrome P450 system) or saturation of outward-directed drug-carrier systems that mediate transmembrane drug flux, such as *MDR1* P-glycoprotein. Saturation of presystemic metabolism or degradation in the gut lumen, the intestinal mucosae, or the liver after oral administration of drugs in humans is relatively common and has been well described for the calcium antagonist verapamil³⁰ and also for fluorouracil.³¹ However, the phenomenon of a dose-dependent decrease in extravascular binding ($V_{d,ss}/F$) as seen here with SCH 66336 is highly unusual, although it has been reported to occur with 3-hour infusions of paclitaxel, presumably as a result of extensive binding to microtubules or micellar encapsulation in its formulation vehicle.³² Further analysis of the absorption and disposition of SCH 66336 in individual cancer patients, with respect to the current findings, should be of great importance for our ability to better understand the role of the various biologic factors that may influence the compound's pharmacokinetic behavior and pharmacologic actions, and effects of other drug administered concomitantly.

In conclusion, this phase I and pharmacologic study with continuous oral bid SCH 66336 has shown that this farnesyl transferase inhibitor can be safely administered using a continuous oral bid dosing schedule. The recommended dose for phase II studies using this treatment schedule is 200 mg bid.

REFERENCES

- Gibbs JB: Ras C-terminal processing enzymes: New drug targets? *Cell* 65:1-4, 1991
- Lowy DR, Willumsen BM: Function and regulation of Ras. *Annu Rev Biochem* 62:851-891, 1993
- Khosravi-Far R, Der CJ: The Ras signal transduction pathway. *Cancer Metastasis Rev* 13:67-89, 1994
- Gibbs JB, Oliff A, Kohl NE: Farnesyltransferase inhibitors: Ras research yields a potential cancer therapeutic. *Cell* 77:175-178, 1994
- Gibbs JB, Kohl NE, Koblansky KS, et al: Farnesyltransferase inhibitors and anti Ras therapy. *Breast Cancer Res Treat* 38:75-83, 1996
- Omer CA, Kohl NE: CA₁A₂X-competitive inhibitors of farnesyltransferase as anti-cancer agents. *Trends Pharmacol Sci* 18:437-444, 1997
- Gibbs JB, Oliff A: The potential of farnesyltransferase inhibitors as cancer chemotherapeutics. *Annu Rev Pharmacol Toxicol* 37:143-166, 1997
- Rowinsky EK, Windle JJ, Von Hoff DD: Ras protein farnesyl transferase: A strategic target for anticancer therapeutic development. *J Clin Oncol* 17:3631-3652, 1999
- Oliff A: Farnesyl transferase inhibitors: Targeting the molecular basis of cancer. *Biochim Biophys Acta* 1423:C19-C30, 1999
- Bos JL: *ras* oncogenes in human cancer: A review. *Cancer Res* 49:4682-4689, 1989
- Prendergast JC: Targeting farnesyltransferase: Is *Ras* relevant? *ASCO Educational Book* Spring:22-28, 1999
- Liu M, Lee S, Yaremko B, et al: SCH 66336, an orally bioavailable tricyclic farnesyl protein transferase inhibitor, demonstrates broad and potent in-vivo antitumor activity. *Proc Am Assoc Cancer Res* 39:270, 1998 (abstr 1843)
- Izbicka E, Lawrence R, Davidson K, et al: Activity of a farnesyl transferase inhibitor (SCH 66336) against a broad range of tumors taken directly from patients. *Proc Am Assoc Cancer Res* 40:524, 1999 (abstr 3454)

14. Liu M, Bryant MS, Chen J, et al: Antitumor activity of SCH 66336, an orally bioavailable tricyclic inhibitor of farnesyl protein transferase in human tumor xenograft models and wap-ras transgenic mice. *Cancer Res* 58:4947-4956, 1998
15. World Health Organization: WHO handbook for reporting results of cancer treatment. Geneva, Switzerland, World Health Organization, 1979 (Offset Publication No. 40)
16. Kim H, Likhari P, Lin CC, et al: High-performance liquid chromatographic analysis of the antitumor agent SCH 66336 in cynomolgus monkey plasma and evaluation of its chiral inversion in animals. *J Chromatogr B Biomed Sci Appl* 728:133-141, 1999
17. Gibaldi M, Perrier D: Noncompartmental analysis based on statistical moment theory, in *Pharmacokinetics* (ed 2). New York, NY, and Basel, Switzerland, Marcel Dekker, 1982, pp 409-417
18. Adjei AA, Erlichman Ch, Davis JN, et al: A phase I trial of the farnesyl protein transferase (FPT) inhibitor SCH 66336: Evidence for biological and clinical activity. *Cancer Res* 60:1871-1877, 2000
19. Hurwitz HI, Colvin OM, Petros WP, et al: Phase I and pharmacokinetic study of SCH 66336, a novel FPTI, using a 2-week on, 2-week off schedule. *Proc Am Soc Clin Oncol* 18:156a, 1999 (abstr 599)
20. Awada A, Eskens FALM, Piccart MJ, et al: A clinical, pharmacodynamic and pharmacokinetic phase I study of SCH 66336 (SCH), an oral inhibitor of the enzyme farnesyl transferase, given once daily in patients with solid tumors. *Clin Cancer Res* 5:3733s, 1999 (suppl, abstr 20)
21. Britten CD, Rowinsky E, Yao S-L, et al: The farnesyl protein transferase (FPTase) inhibitor L-778,123 in patients with solid cancers. *Proc Am Soc Clin Oncol* 18:155a, 1999 (abstr 597)
22. Rubin E, Abbruzzese JL, Morrison BW, et al: Phase I trial of the farnesyl protein transferase inhibitor L-778,123 on a 14 or 28-day schedule. *Proc Am Soc Clin Oncol* 19:178a, 2000 (abstr 689)
23. Schellens J, De Klerk G, Swart M, et al: Phase I and pharmacologic study with the novel farnesyl transferase inhibitor (FTI) R115777. *Proc Am Soc Clin Oncol* 19:184a, 2000 (abstr 715)
24. Hudes G, Schol J, Baab A, et al: Phase I clinical and pharmacokinetic trial of the farnesyl transferase inhibitor R115777 on a 21-day dosing schedule. *Proc Am Soc Clin Oncol* 18:156a 1999 (abstr 601)
25. Zujewski J, Horak ID, Bol CJ, et al: Phase I and pharmacokinetic study of farnesyl transferase inhibitor R115777 in advanced cancer. *J Clin Oncol* 18:927-941, 2000
26. Ryan DP, Eder JP, Supko JG, et al: Phase I clinical trial of the farnesyltransferase (FT) inhibitor BMS-214662 in patients with advanced solid tumors. *Proc Am Soc Clin Oncol* 19:185a, 2000 (abstr 720)
27. Bryant MS, Liu M, Wang S, et al: Pharmacokinetics of a potent orally bioavailable inhibitor of farnesyl protein transferase in the mouse, rat and cynomolgus monkey. *Proc Am Assoc Cancer Res* 39:177, 1998 (abstr)
28. Petit T, Izbicka E, Lawrence RA, et al: Activity of SCH 66336, a tricyclic farnesyltransferase inhibitor, against human tumor colony-forming units. *Ann Oncol* 10:449-453, 1999
29. Lin JH: Dose-dependent pharmacokinetics: Experimental observations and theoretical considerations. *Biopharm Drug Dispos* 15:1-31, 1994
30. Freedman SB, Richmond DR, Ashley JJ, et al: Verapamil kinetics in normal subjects and patients with coronary artery spasm. *Clin Pharmacol Ther* 30:644-652, 1981
31. Wagner JG, Gyves JW, Stetson CL, et al: Steady-state nonlinear pharmacokinetics of 5-fluorouracil during hepatic arterial and intravenous infusions in cancer patients. *Cancer Res* 46:1499-1506, 1986
32. Kearns CM, Gianni L, Egorin MJ: Paclitaxel pharmacokinetics and pharmacodynamics. *Semin Oncol* 22:16-23, 1995 (suppl 6)

Phase I and Pharmacokinetic Study of Farnesyl Protein Transferase Inhibitor R115777 in Advanced Cancer

By J. Zujewski, I.D. Horak, C.J. Bol, R. Woestenborghs, C. Bowden, D.W. End, V.K. Piotrovsky, J. Chiao, R.T. Belly, A. Todd, W.C. Kopp, D.R. Kohler, C. Chow, M. Noone, F.T. Hakim, G. Larkin, R.E. Gress, R.B. Nussenblatt, A.B. Kremer, and K.H. Cowan

Purpose: To determine the maximum-tolerated dose, toxicities, and pharmacokinetic profile of the farnesyl protein transferase inhibitor R115777 when administered orally bid for 5 days every 2 weeks.

Patients and Methods: Twenty-seven patients with a median age of 58 years received 85 cycles of R115777 using an inpatient and outpatient dose escalation schema. Drug was administered orally at escalating doses as a solution (25 to 850 mg bid) or as pellet capsules (500 to 1300 mg bid). Pharmacokinetics were assessed after the first dose and the last dose administered during cycle 1.

Results: Dose-limiting toxicity of grade 3 neuropathy was observed in one patient and grade 2 fatigue (decrease in two performance status levels) was seen in four of six patients treated with 1,300 mg bid. The most frequent clinical grade 2 or 3 adverse events in any cycle included nausea, vomiting, headache, fatigue, anemia, and hypotension. Myelosuppression was mild and infrequent. Peak plasma concentrations of R115777 were achieved within 0.5 to 4 hours after oral

drug administration. The elimination of R115777 from plasma was biphasic, with sequential half-lives of about 5 hours and 16 hours. There was little drug accumulation after bid dosing, and steady-state concentrations were achieved within 2 to 3 days. The pharmacokinetics were dose proportional in the 25 to 325 mg/dose range for the oral solution. Urinary excretion of unchanged R115777 was less than 0.1% of the oral dose. One patient with metastatic colon cancer treated at the 500-mg bid dose had a 46% decrease in carcinoembryonic antigen levels, improvement in cough, and radiographically stable disease for 5 months.

Conclusion: R115777 is bioavailable after oral administration and has an acceptable toxicity profile. Based upon pharmacokinetic data, the recommended dose for phase II trials is 500 mg orally bid (total daily dose, 1,000 mg) for 5 consecutive days followed by 9 days of rest. Studies of continuous dosing and studies of R115777 in combination with chemotherapy are ongoing.

J Clin Oncol 18:927-941. © 2000 by American Society of Clinical Oncology.

THERAPIES DIRECTED against specific molecular targets offer the promise of increased antitumor efficacy with decreased toxicity. The *ras* proto-oncogene encodes a 21-kd guanosine triphosphate-binding protein Ras, which is a critical component in cellular signal transduction associated with cell proliferation, differentiation, and other pleiotropic responses.¹ Activating, oncogenic, point mutations in codons 12, 13, and 61 of the *ras* gene have been observed in approximately 30% of adult human solid tumors, including pancreas, lung, colon, bladder, and other tumors.¹⁻¹¹ The wild-type Ras protein may also contribute to the growth of tumors that are driven by the aberrant activation of growth factor receptors and other tyrosine-specific protein kinases.¹²⁻¹⁶

To function in signal transduction and malignant transformation, Ras must localize to the plasma membrane.¹⁷⁻²⁰ Lacking membrane-binding domains, newly synthesized Ras requires sequential posttranslational enzymatic processing before membrane attachment. The initial and rate-limiting step involves the covalent attachment of a 15-carbon farnesyl moiety via a thioether bond to a single cysteine positioned exactly four amino acids from the carboxyl terminus.²¹ This reaction is catalyzed by the enzyme farnesyl protein transferase. The C-terminal recognition sequence has become known as a CAAX motif to indicate the requirement for a cysteine followed by two

neutral amino acids (A) with a C-terminal serine or methionine for recognition by farnesyl protein transferase. Farnesylation is followed by cleavage of the three terminal amino acids by a CAAX protease.²² The resulting C-terminal farnesylcysteine moiety is further carboxy-O-methylated to create the proper hydrophobicity or molecular recognition features to allow plasma membrane localization

From the Medicine Branch, Division of Clinical Sciences, National Cancer Institute; Clinical Center, National Institutes of Health; and National Eye Institute, Bethesda; SAIC-Frederick, Frederick, MD; Janssen Research Institute, Titusville, NJ; Janssen Research Foundation, Beerse, Belgium; Ortho-Clinical Diagnostics, Rochester, NY; and Johnson and Johnson Research, Sydney, Australia.

Submitted March 2, 1999; accepted November 3, 1999.

Supported in part with federal funds from the National Cancer Institute, National Institutes of Health, under contract no. NO1-CO-56000.

The contents of this publication do not necessarily reflect the views or policies of the Department of Health and Human Services, nor does the mention of trade names, commercial products, or organization imply endorsement by the United States government.

Address reprint requests to Jo Anne Zujewski, MD, Medicine Branch, Division of Clinical Sciences, National Cancer Institute, 9000 Rockville Pike, Bethesda, MD; email zujewski@nih.gov.

© 2000 by American Society of Clinical Oncology.

0732-183X/00/1804-927

within cells.²² The delineation and purification of enzymes involved in Ras processing created the opportunity to downregulate *ras* function in tumor cells by preventing proper localization of the protein. The demonstration that activated, oncogenic Ras lacking the c-terminal cysteine lost cell-transforming activity and the description of simple CAAX tetrapeptide inhibitors of the enzyme farnesyl protein transferase focused drug discovery efforts on this posttranslational step.^{21,23}

Initial reports on the cellular effects of farnesyl protein transferase inhibitors that were CAAX peptidomimetics suggested that this class of agent selectively reversed the *ras*-transformed phenotype in cell lines bearing *ras* mutations.²⁴⁻²⁶ These findings were very promising because polymerase chain reaction (PCR)-based DNA diagnostics were available that would allow the detection of *ras* mutations and possibly the preselection of patients who would be the best candidates for this *ras*-targeted therapy.²⁷ However, subsequent preclinical studies have shown the pharmacology of farnesyl protein transferase inhibitors to be more complex. First, farnesyl protein transferase inhibitors, including R115777, have shown antiproliferative effects in vitro and antitumor effects in vivo in cell lines with wild-type *ras*.²⁸⁻³⁰ The effects of this class of agent are clearly not dependent upon the presence of mutant Ras, although the compounds are highly effective in cell lines transformed by mutant *ras* also.^{25,31-34} Also, it was reported that the K-*ras* isoform of Ras had a much higher affinity for farnesyl protein transferase than the H-*ras* or N-*ras* isoform.³⁵ Inhibitors that were competitive for the Ras substrate-binding site of the enzyme were much less effective in blocking K-*ras* farnesylation in cell-free systems. An additional complicating issue was introduced by the observation that the CVIM CAAX motif of the K-*ras* peptide allowed the molecule to be either farnesylated or geranylgeranylated by geranylgeranyl protein transferase type 1. Geranylgeranyl protein transferase type 1 is quite similar to farnesyl protein transferase but attaches a 20-carbon geranylgeranyl isoprenoid moiety to substrate proteins bearing a CAAX motif with a terminal leucine.³⁶ In intact cell lines bearing K-*ras* mutations, alternative processing of K-*ras* by the geranylgeranyl protein transferase type 1 pathway was shown to produce resistance to some farnesyl protein transferase inhibitors.^{37,38} The results suggested that farnesyl protein transferase inhibitors might be of no practical use in the human tumor setting because K-*ras* mutations account for the vast majority of *ras* mutations in human tumors. However, it has been clearly established that tumors with mutant K-*ras* respond to this class of agent both in vitro and in vivo.^{39,40}

Ironically, as the present clinical studies of R115777 and other compounds are being reported, the biochemical basis

for the antitumor responses obtained in preclinical models is under intense reevaluation. An emerging hypothesis involving Rho B accounts for some of the discrepancies discussed previously. Like K-*ras*, Rho B can be either farnesylated or geranylgeranylated with isolated enzymes or in intact cells.^{41,42} Farnesylated Rho B seems to cooperate in expression of the transformed phenotype downstream of Ras through modulation of cytoskeletal proteins.⁴³ Expression of constructs of Rho B that can only be geranylgeranylated seems to produce antiproliferative and antitransforming effects that are similar to the effects of farnesyl protein transferase inhibitors.⁴⁴ Thus, farnesyl protein transferase inhibitors may produce antitumor effects by altering the balance of farnesylated and geranylgeranylated Rho B in cells.

Although the role of Ras in the antitumor effects of protein farnesyl transferase inhibitors remains ambiguous in preclinical studies, it will be important to assess *ras* gene status in patients entering onto studies of this class of compound. Although the existing data preclude the *ras* gene mutations as an entry criterion for treatment with a farnesyl protein transferase inhibitor, clinical studies may ultimately find a correlation between oncogene status and responses to these compounds. The genetic instability and complexity of human tumor cell lines used for laboratory studies may not be appropriate to the characterization of newer therapies with specific molecular targets.

Regardless of the mechanism, it is clear that this class of compound produces antitumor effects in standard preclinical tumor models, including human tumor xenografts as well as transgenic oncomouse models.^{32,44} The crux of modern cancer research is the translation of preclinical antitumor effects into effective clinical therapy. The first step of this translation are the phase I safety and pharmacokinetic evaluations that allow selection of dose and dose schedules for further evaluation. Presented herein are the phase I data for the first farnesyl protein transferase inhibitor to be evaluated in clinical trials, R115777 (Fig 1). R115777 is a substituted quinolone that is a competitive inhibitor of the CAAX peptide-binding site of farnesyl protein transferase.⁴⁵ The molecule is an extremely potent inhibitor of farnesylation with isolated enzyme inhibition of lamin B1 (50% inhibitory concentration [IC₅₀], 0.8 nmol/L) and K-*ras* peptide (IC₅₀, 7.9 nmol/L).⁴⁰ R115777 is also a potent inhibitor of proliferation of intact cell lines. The IC₅₀ required to inhibit H-*ras* transformed fibroblasts is 1.7 nmol/L, and the IC₅₀ required to inhibit pancreatic and colon cancer cell lines bearing K-*ras* mutations ranges from 16 to 22 nmol/L.⁴⁰ Preclinical studies have demonstrated that R115777 has antitumor effects in murine xenograft models using H-*ras*-transformed fibroblasts⁴⁶ and pancreatic and colon cell lines bearing K-*ras* mutations.³⁰ No

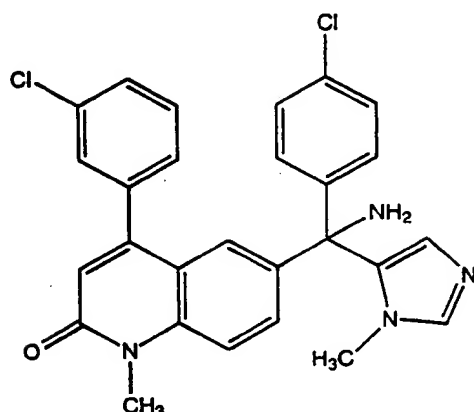


Fig 1. Chemical structure of R115777 or (B)-6-[amino(4-chlorophenyl)](1-methyl-1H-imidazol-5-yl)methyl-4-(3-chlorophenyl)-1-methyl-2(1H)-quinoline.

gross toxicity to the tumor-bearing host has been observed at effective doses of this compound. After oral administration of R115777 to male Wistar rats and male Beagle dogs, plasma concentrations of R115777 declined with a terminal half-life of less than 1.7 hours and 2.1 hours, respectively. The absolute oral bioavailability was 9% and 66% in the rat and dog, respectively (Janssen Research Foundation, Beerse, Belgium, unpublished observations).

PATIENTS AND METHODS

Patient Eligibility

Patients eligible for this trial had to meet the following criteria: pathologic confirmation of advanced cancer; no available therapy proven to improve survival; last dose of radiation therapy or chemotherapy at least 4 weeks before study entry (6 weeks for nitrosoureas or mitomycin); at least 18 years of age; Zubrod performance status of 0 or 1; adequate hepatic function (normal bilirubin, transaminase levels less than two times the upper limit of normal); normal creatinine levels (0.9 to 1.4 mg/dL for males and 0.7 to 1.3 mg/dL for females); and adequate bone marrow function (absolute neutrophil count $>1,500/\mu\text{L}$ and platelet count $>100,000/\mu\text{L}$).

Pregnant patients and lactating mothers were ineligible, as were patients with the following characteristics: extensive prior radiation therapy ($> 25\%$ of bone marrow reserve); previous bone marrow transplantation or high-dose chemotherapy with bone marrow or stem-cell rescue; untreated CNS metastases; concurrent radiation therapy, chemotherapy, hormonal therapy, or immunotherapy; coexisting medical or psychiatric conditions that were likely to interfere with study procedures; or known allergy to imidazole drugs. All patients were required to provide written informed consent according to National Cancer Institute institutional review board guidelines.

Patient Evaluations

Patient evaluations included the following: complete history and physical examination; complete blood count with leukocyte differential; serum sodium, potassium, chloride, CO_2 , blood urea nitrogen, creatinine, calcium, magnesium, total bilirubin, liver transaminases,

Table 1. Dose Escalation Schema

Formulation	Dose Level	Dose Cycle 1 (mg bid \times 10 doses)	Dose Cycle 2 (mg bid \times 10 doses)	Dose Cycle 3 (mg bid \times 10 doses)
Liquid	1	25	50	75
Liquid	2	50	75	125
Liquid	3	75	125	200
Liquid	4	125	200	325
Liquid	5	200	325	525
Liquid	6	325	525	850
Capsule	7	500	800	1,300
Capsule	8	800	800	1,300
Capsule	9	1,300	1,300	1,300

NOTE. Drug was administered orally bid for 10 doses over 5 days every 14 days. The dose level 1 starting dose was 25 mg orally bid (total daily dose, 50 mg) for 5 days.

alkaline phosphatase, lactate dehydrogenase, prothrombin time, partial thromboplastin time, fibrinogen, cholesterol, and triglyceride analyses; urinalysis; pregnancy test (as appropriate); chest radiograph; computed tomography of the chest, abdomen, or pelvis as appropriate; and radionuclide bone scan as appropriate. On-study evaluations included a complete blood count with differential leukocyte count blood chemistry analyses two to three times weekly and radiographic staging studies every 6 weeks (after three 2-week cycles of therapy). Ophthalmologic evaluations, including best visual acuity, ocular history and examination, visual field screening, D-15 color testing, and contrast sensitivity via Pelli-Robson charts (screening tests for abnormalities in visual function⁴⁷), were performed at baseline and during drug administration. Patients with changes in vision that could not be explained by refraction or changes in the anterior segment were to be evaluated with an electroretinogram. This extensive testing was based upon the involvement of several farnesylated proteins on vision⁴⁸ and the development of cataracts in one animal species (rats) used in toxicology studies (Janssen, data on file).

Treatment Plan

A modified phase I dose escalation schema was used as shown in Table 1. The starting dose was 50 mg daily, less than 1/10th of the lethal dose in dogs. This conservative starting dose was chosen because of the wide interspecies variability in the bioavailability of R115777 (data on file) and the importance of the *ras* signal transduction pathway for normal cellular function. A conservative schedule of R115777 administration was chosen: bid oral administration for 5 days followed by a minimum 7-day period of rest per treatment cycle. This schedule was used because (1) toxicology data in dogs demonstrated hematologic toxicity within 4 days of initiation of dosing with full recovery in 14 days, (2) farnesyl transferase inhibitors had not been tested in humans and acute effects of drug administration were not known, and (3) preclinical pharmacokinetic modeling predicted a half-life of 8 to 12 hours, which would allow for approximately 3 days of steady-state concentrations.

During cycle 1, in order to accommodate 24-hour pharmacokinetic sampling after first-dose administration, a single dose was administered on the first day, followed by bid administration for the next 4 days (days 2 through 5). The final (10th) dose of the cycle was administered on the sixth day.

The schema permitted inpatient dose escalation, thereby reducing the number of patients who would be treated at potentially subthera-

peutic doses.^{49,50} Inpatient dose escalation to the next dose level was allowed during the second and subsequent treatment cycles provided that nonhematologic toxicity was less than grade 1 in severity, hematologic toxicity was less than grade 2 in severity in the preceding cycle, and no treatment delays were necessary.

Three patients were enrolled at each dose level and observed for at least 14 days before additional patients were entered at the next dose level. If no dose-limiting toxicity was observed in three of three patients at a single dose level, additional patients were entered at the next higher dose level. If dose-limiting toxicity was observed in one patient, additional patients up to a total of six were entered at the same dose level. If two patients developed dose-limiting toxicity at a single dose level, the maximum-tolerated dose was determined to have been exceeded and accrual ceased at that dose level. The first cycle at a new dose level was considered for dose-limiting toxicity (whether entering trial at that dose level or escalating to that dose level). Subsequently, up to a total of six patients could be entered at one dose level below. The maximum-tolerated dose was defined as the highest dose level at which no more than one of six patients experienced a dose-limiting toxicity that could reasonably be attributed to the study drug.

Toxicity

Toxicities were scored according to National Cancer Institute of Canada Clinical Trial Group expanded toxicity criteria. Nonhematologic dose-limiting toxicity was defined as any grade 3 or greater toxicity observed during the first cycle at any dose level (whether entered at that dose level or escalated to that dose level), with the exception of alopecia, nausea, and vomiting. Hematologic dose-limiting toxicity was defined as the occurrence of an absolute neutrophil count less than 500/ μ L for greater than 3 days or platelet count less than 20,000/ μ L on a single occasion observed during the first cycle. A treatment delay of more than 3 weeks secondary to toxicity or failure to recover hematologic counts was also considered dose limiting.

Antitumor Response

Patients were evaluated for antitumor response after three cycles of therapy and every three cycles thereafter in selected patients who exhibited some evidence of clinical benefit. A complete response was defined as total disappearance of all clinical evidence of disease for at least two measurements separated by at least 4 weeks. A partial response was defined as at least a 50% reduction in the size of all measurable tumor areas as measured by the sum of the products of the greatest perpendicular, bidirectional measurements without the appearance of new lesions. These parameters must have been present for at least two measurement periods separated by at least 4 weeks. Progressive disease was defined as an increase of more than 25% in measurable disease or the development of new lesions. Stable disease was defined as a tumor status that failed to qualify for either an objective response or progressive disease.

Drug Administration

R115777 was administered orally as an aqueous, cherry-flavored liquid for dose levels 1 through 6 (25 to 850 mg bid). Drug substance was dissolved in a solvent of purified water, hydrochloric acid, benzoic acid, and cherry flavor. For dose levels 7, 8, and 9, (500 to 1,300 mg bid) a hard, gelatin capsule formulation containing 100 mg of R115777 capsule became available and was used. Drug was supplied by the Janssen Research Foundation. Patients were required to fast 1 hour before and 1 hour after administration of R115777.

Pharmacokinetics

During cycle 1, a single dose was administered orally on the morning of the first day to characterize the pharmacokinetics of R115777 for 24 hours after a single oral dose. In addition, R115777 elimination was evaluated for up to 72 hours after the 10th dose given on day 6. Venous blood samples were drawn at 0.25, 0.5, 0.75, 1, 1.5, 2, 3, 4, 6, 8, 12, 14, 16, 24, 48, and 72 hours after R115777 administration. Blood samples were also collected during the first cycle on days 3 and 5 just before drug administration to evaluate whether R115777 concentrations had achieved steady state in the blood. For each sample, 7 mL of heparinized blood was collected and immediately placed on ice. Specimens were centrifuged (5 min, 2,500 \times g) as soon as possible to collect the plasma and frozen at -70°C until analyzed. Urine was collected on the last day of drug administration during cycle 1 (day 6) to characterize R115777 urinary excretion. A pre-dose urine sample was collected, and a 20-mL aliquot was retained as a pre-dose sample. Patients' complete urinary output during a 12-hour interval was collected. The urine was mixed, the volume and pH were measured, and the sample was frozen at -20°C until assayed. The plasma and urine samples were alkalized (0.1 mol/L sodium hydroxide), extracted with heptane-isoamyl alcohol (90:10, v/v), and analyzed using a reverse-phase high-performance liquid chromatography column 10 cm \times 4.6 mm internal diameter) packed with 3- μ m-particle-sized C18 BDS-Hypersil (Hypersil, Cheshire, United Kingdom). The mobile phase was 0.01 mol/L ammonium acetate-acetonitrile (52:48) at a flow rate of 0.8 mL/min. The chromatographic peaks of R115777 (retention time approximately 4.3 min) and the internal standard (R121550, retention time approximately 6.3 min) were quantified using ultraviolet detection at 240 nm. The mean overall coefficient of variation, as obtained from independently prepared quality control plasma samples, was 6.7% at 14.9 ng/mL, 7.1% at 124 ng/mL, and 7.1% at 2,064 ng/mL. Urine concentrations of R115777 were determined before and after hydrolysis with beta-glucuronidase (from *Escherichia coli*). The validated quantification limit of R115777 in urine was 1.0 ng/mL before hydrolysis and 20 ng/mL after hydrolysis. The following pharmacokinetic parameters were calculated by standard procedures⁵¹: maximum plasma concentration (C_{max}), time to maximum plasma concentration (t_{max}), minimum concentration in plasma (C_{min} ; trough concentration), area under the plasma concentration versus time curve over a 12-hour dosing interval calculated by trapezoidal summation ($\text{AUC}_{12\text{h}}$), elimination half-life ($t_{1/2}$), and percentage of dose excreted in the urine. The accumulation ratio was calculated as the $\text{AUC}_{12\text{h}}$ ratio of day 6 and day 1. The pharmacokinetics of 27 patients were determined. However, the data of one patient at 1,300 mg were incomplete.

To determine the pharmacokinetic parameters that could predict the occurrence of certain adverse events related to the intake of R115777, the following evaluation was performed. The pharmacokinetic parameters C_{max} , $\text{AUC}_{12\text{sd}}$ (day 1), and $\text{AUC}_{12\text{ss}}$ (day 6) were tested as predictors for the occurrence of nausea, vomiting, diarrhea, and fatigue. A logistic regression analysis was performed by fitting a generalized linear model with a binary link to the data. The logistic regression model allows the binary data to be converted into a continuous relationship between measures of drug exposure and the probability of developing a certain adverse event. Adverse events were coded as binary response variables (yes or no) without taking into account the severity. The model was parameterized via (i) the predictor value corresponding to 50% probability of having a certain adverse event (P_{50}) and (ii) the sigmoidicity parameter, which reflects the steepness of the probability versus predictor curve (n). The best estimates of parameters and their SEs were obtained via a bootstrap analysis. The

number of bootstrap replications was 1,000. The S-PLUS package (Probability, Statistics, & Information, Seattle, WA) was used throughout the analysis.

Flow Cytometric Analysis

Lymphocyte populations were analyzed by three-color flow cytometry at five time points in the first three cycles of treatment. Peripheral blood, collected in sodium heparin, was stained at ambient temperature with a panel of antibodies, lysed using Optilyse C lysing solution (Coulter Corporation, Opalocka, FL), washed with Dulbecco's phosphate-buffered saline (BioWhittaker, Walkersville, MD), and analyzed on a Coulter XL flow cytometer (Coulter Corporation, Hialeah, FL). Total leukocyte populations and lymphocyte subpopulations were analyzed using the following antibody combinations: IgG1/IgG2a/CD3, CD45/CD14/CD3, CD4/CD8/CD3, CD20/CD19/CD3, and CD3/CD16⁺CD56/CD8. Commercial sources for antibodies included Becton Dickinson Immunocytometry Systems (Mountainview, CA), Caltag (Burlingame, CA), Pharmingen (San Francisco, CA), Sigma (St Louis, MO), and Immunotech (Marseille, France). B cells were defined as CD3⁺CD19⁺CD20⁺, natural killer cells as CD3⁺CD16⁺CD56⁺, CD8 cells as CD3⁺CD8⁺, and CD4 cells as CD3⁺CD4⁺. Proportions of CD45RA and CD45RO (naïve v activated/memory cells) within the CD4 population were determined by staining cells with three antibodies, acquiring the lymphocyte population, and gating during analysis on CD4⁺ cells only. Determination of total cells/ μ L expressing a particular phenotype was calculated by multiplying the total WBC count, as determined using a Coulter counter, by the frequency of that population in the lymphocyte gate and the fraction of total WBCs included in the lymphocyte gate. Lymphocyte populations were compared at the five time points using the Wilcoxon rank test for nonparametric assessments of paired data (Statview 5.0; SAS Institute Inc, Cary, NC).

Analysis of Ras and Prenyl Protein Processing

Lymphocyte samples containing approximately 1×10^7 cells were obtained before administration of R115777 and at the end of the 5-day treatment period. Samples were also obtained from healthy untreated volunteers to control for cell preparation and storage. Lymphocytes were stored frozen as pellets before prenyl protein processing was analyzed essentially as described.⁵² Briefly, lymphocyte pellets were resuspended in 0.5 mL of sonication buffer consisting of 20 mmol/L HEPES, 1 mmol/L EDTA, 1 mmol/L MgCl₂, 1 mmol/L dithiothreitol, 1 mmol/L phenylmethylsulfonyl fluoride, and 2 μ mol/L pepstatin. The cell pellets were lysed by sonication for 20 seconds. The lysates were centrifuged at $100,000 \times g$ for 60 min. The resulting supernatants were transferred to microfuge tubes, and the pellets were resuspended in 0.5 mL of sonication buffer. Protein determinations were performed on 5- μ L portions of supernatants and pellets, and samples were diluted to equal protein concentrations in Laemmli sample buffer. Samples (10 to 15 μ L) were separated by electrophoresis on 10% to 20% gradient sodium dodecyl sulfate polyacrylamide minigels and transferred to polyvinylidene fluoride membranes. The membranes were incubated overnight at 4°C with primary antibodies. Primary antibodies from Calbiochem (La Jolla, CA) (lamin B1 and pan-Ras Ab-3) and Santa Cruz Biotechnology (Santa Cruz, CA) (Rho B) were used for the Western blot analysis of these prenylated proteins. The immunostained antigens were visualized using horseradish peroxidase-conjugated secondary antibodies and the Amersham ECL-enhanced chemiluminescent detection system (Amersham, Buckinghamshire, United Kingdom).

ras Mutation Analysis

Paraffin sections of primary tumors or metastatic sites were analyzed. The first section (4 μ m) from each block was stained with hematoxylin and eosin and examined by a pathologist to confirm the presence of cancer and to determine the extent of tumor on the slide. A series of 10- μ m sections were cut for mutation analysis. To minimize possible contamination between samples, the microtome was cleaned to remove excess paraffin and a new blade was used between samples. DNA was extracted from one or more of the remaining sections, and samples were analyzed for the presence of *ras* by a nested PCR protocol, followed by restriction fragment length polymorphism (RFLP) analysis. Restriction enzymes were selected such that wild-type *ras* sequences were cleaved, leaving an intact gel band of the expected size when a mutation was present. Cell-line DNA from both wild-type and, where available, mutant *ras* were used as controls. This nested PCR/RFLP method can detect mutations at H-*ras* intron D and all K-, H-, and N-*ras* mutations at codons 12, 13, and 61 (except for H-*ras* codon 13, which is an extremely rare mutation). Studies with cell-line DNA indicated that this protocol detects one mutant allele in a background of 10 wild-type alleles.

RESULTS

Patient Characteristics

Twenty-seven patients were treated in this phase I study. Patient characteristics are listed in Table 2.

Adverse Events

Table 3 includes all adverse events observed during cycle 1 of therapy considered possibly, probably, or very likely related to R115777. Dose-limiting toxicity was observed at the 1,300-mg dose level in one patient who had a prior history of mild peripheral neuropathy attributed to paclitaxel chemotherapy. During cycle 1, she developed severe burning in her lower extremities, oral cavity, and vaginal area. The pain required opioid analgesics and resolved within 24 hours after withholding of the drug. There were no signs of stomatitis or vaginitis on physical examination. The same patient experienced similar but less severe symptoms during her next treatment cycle at a reduced dose (800 mg bid); however, severe (grade 3) symptoms recurred during her third cycle of therapy at 800 mg bid.

Although not defined as dose-limiting, clinically significant fatigue was observed in patients treated at the higher dose levels (800 mg and 1,300 mg bid). With National Cancer Institute of Canada criteria, grade 2 fatigue (two-level decrease in performance status) was observed in one of three patients who received 1,300 mg bid during the first cycle of therapy and in four of six patients treated at 1,300 mg bid during any cycle (Table 4).

One patient developed a grade 2 increase in his serum creatinine level during his second treatment cycle. The patient's baseline creatinine level was 1.1 mg/dL. He received the first cycle of R115777 at 800 mg bid without a

Table 2. Patient Characteristics (n = 27)

	No. of Patients
Age, years	
Median	58
Range	27-78
Sex	
Male	13
Female	14
Diagnosis	
Colorectal cancer	11
Breast cancer	7
Other*	9
Prior therapies	
No prior therapy	1
Prior chemotherapy	
1-2 prior regimens	12
≥3 prior regimens	14
Prior hormone/immune therapy	
1 prior regimen	8
2 or more	3
Prior radiation therapy	17
Zubrod performance status	
0	5
1	22
ras mutation status	
K-ras codon 12 (colon)	2
K-ras codon 61 (liver)	1
Negative	20
Not available	4

*Other diagnoses were rhabdomyosarcoma, non-Hodgkin's lymphoma, adenocarcinoma of unknown primary, sarcoma (not otherwise specified), esophageal carcinoma, gallbladder carcinoma, hepatoma, melanoma, and non-small-cell lung cancer.

significant change in his serum creatinine level. During cycle 2, in which R115777 was administered at 1,300 mg bid, his creatinine level increased to 3.3 mg/dL on day 6. His creatinine level had normalized by day 30. He received cycle 3 at the 800-mg bid dose without event. Evaluation of urine sediment during cycle 2 was remarkable for renal epithelial cells consistent with an acute tubular injury. Proteinuria was not significant. Other causes of renal dysfunction (eg, contrast dye administration, nonsteroidal analgesics, hypotension) and predisposing factors for renal dysfunction were excluded. Eight additional patients were noted to have increased creatinine levels in this study. In five of these eight patients, grade 1 creatinine elevation was noted and considered at least possibly related to R115777 (three patients at the 1,300-mg bid dose level, one patient at the 800-mg bid dose level, and one patient at the 200-mg bid dose level). In one of these five patients, examination of the urinary sediment was also consistent with acute tubular injury during the first cycle at 1,300 mg bid and during a subsequent cycle at 800 mg bid. In three patients, other

causes were thought more likely to account for the creatinine elevation (obstruction due to malignant disease in two patients and an inferior vena cava thrombosis in one patient).

Another prominent adverse event was nausea and vomiting. At dose levels 1 through 6, an oral liquid formulation was used. This liquid had an unpleasant taste, and nausea and vomiting were frequently reported. Although the capsule formulation was tolerated better than the liquid formulation, at the highest dose levels, the capsule formulation was also associated with grade 1 and 2 nausea and vomiting. Twenty of 27 patients required antiemetic therapy. The choice of antiemetic was made at the discretion of the prescribing physician. Drugs used included ondansetron, granisetron, prochlorperazine, metoclopramide, lorazepam, and promethazine.

One patient with a baseline history of migraines treated with 125 mg bid experienced a grade 3 headache during her first cycle of therapy. This headache was similar in character but more severe than her prestudy headaches. She was able to continue treatment without subsequent events.

Minimal hematopoietic toxicity was observed in this trial. One patient treated with 50 mg bid experienced grade 3 neutropenia. This patient had multiple prior therapies for breast cancer, including radiation. A review of her complete blood counts obtained before study drug administration demonstrated intermittent grade 3 neutropenia. This patient continued to receive study drug at the same dose level with resolution of her neutropenia.

A second patient with a baseline platelet count of 103,000/ μ L developed grade 2 thrombocytopenia (72,000/ μ L) during cycle 1 of R115777 at the 1,300-mg bid dose level. This patient also experienced grade 3 peripheral neuropathy requiring a dose reduction. She was able to continue therapy without delay at the 800-mg bid dose level with resolution of her thrombocytopenia and no subsequent recurrences of thrombocytopenia.

Eight patients required RBC transfusions during this trial. All patients requiring blood transfusions had received prior therapy for their advanced cancer and had multiple blood samples drawn for pharmacokinetic studies and toxicity monitoring.

Several farnesylated proteins are important in maintenance of retinal cytoarchitecture and photoreceptor structure⁴⁸; therefore, all patients were carefully evaluated for ophthalmologic abnormalities. No abnormalities were noted in D-15 color vision and contrast sensitivity testing. Two patients had small unilateral visual field defects while on therapy. In one patient, the visual field defect resolved during continued R115777 therapy. In the second patient, a possible defect in the same area was noted at baseline that became more apparent after initiation of therapy. Both

Table 3. Cycle 1 Toxicities Related to Study Drug by Dose Level

	Dose																										
	25			50			75			125			200			325			500			800			1,300		
	Grade 1	Grade 2	Grade 3	Grade 1	Grade 2	Grade 3	Grade 1	Grade 2	Grade 3	Grade 1	Grade 2	Grade 3	Grade 1	Grade 2	Grade 3	Grade 1	Grade 2	Grade 3	Grade 1	Grade 2	Grade 3	Grade 1	Grade 2	Grade 3	Grade 1	Grade 2	Grade 3
Nausea	1			2			1			2			1			1			2			2	1		3		
Vomiting				2																		2	1		1		
Fatigue				1						1						1			2			3			2	1	
Lethargy																			1								
Anorexia																			2						1		
Headache				1						1	1					1			1						1		
Hypotension													1												2		
Arthralgia							1									1											
Taste change	2												1														
Heartburn										1			1												2		
Constipation																1											
Hiccoughs										1						1											
Bloating																									2		
Neurocortical													1						1			1			1		
Xerostomia										1																	
Pharyngitis																2											
Chills	1																		1								
Dizziness																			1								
Neuropathy																										1	
Creatinine																									2		
Thrombocytopenia																									1		
Neutropenia						1																					
Hemoglobin																		1		1							
Hypomagnesemia																									2		
Hypokalemia																										1	

NOTE. This table includes the number of patients who experienced toxicity, at maximum grade per patient, at each dose level during their first cycle of therapy. Three patients received cycle 1 at each dose level. Toxicities were considered possibly, probably, or very likely related to study drug.

patients were asymptomatic. Retinal examinations were remarkable for the development of abnormalities during drug administration in four patients, including cotton wool spots and small retinal hemorrhages (two patients), small hemorrhage (one patient), and Roth's spots (one patient). These four patients also had a history of diabetes, hypertension, or anemia. All patients were asymptomatic, and the ophthalmologic findings were thought to be consistent with those observable in a chronically ill population. No new or worsening cataracts were noted in this trial.

Several serious adverse events were observed during this trial that were not considered related to the study drug. One patient with history of pulmonary embolism developed an inferior vena cava clot at the site of an inferior vena cava filter. He was taken off study and treated with anticoagulant therapy. One patient with melanoma and a prior history of brain metastasis treated with radiation therapy experienced an unwitnessed seizure. Subsequent magnetic resonance imaging revealed new and enlarged brain metastases. One patient with a history of hypertension experienced an episode of confusion. Imaging studies were consistent with

a new small cerebral hemorrhage thought secondary to hypertension. One patient developed a small pericardial effusion and atrial arrhythmia thought to be related to progressive malignant disease.

Pharmacokinetics

R115777 was rapidly absorbed, with peak plasma concentrations reached within 0.5 to 3 hours after administration of the oral solution and within 1.5 to 4 hours after administration of the pellet capsules. Pharmacokinetic parameters are shown in Table 5. Representative concentration-time profiles of (mean \pm SD) R115777 are shown in Fig 2 for a patient receiving 125 mg bid administered as an oral solution and 500 mg bid administered as a capsule. Within the 25- to 1,300-mg bid dose range, C_{max} values ranged from 93.0 to 3,585 ng/mL on day 1 and from 59.2 to 2,946 ng/mL on day 6, and AUC_{12h} values ranged from 289 to 13,531 ng \cdot h/mL on day 1 and from 315 to 15,724 ng \cdot h/mL on day 6. On day 6, C_{min} values ranged from 6.7 to 363 ng/mL. The elimination of R115777 from plasma was biphasic. The half-life associated with the first elimination

Table 4. Toxicities Related to R115777 During All Cycles by Dose Level (n = 85 cycles)

	Dose															
	50 mg (6 patients, 7 cycles)		75 mg (8 patients, 10 cycles)		125 mg (7 patients, 9 cycles)		200 mg (7 patients, 10 cycles)		325 mg (7 patients, 7 cycles)		500 mg (9 patients, 16 cycles)		800 mg (10 patients, 14 cycles)		1,300 mg (6 patients, 9 cycles)	
	Grade		Grade		Grade		Grade		Grade		Grade		Grade		Grade	
	2	3	2	3	2	3	2	3	2	3	2	3	2	3	2	3
Nausea	1		2					1			2		1	1	1	
Vomiting							2						2	1	1	
Fatigue			2								2		2		4	
Headache					1	1							1			
Hypotension													2		1	
Hypertension								1								
Arthralgia			1													
Myalgia											1					
Edema							1									
Fever							1									
Pericardial			1													
Neuropathy														1		1
Neurocortical								1								
Neutropenia		1														
Hemoglobin	1									1		2	1	1		1
Thrombocytopenia																
Thrombocytosis													1		1	
Creatinine															1	
Hypokalemia													2		2	
Hypomagnesemia															1	

NOTE. This table includes the number of patients who experienced toxicities greater than grade 1, at maximum grade per patient, that were considered possibly, probably, or very likely related to study drug, at each dose during all cycles of therapy. The 500-mg level includes toxicities observed in patients receiving the 500-mg capsule formulation or the 525-mg liquid formulation. The 800-mg level includes toxicities observed in patients receiving the receiving 800-mg capsule formulation and the 850-mg liquid formulation of R115777. Patients experiencing toxicities at more than one dose level are reported at all dose levels at which the toxicity was observed. Three patients received three cycles at the 25-mg dose, and there were no grade 3 or 4 adverse events observed.

phase was 5.27 ± 3.24 hours (SEM + SD) for the oral solution (n = 17) and 4.34 ± 1.4 hours for the pellet capsule (n = 9). The terminal half-life associated with the second phase of elimination varied with the ability to quantify R115777 in plasma. Its median value was about 16 hours. Steady-state conditions were obtained within 2 to 3 days of bid dosing. The accumulation ratio was 1.09 ± 0.28 for the oral solution and 0.92 ± 0.20 for the capsule and indicates little accumulation of R115777 after a 5-day bid dosing regimen.

Plots of the individual values of C_{max} and AUC_{12h} , evaluated after the first dose on day 1 and the last dose on day 6, versus the administered dose of R115777 (Fig 3) indicate a consistent dose-proportional increase in the 25 to 325-mg dose range for the oral solution. For the capsule, a dose-proportional increase was observed in the 500- to 1,300-mg dose range after the first dose on day 1. However, at day 6, AUC_{12h} and C_{max} seemed to increase less than dose proportional. Since vomiting occurred only during one out of 11 assessments for the pharmacokinetics of the 800-

and 1,300-mg doses, it is not likely that the deviation from dose proportionality is the result of drug loss from emesis. The data also suggest that the bioavailability of the capsules is less than that of the oral solution. Furthermore, the data suggest substantial interindividual variability in the oral bioavailability of R115777.

The urinary excretion of unchanged R115777 (n = 15) was negligible, as less than 0.1% of the administered oral dose was excreted in the urine as unchanged drug. In addition, $16.5 \pm 12.2\%$ (mean \pm SD) of the administered dose was excreted in the urine as the glucuronide conjugate of R115777.

The estimates of the logistic regression model parameters, as listed in Table 6, related frequently observed adverse events with pharmacokinetic parameters. According to the model, fatigue was the only response for which the probability of occurrence could be predicted reliably on the basis of C_{max} and AUCs. The $AUC_{12h(ss)}$ corresponding to a 50% probability to develop fatigue was estimated at $4,210 \pm 1,390$ ng \cdot h/mL (mean \pm SD).

Table 5. Pharmacokinetic Parameters

Parameter	Oral Solution					
	25 mg	50 mg	75 mg	125 mg	200 mg	325 mg
Day 1						
t_{max} , hours	0.8 ± 0.3	1.4 ± 0.6	1.1 ± 0.4	1.5 ± 0.7	1.3 ± 0.3	1.8 ± 1
C_{max} , ng/ml	147 ± 64	266 ± 90	264 ± 140	646 ± 109	712 ± 474	2,045 ± 933
AUC_{12h} , ng · h/ml	470 ± 254	1,005 ± 258	1,021 ± 615	2,475 ± 690	2,616 ± 1,541	8,891 ± 4,045
$t_{1/2}$, hours	5.6 ± 2.0	5.0 ± 1.3	9.1 ± 6.4	4.4 ± 1.9	4.9 ± 1.4	2.7 ± 0.2
Day 6						
t_{max} , hours	1.1 ± 0.4	1.4 ± 0.3	2.2 ± 1.5	1.9 ± 0.3	1.5 ± 0.5	1.8 ± 0.3
C_{min} , ng/ml	10.0 ± 3.0	24.0 ± 15.0	28.0 ± 6.0	84.0 ± 38.0	66.0 ± 46.0	148 ± 89
C_{max} , ng/ml	123 ± 87	285 ± 101	274 ± 51	528 ± 102	778 ± 470	1,549 ± 663
AUC_{12h} , ng · h/ml	506 ± 273	1,108 ± 507	1,207 ± 330	2,537 ± 396	2,940 ± 1,736	7,651 ± 3,070
$t_{1/2terminal}$, hours	12.6 ± 13.8	12.8 ± 8.5	11.5 ± 4.7	20.7 ± 7.5	58.3 ± 48.4	18 ± 7.7
Accum index	1.1 ± 0.2	1.1 ± 0.3	1.3 ± 0.4	1.1 ± 0.3	1.1 ± 0.3	0.9 ± 0.1
Parameter	Capsule					
	500 mg		800 mg		1,300 mg	
Day 1						
t_{max} , hours	3.4 ± 0.6		3.0 ± 1.0		1.8 ± 0.3	
C_{max} , ng/ml	1,637 ± 996		1,476 ± 569		2,521 ± 1,038	
AUC_{12h} , ng · h/ml	9,304 ± 7,669		7,134 ± 2,526		11,970	
$t_{1/2}$, hours	3.8 ± 0.5		5.2 ± 1.2		7.1 ± 6.7	
Day 6						
t_{max} , hours	3.7 ± 0.6		2.8 ± 1.3		1.6	
C_{min} , ng/ml	183 ± 115		187 ± 153		115	
C_{max} , ng/ml	1,656 ± 1,124		1,589 ± 969		1,115	
AUC_{12h} , ng · h/ml	8,701 ± 6,092		6,951 ± 3,906		5,935	
$t_{1/2terminal}$, hours	31.5 ± 17.1		24.6 ± 9.1		13.0	
Accum index	1.0 ± 0.2		0.9 ± 0.2		0.6	

NOTE. Pharmacokinetic parameters (mean ± SD, n = 3 per dose level or when SD is omitted, n = 2) of R115777 in patients with advanced incurable cancer were evaluated in cycle 1 after the first dose on day 1 and after the last dose on day 6. R115777 was given bid as an oral solution (25 to 325 mg) and as pellet capsules (500 to 1,300 mg).

The model prediction for nausea had a borderline significance. Vomiting and diarrhea could not be related to any of the pharmacokinetic parameters.

Flow Cytometric Analysis

The effect of farnesyltransferase inhibitors on T-, B-, and natural killer-cell populations was assessed by flow cytometry. To assess changes in the threshold for activation of the cells, the expression of early and late activation markers (CD69 and HLA-DR, respectively) and CD45 isoform markers of naive and activated/memory subpopulations was examined in CD4 populations. Finally, atypical CD8 populations expressing CD57 and lacking in CD28 expression expand after chemotherapy or transplantation, in human immunodeficiency virus and in the extreme elderly, in a process that may reflect terminal differentiation of chronically activated cells.^{53,54} These CD8 subpopulations were therefore assessed.

Flow cytometric analyses were performed at five time points: pretreatment (cycle 1, day 1), end of the first drug treatment (cycle 1, day 6), end of the first cycle (cycle 1, day

14), end of the second cycle (cycle 2, day 14), and end of the third cycle (cycle 3, day 14). All 27 patients were assessed before the start of therapy, 21 were assessed through the end of two cycles of treatment and recovery, 16 were assessed through three cycles, and two were observed after four and six cycles.

The absolute numbers (cells/ μ L) of all peripheral-blood lymphocyte populations assessed (CD4, CD8, total CD3, B, and natural killer cells) decreased during the first 5-day treatment period ($P[CD4] = .047$, $P[CD8] = .01$, $P[\text{natural killer}] = .001$, $P[B] = .36$) but recovered to pretreatment levels by the end of cycle 1 or cycle 2. T-cell subsets and B-cell populations at the end of the third cycle (cycle 3, day 14) were reduced 30% to 35% compared with pretreatment levels ($P[CD4] = .001$, $P[CD8] = .001$, $P[\text{natural killer}] = .08$, $P[B] = .007$) but remained within normal adult ranges. The reduction in numbers persisted in the two individuals observed for longer periods. The drop in T and B cells was associated primarily with a decrease in the overall frequency of lymphocytes from an average of $21\% \pm 2.3\%$ at baseline (cycle 1, day 1) to $16.6\% \pm 2.3\%$ at cycle 3, day

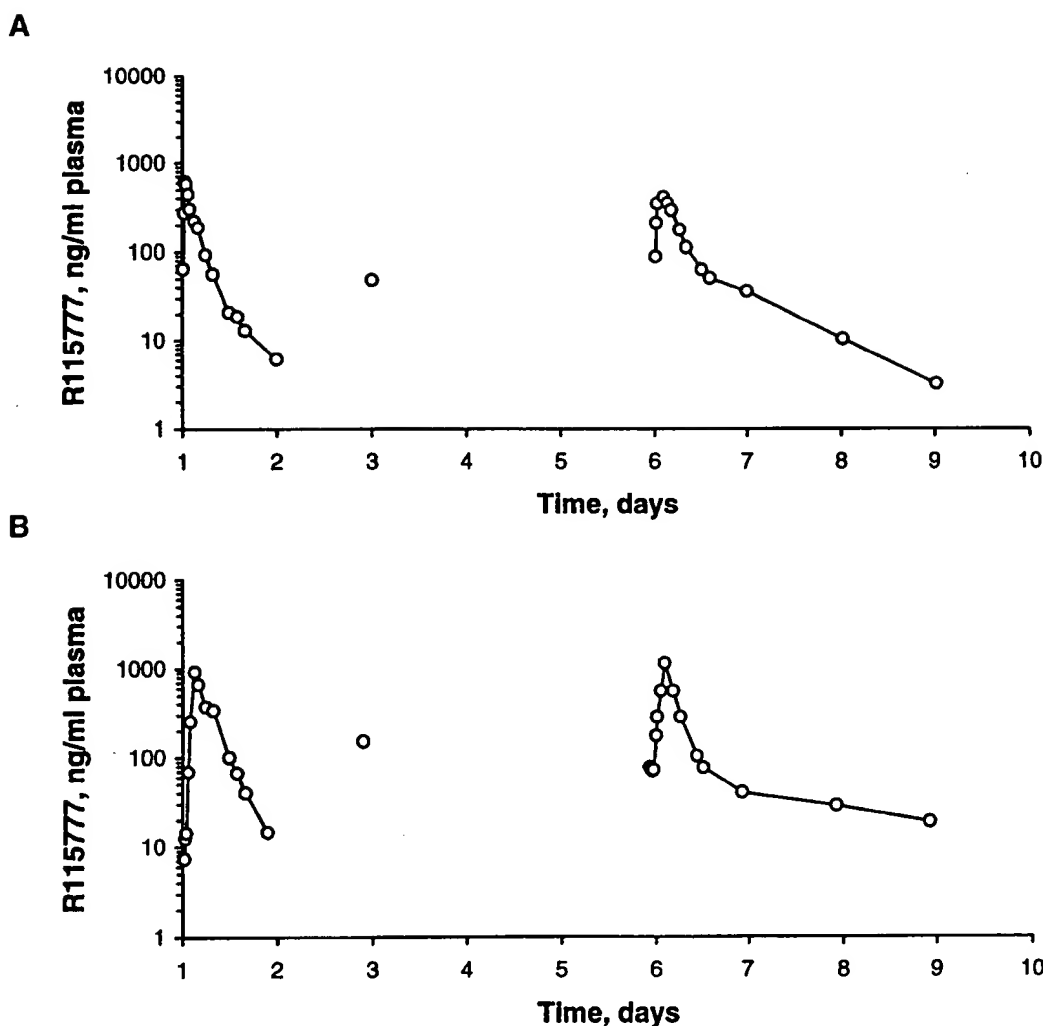


Fig 2. Representative concentration-time profiles of R115777 given bid to patients as an oral solution (A, 125 mg) and as capsules (B, 500 mg).

14; this corresponded to an average decrease in the total number of lymphocytes from $1,454 \pm 166$ cells/ μ L to $1,026 \pm 114$ cells/ μ L. The total WBC count did not change significantly ($7.3 \pm 0.71 \times 10^3/\mu$ L v $7.1 \pm 0.77 \times 10^3/\mu$ L) at these time points. Thus, although a 14-day period was sufficient for recovery of lymphocyte levels after the first two cycles, it was not sufficient for the third.

The percentages of T-cell subsets and B and natural killer cells within the total lymphocyte population remained remarkably constant throughout the study. Furthermore, the frequency of expression of activation markers (HLA-DR), of naive and memory phenotypes in CD4 cells, and of atypical chronically activated CD8 cells remained consistent within each patient. This lack of changes in subpopulations of T cells would be consis-

tent with either altered trafficking of lymphocytes within the peripheral blood or with a nonspecific loss of lymphocyte populations.

Analysis of Ras and Prenyl Protein Processing

The processing of the prenylated protein lamin B1, Ras, and Rho B was studied in lymphocytes using a technique initially developed to study the effects of farnesyl protein transferase inhibitors in tumor cells in tissue culture. The method measures levels of prenylated proteins in particulate membrane fractions and the appearance of unprenylated proteins in the soluble, cytosolic fractions. Strong signals for Rho B and Ras were observed in all particulate membrane fractions. Levels were not decreased by treatment with high doses of R115777 (500, 800, and 1,300 mg).

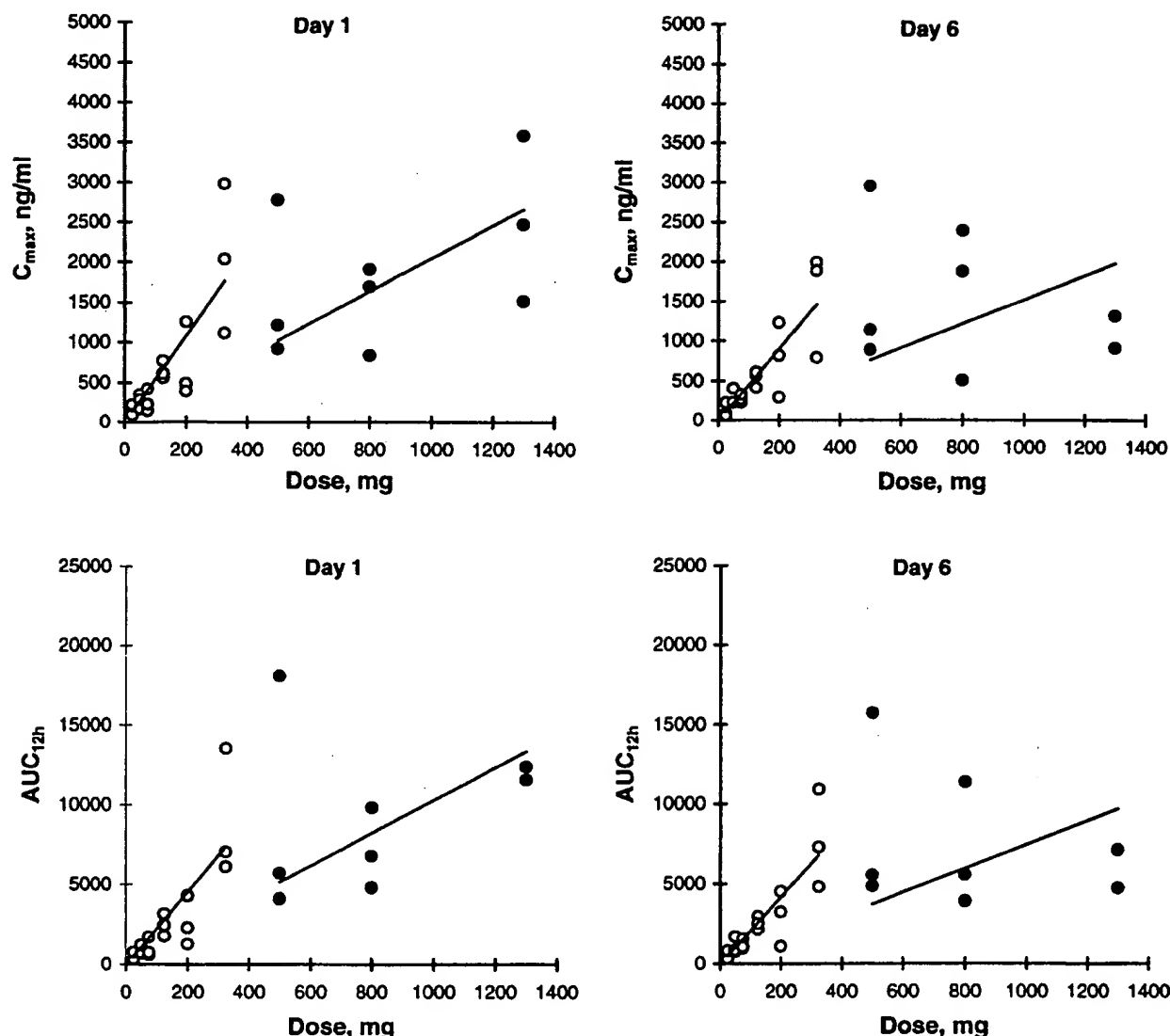


Fig 3. Individual values of C_{max} and AUC_{12h} versus bid dose, evaluated in cycle 1 after the first dose on day 1 and after the last dose on day 6. The oral solution and the oral pellet capsule are represented by open and closed circles, respectively. The trendlines are the regression lines with the intercept set at zero.

There was no appearance of Rho B in soluble fractions after treatment with R115777, an observation consistent with the posttranslational modification of the protein by geranylgeranyltransferase. Evaluation of soluble, unfarnesylated Ras revealed that an antigen appearing randomly in patient and healthy volunteer samples cross-reacted with the pan-Ras antibody. The cross-reactivity seemed to be associated with erythrocyte contamination and hemolysis in samples. This prevented an accurate assessment of soluble unfarnesylated Ras. However, there was no evidence of a treatment-related increase in soluble Ras in

the samples. Lamin B1 immunoreactivity was at the limits of detection and could not be reliably measured. It is known that lamin B1 expression is restricted to certain tissues and predominates in proliferating tissues.⁵⁵ The low levels of lamin B1 compared with those obtained in cell lines grown in culture may reflect the lack of cell proliferation in the peripheral-blood lymphocyte compartment. Although peripheral-blood lymphocytes may be attractive for monitoring the effects of prenylation inhibitors because of their accessibility, the lack of cell turnover may preclude their utility in biomarker studies.

Table 6. Estimates and SEs of Parameters of the Logistic Model Fitted to All Combinations of Responses and Predictors

Response/Predictor	Units	Parameters	Estimates	SEs	P
Nausea					
C_{max}	ng/mL	P_{50}	384	174	.0371
	-	n	1.21	0.662	.0793
AUC_{12} (sd)	ng · h/mL	P_{50}	1420	676	.0459
	-	n	1.11	0.59	.0723
AUC_{12} (ss)	ng · h/mL	P_{50}	1530	705	.0401
	-	n	1.13	0.667	.104
Vomiting					
C_{max}	ng/mL	P_{50}	1540	2290	.506
	-	n	0.0795	0.427	.854
AUC_{12} (sd)	ng · h/mL	P_{50}	8580	12700	.506
	-	n	0.0835	0.361	.819
AUC_{12} (ss)	ng · h/mL	P_{50}	8650	12800	.505
	-	n	0.223	0.434	.612
Diarrhea					
C_{max}	ng/mL	P_{50}	4370	6480	.506
	-	n	0.343	0.446	.449
AUC_{12} (sd)	ng · h/mL	P_{50}	16800	21600	.443
	-	n	0.433	0.439	.334
AUC_{12} (ss)	ng · h/mL	P_{50}	12400	17200	.478
	-	n	0.466	0.518	.376
Fatigue					
C_{max}	ng/mL	P_{50}	1040	355	.00745
	-	n	1.48	0.611	.0233
AUC_{12} (sd)	ng · h/mL	P_{50}	4210	1390	.00553
	-	n	1.62	0.654	.0205
AUC_{12} (ss)	ng · h/mL	P_{50}	4230	1450	.00717
	-	n	1.54	0.661	.0279

Antitumor Response

Twenty-seven patients were treated on this phase I trial. Two patients did not complete a total of three cycles (6 weeks) of therapy for reasons other than disease progression (one patient for noncompliance and one patient for development of inferior vena cava thrombosis) and were not evaluated for a response. By the end of 6 weeks of therapy, 17 patients had developed progressive disease and therapy was discontinued. Among eight patients who had had stable disease after three cycles of therapy, four continued therapy with R115777 and their disease remained stable for 2 to 5 months. One patient with metastatic colon cancer involving the mediastinum and lung experienced improvement in symptoms (decreased cough) and a carcinoembryonic antigen decrease from 2,991 to 1,626 ng/mL. This patient developed progressive disease after 5 months of R115777 therapy.

DISCUSSION

This phase I trial attempted to determine the maximum-tolerated dose of R115777 when administered orally twice daily for 5 consecutive days followed by 7 to 9 days of rest. The maximum-tolerated dose as defined in the protocol was

not reached and dosing was terminated at the highest dose level (1,300 mg bid; total daily dose, 2,600 mg).

Only one dose-limiting toxicity was observed in one of six patients who received R115777 1,300 mg bid. This patient developed grade 3 peripheral neuropathy, described as a painful burning sensation in the extremities, oral cavity, and vaginal area. Although not defined as dose limiting, grade 2 fatigue (decrease in two performance status levels) was observed in four of six patients at the 1,300-mg bid dose level and two of nine patients at the 800-mg bid dose level. Grade 1 to 2 increases in serum creatinine levels and urinary findings consistent with acute tubular injury were noted in two patients treated with the 1,300-mg dose, which suggests that R115777 may be nephrotoxic at high doses. Therefore, we recommend that patients maintain adequate hydration during R115777 therapy and that concurrent treatment with agents known to cause renal tubular injury be avoided. Minimal hematopoietic toxicity was observed in this trial, possibly due to the interrupted schedule.

Pharmacokinetic studies demonstrate that R115777 is orally bioavailable with plasma concentrations reaching those necessary for an antitumor effect in preclinical studies. Dose-proportional pharmacokinetics in the 25- to

325-mg dose range were noted for the oral solution throughout the 5-day dosing regimen. For the capsule, dose proportionality could be demonstrated in the 500- to 1,300-mg dose range after the first dose on day 1 but not after the last dose on day 6. Furthermore, the data suggest that the bioavailability of the capsules is less than that of the oral solution. However, because of the limited data and the high interindividual variability, more data are needed to investigate these observations. The pharmacokinetics of R115777 will be further explored in the drug development of R115777 to allow correlation of pharmacokinetic parameters with patient characteristics, disease state, liver function, and concomitant medication using population pharmacokinetic analysis techniques. Also, other drug formulations and the effect of food will be evaluated. Determination of the therapeutic level will allow assessment of the importance of the interindividual pharmacokinetic variability.

No objective tumor responses were observed in this phase I trial, although one patient with colon cancer metastatic to lungs experienced an improvement in her cough and decreased carcinoembryonic antigen levels. *ras* mutation analysis was performed on tumor specimens of patients participating in this trial. Three of 23 tumor specimens tested were positive for a *ras* mutation. The low frequency of *ras* mutations in this study can be attributed to the small sample size and patient selection factors. We also had other trials open at our institution for patients with known *ras* mutations, which may also have been a contributing factor. The results of phase II studies will be necessary to correlate *ras* mutation status with clinical response.

Although the protocol-defined maximum-tolerated dose was not achieved in this trial, analysis of toxicity data from all cycles and the pharmacokinetic data suggest that 500 mg bid for 5 days every 14 days is an appropriate dose for phase II studies. Pharmacokinetic studies demonstrate that 500 mg orally twice daily achieves plasma concentrations correlating with an antitumor effect in preclinical studies. The most frequent clinically significant adverse event related to R115777 was fatigue. Two of seven patients treated with 800 mg bid and four of six patients treated at 1,300 mg bid reported grade 2 worsening of performance status. All patients had advanced cancer and virtually all of them had received multiple previous therapies that could have contributed to declines in performance status. Nonetheless, the association of increasing frequency of significant performance status reduction with doses greater than 500 mg bid is reasonably strong. Clinical applications of this schedule might be in combination with cytotoxic chemotherapy, especially in light of the finding that cisplatin and paclitaxel have been demonstrated to have additive to synergistic effects when combined with farnesyl protein transferase

inhibitors.⁵⁶ It remains to be seen whether the dose and schedule defined in this trial has utility as a chronic single-agent therapy, because only two patients received R115777 for at least 2 months. Further evaluation of this schedule can be addressed further in phase II studies with defined patient populations.

Further support for phase II testing with R115777 at the 500-mg orally, twice-daily schedule comes from pharmacokinetic data showing a possible deviation from dose proportionality for the oral bioavailability of R115777 at doses greater than 500 mg after repeated dosing. Our initial attempts to develop a surrogate biochemical correlate to monitor farnesyl protein transferase inhibition in peripheral-blood lymphocytes failed to detect changes that have been seen in cell culture studies. It remains to be determined whether the problem is associated with technical limitations of the assay or was due to the lack of protein turnover in the normally quiescent lymphocyte compartment.

In addition to the role mutant Ras may play in proliferation and apoptotic resistance in fibroblastic and epithelial malignancies,⁵⁷ Ras proteins also play a central role in both the activation⁵⁸ and apoptotic pathways⁵⁹ of normal T and natural killer cells. Maintenance of homeostasis in T-cell populations in adults involves a complex interplay of low-level proliferation of peripheral cells, replenishment by maturation of new naive cells from the thymus, and loss of cells by apoptosis.⁶⁰⁻⁶³ The effect of inhibition of farnesyl protein transferase on T-cell homeostasis is unknown but an important concern in a chronically administered treatment. Natural killer cells, in contrast to T cells, are relatively short-lived, but little is known of the mechanisms regulating natural killer homeostasis. For these reasons, the effect of farnesyl protein transferase inhibitors on T-, B-, and natural killer-cell populations was assessed by flow cytometry. A small decrease in the total number of lymphocytes was noted at the end of the third cycle of therapy in this trial. Although this decrease was not of clinical significance, these data suggest the need for monitoring of the lymphocyte populations in long-term or continuous-treatment trials with R115777.

This study indicates that R115777 is orally bioavailable with an acceptable safety profile. This first clinical trial with a farnesyl protein transferase inhibitor suggests further investigations are warranted. Major challenges with this and other agents that are considered cytostatic are dose and schedule selection and sequencing in combination with other cancer treatments. Early clinical trials of these and other similar compounds should continue exploratory studies of potential novel surrogate end points of drug effect⁶⁴ (for example, levels of farnesylated proteins). These studies will help select optimal dosing schedules for definitive trials that would assess time to progression and, ultimately,

overall survival. It may be necessary to administer farnesyl protein transferase inhibitors chronically or in combination with other therapies for maximum clinical benefit. A phase I study of chronic dosing with R115777 suggests that myelosuppression occurs at significantly lower doses than has been observed in this phase I trial using an interrupted schedule.⁶⁵ The different toxicity profiles seen with the intermittent versus chronic dosing schedules have implications for sequencing with other agents that cause myelosuppression. Preclinical data with various farnesyl protein transferase inhibitors demonstrate synergy or additive effects with the traditional chemotherapy agents⁵⁶ and radiation therapy.⁶⁶ At the same time, preclinical data continue to underscore that *ras* (mutated or wild-type) is not the sole target of farnesyl transferase inhibition.⁶⁷ The fact that *ras*

mutation status does not predict preclinical anticancer activity²⁸ suggests that phase II trials should target a wide variety of malignancies (including lung, breast, colon, ovarian, and hematologic malignancies), regardless of the incidence of *ras* mutations. Studies of continuous dosing and studies of R115777 in combination with other antineoplastic agents are ongoing.

ACKNOWLEDGMENT

The authors acknowledge Tanya Applegate, Caroline Fuery, Natalie Robert, Michele Steinmann, Jianbo Sun, and Jackie Toner for their contributions to the *ras* mutation analysis; Louise R. Finch, Christine Maloney, Annie Lennon-Gold, and Sylvia Avery for their research assistance; and David Venzon for the statistical review of the manuscript.

REFERENCES

1. Barbacid M: *ras* genes. *Annu Rev Biochem* 56:779-827, 1987
2. Grunewald K, Lyons J, Frohlich A, et al: High frequency of Ki-ras codon 12 mutations in pancreatic adenocarcinomas. *Int J Cancer* 43:1037-1041, 1989
3. Forrester K, Almoguera C, Han K, et al: Detection of high incidence of K-ras oncogenes during human colon tumorigenesis. *Nature* 327:298-303, 1987
4. Vogelstein B, Fearon ER, Hamilton SR, et al: Genetic alterations during colorectal-tumor development. *N Engl J Med* 319:525-532, 1988
5. Reynolds SH, Anna CK, Brown KC, et al: Activated proto-oncogenes in human lung tumors from smokers. *Proc Natl Acad Sci USA* 88:1085-1089, 1991
6. Knowles MA, Williamson M: Mutation of H-ras is infrequent in bladder cancer: Confirmation by single-strand conformation polymorphism analysis, designed restriction fragment length polymorphisms, and direct sequencing. *Cancer Res* 53:133-139, 1993
7. Almoguera C, Shibata D, Forrester K, et al: Most human carcinomas of the exocrine pancreas contain mutant c-K-ras genes. *Cell* 53:549-554, 1988
8. Bos JL, Fearon ER, Hamilton SR, et al: Prevalence of *ras* gene mutations in human colorectal cancers. *Nature* 327:293-297, 1987
9. Mills NE, Fishman CL, Rom WN, et al: Increased prevalence of K-ras oncogene mutations in lung adenocarcinoma. *Cancer Res* 55:1444-1447, 1995
10. Bos JL: *ras* oncogenes in human cancer: A review. *Cancer Res* 49:4682-4689, 1989 [published erratum appears in *Cancer Res* 50:1352, 1990]
11. Moriyama N, Umeda T, Akaza H, et al: Expression of *ras* p21 oncogene product on human bladder tumors. *Urol Int* 44:260-263, 1989
12. Clark GJ, Der CJ: Aberrant function of the *Ras* signal transduction pathway in human breast cancer. *Breast Cancer Res Treat* 35:133-144, 1995
13. Janes PW, Daly RJ, deFazio A, et al: Activation of the *Ras* signalling pathway in human breast cancer cells overexpressing *erbB-2*. *Oncogene* 9:3601-3608, 1994
14. Patton SE, Martin ML, Nelsen LL, et al: Activation of the *ras*-mitogen-activated protein kinase pathway and phosphorylation of *ets-2* at position threonine 72 in human ovarian cancer cell lines. *Cancer Res* 58:2253-2259, 1998
15. Feldkamp M, Lau N, Guha A: Astrocytomas are growth-inhibited by farnesyl transferase inhibitors through a combination of anti-proliferative and antiangiogenic activities. *Proc Am Assoc Cancer Res* 39:318, 1998 (abstr)
16. Guha A, Feldkamp MM, Lau N, et al: Proliferation of human malignant astrocytomas is dependent on *Ras* activation. *Oncogene* 15:2755-2765, 1997
17. Kato K, Der CJ, Buss JE: Prenoids and palmitate: Lipids that control the biological activity of *Ras* proteins. *Semin Cancer Biol* 3:179-188, 1992
18. Casey PJ, Solksi PA, Der CJ, et al: p21*ras* is modified by a farnesyl isoprenoid. *Proc Natl Acad Sci USA* 86:8323-8327, 1989
19. Der CJ, Cox AD: Isoprenoid modification and plasma membrane association: Critical factors for *ras* oncogenicity. *Cancer Cells* 3:331-340, 1991
20. Jackson JH, Cochrane CG, Bourne JR, et al: Farnesol modification of Kirsten-*ras* exon 4B protein is essential for transformation. *Proc Natl Acad Sci USA* 87:3042-3046, 1990
21. Reiss Y, Goldstein JL, Seabra MC, et al: Inhibition of purified p21*ras* farnesyl:protein transferase by Cys-AAX tetrapeptides. *Cell* 62:81-88, 1990
22. Gutierrez L, Magee AI, Marshall CJ, et al: Post-translational processing of p21*ras* is two-step and involves carboxyl-methylation and carboxy-terminal proteolysis. *EMBO J* 8:1093-1098, 1989
23. Kato K, Cox AD, Hisaka MM, et al: Isoprenoid addition to *Ras* protein is the critical modification for its membrane association and transforming activity. *Proc Natl Acad Sci USA* 89:6403-6407, 1992
24. Kohl NE, Mosser SD, deSolms SJ, et al: Selective inhibition of *ras*-dependent transformation by a farnesyltransferase inhibitor. *Science* 260:1934-1937, 1993 (see comments)
25. James GL, Goldstein JL, Brown MS, et al: Benzodiazepine peptidomimetics: Potent inhibitors of *Ras* farnesylation in animal cells. *Science* 260:1937-1942, 1993 (see comments)
26. Garcia AM, Rowell C, Ackermann K, et al: Peptidomimetic inhibitors of *Ras* farnesylation and function in whole cells. *J Biol Chem* 268:18415-18418, 1993
27. Ward R, Hawkins N, O'Grady R, et al: Restriction endonuclease-mediated selective polymerase chain reaction: A novel assay for the detection of K-ras mutations in clinical samples. *Am J Pathol* 153:373-379, 1998

28. Todd AV, Applegate TL, Fuery CJ, et al: Farnesyl transferase inhibitor (FTI): Effect of ras activation. *Proc Am Assoc Cancer Res* 39:317, 1998 (abstr)
29. Sepp-Lorenzino L, Ma Z, Rands E, et al: A peptidomimetic inhibitor of farnesyl:protein transferase blocks the anchorage-dependent and -independent growth of human tumor cell lines. *Cancer Res* 55:5302-5309, 1995
30. Smets G, Xhonneux B, Cornelissen F, et al: R115777, a selective farnesyl protein transferase inhibitor (FTI), induces anti-angiogenic, apoptotic and anti-proliferative activity in CAPAN-2 and LoVo tumor xenografts. *Proc Am Assoc Cancer Res* 39:318, 1998 (abstr)
31. Kohl NE, Wilson FR, Mosser SD, et al: Protein farnesyltransferase inhibitors block the growth of ras-dependent tumors in nude mice. *Proc Natl Acad Sci USA* 91:9141-9145, 1994
32. Kohl NE, Omer CA, Conner MW, et al: Inhibition of farnesyltransferase induces regression of mammary and salivary carcinomas in ras transgenic mice. *Nat Med* 1:792-797, 1995 (see comments)
33. Mangues R, Corral T, Kohl NE, et al: Antitumor effect of a farnesyl protein transferase inhibitor in mammary and lymphoid tumors overexpressing N-ras in transgenic mice. *Cancer Res* 58:1253-1259, 1998
34. Sun J, Qian Y, Hamilton AD, et al: Ras CAAX peptidomimetic FTI 276 selectively blocks tumor growth in nude mice of a human lung carcinoma with K-Ras mutation and p53 deletion. *Cancer Res* 55:4243-4247, 1995
35. James GL, Goldstein JL, Brown MS: Polylysine and CVIM sequences of K-RasB dictate specificity of prenylation and confer resistance to benzodiazepine peptidomimetic in vitro. *J Biol Chem* 270:6221-6226, 1995
36. Yokoyama K, McGeedy P, Gelb MH: Mammalian protein geranylgeranyltransferase-I: Substrate specificity, kinetic mechanism, metal requirements, and affinity labeling. *Biochemistry* 34:1344-1354, 1995 (published erratum appears in *Biochemistry* 34:14270), 1995
37. Whyte DB, Kirschmeier P, Hockenberry TN, et al: K- and N-Ras are geranylgeranylated in cells treated with farnesyl protein transferase inhibitors. *J Biol Chem* 272:14459-14464, 1997
38. Rowell CA, Kowalczyk JJ, Lewis MD, et al: Direct demonstration of geranylgeranylation and farnesylation of Ki-Ras in vivo. *J Biol Chem* 272:14093-14097, 1997
39. Liu M, Bryant MS, Chen J, et al: Antitumor activity of SCH 66336, an orally bioavailable tricyclic inhibitor of farnesyl protein transferase, in human tumor xenograft models and wap-ras transgenic mice. *Cancer Res* 58:4947-4956, 1998
40. End D, Skrzat S, Devine A, et al: R115777, a novel imidazole farnesyl protein transferase inhibitor (FTI): Biochemical and cellular effects in H-ras and K-ras dominant systems. *Proc Am Assoc Cancer Res* 39:270, 1998
41. Armstrong SA, Hannah VC, Goldstein JL, et al: CAAX geranylgeranyl transferase transfers farnesyl as efficiently as geranylgeranyl to RhoB. *J Biol Chem* 270:7864-7868, 1995
42. Lebowitz PF, Casey PJ, Prendergast GC, et al: Farnesyltransferase inhibitors alter the prenylation and growth-stimulating function of RhoB. *J Biol Chem* 272:15591-15594, 1997
43. Tapon N, Hall A: Rho, Rac and Cdc42 GTPases regulate the organization of the actin cytoskeleton. *Curr Opin Cell Biol* 9:86-92, 1997
44. Du W, Liebowitz P, Prendergast G: Cell growth inhibition by farnesyltransferase inhibitors is mediated by gain of geranylgeranylated Rho B. *Mol Cell Biol* 19:1831-1840, 1999
45. Venet M, Angibaud P, Sanz G, et al: Synthesis and in-vitro structure-activity relationships of imidazolyl-2-quinolinones as farnesyl protein transferase inhibitors (FTI). *Proc Am Assoc Cancer Res* 39:318, 1998
46. Skrzat S, Angibaud P, Venet M, et al: R115777, a novel imidazole farnesyl protein transferase inhibitor (FTI) with potent oral antitumor activity. *Proc Am Assoc Cancer Res* 39:316, 1998 (abstr)
47. Miyake Y, Horiguchi M, Tomita N, et al: Occult macular dystrophy. *Am J Ophthalmol* 122:644-653, 1996
48. Pittler SJ, Fliesler SJ, Fisher PL, et al: In vivo requirement of protein prenylation for maintenance of retinal cytoarchitecture and photoreceptor structure. *J Cell Biol* 130:431-439, 1995
49. Christian MC, Korn EL: The limited precision of phase I trials. *J Natl Cancer Inst* 86:1662-1663, 1994 (editorial; comment)
50. Simon R, Freidlin B, Rubinstein L, et al: Accelerated titration designs for phase I clinical trials in oncology. *J Natl Cancer Inst* 89:1138-1147, 1997
51. Gibaldi M, Perier D: *Pharmacokinetics*. New York, NY, Marcel Dekker, Inc (1982)
52. Yan N, Ricca C, Fletcher J, et al: Farnesyltransferase inhibitors block the neurofibromatosis type I (NF1) malignant phenotype. *Cancer Res* 55:3569-3575, 1995
53. Nocieri MM, Telford W, Russo C: Postthymic development of CD28- CD8+ T cell subset: Age-associated expansion and shift from memory to naive phenotype. *J Immunol* 162:3327-3335, 1999
54. d'Angelo AD, Monier S, Pilling D, et al: CD57+ T lymphocytes are derived from CD57- precursors by differentiation occurring in late immune responses. *Eur J Immunol* 24:1503-1511, 1994
55. Broers JL, Machiels BM, Kuijpers HJ, et al: A- and B-type lamins are differentially expressed in normal human tissues. *Histochem Cell Biol* 107:505-517, 1997
56. Moasser MM, Sepp-Lorenzino L, Kohl NE, et al: Farnesyl transferase inhibitors cause enhanced mitotic sensitivity to Taxol and epothilones. *Proc Natl Acad Sci USA* 95:1369-1374, 1998
57. Peli J, Schroter M, Rudaz C, et al: Oncogenic Ras inhibits Fas ligand-mediated apoptosis by downregulating the expression of Fas. *Embo J* 18:1824-1831, 1999
58. Gomez J, Gonzalez A, Martinez AC, et al: IL-2-induced cellular events. *Crit Rev Immunol* 18:185-220, 1998
59. Downward J: Ras signalling and apoptosis. *Curr Opin Genet Dev* 8:49-54, 1998
60. Mackall C, Hakim F, Gress R: T cell regeneration: All repertoires are not created equal. *Immunol Today* 18:245-251, 1997
61. Ho DD, Neumann AU, Perelson AS, et al: Rapid turnover of plasma virions and CD4 lymphocytes in HIV-1 infection. *Nature* 373:123-126, 1995 (see comments)
62. Hakim FT, Cepeda R, Kaime S, et al: Constraints on CD4 recovery postchemotherapy in adults: Thymic insufficiency and apoptotic decline of expanded peripheral CD4 cells. *Blood* 90:3789-3798, 1997
63. Tanchot C, Rocha B: Peripheral selection of T cell repertoires: The role of continuous thymus output. *J Exp Med* 186:1099-1106, 1997
64. Gelmon KA, Eisenhaur EA, Harris AL, et al: Anticancer agents targeting signaling molecules and cancer cell environment: Challenges for drug development? *J Natl Cancer Inst* 91:1281-1287, 1999
65. Hudes G, Schol J, Baab J, et al: Phase I clinical and pharmacokinetic trial of the farnesyltransferase inhibitor R115777 on a 21-day dosing schedule. *Proc Am Soc Clin Oncol* 18:156a, 1999 (abstr)
66. Bernhard EJ, McKenna WG, Hamilton AD, et al: Inhibiting Ras prenylation increases the radiosensitivity of human tumor cell lines with activating mutations of ras oncogenes. *Cancer Res* 58:1754-1761, 1998
67. Prendergast GC, Davide JP, deSolms SJ, et al: Farnesyltransferase inhibition causes morphological reversion of ras-transformed cells by a complex mechanism that involves regulation of the actin cytoskeleton. *Mol Cell Biol* 14:4193-4202, 1994

Second-Generation Peptidomimetic Inhibitors of Protein Farnesyltransferase Demonstrating Improved Cellular Potency and Significant in Vivo Efficacy

Stephen J. O'Connor,* Kenneth J. Barr,* Le Wang,[†] Bryan K. Sorensen,[†] Andrew S. Tasker,^{||} Hing Sham,[†] Shi-Chung Ng,[†] Jerome Cohen,[†] Edward Devine,[†] Sajeev Cherian,[†] Badr Saeed,[†] Haichao Zhang,[†] Jang Yun Lee,[†] Robert Warner,[†] Stephen Tahir,[†] Peter Kovar,[†] Patricia Ewing,[†] Jeffrey Alder,[†] Michael Mitten,[†] Juan Leal,[†] Kennan Marsh,[†] Joy Bauch,[†] Daniel J. Hoffman,[†] Said M. Sebt,[§] and Saul H. Rosenberg[†]

Departments of Cancer Research D-47B, General Pharmacology and Experimental Therapeutics D-47T, and Experimental Sciences D-4EK, Abbott Laboratories, Abbott Park, Illinois 60064-3500, and H. Lee Moffitt Cancer Center and Research Institute, Department of Biochemistry and Molecular Biology, University of South Florida, 12902 Magnolia Drive, Tampa, Florida 33612

Received April 20, 1999

The synthesis and evaluation of analogues of previously reported farnesyltransferase inhibitors, pyridyl benzyl ether **3** and pyridylbenzylamine **4**, are described. Substitution of **3** at the 5-position of the core aryl ring resulted in inhibitors of equal or less potency against the enzyme and decreased efficacy in a cellular assay against Ras processing by the enzyme. Substitution of **4** at the benzyl nitrogen yielded **26**, which showed improved efficacy and potency and yet presented a poor pharmacokinetic profile. Further modification afforded **30**, which demonstrated a dramatically improved pharmacokinetic profile. Compounds **26** and **29** demonstrated significant in vivo efficacy in nude mice inoculated with MiaPaCa-2, a human pancreatic tumor-derived cell line.

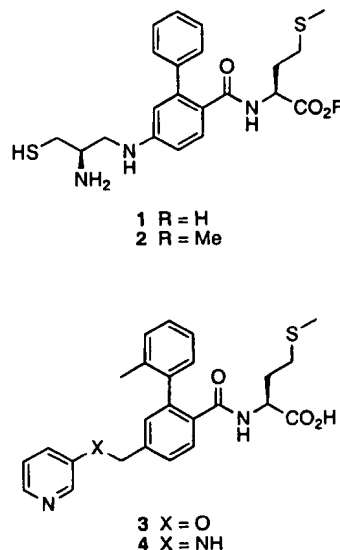
Introduction

Ras proteins are key elements in signal transduction from cell-surface receptor tyrosine kinases through the cytoplasm to the cell nucleus.¹ Mutations in *ras* genes lead to constitutively activated Ras proteins resulting in uncontrolled cell growth.^{2,3} Mutated Ras proteins are found in a number (30–50%) of human tumors including ~30% of lung cancers, 50% of colon cancers, and 90% of pancreatic cancers.⁴ Therefore, inhibition of oncogenic Ras function should be a viable therapy for these types of tumors.^{5–7}

Newly synthesized Ras proteins undergo a series of posttranslational modifications to provide the active species.^{8–12} The first modification occurs by the transfer of a farnesyl group from farnesylpyrophosphate to the cysteine near the C-terminus (CAAX box). Farnesylation is followed by proteolytic cleavage of the AAX group and subsequent O-methylation of the new C-terminus. This truncated peptide migrates to the cell surface and anchors to the membrane using the attached farnesyl chain. **The only step required for activation of Ras is the farnesylation of the cysteine thiol.** This reaction is catalyzed by the enzyme protein farnesyltransferase (FTase). Inhibition of this enzyme has been shown to reduce Ras function both in vitro and in vivo.^{13–24} Therefore, the inhibition of FTase represents an intriguing target for cancer chemotherapy.^{25,26}

We recently reported²⁷ a series of compounds related to FTI-276, **1**, a potent inhibitor of FTase (Chart 1).^{28,29}

Chart 1. Structures of FTase Inhibitors 1–4



We successfully replaced the metabolically labile cysteine with a 3-pyridyl substituent and also determined that ortho-substitution of the biphenyl moiety with sterically demanding groups provided an unexpected yet critical boost in potency. Compound **3**, with a 3-oxypyridyl linkage and an *o*-tolylbiphenyl spacer, possesses an IC₅₀ value of 0.4 nM. The ability of **3** to prevent farnesylation of Ras in whole cells (Ras processing, ED₅₀ = 0.35 μM) equaled that of FTI-277, **2**, an ester prodrug of **1**. Although equipotent to FTI-276, compound **3** was not active against human tumor xenografts (MiaPaCa) in nude mice. We ascribed the inactivity of **3** to several factors. Pharmacokinetic studies in the rat demonstrated a very short plasma half-life, and the overall oral bioavailability (6%) was very poor. In addition, **3**

* To whom correspondence should be addressed. Present address for S. J. O'Connor: Pharmaceutical Division, Bayer, 400 Morgan Lane, West Haven, CT 06516-4175. Present address for K. J. Barr: Sunesis Pharmaceuticals, Inc., 3696 Haven Ave, Suite C, Redwood City, CA 94063.

[†] Abbott Laboratories.

[§] University of South Florida.

^{||} Present address: Amgen, 1840 DeHavilland Dr, Thousand Oaks, CA 91320-1789.

may not possess activity sufficient to inhibit the growth of such an aggressive human tumor cell line. Therefore, we set out to improve upon **3** by augmenting its potency and pharmacokinetic profile. Our efforts concentrated on altering the heterocyclic ring electron density and increasing the lipophilicity of **3** and its aminopyridyl analogue **4**. These alterations included substitution on the biphenyl core of **3**, appending groups to the amino linkage of **4**, or replacement of the pyridine ring altogether. The results of our work are presented here.

Chemistry

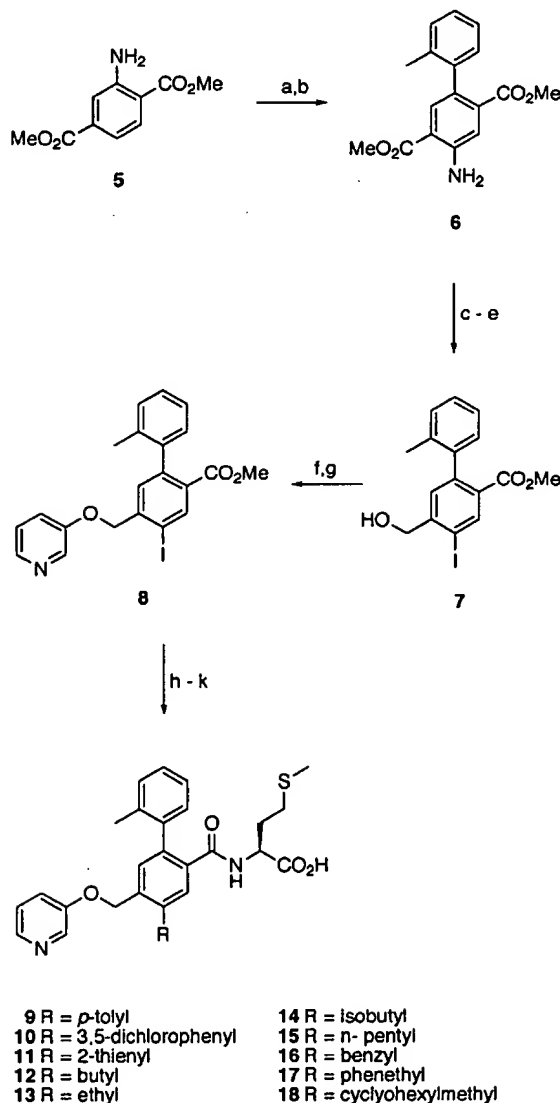
Analogues of **3** substituted at the 5-position of the biphenyl ring were prepared by Suzuki coupling of iodide **7** with boronic acids or alkylboranes according to published procedures (Scheme 1).³⁰ The boronic acids used were commercially available. The boranes were either purchased (triethylborane, tributylborane, and benzyl-9-BBN), prepared by hydroboration (tripentylborane), or prepared by reaction of the appropriate lithium or Grignard reagents with 9-methoxy-9-BBN (isobutyl, phenethyl, cyclohexylmethyl).³¹ The coupled benzoate esters were converted to the final compounds as previously described.²⁷

Analogues of amine **4** were prepared in the following manner. The appropriate amino heterocycle was reacted with an aldehyde to form the Schiff base. Reduction with NaBH₄ or Na(OAc)₃BH provided the secondary amine, which was deprotonated with *n*-BuLi or sodium bis(trimethylsilyl)amide) and coupled to a halomethylbiphenyl ester²⁷ as shown in Scheme 2. 5-Fluoro-3-aminopyridine was prepared from the 5-fluoronicotinic acid³² as shown in Scheme 4, while the pyrimidine analogue was made according to the route outlined in Scheme 5. The amides **23** and **24** were prepared by acylation of 3-aminopyridine with benzoyl or phenylacetyl chloride. The benzenesulfonamide arose from sulfonylation of 3-aminopyridine with benzenesulfonyl chloride. Each of these compounds was deprotonated and reacted with the bromomethylbiphenyl ester using the same procedure as the secondary amines. Thiazole amines were prepared analogously to the amino heterocycles and reacted with the bromide using diisopropylethylamine as an HCl scavenger. Conversion to the final compounds was straightforward.²⁷

Results and Discussion

The results of modification of **3** at the 5-position are summarized in Table 1. Examination of the data for **3**, **9**, **10**, and **11** reveals that aryl substitution at the 5-position was severely detrimental to potency against the enzyme with respect to the parent compound, whereas the activity dropped 2–3 orders of magnitude. We were less discouraged by the results of alkyl substitution. Compounds **12**–**15** demonstrate that small alkyl substituents are far better tolerated and that slightly longer, unbranched groups are somewhat favored, suggesting the presence of a narrow hydrophobic pocket. The benzyl and phenethyl analogues of **3** are equipotent to the parent compound. The diminished activity of the similarly lipophilic, yet more sterically demanding, cyclohexylmethyl analogue **18** adds credence to our postulation of a more narrow lipophilic pocket. Each of the 5-substituted analogues of **3** was

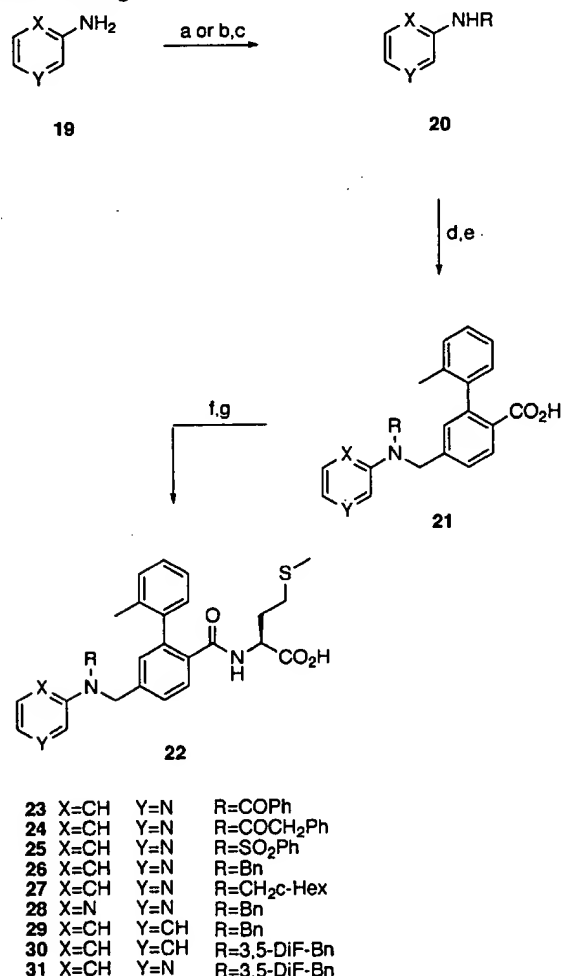
Scheme 1. Synthesis of FTase Inhibitors Containing an Ether Linkage^a



^a Reagents: (a) Br₂, pyridine/CH₂Cl₂; (b) Pd(OAc)₂, PPh₃, *o*-tolylboronic acid, aq Na₂CO₃, toluene, reflux; (c) NaNO₂, NaI, 3 N HCl, acetone; (d) aq NaOH, THF/MeOH; (e) BH₃·THF; (f) PPh₃/CBr₄, CH₂Cl₂; (g) K-O-3-Pyr, BnNEt₃Br, CH₂Cl₂; (h) R-B(OH)₂, Pd(OAc)₂, PPh₃, aq Na₂CO₃, toluene, reflux; or R₃B/R-9-BBN, Cl₂PdDPPF, base, DMF, 65 °C; (i) NaOH, aq EtOH, reflux; (j) Met(OMe)·HCl, NEt₃, EDCI, HOBT, DMF; (k) LiOH, aq THF/MeOH.

notably less active in the whole-cell Ras processing assay (ED₅₀'s ≥ 1 μM).

The results of modifications of **4**, the amine series, are summarized in Table 2. Acylation or sulfonylation of the nitrogen resulted in significant reduction in potency against the enzyme (compare **23**–**25** with **4**). The benzoyl (53 nM) and phenylacetyl (39 nM) substituted analogues were ~100 times less active against the enzyme than the NH compound. The sulfonyl derivative **25** was slightly better at 7 nM, a loss of only 15-fold. The reverse effect was observed with N-alkylation. With an IC₅₀ value of 100 pM, benzyl derivative **26** demonstrates a 4-fold increase in potency over the parent compound, suggesting that the reduction in potency observed for the acylated analogues was due principally to the electron-withdrawing nature of the substituents.

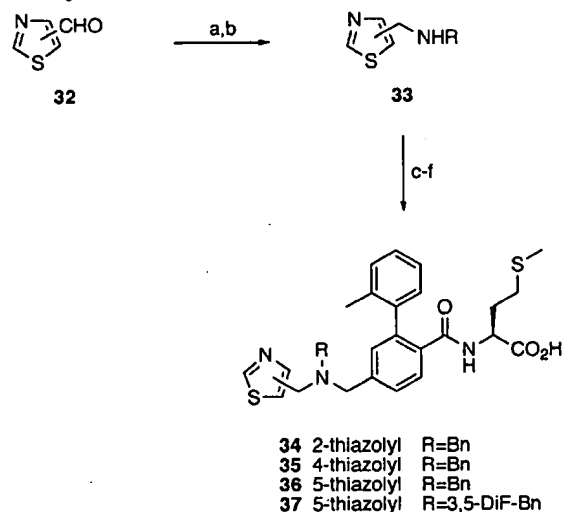
Scheme 2. Synthesis of FTase Inhibitors Containing an Amino Linkage^a

^a Reagents: (a) R-COCl or R-SO₂Cl, NEt₃, CH₂Cl₂; (b) RCHO, toluene, reflux (-H₂O); (c) NaBH₄, EtOH; (d) *n*-BuLi or NaHMDS, THF, then methyl 4-bromomethyl-2-(2-methylphenyl)benzoate; (e) NaOH, aq EtOH, reflux; (f) Met(OMe)·HCl, NEt₃, EDCI, HOBt, DMF; (g) LiOH, aq THF/MeOH.

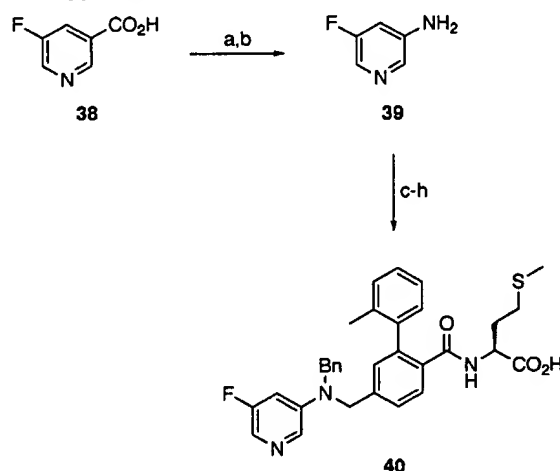
The improvement in cellular potency was even more dramatic, in that the ED₅₀ for **26** was measured to be 13 nM, a 20-fold increase. Thus **26** is the first compound we prepared possessing whole-cell activity greater than that of our original lead, FTI-277.

Despite the substantial improvement in the activity demonstrated by **26**, the pharmacokinetic behavior remained poor. The iv half-life was less than 1 h (see column 7, Table 2), and the systemic area under the curve (AUC) was well below 1 μg·h/mL upon intraduodenal (id) dosing, though the portal vein AUC was reasonable at 3 μg·h/mL. The discrepancy in AUC values is indicative of dramatic first-pass effects in the liver. In fact, after dosing compound **26** in rats over 80% of the dose can be recovered from the bile as unchanged drug.

In an attempt to improve upon the pharmacokinetic profile of **26**, we prepared the cyclohexylmethyl analogue **27** and fluoro-substituted pyridine analogue **40**. The rationale was that the cyclohexyl group might add some additional lipophilicity while the 5-fluoro derivative should be less basic than the parent pyridine. Both of these new substrates proved to be essentially equipotent with **26**. However, they each demonstrated a

Scheme 3. Synthesis of FTase Inhibitors Containing a Variously Linked Thiazole Moiety^a

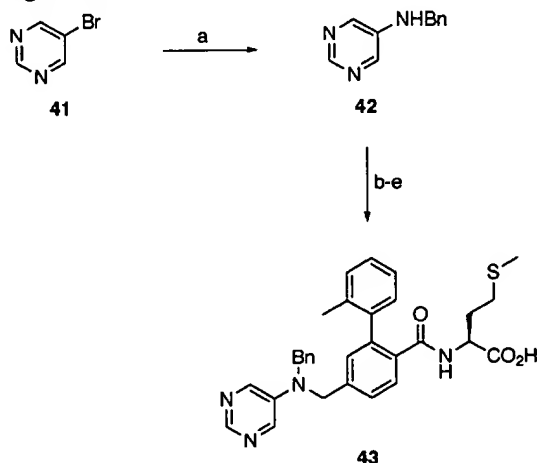
^a Reagents: (a) R-NH₂ toluene, reflux (-H₂O); (b) NaBH₄, EtOH; (c) methyl 4-bromomethyl-2-(2-methylphenyl)benzoate, Et-NiPr₂, CH₃CN, rt-60 °C; (d) NaOH, aq EtOH, reflux; (e) Met(OMe)·HCl, NEt₃, EDCI, HOBt, DMF; (f) LiOH, aq THF/MeOH.

Scheme 4. Synthesis of FTase Inhibitor 3-Fluoropyridine Analogue **40**^a

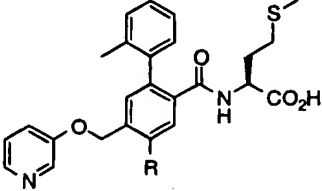
^a Reagents: (a) DPPA, NMM, ClCH₂CH₂Cl, rt-80 °C, then BnOH, cat. CuCl, reflux; (b) NH₄HCO₂, Pd/C, MeOH, reflux; (c) RCHO, toluene, reflux (-H₂O); (d) NaBH₄, EtOH; (e) *n*-BuLi, THF, then methyl 4-bromomethyl-2-(2-methylphenyl)benzoate, -30-0 °C; (f) NaOH, aq EtOH, reflux; (g) Met(OMe)·HCl, NEt₃, EDCI, HOBt, DMF; (h) LiOH, aq THF/MeOH.

reduced plasma half-life, and both reduced iv and systemic AUCs compared to **26**.

We prepared less basic heterocycles in an attempt to improve pharmacokinetics. The pyrimidine and pyrazine compounds possessed potent in vitro enzyme activity but were of lower potency in the cellular assay (compare compounds **43** and **28** with **26**). The potency of the variously substituted thiazole analogues displayed a clear regiochemical preference (compounds **34-36**, Table 2), the 5-substituted derivative proving to be substantially more active (0.5 nM) than either the 2- or 4-substituted isomers (7 and 16 nM, respectively). However, these compounds demonstrated notably reduced activity in the Ras processing assay than the corresponding pyridine analogue (e.g. compound **36**,

Scheme 5. Synthesis of FTase Inhibitor Pyrimidine Analogue 43^a

^a Reagents: (a) 5-aminopyrimidine, BnNH_2 , Cu_2O_3 , K_2CO_3 , reflux; (b) NaHMDS, THF, then methyl 4-bromomethyl-2-(2-methylphenyl)benzoate, rt, reflux; (c) NaOH, aq EtOH, reflux; (d) Met(OMe)·HCl, NEt_3 , EDCI, HOBt, DMF; (e) LiOH, aq THF/MeOH.

Table 1. Results of Substitution at the 5-Position of 3^a


compd	R	IC ₅₀ (nM)	ED ₅₀ (μM)
3	H	0.4 ± 0.2	0.4
9	4-(CH ₃)C ₆ H ₄ -	370	ND
10	3,5-Cl ₂ C ₆ H ₃ -	95	ND
11	2-thiophenyl	510	ND
12	ethyl	11 ± 1	ND
13	<i>n</i> -butyl	3	<10
14	isobutyl	29	>10
15	pentyl	2	1
16	PhCH ₂ -	1	>1
17	PhCH ₂ CH ₂ -	0.5	1
18	C ₆ H ₁₁ CH ₂ -	12	1

^a Unless statistical limits are given, the compounds were assayed once. The reliability of the in vitro assay is ±50%. The reliability of the cell-based assay is ±50–100%. Potencies that differ by more than 3-fold should be considered statistically different.

ED₅₀ = 300 nM). Additionally, none of the alternate heterocycles produced an improvement in the pharmacokinetic profile. Interestingly, although the iv AUC for compound 43 (10.4 μg·h/mL) was improved relative to 26, it was subject to efficient first-pass clearance (systemic AUC ~ 0.02 μg·h/mL).

Carbocyclic replacement of the heterocycle resulted in some interesting findings. Benzene analogue 29 possessed enzyme inhibitory potency comparable to that of the heterocyclic analogues. Though the cellular potency (ED₅₀ = 400 nM) was reduced, it was not decreased any more than observed in the non-pyridine heterocycles. Unfortunately, the pharmacokinetics showed no improvement. Compound 29 possessed similar iv half-life and portal vein AUC in rat with respect to 26, and a similarly low systemic AUC was observed.

During the process of defining the SAR of 29, the 3,5-

difluorobenzyl analogue 30 was prepared, and this compound provided the best pharmacokinetic profile observed in the entire series, yielding a systemic AUC by oral administration of nearly 11 μg·h/mL. Unfortunately, as we observed previously with other inhibitors, only the in vitro potency was maintained (0.4 nM); the Ras processing efficiency fell off substantially (~1 μM). The remarkable improvement in bioavailability of 30 prompted us to replace the *N*-benzyl substituent with the 3,5-difluorobenzyl moiety in the more potent compounds pyridyl 26 and thiazolyl 36. Although both compounds maintained comparable in vitro and cellular activity, neither possessed substantially better pharmacokinetics than the parent benzyl derivatives. Other inhibitors (data not shown) bearing this group also failed to demonstrate any improvement in pharmacokinetic behavior. We have no explanation for this isolated observation.

Of the numerous farnesyltransferase inhibitors prepared during the course of our work in this area, several compounds, including some of those reported in this study, were also tested against the related enzyme geranylgeranyltransferase 1 (GGT1ase). In nearly all cases examined the decrease in binding affinity observed was greater than 4 orders of magnitude. For example, compound 3 is 0.4 nM against FTase and 28 μM against GGT1ase.

In Vivo. Based upon the results presented, we investigated the activity of pyridine 26 and aniline 29 in vivo. In selecting these compounds, we compared a potent heterocyclic inhibitor with its carbocyclic counterpart. The compounds were tested against subcutaneous xenografts in nude mice. The first cell line we selected was MiaPaCa-2, which is derived from a human pancreatic tumor containing a *K-ras* mutation at codon 12 (Gly12Cys). In addition, the cell line contains a mutation in the binding domain of p53 at position 248 (Arg248Trp), considered a "hot spot" in human p53 cancers. This cell line quickly (~16 days) produces 1-g tumors and is nonresponsive toward the majority of conventional cytotoxic agents. The ED₅₀ of 26 against MiaPaCa-2 is less than 50 nM (91% inhibition of Ras processing at 50 nM). Like data for 29 is not available at this time.

During the experiments approximately 8-week-old nude mice (10/study group) were inoculated subcutaneously in the right flank with 0.5 mL of a 1:20 brei of MiaPaCa cells on study day 0. Therapy was initiated on study day 1 and consisted of continuous once daily dosing of compound 26 at either 25, 50, or 100 mg/kg/day (mpk/day) ip. The protocol involving aniline derivative 29 was identical to that of the pyridine derivative 26, except that doses of 25 and 12.5 mpk (ip) were used. The vehicle employed was a phosphate-buffered saline (PBS) solution with NaOH added. Vehicle was administered as the untreated control, while cyclophosphamide was used as the positive control. Measurement of tumors began on study day 6. Tumor mass was estimated by measuring length and width of the tumor with digital calipers and applying the following formula: $(L \times W^2)/2$. Mice were euthanized when tumors reached at least 1 g, and death due to drug toxicity was also monitored. Figure 1 shows select examples which illustrate our results. At the 25 mpk/day dose, 26

Table 2. Results of Modifications to the Aminopyridine Moiety of 4

compd	R ₁	R ₂	IC ₅₀ (nM)	ED ₅₀ (μM)	T _{1/2} (h)	AUC (μg·h/mL)	
						iv	systemic
4	H	3-pyridyl	0.4	3	ND	ND	ND
23	PhCO-	3-pyridyl	53	>1	ND	ND	ND
24	PhCH ₂ CO-	3-pyridyl	39	>1	ND	ND	ND
25	PhSO ₂ -	3-pyridyl	7	ND	ND	ND	ND
26	PhCH ₂ -	3-pyridyl	0.10 ± 0.04 ^a	0.013 ± 0.005 ^a	0.83 ± 0.21	3.0 ± 0.7	0.5 ± 0.1 ^a
						2.5 ± 0.7	0.11 ± 0.03 ^b
27	C ₆ H ₁₁ CH ₂ -	3-pyridyl	0.1	0.01	<0.4	1.0 ± 0.3	0.1 ± 0.1
40	PhCH ₂ -	5-F-3-pyridyl	0.1	0.03	<0.4	2.4 ± 0.9	0.4 ± 0.3 ^a
43	PhCH ₂ -	5-pyrimidyl	0.4	0.09	0.5	10.4 ± 6.0	0.02 ± 0.02 ^a
28	PhCH ₂ -	2-pyrazinyl	0.8	0.05	<0.4	1.8 ± 0.3	0.9 ± 0.7 ^a
34	PhCH ₂ -	2-thiazolylmethyl	7	>1	ND	ND	ND
35	PhCH ₂ -	4-thiazolylmethyl	16	>1	ND	ND	ND
36	PhCH ₂ -	5-thiazolylmethyl	0.4	0.3	<0.4	3.2 ± 0.3	1.6 ± 0.6 ^a
29	PhCH ₂ -	Ph-	1.4 ± 0.5 ^a	0.40 ± 0.06 [†]	0.8	1.9 ± 0.3	0.6 ± 0.1 ^a
30	3,5-F ₂ -C ₆ H ₃ CH ₂ -	Ph-	0.4	1	1.9	14.3 ± 4.4	10.8 ± 5.1 ^b
31	3,5-F ₂ -C ₆ H ₃ CH ₂ -	3-pyridyl	1.4	0.05	1.0 ± 0.1	3.56 ± 0.30	0.14 ± 0.02 ^b
37	3,5-F ₂ -C ₆ H ₃ CH ₂ -	5-thiazolylmethyl	0.2	0.5	1.13	2.4 ± 0.8	0.3 ± 0.1 ^b

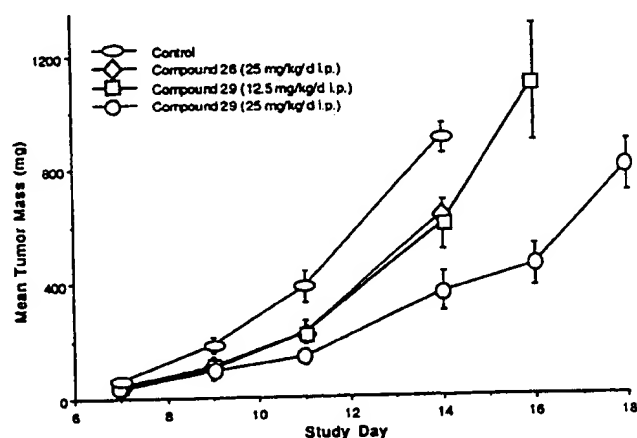
^a Intraduodenal dosing. ^b Oral dosing. [†] *n* = 3.[†] *n* = 2. Unless statistical limits are given, the compounds were assayed once. The reliability of the in vitro assay is ±50%. The reliability of the cell-based assay is ±50–100%. Potencies that differ by more than 3-fold should be considered statistically different.

Figure 1. Antitumor efficacy of 26 and 29 vs untreated control against MiaPaCa-2 subcutaneous tumors in nude mice. Mice were inoculated subcutaneously in the right flank on study day 0. Therapy was initiated on study day 1 and consisted of continuous once daily dosing ip of compound 26 or 29 at the indicated doses.

demonstrates a notable reduction in mean tumor mass for the animals studied. Compound 29 nearly matches this reduction at one-half the dosage (12.5 mpk/day) and shows a marked further improvement at the original higher dose. Thus, initial evidence of a dose-response has been established.

In a similar study we investigated the antitumor efficacy of 26 against the slower developing human lung adenocarcinoma A-549, one of the NCI panel of 60 cell lines. The genetic lesions found in A-549 include a point mutation in *K-ras* at codon 12 (Gly12Ser). The cell line exhibits low levels of P-glycoprotein and bcl-2 expression in comparison to the other cell lines in the panel. A-549 displays wild-type p53, and so presumably the p53-dependant pathway of growth arrest and apoptosis may

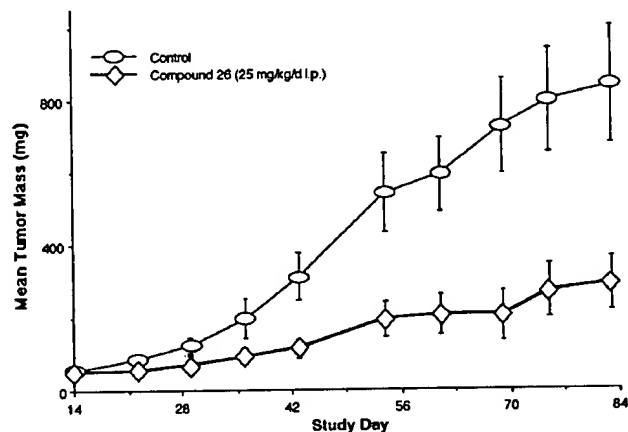


Figure 2. Antitumor efficacy of 26 vs untreated control against A-549 subcutaneous tumors in nude mice. Mice were inoculated subcutaneously in the right and left flanks on study day 0. Therapy was initiated on study day 19 and consisted of continuous once daily dosing of compound 26 at 25 mpk/day ip. Injections were stopped from days 45–53 and restarted on day 54.

still function. The ED₅₀ of 26 against A-549 is about 1 μM, suggesting the compound to be far less active against this line than the MiaPaCa-2 line.

Here therapy was initiated on study day 19 and consisted of continuous once daily dosing of compound 26 at 25 mpk/day ip. Injections were stopped from days 45–53 and restarted on day 54. The data presented in Figure 2 illustrates that a noteworthy reduction in mean tumor mass was once again observed in animals treated with 26 versus untreated controls.

In the MiaPaCa trial with inhibitors 26 and 29, all mice inoculated with transformed cells developed tumors. The mean value for days to reach 1 g of tumor mass within the untreated control group was 16. Treat-

ment with cyclophosphamide at 25 mg/kg on days 1, 5, and 9 as a positive control produced a mean delay to 1 g of tumor mass of 3 days. At an equivalent dosage, daily administration of the pyridine analogue **26** produced a mean delay in tumor growth of 2 days, while results from the aniline analogue **29** equaled that of the positive control at 3 days. This result was intriguing because we had observed previously that cellular potency was often predictive of in vivo efficacy, and yet **29** had demonstrated reduced activity in the cellular potency assay with respect to **26**. None of the numerous other compounds in the aniline series demonstrated significant in vivo efficacy against the MiaPaCa cell line (data not shown). The reason for the increased efficacy of **29** is not clear to us at this time. The pharmacokinetic profiles of the two compounds are not markedly different, as both inhibitors possess rather short half-lives and neither provides a systemic AUC above 1 $\mu\text{g}\cdot\text{h/mL}$. One plausible explanation is that the aniline derivative may experience better tissue distribution, but we have no experimental confirmation of this at present. Despite this unexpected finding, these experiments clearly highlight the potential of farnesyltransferase inhibitors as effective antitumor drugs.

Conclusion

We have demonstrated that certain tertiary amine derivatives of CAAX mimetics are extremely potent inhibitors of farnesyltransferase. *N*-Benzyl-3-aminopyridine analogue **26** possesses potent in vitro and cellular activity and demonstrated significant activity in MiaPaCa and A-549 xenografts in nude mice. Aniline derivative **29** is also a potent inhibitor of farnesyltransferase in vitro as well as in vivo. Efforts are currently underway to improve the in vivo profile of these inhibitors, and the results will be presented in due course.

Experimental Section

General. Proton magnetic resonance spectra were obtained on a Nicolet QE-300 (300 MHz), a General Electric GN-300 (300 MHz), or a Varian Unity 500 (500 MHz) instrument. Chemical shifts are reported as δ values (ppm) downfield relative to Me_4Si as an internal standard. Mass spectra were obtained with a Hewlett-Packard HP5965 spectrometer; CI/NH_3 indicates chemical ionization mode in the presence of ammonia. Combustion analyses were performed by Robertson Microlit Laboratories, Inc., Madison, NJ. Melting points were determined on a Buchi melting point apparatus with a silicone oil bath and are uncorrected. Chromatographies were carried out in flash mode using silica gel 60 (230–400 mesh) from E. Merck.

General Procedure for the Hydrolysis of Benzoate Esters to Benzoic Acids. To a solution of the biphenyl benzoate²⁷ in MeOH at room temperature was added a solution of 4 M NaOH in water (total reaction concentration ~ 1 M). The mixture was brought to reflux and maintained until TLC analysis indicated complete consumption of starting material. The mixture was cooled to room temperature and the MeOH removed on a rotary evaporator. The resulting solution was extracted with ethyl acetate, and the aqueous phase was then cooled to 0 °C and acidified by the careful addition of concentrated aq HCl. The mixture was extracted with 2 portions of ethyl acetate, dried over MgSO_4 , filtered, and concentrated to give the desired compound.

General Procedure for the Conversion of Benzoic Acids to Benzoylmethionine Methyl Esters. A solution of benzoic acid in DMF was treated sequentially with HOBt (110 mol %), EDCI (110 mol %), and L-methionine methyl ester

hydrochloride (130 mol %). The suspension was stirred for 15 min, then triethylamine (180 mol %) was added, and the mixture was stirred for 24 h. The reaction was quenched by transfer into ethyl acetate and extraction with water, saturated aqueous NaHCO_3 , and brine. The solution was then dried over Na_2SO_4 , filtered, and concentrated. The residue was purified by column chromatography on silica gel (ethyl acetate/hexanes) to provide the desired compound.

General Procedure for Hydrolysis of Methionine Methyl Esters. The methionine ester was dissolved in 3:1 THF/MeOH and cooled in an ice bath. The solution was treated with aqueous LiOH (200 mol %) and the mixture stirred until judged complete by TLC analysis. The solution was concentrated to remove the organic fractions and diluted with water and the pH of the solution adjusted to ~ 4 with aqueous HCl. If a solid precipitate formed, the product was collected by filtration. If an oil formed or if the solid was not isolable, the aqueous mixture was extracted with ethyl acetate, and the extracts were dried over sodium sulfate, filtered, and concentrated. These procedures generally gave material of suitable purity. If not, the compound was purified by column chromatography on silica gel or reverse-phase preparative HPLC.

Dimethyl 2-Amino-5-(2-methylphenyl)terephthalate (6). To a -12 °C suspension in dichloromethane of 2-amino-terephthalate (10.5 g, 50.0 mmol) and pyridine (8.1 mL, 100.0 mmol) was added a solution of bromine (2.6 mL, 52.5 mmol) in dichloromethane (25 mL) over 0.5 h, and the reaction mixture was warmed slowly to ambient temperature and stirred overnight. Aqueous workup followed by recrystallization from 95% ethanol gave the desired compound (11.13 g, 77%, mp 113–116 °C). ^1H NMR (CDCl_3): δ 8.09 (s, 1H), 7.05 (s, 1H), 5.80 (bs, 2H), 3.93 (s, 3H), 3.88 (s, 3H). MS (DCI , NH_3): 305 ($\text{M} + \text{NH}_4$)⁺. A solution of palladium acetate (0.26 g, 1.2 mmol) and triphenylphosphine (1.21 g, 4.6 mmol) in 100 mL of toluene was stirred for 10 min at ambient temperature, and then the above product (11.13 g, 38.6 mmol), 2-methylphenylboronic acid (5.77 g, 42.4 mmol), ethanol (18 mL), and aqueous 2 M sodium carbonate (157 mL) were added. The reaction mixture was warmed to reflux and stirred for 18 h. The reaction mixture was cooled to ambient temperature and diluted with ether. The aqueous phase was extracted with ether. The combined organic layers were washed with water, dried, filtered, and concentrated in vacuo to give an orange oil. Chromatography on silica gel (25% ethyl acetate–hexanes) gave compound **6** (9.6 g, 83%) as a yellow solid. ^1H NMR (CDCl_3): δ 8.54 (s, 1H), 7.66 (s, 1H), 7.17–7.32 (m, 3H), 7.04 (d, 1H), 3.93 (s, 3H), 3.63 (s, 3H), 2.05 (s, 3H). MS (CI/NH_3): 428 ($\text{M} + \text{NH}_4$)⁺.

Methyl 2-(2-Methylphenyl)-4-hydroxymethyl-5-iodobenzoate (7). A mixture of compound **6** (7.00 g, 23.4 mmol) and aqueous 3 M HCl (50 mL) in acetone (500 mL) was cooled to 0 °C and a solution of NaNO_2 (1.78 g, 25.7 mmol) in water (20 mL) was added dropwise. The reaction mixture was stirred for 1 h, and then urea (0.53 g, 8.88 mmol) was added followed by a solution of KI (6.79 g, 40.9 mmol) in water (20 mL), during which time the reaction temperature remained below 0 °C. The reaction mixture was stirred for 0.5 h, then the cold bath was removed, and stirring was continued for 2 h. The reaction mixture was diluted with water (400 mL), and NaHSO_3 was added until the brown color disappeared. The reaction mixture was filtered, and the solid material collected was recrystallized from 5% aqueous ethanol to give the desired compound (6.46 g, 67%, mp 105–109 °C). ^1H NMR (CDCl_3): δ 8.53 (s, 1H), 7.65 (s, 1H), 7.37–7.51 (m, 3H), 7.06 (d, 1H), 3.93 (s, 3H), 3.64 (s, 3H), 2.07 (s, 3H). MS (CI/NH_3): 428 ($\text{M} + \text{NH}_4$)⁺. This material was dissolved in 60 mL of THF and cooled in an ice bath. The ice-cold solution was treated sequentially with 15 mL of MeOH and aqueous LiOH (0.69 g in 25 mL of water), and the mixture was stirred for 68 h during which time the bath melted. The solution was concentrated to remove the organics and diluted with 100 mL of water. The aqueous mixture was extracted with 2 portions of ether and set aside. The ethereal extracts were combined and washed with water. The aqueous fractions were combined, and the pH was

adjusted to <2 with 1 M aq NaHSO₄. The mixture was extracted with 3 portions of ether, and the combined ethereal extracts were dried over MgSO₄, filtered, and concentrated to provide the crude acid (5.71 g, 92%) which was used without further purification. The acid (5.60 g, 14.06 mmol) was dissolved in 30 mL of dry THF and cooled in an ice bath. Borane (28.0 mL of a 1 M in THF, 28.0 mmol) was added dropwise, and the mixture was stirred for 2 h. The ice bath was removed, and after 2 h stirring, the solution was recooled to in an ice bath and quenched by the careful addition of 25 mL of 20% aqueous THF (*caution!!* vigorous evolution of gas), followed by 25 mL of 4 N aqueous H₂SO₄. The mixture was stirred an additional 10 min and diluted with 200 mL of water. This mixture was extracted with 3 portions of ethyl acetate, and the combined extracts were washed with water and saturated aqueous NaHCO₃. The solution was dried over MgSO₄, filtered, and concentrated. The residue was purified by column chromatography on silica gel (20% ethyl acetate/hexanes) to give compound 7, 3.93 g (73%, 67% overall). ¹H NMR (CDCl₃): δ 8.41 (s, 1H), 7.34 (s, 1H), 7.17–7.39 (m, 3H), 7.06 (d, 1H), 4.72 (d, 2H), 3.62 (s, 3H), 2.06 (s, 3H). MS (CI/NH₃): 400 (M + NH₄)⁺.

Methyl 2-(2-Methylphenyl)-4-(3-pyridyloxymethyl)-5-iodobenzoate (8). Compound 7 (830 mg, 2.17 mmol) in dichloromethane was cooled in an ice/acetone bath, carbon tetrabromide (864 mg, 2.60 mmol) was added, followed by triphenylphosphine (626 mg, 2.39 mmol), and the reaction mixture was warmed to 0 °C over 1 h. The cold bath was then removed, and stirring was continued for 2 h. The reaction mixture was concentrated in vacuo and purified by chromatography on silica gel (5% ethyl acetate–hexanes) to give the bromide (1.1 g) which also contained some triphenylphosphine. This material was used directly. To a solution of benzyltriethylammonium bromide (1.18 g, 4.34 mmol) in 10 mL of CH₂Cl₂ was added 3-hydroxypyridine potassium salt (586 mg, 4.34 mmol), and the mixture was stirred for 15 min. A solution of the above bromide (960 mg, 2.17 mmol) in 4 mL of CH₂Cl₂ was added, and the reaction mixture was stirred overnight. The reaction mixture was washed with water, dried, filtered, and concentrated in vacuo. Chromatography on silica gel (35% ethyl acetate–hexanes) gave compound 8 (480 mg, 49%). ¹H NMR (CDCl₃): δ 8.45 (s, 1H), 8.39 (bs, 1H), 8.28 (m, 1H), 7.39 (s, 1H), 7.15–7.31 (m, 3H), 7.03 (d, 1H), 5.14 (s, 2H), 3.63 (s, 3H), 2.02 (s, 3H). MS (CI/NH₃): 460 (MH)⁺.

General Procedures for Conversion of Iodide 8 to Aryl- or Alkylbiphenyl. **Procedure A: Arylboronic Acids.** **4-(3-Pyridyloxymethyl)-5-(4-methylphenyl)-2-(2-methylphenyl)benzoylmethionine (9).** To a solution of tetrakis(triphenylphosphine)palladium(0) (2 mg) in toluene (1 mL) was added a solution of 8 (100 mg, 0.22 mmol) in toluene (3 mL). The mixture was stirred for 10 min; then a solution of 4-methylphenylboronic acid (33 mg, 0.24 mmol) in ethanol (2 mL) and aqueous 2 M sodium carbonate were added. The reaction mixture was stirred overnight at reflux, additional catalyst (20 mg), boronic acid (20 mg), and base (0.5 mL) were added, and reflux was continued for 4 h. The reaction mixture was cooled to ambient temperature, diluted with ether, washed with water and brine, dried over sodium carbonate, filtered, and concentrated in vacuo. Chromatography on silica gel (30% ethyl acetate–hexanes) gave the *p*-tolyl analogue (98 mg). Hydrolysis, methionine methyl ester coupling, and methyl ester hydrolysis were carried out as previously described. ¹H NMR (CDCl₃): δ 8.31 (d, 1H), 8.19 (dd, 1H), 7.90 (d, 1H), 7.42 (s, 1H), 7.40–7.20 (m, 10H), 6.07 (d, 1H), 5.08 (m, 2H), 4.62 (m, 1H), 2.40 (s, 3H), 2.25–2.10 (m, 5H), 2.02 (s, 3H), 2.00–1.55 (m, 2H). MS (CI/NH₃): 541 (M + H)⁺. Anal. (C₂₉H₃₄N₂O₄S·0.50H₂O) C, H, N.

4-(3-Pyridyloxymethyl)-5-(3,5-dichlorophenyl)-2-(2-methylphenyl)benzoylmethionine (10). The side chain was attached using procedure A and commercial 3,5-dichlorophenylboronic acid. Hydrolysis, methionine methyl ester coupling, and methyl ester hydrolysis were carried out as previously described. ¹H NMR (CDCl₃): δ 8.37 (d, 1H), 8.21 (d, 1H), 7.85 (d, 1H), 7.44 (s, 1H), 7.40–7.20 (m, 9H), 6.08 (d, 1H), 5.03 (s,

2H), 4.62 (m, 1H), 2.25–2.05 (m, 5H), 2.02 (s, 3H), 1.95 (m, 1H), 1.64 (m, 1H). MS (CI/NH₃): 595 (M + H)⁺. Anal. (C₃₁H₂₈Cl₂N₂O₄S·0.20H₂O) C, H, N.

4-(3-Pyridyloxymethyl)-5-(2-thienyl)-2-(2-methylphenyl)benzoylmethionine (11). The side chain was attached using procedure A and commercial 2-thienylboronic acid. Hydrolysis, methionine methyl ester coupling, and methyl ester hydrolysis were carried out as previously described. ¹H NMR (CDCl₃): δ 8.38 (d, 1H), 8.20 (dd, 1H), 8.03 (s, 1H), 7.43 (s, 1H), 7.39 (dd, 1H), 7.38–7.20 (m, 6H), 7.15 (dd, 1H), 7.08 (m, 1H), 6.07 (d, 1H), 5.10 (m, 2H), 4.61 (m, 1H), 2.20–2.05 (m, 5H), 2.02 (s, 3H), 1.93 (m, 1H), 1.62 (m, 1H). MS (CI/NH₃): 533 (MH)⁺. Anal. (C₂₉H₂₇LiN₂O₄S₂·0.45H₂O) C, H, N.

Procedure B: Commercial Alkylboranes. **N-2-(2-Methylphenyl)-4-(3-pyridyloxymethyl)-5-butylbenzoylmethionine (12).** Tributylborane (0.10 mL, 0.41 mmol) was added to 2 mL of degassed DMF followed by the sequential addition of 150 mg (0.33 mmol) of iodide 8, 8 mg (0.01 mmol) of Cl₂PdDPPF, and 212 mg (1.0 mmol) of K₂CO₃. The mixture was placed in an oil bath preheated to 65 °C and stirred at that temperature for 3 h. The mixture was poured into water and extracted with 2 portions of ethyl acetate. The combined aqueous layers were rinsed with water and brine, dried over Na₂SO₄, filtered, and concentrated to give the crude product, which was used directly. Hydrolysis, methionine methyl ester coupling, and methyl ester hydrolysis were carried out as previously described. ¹H NMR (DMSO-*d*₆): δ 8.35 (d, 1H), 8.18 (dd, 1H), 8.09 (dd, 1H), 7.47 (m, 1H), 7.37 (s, 1H), 7.35 (dd, 1H), 7.26 (s, 1H), 7.19 (m, 2H), 7.11 (m, 2H), 5.26 (s, 2H), 4.2 (m, 1H), 2.73 (dd, 2H), 1.98–2.21 (m, 5H), 1.96 (s, 3H), 1.77–1.90 (m, 4H), 1.40 (sextet, 2H), 0.93 (t, 3H). MS (CI/NH₃): 507 (MH)⁺. Anal. (C₂₉H₃₄N₂O₄S·0.50H₂O) C, H, N.

N-2-(2-Methylphenyl)-4-(3-pyridyloxymethyl)-5-ethylbenzoylmethionine (13). The side chain was attached using procedure B and commercial triethylborane. Hydrolysis, methionine methyl ester coupling, and methyl ester hydrolysis were carried out as previously described. ¹H NMR (DMSO-*d*₆): δ 8.38 (d, 1H), 8.18 (d, 1H), 7.93 (m, 1H), 7.51 (m, 1H), 7.40 (s, 1H), 7.35 (m, 1H), 7.28 (bs, 1H), 7.20 (m, 2H), 7.13 (m, 2H), 5.27 (s, 2H), 4.12 (m, 1H), 2.78 (q, 2H), 2.20–2.00 (m, 5H), 1.96 (s, 3H), 1.90–1.60 (m, 2H), 1.26 (t, 3H). MS (CI/NH₃): 479 (MH)⁺. Anal. (C₂₇H₃₀N₂O₄S·1.00H₂O) C, H, N.

N-2-(2-Methylphenyl)-4-(3-pyridyloxymethyl)-5-pentylbenzoylmethionine (15). The side chain was attached using procedure B and triptentylborane (prepared in situ by the hydroboration of 1-pentene with BH₃·THF). Hydrolysis, methionine methyl ester coupling, and methyl ester hydrolysis were carried out as previously described. ¹H NMR (DMSO-*d*₆): δ 8.37 (d, 1H), 8.18 (dd, 1H), 8.09 (dd, 1H), 7.48 (m, 1H), 7.36 (s, 1H), 7.34 (m, 1H), 7.26 (bs, 1H), 7.19 (m, 2H), 7.13 (m, 2H), 5.26 (s, 2H), 4.21 (m, 1H), 2.73 (m, 2H), 2.20–2.00 (m, 5H), 1.96 (s, 3H), 1.90–1.60 (m, 4H), 1.36 (m, 4H), 0.86 (t, 3H). MS (CI/NH₃): 521 (MH)⁺. Anal. (C₃₀H₃₆N₂O₄S) C, H, N.

4-(3-Pyridyloxymethyl)-5-phenylmethyl-2-(2-methylphenyl)benzoylmethionine (16). The side chain was attached using procedure B and commercial 9-methoxy-9-BBN. Hydrolysis, methionine methyl ester coupling, and methyl ester hydrolysis were carried out as previously described. ¹H NMR (CDCl₃): δ 8.27 (d, 1H), 8.19 (dd, 1H), 7.88 (s, 1H), 7.40–7.00 (m, 12H), 6.00 (d, 1H), 5.08 (d, 1H), 5.01 (d, 1H), 4.62 (m, 1H), 4.15 (s, 2H), 2.20–2.05 (m, 5H), 2.02 (s, 3H), 1.92 (m, 1H), 1.60 (m, 1H). MS (CI/NH₃): 541 (MH)⁺. Anal. (C₃₂H₃₂N₂O₄S·0.25H₂O) C, H, N.

Procedure C: Synthetic Alkylboranes. **N-2-(2-Methylphenyl)-4-(3-pyridyloxymethyl)-5-isobutylbenzoylmethionine (14).** To a solution of *t*-butyllithium (0.75 mL of a 1.7 M solution in pentane, 1.28 mmol) in 1 mL of dry ether at –78 °C was added a solution of 74 μL (0.64 mmol) of isobutyl iodide in 1 mL of ether. After stirring for 30 min at –78 °C, 9-methoxy-9-BBN (0.66 mL of a 1.0 M solution in hexanes, 0.66 mmol) was added, and the mixture was warmed to 0 °C for 30 min and then allowed to reach room temperature. The mixture was treated with 218 mg (0.53 mmol) of iodide 8 in 4 mL of degassed DMF followed by 13 mg (0.02 mmol) of Cl₂-

PdDPPF and 338 mg (1.59 mmol) of anhydrous K_3PO_4 . The solution was heated to 65 °C at first under a N_2 stream (to remove the volatile organics) and then for 2 h additional. After cooling to room temperature, the mixture was poured into water and extracted with 3 portions of ethyl acetate. The combined organic extracts were washed with water and brine, dried over Na_2SO_4 , filtered, and concentrated. The residue was purified by column chromatography (18 g SiO_2 , 30% ethyl acetate/hexanes) to provide the isobutyl derivative. Hydrolysis, methionine methyl ester coupling, and methyl ester hydrolysis were carried out as previously described. 1H NMR (DMSO- d_6): δ 8.35 (d, 1H), 8.18 (dd, 1H), 8.06 (dd, 1H), 7.49 (dq, 1H), 7.35 (s, 1H), 7.33 (dd, 1H), 7.27 (s, 1H), 7.18 (m, 2H), 7.03 (m, 2H), 5.25 (s, 1H), 4.22 (m, 1H), 2.63 (dd, 2H), 2.12 (heptet, 1H), 2.03 (m, 4H), 1.96 (s, 3H), 1.64–1.90 (m, 3H), 0.96 (d, 6H). MS (CI/NH $_3$): 507, 489, 221, 204. Anal. ($C_{29}H_{34}N_2O_4S \cdot 0.50H_2O$) C, H, N.

***N*-2-(2-Methylphenyl)-4-(3-pyridyloxymethyl)-5-phenethylbenzoylmethionine (17).** The side chain was attached using procedure C and commercial phenethyl bromide. Hydrolysis, methionine methyl ester coupling, and methyl ester hydrolysis were carried out as previously described. 1H NMR (CDCl $_3$): δ 8.47 (m, 1H), 8.26 (d, 1H), 8.13 (dd, 1H), 7.65 (dd, 1H), 7.50 (s, 1H), 7.48 (m, 1H), 7.40–7.25 (m, 4H), 7.25–7.00 (m, 6H), 5.30 (s, 2H), 4.22 (m, 1H), 2.99 (m, 4H), 2.25–2.00 (m, 5H), 1.97 (s, 3H), 1.95–1.60 (m, 2H). MS (CI/NH $_3$): 555 (MH $^+$). Anal. ($C_{33}H_{34}N_2O_4S \cdot 1.00TFA$) C, H, N.

***N*-2-(2-Methylphenyl)-4-(3-pyridyloxymethyl)-5-cyclohexylmethylbenzoylmethionine (18).** The side chain was attached using procedure C and commercial bromomethylcyclohexane. Hydrolysis, methionine methyl ester coupling, and methyl ester hydrolysis were carried out as previously described. 1H NMR (CDCl $_3$): δ 12.60 (bs, 1H), 8.40–8.20 (m, 1H), 8.20–8.10 (m, 2H), 7.52 (m, 1H), 7.40–7.25 (m, 4H), 7.20 (m, 2H), 7.14 (m, 2H), 5.23 (s, 2H), 4.21 (m, 1H), 2.62 (m, 1H), 2.20–2.00 (m, 5H), 1.96 (s, 3H), 1.90–1.50 (m, 3H), 1.30–0.90 (m, 5H). MS (CI/NH $_3$): 547 (MH $^+$). Anal. ($C_{32}H_{38}N_2O_4S \cdot 0.35CH_3CN$) C, H, N.

***N*-Benzoyl-3-aminopyridine.** A solution of 3-aminopyridine (0.94 g, 10.00 mmol) and *N*-methylmorpholine (1.32 mL, 12.00 mmol) in 10 mL of CH_2Cl_2 was cooled in an ice/acetone bath and treated dropwise with benzoyl chloride (1.20 mL, 11.00 mmol). The mixture was stirred for 6 h during which time the cold bath melted. The solution was diluted with 50 mL of ethyl ether and extracted with water, 2 M aqueous Na_2CO_3 , water, and brine. The organic phase was dried over Na_2SO_4 , filtered, and concentrated. The residue was purified by column chromatography (3:1 ethyl acetate/hexanes) to give 1.52 g (77%) of *N*-benzoyl-3-aminopyridine. 1H NMR (CDCl $_3$): δ 8.70 (d, 1H), 8.37 (m, 2H), 8.28 (m, 1H), 7.90 (m, 2H), 7.57 (m, 1H), 7.49 (m, 2H), 7.34 (dd, 1H). MS (CI/NH $_3$): 199 (MH $^+$).

General Procedure for the Formation of Tertiary Amines and Amides. Procedure D: ***N*-[4-(*N*-Benzoyl-3-pyridyl-3-ylaminomethyl)-2-(2-methylphenyl)benzoyl]methionine (23).** A solution of methyl 2-(2-methylphenyl)-4-bromomethylbenzoate (175 mg, 0.55 mmol) in 1 mL of dry DMF was cooled in an ice bath and treated with NaH (26 mg of a 60% mineral oil dispersion, 0.66 mmol) followed by a solution of *N*-benzoyl-3-aminopyridine (119 mg, 0.60 mmol) in 1 mL of dry DMF. The mixture was stirred for 3 h and quenched by the addition of water. The suspension was poured into water and extracted with 3 portions of ethyl acetate. The combined organic extracts were washed with water and brine, dried over Na_2SO_4 , filtered, and concentrated. The residue was purified by column chromatography (1:1 ethyl acetate/hexanes) to give the alkylated product. Hydrolysis, methionine methyl ester coupling, and methyl ester hydrolysis were carried out as previously described. 1H NMR (DMSO- d_6): δ 12.54 (bs, 1H), 8.24 (dd, 1H), 8.13 (m, 2H), 7.61 (m, 1H), 7.43 (m, 2H), 7.29 (m, 6H), 7.00–7.21 (m, 5H), 5.21 (s, 2H), 4.18 (m, 1H), 1.97–2.22 (m, 2H), 1.94 (s, 6H), 1.63–1.88 (m, 2H). MS (CI/NH $_3$): 554 (MH $^+$). Anal. ($C_{32}H_{31}N_3O_4S \cdot 0.50H_2O$) C, H, N.

***N*-[4-(*N*-Phenylacetyl-*N*-pyrid-3-ylaminomethyl)-2-(2-methylphenyl)benzoyl]methionine (24).** Prepared using

procedure D and phenylacetyl chloride. 1H NMR (DMSO- d_6): δ 8.49 (d, 1H), 8.30 (d, 1H), 8.09 (d, 1H), 7.61 (dt, 1H), 7.42 (m, 2H), 7.24 (dd, 1H), 6.91–7.23 (m, 10H), 4.91 (bs, 2H), 4.19 (m, 1H), 3.50 (bs, 2H), 1.98–2.22 (m, 2H), 1.96 (bs, 6H), 1.62–1.88 (m, 2H). MS (CI/NH $_3$): 568 (MH $^+$). Anal. ($C_{33}H_{33}N_3O_4S$) C, H, N.

***N*-[4-(*N*-Phenylsulfonyl-*N*-pyrid-3-ylaminomethyl)-2-(2-methylphenyl)benzoyl]methionine (25).** Prepared using procedure D and *p*-toluenesulfonyl chloride. 1H NMR (DMSO- d_6): δ 8.42 (d, 1H), 8.30 (s, 1H), 8.12 (d, 1H), 7.76 (m, 1H), 7.60–7.73 (m, 4H), 7.53 (m, 1H), 7.38 (m, 3H), 7.19 (m, 2H), 6.90–7.15 (m, 3H), 4.91 (s, 2H), 4.17 (m, 1H), 1.93–2.20 (m, 3H), 1.92 (s, 3H), 1.61–1.90 (m, 6H). MS (CI/NH $_3$): 590 (MH $^+$). Anal. ($C_{31}H_{31}N_3O_5S_2 \cdot 0.31H_2O$) C, H, N.

General Procedure E: Preparation of *N*-Alkylamino Heterocycles. *N*-Benzyl-3-aminopyridine. A mixture of 94.12 g (1.00 mol) of 3-aminopyridine and 102 mL (1.00 mol) of benzaldehyde in 300 mL of toluene were heated to reflux. A Dean-Stark trap was used to collect the water removed by the azeotrope. When the theoretical amount of water was collected (~3 h) the mixture was cooled to room temperature and concentrated in vacuo to remove the toluene. The residue was dissolved in 300 mL of ethanol and added dropwise to a solution of 55.70 g (1.50 mol) of $NaBH_4$ in ethanol at 0 °C. The ice bath was removed, and the thick solution was stirred for 2 h at ambient temperature and 6 h at reflux. The mixture was cooled to 50 °C and treated with 1 L of 4 N aqueous NaOH such that the temperature was maintained between 50 and 60 °C, and stirring was continued overnight. The cooled mixture was extracted with 3 portions of ethyl acetate, and the combined organic extracts were washed with 2 portions of water and 2 portions of brine, dried over Na_2SO_4 , filtered, and concentrated to a volume of ~500 mL. This concentrate was heated to obtain a solution, filtered hot, and allowed to slowly cool to room temperature. The solid was collected by filtration, the mother liquor was concentrated to approximately 250 mL, and the same procedure was repeated. The total amount of crystalline material collected was 138.90 g (75%). 1H NMR (CDCl $_3$): δ 8.09 (d, 1H), 7.97 (dd, 1H), 7.28–7.44 (m, 5H), 7.06 (dd, 1H), 6.98 (ddd, 1H), 4.35 (d, 2H), 4.16 (bs, 1H). MS (CI/NH $_3$): 185 (MH $^+$).

Methyl 4-(*N*-Benzyl-*N*-3-pyridylaminomethyl)-2-(2-methylphenyl)benzoate. A solution of *n*-BuLi (49.8 mL of a 1.6 M solution in hexanes, 79.7 mmol) in 50 mL of dry THF was cooled to –30 °C and treated dropwise with a solution of 15.0 g (81.7 mmol) of *N*-benzyl-3-aminopyridine in 20 mL of dry THF. The mixture was stirred at this temperature for 30 min, and then methyl 4-bromomethyl-2-(2-methylphenyl) benzoate²⁷ (13.0 g, 40.9 mmol) in 30 mL of dry THF was added dropwise. The temperature was raised to –10 °C, stirred for 2 h, and quenched with water. The solvent was removed in vacuo and the residue partitioned into ether. The ether layer was dried over Na_2SO_4 , filtered, and concentrated. The residue was purified by column chromatography (50% ethyl acetate/hexanes) to give 13.5 g (78%) of the desired compound. 1H NMR (CDCl $_3$): δ 8.17 (d, 1H), 7.97 (dd, 1H), 7.94 (d, 1H), 7.14–7.38 (m, 10H), 6.90–7.13 (m, 4H), 4.72 (s, 2H), 4.68 (s, 2H), 3.62 (s, 3H), 2.02 (s, 3H). MS (CI/NH $_3$): 423 (MH $^+$).

4-(*N*-Benzyl-*N*-3-pyridylaminomethyl)-2-(2-methylphenyl)benzoylmethionine (26). The ester obtained above was converted to the final product as previously described. 1H NMR (DMSO- d_6): δ 8.18 (d, 1H), 8.03 (bs, 1H), 7.82 (bs, 1H), 7.48 (d, 1H), 7.30 (m, 6H), 7.19 (m, 2H), 7.10 (m, 4H), 4.84 (s, 2H), 4.79 (s, 2H), 1.96–2.23 (m, 5H), 1.96 (s, 3H), 1.63–1.89 (m, 2H). MS (CI/NH $_3$): 540 (MH $^+$). Anal. ($C_{32}H_{33}N_3O_3S$) C, H, N.

4-(*N*-Cyclohexylmethyl-*N*-3-pyridylaminomethyl)-2-(2-methylphenyl)benzoylmethionine (27). Prepared by the same sequence as compound 26 substituting cyclohexanecarboxaldehyde for benzaldehyde. 1H NMR (DMSO- d_6): δ 8.18 (d, 1H), 7.79 (d, 1H), 7.44 (d, 1H), 7.25 (d, 1H), 7.03–7.19 (m, 6H), 6.97 (s, 1H), 4.71 (s, 2H), 4.19 (ddd, 1H), 2.14 (m, 1H), 1.96–2.10 (m, 4H), 1.95 (s, 3H), 1.57–1.89 (m, 8H), 1.17 (m, 3H), 1.01 (m, 2H). MS (ESI $^+$): 546 (MH $^+$); (ESI $^-$): 544 (M $^-$). Anal. ($C_{32}H_{39}N_3O_3S \cdot 0.99H_2O$) C, H, N.

4-(*N*-Benzyl-*N*-3-pyrazinylaminomethyl)-2-(2-methylphenyl)benzoylmethionine (28). Prepared by the same sequence as compound 26 substituting aminopyrazine for 3-aminopyridine. ¹H NMR (DMSO-*d*₆): δ 1.46–2.09 (comp, 10H), 3.59–3.70 (br, 1H), 4.83–4.95 (comp, 4H), 6.90–6.95 (br, 1H), 7.00 (s, 1H), 7.04–7.34 (comp, 10H), 7.49 (d, 1H), 7.80 (d, 1H), 8.04–8.05 (m, 1H), 8.07–8.10 (m, 1H). HRMS (ESI+) calcd for the protonated acid C₃₁H₃₂N₄O₃S, 541.2273; obsd, 541.2268. Anal. (C₃₁H₃₁LiN₄O₃S·1.40H₂O·0.25CH₃CN) C, H, N.

4-(*N*-Benzyl-*N*-phenylaminomethyl)-2-(2-methylphenyl)benzoylmethionine (29). Prepared by the same sequence as compound 26 substituting aniline for 3-aminopyridine. ¹H NMR (MeOH-*d*₄): δ 1.55–1.69 (m, 1H), 1.73–2.14 (comp, 9H), 4.16–4.28 (br, 1H), 4.65 (s, 2H), 4.70 (s, 2H), 6.59–6.66 (m, 1H), 6.73 (d, 2H), 7.03–7.13 (comp, 3H), 7.15–7.28 (comp, 8H), 7.34 (dd, 1H), 7.62 (d, 1H). MS (CI/NH₃): 539 (MH⁺). Anal. (C₃₃H₃₃LiN₂O₃S·1.0LiOH·0.85H₂O) C, H, N.

4-(*N*-3,5-Difluorobenzyl-*N*-phenylaminomethyl)-2-(2-methylphenyl)benzoylmethionine (30). Prepared by the same sequence as compound 26 substituting aniline for 3-aminopyridine and 3,5-difluorobenzaldehyde for benzaldehyde. ¹H NMR (MeOH-*d*₄): δ 7.7–7.8 (m, 1H), 7.3–7.4 (d, 1H), 7.0–7.3 (m, 7H), 6.8–6.9 (m, 3H), 6.6–6.8 (m, 4H), 4.88 (s, 2H), 4.85 (s, 2H), 4.1–4.22 (m, 1H), 1.7–2.1 (m, 10H). MS (ESI-): 573 (M – Li). Anal. (C₃₃H₃₁F₂N₂O₃SLi·1.70H₂O) C, H, N.

4-(*N*-3,5-Difluorobenzyl-*N*-3-pyridylaminomethyl)-2-(2-methylphenyl)benzoylmethionine (31). Prepared by the same sequence as compound 26 substituting 3,5-difluorobenzaldehyde for benzaldehyde. ¹H NMR (DMSO-*d*₆): δ 1.48–1.76 (comp, 2H), 1.85–2.05 (comp, 8H), 3.62–3.74 (br, 1H), 4.80 (s, 2H), 4.86 (s, 2H), 6.92–7.23 (comp, 11H), 7.33 (dd, 1H), 7.52 (d, 1H), 7.84 (dd, 1H), 8.03 (d, 1H). MS (CI/NH₃): 576 (MH⁺). Anal. (C₃₂H₃₀LiF₂N₃O₃S·2.15H₂O) C, H, N.

***N*-Benzyl-2-aminomethylthiazole.** Prepared by the same method as *N*-benzyl-3-aminopyridine using benzylamine and 2-thiazolecarboxaldehyde. ¹H NMR (CDCl₃): δ 7.74 (d, 1H), 7.29–7.40 (m, 3H), 7.13–7.18 (m, 3H), 4.16 (s, 2H), 3.88 (s, 2H), 1.93 (bs, 1H). MS (CI/NH₃): 205 (MH⁺).

Methyl 4-(*N*-Benzyl-*N*-2-aminomethylthiazolylmethyl)-2-(2-methylphenyl)benzoate. A solution of 373 mg (1.0 mmol) of methyl 4-bromomethyl-2-(2-methylphenyl)benzoate, 225 mg (1.1 mmol) of *N*-benzyl-2-aminomethylthiazole, and 0.21 mL (1.2 mmol) of *N,N*-diisopropylethylamine in 2 mL of CH₃CN was heated to reflux for 4 h. The mixture was poured into water and extracted with 3 portions of ethyl acetate. The combined organic extracts were washed with 2 portions of water, and 1 portion of brine, dried (Na₂SO₄), filtered, and concentrated. The residue was purified by column chromatography (25% ethyl acetate/hexanes) to give 279 mg of the desired product. ¹H NMR (CDCl₃): δ 7.94 (d, 1H), 7.69 (d, 1H), 7.55 (dd, 1H), 7.41 (m, 2H), 7.17–7.38 (m, 8H), 7.06 (d, 1H), 3.94 (s, 2H), 3.72 (d, 2H), 3.68 (d, 2H), 3.60 (s, 3H), 2.03 (s, 3H). MS (CI/NH₃): 443 (MH⁺).

***N*-[4-(*N*-Benzyl-*N*-thiazol-2-ylmethylaminomethyl)-2-(2-methylphenyl)benzoyl]methionine (34).** The ester obtained above was converted to the final product as previously described. ¹H NMR (DMSO-*d*₆): δ 8.09 (d, 1H), 7.72 (d, 1H), 7.66 (d, 1H), 7.50 (m, 2H), 7.38 (m, 4H), 7.23 (m, 4H), 7.14 (m, 2H), 4.20 (ddd, 1H), 3.89 (s, 2H), 3.70 (s, 2H), 3.68 (s, 2H), 2.09 (m, 4H), 1.96 (s, 3H), 1.63–1.90 (m, 2H). MS (CI/NH₃): 560 (MH⁺). Anal. (C₃₁H₃₃N₃O₃S₂·0.32H₂O) C, H, N.

***N*-[4-(*N*-Benzyl-*N*-thiazol-4-ylmethylaminomethyl)-2-(2-methylphenyl)benzoyl]methionine (35).** Prepared by the same sequence as compound 34 substituting 4-thiazolecarboxaldehyde for 2-thiazolecarboxaldehyde. ¹H NMR (DMSO-*d*₆): δ 9.08 (d, 1H), 8.13 (d, 1H), 7.58 (d, 1H), 7.49 (s, 2H), 7.40 (d, 2H), 7.31 (t, 2H), 7.22 (m, 4H), 7.11 (m, 2H), 4.21 (m, 1H), 3.77 (s, 2H), 3.67 (s, 2H), 3.62 (s, 2H), 1.98–2.23 (m, 5H), 1.97 (s, 3H), 1.63–1.90 (m, 2H). MS (ESI-): 558 (M – H). Anal. (C₃₁H₃₃N₃O₃S₂·0.49H₂O) C, H, N.

***N*-[4-(*N*-Benzyl-*N*-thiazol-5-ylmethylaminomethyl)-2-(2-methylphenyl)benzoyl]methionine (36).** Prepared by

the same sequence as compound 34 substituting 5-thiazolecarboxaldehyde for 2-thiazolecarboxaldehyde. ¹H NMR (DMSO-*d*₆): δ 12.4 (bs, 1H), 9.03 (s, 1H), 8.12 (d, 1H), 7.79 (s, 1H), 7.48 (dd, 2H), 7.35 (m, 4H), 7.04–7.28 (m, 6H), 4.21 (ddd, 1H), 3.81 (s, 2H), 3.61 (s, 2H), 3.58 (s, 1H), 1.98–2.21 (m, 5H), 1.96 (s, 3H), 1.61–1.89 (m, 2H). MS (CI/NH₃): 560 (MH⁺). Anal. (C₃₁H₃₃N₃O₃S₂·0.78H₂O) C, H, N.

4-(*N*-3,5-Difluorobenzyl-*N*-5-thiazolylmethylaminomethyl)-2-(2-methylphenyl)benzoylmethionine (37). Prepared by the same sequence as compound 34 substituting 5-thiazolecarboxaldehyde for 2-thiazolecarboxaldehyde and 3,5-difluorobenzylamine for benzylamine. ¹H NMR (MeOH-*d*₄): δ 8.95 (s, 1H), 7.78 (s, 1H), 7.6–7.7 (m, 1H), 7.4–7.5 (m, 1H), 7.05–7.30 (m, 5H), 6.95–7.05 (m, 2H), 6.85–6.95 (m, 1H), 4.95 (s, 2H), 4.1–4.22 (m, 1H), 3.9 (s, 2H), 4.7 (m, 2H), 4.6 (s, 2H), 2.25 (s, 2H), 1.6–2.1 (m, 8H). MS (ESI-): 594 (M – Li). Anal. (C₃₁H₃₁F₂N₃O₃S₂·0.41H₂O) C, H, N.

3-Fluoro-5-aminopyridine (39). A suspension of 423 mg (3.0 mmol) of 5-fluoronicotinic acid (38) in 10 mL of CICH₂-CH₂Cl was added 0.36 mL (3.3 mmol) of NMM. After stirring for 10 min, 0.71 mL (3.3 mmol) of DPPA was added dropwise and stirring continued for 30 min. The mixture was then slowly heated to 75 °C, wherein gas bubbles began to evolve. The temperature was maintained at 75 °C for 1 h, then 0.46 mL (4.5 mmol) of benzyl alcohol and ~10 mg of CuCl were added, and the mixture was heated to reflux for 3 h. After cooling to room temperature, the mixture was concentrated in vacuo and the residue purified by column chromatography (40% ethyl acetate/hexanes) to give 415 mg (56%) of 3-fluoro-5-benzyloxycarbonylaminopyridine. ¹H NMR (CDCl₃): δ 8.21 (s, 1H), 8.18 (d, 1H), 7.98 (dd, 1H), 7.31–7.43 (m, 5H), 7.05 (bs, 1H), 5.22 (s, 2H). MS (CI/NH₃): 247 (MH⁺). The benzyloxycarbonyl derivative (408 mg, 1.66 mmol) was dissolved in 10 mL of MeOH, and the solution was degassed by a vacuum/N₂ purge sequence. To the solution were added 50 mg of 10% Pd/C and 522 mg of ammonium formate, and the mixture was heated to reflux for 1.5 h before cooling to room temperature. The mixture was diluted with 40 mL of ethyl acetate and filtered through a 1 in. by 2 in. pad of SiO₂, which was washed well with ethyl acetate. The filtrate was concentrated to give 181 mg (97%) of aminopyridine 39. ¹H NMR (CDCl₃): δ 7.93 (t, 1H), 7.89 (d, 1H), 6.71 (dt, 1H). MS (CI/NH₃): 113 (MH⁺).

4-(*N*-Benzyl-*N*-5-fluoro-3-pyridylaminomethyl)-2-(2-methylphenyl)benzoylmethionine (40). Prepared by the same sequence as compound 26 substituting 5-fluoro-3-aminopyridine for 3-aminopyridine. ¹H NMR (DMSO-*d*₆): δ 8.12 (d, 1H), 7.91 (t, 1H), 7.75 (d, 1H), 7.47 (d, 1H), 7.21–7.38 (m, 6H), 7.19 (m, 2H), 7.10 (m, 3H), 6.92 (dt, 1H), 4.86 (s, 2H), 4.82 (s, 2H), 4.21 (m, 1H), 1.96–2.22 (m, 5H), 1.95 (s, 3H), 1.74–1.89 (m, 2H). MS (CI/NH₃): 558 (MH⁺). Anal. (C₃₂H₃₂FN₃O₃S·0.46H₂O) C, H, N.

***N*-Benzyl-5-aminopyrimidine (42).** A heterogeneous mixture of 5-bromopyrimidine (41) (1.62 g, 10.0 mmol), benzylamine (6.49 g, 60.0 mmol), potassium carbonate (1.66 g, 12.0 mmol), and CuO (40.0 mg, 0.500 mmol) was heated to reflux for 18 h. Vacuum filtration was followed by concentration of the filtrate. Flash column chromatography eluting with 30:70 hexane/ethyl acetate afforded 1.40 g of the title compound (76% yield). ¹H NMR (CDCl₃): δ 4.22–4.33 (br, 1H), 4.36 (d, 2H), 7.27–7.41 (comp, 5H), 8.13 (s, 2H), 8.59 (s, 1H). MS (CI/NH₃): 186 (MH⁺).

4-(*N*-Benzyl-*N*-pyrimid-5-ylaminomethyl)-2-(2-methylphenyl)benzoylmethionine (43). Compound 42 was converted to the title compound in 24% overall yield by the same protocol as for 28. ¹H NMR (DMSO-*d*₆): δ 1.48–1.74 (br comp, 2H), 1.86–2.08 (br comp, 8H), 3.62–3.74 (br, 1H), 4.83 (s, 2H), 4.89 (s, 2H), 6.92–7.03 (br, 1H), 7.04–7.38 (comp, 11H), 7.52 (d, 1H), 8.22 (s, 2H), 8.42 (s, 1H). HRMS (FAB+) calcd for C₃₁H₃₂N₄O₃S, 541.2273; obsd, 541.2254. Anal. (C₃₁H₃₁LiN₄O₃S·1.75H₂O) C, H, N.

In Vitro Enzyme Assays. In vitro IC₅₀ data were determined against FTase and GGTase1 (purified from bovine brain) using the SPA assay (scintillation proximity assay; Amersham, Arlington Heights, IL). The substrates used were

[³H]farnesyl pyrophosphate and a biotin-linked k-Ras(B) decapeptide (KKSKTKCVIM for FTase or CVLL decapeptide for GGTase1). The radioactivity captured by the SPA beads were counted by a Packard Topcount, and data were stored and analyzed in an Oracle-based database.

Cellular Assays for Inhibition of Ha-Ras Processing. Subconfluent NIH3T3 *ras*-transformed cells were used for the Ras processing assay. Briefly, cells were dosed with various compounds, and lysates were prepared. They were boiled for 5 min in the Laemmli sample buffer, and proteins were resolved on a 15% Tris-Gly gel (Bio-Rad, Richmond, CA). Proteins were then transferred to nitrocellulose membranes. The blots were probed with antibody Y13-238 to Ras purified from hybridoma. Ras bands were visualized by ECL technique (ECL kit, Amersham, Arlington Heights, IL), and signals were quantified by densitometry using an image analysis program Image-Pro Plus (Media Cybernetics, Silver Spring, MD).

Acknowledgment. We thank Prof. A. D. Hamilton (Yale University) for fruitful discussions during the course of this research. In addition, we thank Mr. William Arnold for the large-scale preparation of several key intermediates.

References

- Barbacid, M. Ras Genes. *Annu. Rev. Biochem.* 1987, 56, 779.
- Cox, A. D.; Der, C. J. Farnesyltransferase inhibitors and cancer treatment: targeting simply Ras? *Biochim. Biophys. Acta* 1997, 1333, F51–71.
- Klaris, H.; Spandidos, D. A. Mutations of ras Genes in Human Tumors (Review). *Int. J. Oncol.* 1995, 7, 413–421.
- Bos, J. L. ras Oncogenes in Human Cancer: A Review. *Cancer Res.* 1989, 49, 4682–4689.
- Gibbs, J. B.; Oliff, A.; Kohl, N. E. Farnesyltransferase Inhibitors: Ras Research Yields a Potential Cancer Chemotherapeutic. *Cell* 1994, 77, 175.
- Gibbs, J. B.; Oliff, A. The Potential of Farnesyltransferase Inhibitors as Cancer Chemotherapeutics. *Annu. Rev. Pharmacol. Toxicol.* 1997, 37, 143–166.
- Singh, S. B.; Lingham, R. B. Farnesyl-Protein Transferase Inhibitors in Early Development. *Exp. Opin. Invest. Drugs* 1996, 5, 1589–1599.
- Casey, P. J.; Solski, P. A.; Der, C. I.; Buss, J. E. p21 Ras is Modified by a Farnesyl Isoprenoid. *Proc. Natl. Acad. Sci. U.S.A.* 1989, 86, 8223.
- Cox, A. D.; Der, C. J. Protein prenylation: more than just glue? *Curr. Opin. Cell Biol.* 1992, 4, 1008–1016.
- Hancock, J. F.; Magee, A. I.; Childs, J. E.; Marshall, C. J. All ras proteins are polyisoprenylated but only some are palmitoylated. *Cell* 1989, 57, 1167–1177.
- Newman, C. M.; Magee, A. I. Posttranslational processing of the ras superfamily of small GTP-binding proteins. *Biochim. Biophys. Acta* 1993, 1155, 79–96.
- Schafer, W. R.; Rine, J. Protein prenylation: genes, enzymes, targets, and functions. *Annu. Rev. Genet.* 1992, 26, 209–237.
- deSolms, S. J.; Deana, A. A.; Giuliani, E. A.; Graham, S. L.; Kohl, N. E.; Mosser, S. D.; Oliff, A. I.; Pompliano, D. L.; Rands, E.; Scholtz, T. H.; Wiggins, J. M.; Gibbs, J. B.; Smith, R. L. Pseudopeptide Inhibitors of Protein Farnesyltransferase. *J. Med. Chem.* 1995, 38, 3967–3971.
- deSolms, S. J.; Giuliani, E. A.; Graham, S. L.; Koblan, K. S.; Kohl, N. E.; Mosser, S. D.; Oliff, A. I.; Pompliano, D. L.; Rands, E.; Scholtz, T. H.; Wiscourt, C. M.; Gibbs, J. B.; Smith, R. L. N-Arylalkyl pseudopeptide inhibitors of farnesyltransferase. *J. Med. Chem.* 1998, 41, 2651–2656.
- Graham, S. L.; deSolms, S. J.; Giuliani, E. A.; Kohl, N. E.; Mosser, S. D.; Oliff, A. I.; Pompliano, D. L.; Rands, E.; Breslin, M. J.; Deanna, A. A.; Garsky, V. M.; Scholtz, T. H.; Gibbs, J. B.; Smith, R. L. Pseudopeptide Inhibitors of Ras Farnesyl-protein Transferase. *J. Med. Chem.* 1994, 37, 725.
- Hunt, J. T.; Lee, V. G.; Leftheris, K.; Seizinger, B.; Carboni, J.; Mabius, J.; Ricca, C.; Yan, N.; Manne, V. Potent, Cell Active, Non-Thiol Tetrapeptide Inhibitors of Farnesyltransferase. *J. Med. Chem.* 1996, 39, 353–358.
- James, G. L.; Goldstein, J. L.; Brown, M. S.; Rawson, T. E.; Somers, T. T.; McDowell, R. S.; Crowley, C.; Lucas, B.; Levinson, A.; Marsters, J. C. Benzodiazepine Peptidomimetics: Potent Inhibitors of Ras Farnesylation in Animal Cells. *Science* 1993, 260, 1937.
- Kohl, N. E.; Wilson, F. R.; Mosser, S. D.; Giuliani, E.; Conner, M. W.; Anthony, N. J.; Holtz, W. J.; Gomez, R. P.; Lee, T.-J.; Smith, R. L.; Graham, S. L.; Hartman, G. D.; Gibbs, J. B.; Oliff, A. Protein Farnesyltransferase Inhibitors Block the Growth of Ras-Dependent Tumors in Nude Mice. *Proc. Natl. Acad. Sci. U.S.A.* 1994, 91, 9141.
- Leftheris, K.; Kline, T.; Vite, G. D.; Cho, Y. H.; Bhilde, R. S.; Patel, D. V.; Patel, M. M.; Schmidt, R. J.; Weller, H. N.; Andahazy, M. L.; Carboni, J. M.; Cullo-Brown, J. L.; Lee, F. Y.; Ricca, C.; Rose, W. C.; Yan, N.; Barbacid, M.; Hunt, J. T.; Meyers, C. A.; Seizinger, B. R.; Zahler, R.; Manne, V. Development of Highly Potent Inhibitors of Ras Farnesyltransferase Possessing Cellular and *In Vivo* Activity. *J. Med. Chem.* 1996, 39, 224–236.
- Mallams, A. K.; Rossman, R. R.; Doll, R. J.; Girijavallabhan, V. M.; Ganguly, A. K.; Petrin, J.; Wang, L.; Patton, R.; Bishop, W. R.; Carr, D. M.; Kirschmeier, P.; Catino, J. J.; Bryant, M. S.; Chen, K.-J.; Korfmaier, W. A.; Nardo, C.; Wang, S.; Nomeir, A. A.; Lin, C.-C.; Li, Z. C. Inhibitors of Farnesyl Protein Transferase. 4-Amido, 4-Carbamoyl, and 4-Carboxamido Derivatives of 1-(8-Chloro-6,11-dihydro-5H-benzo[5,6]-cyclohepta[1,2-b]pyridin-11-yl)piperazine and 1-(3-Bromo-8-chloro-6,11-dihydro-5H-benzo[5,6]-cyclohepta[1,2-b]pyridin-11-yl)piperazine. *J. Med. Chem.* 1998, 41, 877.
- McNamara, D. J.; Leonard, D. M.; Shuler, K. R.; Kaltenbronn, J. S.; Quin, J., III; Bur, S.; Thomas, C. E.; Doherty, A. M.; Scholten, J. D.; Zimmerman, K. K.; Gibbs, B. S.; Gowan, R. C.; Latash, M. P.; Leopold, W. R.; Przybranowski, S. A.; Sebolt-Leopold, J. S. C-Terminal Modifications of Histidyl-N-benzylglycinamides To Give Improved Inhibition of Ras Farnesyltransferase, Cellular Activity, and Anticancer Activity in Mice. *J. Med. Chem.* 1997, 41.
- Nagasu, T. Y.; Rowell, C.; Lewis, M. D.; Garcia, A. M. Inhibition of Human Tumor Xenograft Growth by Treatment with the Farnesyltransferase Inhibitor B956. *Cancer Res.* 1995, 55, 5310.
- Njoroge, F. G.; Vibulbhan, B.; Rane, D. F.; Bishop, W. R.; Petrin, J.; Patton, R.; Bryant, M. S.; Chen, K.-J.; Nomeir, A. A.; Lin, C.-C.; Liu, M.; King, I.; Chen, J.; Lee, S.; Yaremko, B.; Dell, J.; Lipari, P.; Malkowski, M.; Li, Z.; Catino, J.; Doll, R. J.; Girijavallabhan, V.; Ganguly, A. K. Structure-Activity Relationship of 3-Substituted N-(Pyridinylacetyl)-4-(8-chloro-5,6-dihydro-11H-benzo[5,6]cyclohepta[1,2-b]pyridin-11-ylidene)-piperidine Inhibitors of Farnesyl-Protein Transferase: Design and Synthesis of *In Vivo* Active Antitumor Compounds. *J. Med. Chem.* 1997, 40, 4290–4301.
- Njoroge, F. G.; Taveras, A. G.; Kelly, J.; Remiszewski, S.; Mallams, A. K.; Wolin, R.; Afonso, A.; Cooper, A. B.; Rane, D. F.; Liu, Y. T.; Wong, J.; Vibulbhan, B.; Pinto, P.; Deskus, J.; Alvarez, C. S.; del Rosario, J.; Connolly, M.; Wang, J.; Desai, J.; Rossman, R. R.; Bishop, W. R.; Patton, R.; Wang, L.; Kirschmeier, P.; Bryant, M. S.; et al. (+)-4-[2-[4-(8-Chloro-3,10-dibromo-6,11-dihydro-5H-benzo[5,6]cyclohepta[1,2-b]pyridin-11-(R)-yl)-1-piperidinyl]-2-oxo-ethyl]-1-piperidinecarboxamide (SCH-66336): A very potent farnesyl protein transferase inhibitor of Ras Farnesyltransferase: A New Therapeutic Target. *J. Med. Chem.* 1997, 40, 2971–2990.
- Sebt, S. M.; Hamilton, A. D. New Approaches to Anticancer Drug Design Based on the Inhibition of Farnesyltransferase. *DDT* 1998, 3, 26–33.
- (a) Augeri, D. J.; O'Connor, S. J.; Janowick, D.; Szczepankiewicz, B.; Sullivan, G.; Larsen, J.; Kalvin, D.; Cohen, J.; Devine, E.; Zhang, H.; Cherian, S.; Saeed, B.; Ng, S.-C.; Rosenberg, S. Potent and Selective Non-Cysteine-Containing Inhibitors of Protein Farnesyltransferase. *J. Med. Chem.* 1998, 41, 4288–4300. (b) Shen, W.; Fakhoury, S.; Donner, G.; Henry, K.; Lee, J. Y.; Zhang, H.; Cohen, J.; Warner, R.; Saeed, B.; Cherian, S.; Tahir, S.; Kovar, S.; Bauch, J.; Ng, S.-C.; Marsh, K.; Sham, H.; Rosenberg, S. Potent Inhibitors of Protein Farnesyltransferase: Heteroarenes as Cysteine Replacements. *Bioorg. Med. Chem. Lett.* 1999, 9, 703–708.
- Sun, J.; Qian, Y.; Hamilton, A. D.; Sebt, S. M. Ras CAAX Peptidomimetic FTI-276 Selectively Blocks Tumor Growth in Nude Mice of a Human Lung Carcinoma With K-Ras Mutation and p53 Deletion. *Cancer Res.* 1995, 55, 4243–4247.
- Qian, Y.; Vogt, A.; Sebt, S. M.; Hamilton, A. D. Design and Synthesis of Non-Peptide Ras CAAX Mimetics as Potent Farnesyltransferase Inhibitors. *J. Med. Chem.* 1996, 39, 217–223.
- Miyaura, N.; Suzuki, A. Palladium-catalyzed cross-coupling reactions of organoboron compounds. *Chem. Rev.* 1995, 95, 2457.
- O'Connor, S. J.; Williard, P. G. Strategy for the Synthesis of the C₁₀-C₁₅ Portion of Amphidinolide-A. *Tetrahedron Lett.* 1989, 30.
- Carlsson, L. A. F.; Helgstrand, A. J. E.; Stjernstrom, N. E. 5-Fluoro-3-Pyridinemethanol Esters Thereof and Therapeutically Acceptable Salts Thereof. *Aktiebolaget Astra US 3,637,714*, 1972.



K

PII: S0959-8049(99)00132-X

Original Paper

Effect of Novel CAAX Peptidomimetic Farnesyltransferase Inhibitor on Angiogenesis *In Vitro* and *In Vivo*

W.-Z. Gu, S.K. Tahir, Y.-C. Wang, H.-C. Zhang, S.P. Cherian, S. O'Connor, J.A. Leal, S.H. Rosenberg and S.-C. Ng

Cancer Research, Pharmaceutical Product Research Division, Abbott Laboratories, Department 4N6 AP9/2, Abbott Park, Illinois, U.S.A.

Ras oncogenes can contribute to tumour development by stimulating vascular endothelial growth factor (VEGF)-dependent angiogenesis. The effect of Ras on angiogenesis may be affected by farnesyltransferase inhibitors (FTI) since farnesylation of Ras is required for its biological activity. In this paper we evaluated the effect of A-170634, a novel and potent CAAX FTI on angiogenesis. Human umbilical vein endothelial cell (HUVEC) tube formation and VEGF secretion were used to assess the effect of A-170634 on angiogenesis *in vitro*. *In vivo*, nude mice were injected with the K-ras mutant colon carcinoma cell line HCT116 and treated subcutaneously with A-170634 using osmotic minipump infusion for 10 days. The effect of A-170634 on corneal angiogenesis *in vivo* was assessed using pellets containing hydron, VEGF, A-170634 or vehicle. *In vitro*, A-170634 selectively inhibited farnesyltransferase activity over the closely related geranylgeranyltransferase I, inhibited Ras processing, blocked anchorage-dependent and -independent growth of HCT116 K-ras mutated cells, decreased HUVEC capillary structure formation, decreased VEGF secretion from tumour cells and HUVEC growth stimulating activity in a dose-dependent manner. *In vivo*, tumour growth was decreased by 30% and vascularisation in and around the tumours was reduced by 41% following drug-treatment with no apparent toxicity to the animals. VEGF-induced corneal neovascularisation was reduced by 80% following A-170634 treatment for 7 days. The data presented here demonstrated that A-170634 was a potent and selective peptidomimetic CAAX FTI with anti-angiogenic properties. These results implied that A-170634 may affect tumour growth *in vivo* by one or more antitumour pathways. © 1999 Elsevier Science Ltd. All rights reserved.

Key words: angiogenesis, farnesyltransferase inhibitor (FTI), ras, vascular endothelial growth factor (VEGF)

Eur J Cancer, Vol. 35, No. 9, pp. 1394–1401, 1999

INTRODUCTION

ONCOGENIC K-ras MUTATION is a frequent genetic event in certain human cancers including pancreatic, colorectal, lung and bladder carcinomas [1–3]. Ras protein p21, a GTP binding protein, is involved in the regulation of cell growth through its various pathways in signal transduction [4–6]. Ras participates in the signalling cascade initiated by platelet derived growth factor [1, 7, 8] through receptor protein tyro-

sine kinase and various adaptor molecules to downstream signal transducers [6, 9]. However, when oncogenic ras loses its intrinsic GTPase activity and is constitutively bound to GTP, it leads to continuous propagation of growth signals within the cell [1]. To acquire biological activity, Ras must associate with the inner surface of the plasma membrane, both in normal and transformed cells [10–12]. In order to be active, Ras requires a series of post-translational modifications. The first and obligatory step, the addition of a farnesyl group to its carboxy-terminal 'CAAX' motif, is catalysed by farnesyl transferase (FTase) [4, 13]. Inhibition of Ras farnesylation is a promising approach for developing a new gen-

Correspondence to S.-C. Ng, e-mail: shi-chung.c.ng@abbott.com
Received 18 Mar. 1999; revised 10 May 1999; accepted 11 May 1999.

eration of mechanism-based anticancer drugs [13–15] since farnesyl transferase inhibitors (FTI) disrupt mutant Ras protein farnesylation *in vitro* and suppress tumour growth *in vivo*.

There is evidence to suggest that *ras* oncogenes can contribute to tumour development directly by promoting tumour cell proliferation and indirectly by stimulating vascular endothelial growth factor (VEGF)-dependent angiogenesis. Mutant *ras* expression is not only required to maintain the transformed phenotype of tumour cells but also critical for tumour progression and metastasis, which is partly mediated by constitutively upregulated expression of tumour angiogenesis factors [16, 17]. There is considerable interest in the role of angiogenesis factors such as VEGF/vascular permeability factor (VEGF/VPF) on tumorigenesis since it is expressed by many human and animal tumours [17, 18] and yet it is a growth factor specific for vascular endothelial cells. The expression of VEGF in a variety of tumours suggests that the growth of solid tumours is dependent on VEGF angiogenesis [9, 19–21]. This has been demonstrated in several recent studies supporting the idea that inhibition of VEGF-induced angiogenesis suppresses tumour growth *in vivo* [22, 23].

We have recently developed and investigated the effect of A-170634, a novel CAAX peptidomimetic FTI, on tumour angiogenesis *in vitro* and *in vivo*. In this report the effect of A-170634 on angiogenesis was assessed by human umbilical vein endothelial cell (HUVEC) tube formation assay as well as tumour cell VEGF secretion *in vitro*. *In vivo* effects of A-170634 were investigated in a xenograft mouse model and in a rat corneal angiogenesis model.

MATERIALS AND METHODS

Chemistry of A-170634

A-170634 was designed as a non-cysteine containing peptidomimetic of the CAAX motif of the *ras* protein. The compound was derived from FTI-277 as the template [24] by replacing the N-terminal cysteine with a 3-pyridylamino-methyl group through combinatorial chemistry efforts. The structure of A-170634 is N-[4-(3-pyr-NH-CH₂)-2-phenyl-benzoyl]methionine methyl ester·HCl (Figure 1a). Details on the structure activity relationship will be reported elsewhere.

Cell cultures

NIH3T3 transformed H- and K-*ras* cell lines were kindly provided by Channing Der (University of North Carolina, U.S.A.). HCT116 was purchased from American Type Culture Collection (ATCC, Rockville, Maryland, U.S.A.). Both NIH3T3 and HCT116 cells were cultured in Dulbecco's Modified Eagle's Medium (DMEM), supplemented with 10% fetal bovine serum (FBS), and 1% antibiotic-antimycotic (Gibco, Grand Island, New York, U.S.A.). NIH3T3 *ras* transformed cells were cultured at 37°C in a humidified chamber containing 90% air and 10% CO₂, whilst HCT116 was cultured in a humidified 95% air and 5% CO₂ atmosphere. Normal HUVEC were purchased from Clonetics (San Diego, California, U.S.A.) and cultured with endothelial growth medium (EGM Bulletkit) supplemented with 3% FBS, bovine brain extract (12 µg/ml), human epidermal growth factor (10 ng/ml), hydrocortisone acetate (1 µg/ml) and gentamycin-1000 (50 µg/ml). Matrigel was obtained from Collaborative Research (Bedford, Massachusetts, U.S.A.).

Ras processing assay

Cells for Ras processing were harvested from subconfluent cultures of NIH3T3 H-*ras* transformed cells and HCT116 cell lines. Cell lysates were prepared by removing culture medium, washing twice with PBS, and the addition of Laemmli sample electrophoresis buffer (Sigma, St Louis, Missouri, U.S.A.). Lysates were boiled for 5 min and then separated on a 15% Tris-Glycine gel (Bio-Rad, Richmond, California, U.S.A.). Cellular proteins were transferred to nitrocellulose membranes (Schleicher & Schuell Optitran BA-S 83) and incubated in blocking buffer (2% nonfat dry milk, 3% bovine serum albumin) overnight. The HCT116 blot was probed with a pan anti-Ras antibody from Transduction Labs (Lexington, Kentucky, U.S.A.) whereas the H-Ras specific antibody Y13-238 was used for the NIH3T3 H-*ras* blot. The blots were subsequently probed with horseradish conjugated antimouse Ig (Amersham, Arlington Heights, Illinois, U.S.A.). Ras bands were visualised by enhanced chemiluminescence (ECL kit, Amersham, Arlington Heights, Illinois, U.S.A.) and quantified by densitometry using an image analysis program Image-Pro Plus (Media Cybernetics, Silver Spring, Maryland, U.S.A.).

Anchorage-dependent proliferation assay

HCT116 cells were harvested from subconfluent culture in 75 cm² culture flasks (Costar, Cambridge, Massachusetts, U.S.A.). Approximately 1 × 10⁴ HCT116 cells were seeded in each well of 24-well culture plates (Costar) and allowed to grow for 24 h. Cells were treated with varying concentrations of A-170634 in medium containing 5% FBS and re-fed every 2 days with medium containing compound or vehicle. After 4 days of incubation, cell proliferation was quantified using non-radioactive alamarBlue (Alamar Biosciences, Sacramento, California, U.S.A.). The plates were read by a CytoFluor

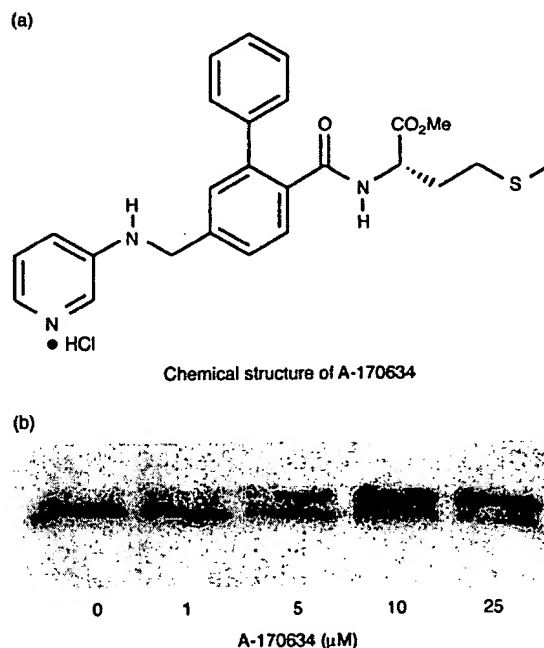


Figure 1. (a) Chemical structure of A-170634. (b) Western blot analysis of *ras* processing. A-170634 inhibited *ras* processing in HCT116 cells. The growing cells were treated with varying concentrations of A-170634 for 48 h. Upper bands are unprocessed *ras* and lower bands are processed *ras*.

2300 fluorescence measurement system (Millipore, Bedford, Massachusetts, U.S.A.) and cell growth was measured by fluorescence intensity and expressed by percentage of inhibition relative to controls.

Soft agar colony formation assay

For anchorage-independent growth, 15 000 HCT116 cells were seeded on to each well of 24-well culture plates on a 0.35% top agar layer overlaid with 0.7% agar with the same medium supplemented with 10% FBS. Both agar layers contained the test compound A-170634. Cultures were re-fed with compound or vehicle twice a week. After 10–14 days of incubation, colonies from duplicate wells were photographed using a Sony CCD camera and quantified by Image-Pro Plus.

Tube formation assay

The effect of A-170634 on the capacity of HUVEC to form a capillary-like network on matrix substratum was studied using a modified method described previously by Schnaper [25]. Briefly, HUVEC passages two to eight grown subconfluently on 75 cm² culture flask were used for the assays. Matrigel was thawed at 4°C overnight. 80 µl of matrigel/well was coated on to each well in two-chamber slides (Nunc, Naperville, Illinois, U.S.A.) and allowed to polymerize at 37°C for 30 min. Approximately 60 000 cells in 1 ml of medium were seeded into each well. After 1 h of incubation, another 1 ml of medium with different doses of test compounds or vehicle was added to each well. A two-dimensional capillary structure was formed after a 12 h incubation. The cell cultures were fixed and stained with Diff-Quik differential staining set (Baxter, Waukegan, Illinois, U.S.A.) and photographed with a Nikon Diaphot 300 microscope and Nikon N6006 camera. Tube formation was scored manually and expressed relative to controls.

VEGF secretion

VEGF secretion was measured by quantitative sandwich enzyme immunoassay technique with a quantikine kit (R&D, Minneapolis, Minnesota, U.S.A.). The assay was performed according to manufacturer instructions [26]. Briefly, a monoclonal antibody (MAb) specific for VEGF₁₆₅ was prepared from mice immunised with purified protein derived from VEGF antigen of insect SS21 cells and precoated on to a 96-well microtitre plate. 200 µl of control, compound treated culture supernatant or serially diluted VEGF standards were added to the plates and incubated for 2 h at room temperature. After washing the wells three times, 200 µl of polyclonal antibody against VEGF conjugated to horseradish peroxidase was added to each well and incubated for 2 h. Wells were washed three times and then the enzyme reaction was carried out at 37°C for 20 min with stabilised hydrogen peroxide and tetramethylbenzidine as substrates. The plates were read by a plate reader (SLT Lab Instruments, Austria) and VEGF content of the samples was estimated from the standard curve determined from serially diluted VEGF standards. The VEGF secretion was normalised to cell number by dividing it by the fluorescence intensity obtained from previous HCT116 cell proliferation assays.

HUVEC growth stimulating activity

We tested whether endothelial cell proliferation was stimulated by VEGF from HCT116 conditioned medium. Briefly, 5000 HUVEC were seeded in each well of a 96-well

microtitre plate and allowed to grow for 24 h. The conditioned medium from either control or compound treated HCT116 cells from the previously described proliferation assay was added to each well of the HUVEC culture. After 2 days of incubation, endothelial cell growth was quantified by alamarBlue assay as described above.

Human tumour xenograft in nude mice

Male BR nu/nu mice aged 8 weeks (Charles River, Maine, U.S.A.) were housed in barrier facilities with food and water *ad libitum*. 5 000 000 HCT116 cells were inoculated intradermally into mouse ventral skin on day 0. Mice with tumours of equal size were randomly divided into control ($n=8$) and treatment ($n=8$) groups, and minipumps (Alzet, Palo Alto, California, U.S.A.) containing 50 mg/kg/day A-170634 or vehicle (0.1% DMSO in saline) were implanted subcutaneously (s.c.) into the back of each mouse on day 3. Tumour volume was estimated by measuring length and width of the tumour mass with digital calipers and by applying the formula $(L \times W^2)/2$ every 3 days. After 10 days of treatment, tumour skin was dissected from each mouse and analysed for vessel density. To quantify macroscopic blood vessels, we removed the tumours with the surrounding skin. The tumours and skin were laid out flat, imaged using a Sony CCD camera attached to a dissection microscope. Image-Pro Plus was then used to segment the blood vessels based on contrast differences and quantified by determining the total pixels (area) of the blood vessels. The area of blood vessels from drug treated animals was expressed as a per cent of untreated controls.

Rat corneal angiogenesis model

The effect of A-170634 was assayed *in vivo* using the corneal angiogenesis model in female Sprague-Dawley rats (Charles River, Maine, U.S.A.), as previously described [27]. Rat eyes were divided into control, low-dose (0.5 µg/kg) and high-dose (1 µg/kg) treatment groups ($n=4$ for each group). Briefly, 10 µl aliquots made of hydron (12% in ethanol), a slow-release polymer, polyhydroxyethylmethacrylate (polyHEMA, Sigma, St Louis, Missouri, U.S.A.), human recombinant VEGF (Collaborative Research, Bedford, Massachusetts, U.S.A.), A-170634 or vehicle were pipetted on to the flat surface of an inverted sterile polypropylene column, and allowed to polymerise for 2 h in a laminar flow hood. Using a dissection microscope, a 2 mm lamellar corneal incision was cut approximately 1 mm from the centre of the cornea into the stroma and 1–1.5 mm from the temporal limbus with a no. 11 surgical blade (Bard-Parker, Becton Dickson Acute-Care, Franklin Lakes, New Jersey, U.S.A.). The pocket was made with a curved iris spatula (Fine Science Tools, Belmont, California, U.S.A.) and the pellets were implanted into corneas of anaesthetised rats. Postsurgery, antibiotic ointment was applied to the operated eyes to prevent infection and to decrease irritation of the ocular surface. After 7 days the anaesthetised rats were perfused with 250 ml of saline via the left ventricle followed by 20 ml of India ink (1:50 dilution). Corneas were carefully removed and fixed with formalin. The corneas were laid flat by making three counterlateral cuts and imaged using a Sony CCD camera attached to a dissection microscope. Neovascularisation was determined by measuring blood vessel density as described above. Neovascularisation from animals receiving drug was expressed as a per cent of untreated controls \pm standard deviation (S.D.).

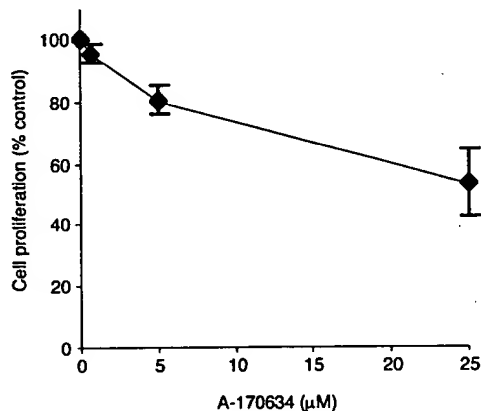


Figure 2. A-170634 blocked HCT116 anchorage-dependent growth. HCT116 cells were plated in 24-well culture plates, allowed to attach for 24 h and then treated with different concentrations of A-170634 for 4 days. Cell proliferation was determined by alamarBlue assay. Data represents the average (\pm standard deviation, S.D.) of three experiments.

RESULTS

A-170634 inhibits anchorage-dependent and -independent tumour cell growth

For anchorage-dependent growth, HCT116 cell proliferation was inhibited 5, 20 and 47% by 0.5, 5 and 25 μ M A-170634, respectively (Figure 2). We further tested whether anchorage-independent growth of NIH3T3 H- and K-*ras* as well as HCT116 cell lines was inhibited by A-170634. We observed that colony formation was inhibited in a dose-dependent manner following treatment with A-170634 in all three cell lines. HCT116 anchorage-independent growth was inhibited by 2, 35 and 48% following 0.1, 0.5 and 1 μ M A-170634 treatment, respectively. The ED_{50} was 0.5, 3.1 and 1.1 μ M for NIH3T3 H-, K-*ras* and HCT116 cells, respectively. We also observed that a reduction in soft agar colony number was accompanied by a reduction in colony size (data not shown).

A-170634 was a potent and selective FTI on FTase over geranylgeranyltransferase I (GGTase I). The concentration of A-170634 required to inhibit *ras* farnesylation by 50% (IC_{50}) was 120 nM whilst for geranylgeranylation it was as high as 18000 nM. The IC_{50} of the free acid form of A-170634 was 6.8 nM. In whole cells A-170634 inhibited post-

translational *Ras* processing in a dose-dependent manner in both NIH3T3 H-*ras* and HCT116 cells (Figure 1b). The ED_{50} was 3.3 and 5 μ M, respectively.

A-170634 inhibits HUVEC tube formation

We tested the effect of A-170634 on HUVEC tube formation *in vitro*. Tubulogenesis was induced in vascular endothelial cells by plating them on to the surface of matrigel for several hours. Figure 3 shows the branching vessel-like structures formed by HUVEC. When A-170634 was added to the culture, there was a decrease in both the number and thickness of vessel formation in a dose-dependent manner. There was approximately a 60% reduction in tubular structure following 25 μ M A-170634 treatment for 12 h. The ED_{50} of A-170634 was 16 μ M.

A-170634 reduces VEGF secretion

At the end of the HCT116 proliferation experiment, the culture supernatant was harvested and stored at -80°C to evaluate VEGF levels by ELISA assay. The test cell number was approximately 1×10^6 per well in 24-well culture plates. The VEGF level released from 1×10^6 cells after 24 h of incubation was ~ 800 pg/ml. VEGF levels declined following A-170634 treatment in a time (data not shown) and dose-dependent manner. VEGF levels were reduced by 16, 31 and 45% relative to the control following treatment with 0.5, 5 and 25 μ M A-170634 for 2 days, respectively (Figure 4a). The data of VEGF secretion was normalised to HCT116 cell number.

A-170634 inhibits HUVEC growth stimulating activity

To test the effect of VEGF on endothelial cell growth stimulating activity, HUVEC were cultured with conditioned medium from HCT116 cell cultures. Endothelial cell growth increased 80% when cultured with conditioned medium for 2 days as compared with controls. There was less growth stimulating activity (56, 38 and 5%) in HUVEC when they were incubated with the conditioned medium from HCT116 cells previously treated with 0.5, 5 and 25 μ M A-170634, respectively (Figure 4b). The decrease in HUVEC growth stimulating activity of the conditioned medium from HCT116 cells treated with A-170634 was probably not due to the presence of residual compound in the medium since A-170634 had little direct effect on HUVEC cell proliferation (data not shown).

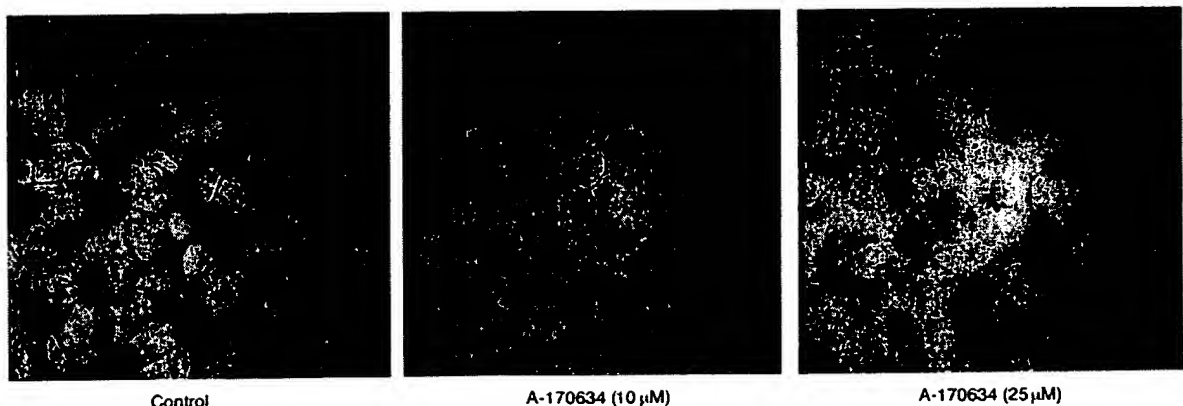


Figure 3. A-170634 disrupted HUVEC tube formation. HUVEC tube formation was reduced in a dose-dependent manner following treatment with A-170634 ($EC_{50} = 16 \mu\text{M}$). The cells were fixed with methanol, stained by Diff-Quik and imaged with a colour CCD camera attached to a Nikon inverted microscope.

A-170634 reduces growth and angiogenesis of human xenograft in nude mice

All nude mice developed tumours after intradermal inoculation of HCT116 cells. Tumours in mouse skin became palpable after 2 days of inoculation. HCT116 tumour volumes between 200–300 mm³ were obtained after 7–10 days of growth. In the treatment group, 50 mg/kg/day of A-170634 was administered via minipumps for 10 days and tumour growth was reduced by approximately one-third as compared with controls. The reduction of HCT116 tumour growth in nude mice was accompanied by a 41% reduction in vascularisation in and around the tumour following A-170634 treatment as compared with controls (Figure 5).

A-170634 inhibits corneal angiogenesis in rats

Pellets containing slow release hydroxyethyl methacrylate (hydron) and VEGF with vehicle or A-170634 were implanted into rat intracorneal micropockets. Limbal capillaries started to sprout into the avascular corneas towards the pellet

2–3 days after surgery. In control eyes the number of vessels increased and hair-like vessels approached or reached the pellet at day 7. In contrast to controls, 0.5 and 1 µg/kg A-170634 treatment significantly inhibited sprouting neovessel growth (Figure 6a). Vessel density from controls and treatment rat corneas were quantified by image analysis at day 7. Neovascular density in A-170634 (0.5 and 1 µg/kg) treated corneas was reduced by 42 and 80% as compared with controls ($P < 0.05$ and $P < 0.00001$, respectively) (Figure 6b).

DISCUSSION

The data presented here demonstrated that A-170634 is a potent and selective peptidomimetic CAAX FTI that may exert its effects on tumour growth *in vivo* by suppressing tumour angiogenesis. We selected HCT116 cells for *in vitro* and *in vivo* studies because it is a representative K-ras mutated human colon carcinoma cell line and it is also known to express high levels of VEGF [28]. The reduction of HCT116 tumour growth following A-170634 treatment *in vivo* may be due to a combination of direct and indirect effects. A-170634 may directly affect tumour cell proliferation through the inhibition of Ras processing. From our *in vitro* results, it was clear that A-170634 suppressed HCT-116 K-ras proliferation as well as Ras processing. In addition, we do not exclude the possible direct effect of FTI on the induction of apoptosis in HCT116 tumour *in vivo*. The idea that FTI could suppress tumour cell proliferation directly through apoptosis was first suggested by Rak and colleagues [29], and later demonstrated in both cell culture [30] and in transgenic tumour models [31]. In MMTV-V-H-ras model, L-744,832 treated salivary tumour exhibited more than a 10-fold increase in apoptosis as measured by TUNEL analysis, and this apoptotic pathway was largely p53 independent. However, in a mammary ras/myc transgenic tumour model, the increase in apoptosis was much more modest, even though tumour regression occurred in both tumour models after FTI treatment [31]. These studies showed that both apoptotic and non-apoptotic pathways could be involved in tumour regression, and the relative contribution of such pathways may vary with different tumour types.

The direct effects of A-170634 on tumour growth *in vivo* may not adequately account for the fact that the effect of some FTIs *in vivo* was greater than what would be predicted *in vitro* [9]. The observation that A-170634 suppressed VEGF release by HCT116 cells *in vitro* also suggested that it may exert its effect on tumour growth *in vivo* by suppressing tumour angiogenesis. A decrease in the vascularisation in and around HCT116 tumour xenografts in nude mice and a reduction in neovascularisation in the rat cornea *in vivo* helped to demonstrate further the anti-angiogenic effects of A-170634. The cornea model is a reliable and reproducible system to evaluate angiogenic and anti-angiogenic compounds *in vivo* since it induced a persistent and aggressive neovascular response by directly stimulating blood vessel growth rather than indirectly by stimulating inflammation [27, 32]. One could argue that local concentrations of A-170634 released by the hydron pellet in the cornea are higher than that in the circulation and acting in a nonspecific, cytotoxic manner. This did not appear to be the case since we did not observe any necrotoxicity within the cornea following treatment. We chose to use recombinant VEGF rather than HCT116 conditioned medium to demonstrate the effect of A-170634 on neovascularisation due to the technical diffi-

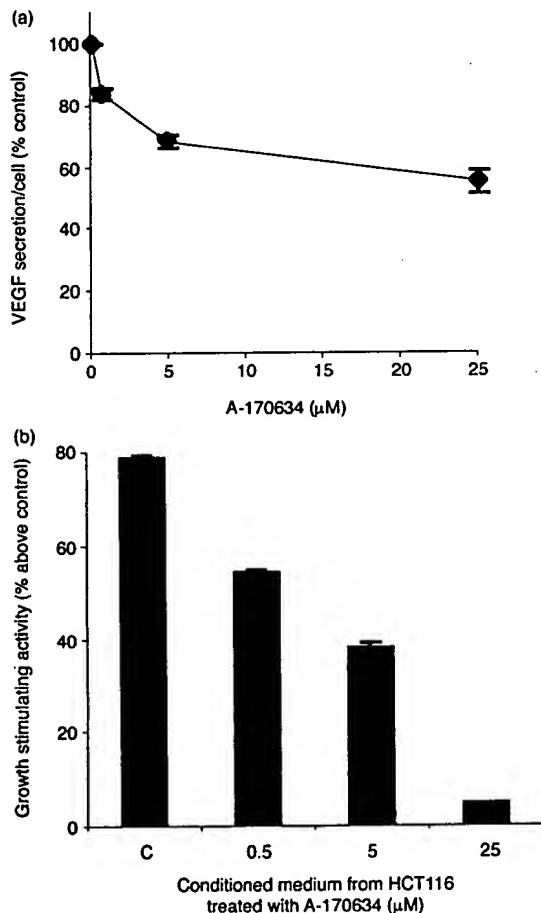


Figure 4. (a) VEGF secretion by HCT116 cells decreased in a dose-dependent manner following treatment with different concentrations of A-170634. VEGF was measured in culture medium with ELISA assay (R&D) and normalised for cell number using alamarBlue assay. Data represents the average (\pm standard deviation, S.D.) of three experiments. (b) The effect of A-170634 on HUVEC growth stimulating activity *in vitro*. HUVEC were seeded in 96-well culture plates and grown for 24 h. Cells were treated with conditioned medium harvested from A-170634 treated HCT116 cells. HUVEC growth was determined by alamarBlue assay. Data represents the average (\pm standard deviation, S.D.) of three experiments.

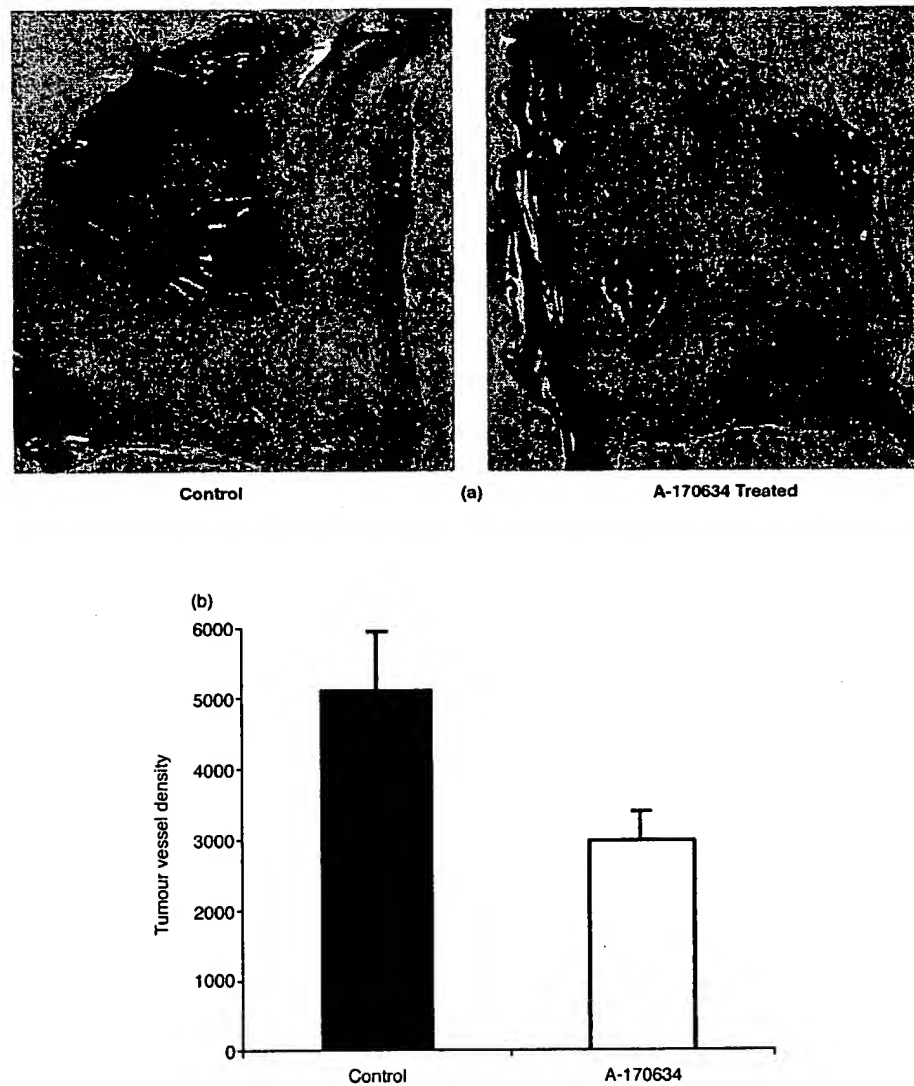


Figure 5. A-170634 reduced growth and vessel density of human tumour xenograft in nude mice. (a) mice were inoculated intradermally with HCT116 cells and treated with 50 mg/kg/day of A-170634 or vehicle for 10 days. Tumour volume decreased following A-170634 treatment as compared with controls ($P < 0.05$). (b) Tumour vessel density from each mouse was measured by image analysis. Vessel density around tumours decreased following A-170634 treatment as compared with controls ($P < 0.05$). Data represents the average (\pm standard deviation, S.D.) from each group.

culties of adding enough medium in a 10 μ l pellet which also included hydron and compound. More recently, we have observed significant inhibition of angiogenesis in the mouse corneal model following systemically treatment with a A-170634 analogues (data not shown).

A-170634 may act directly as an anti-angiogenic agent *in vivo* either by inhibiting endothelial cell proliferation and differentiation or indirectly by inhibiting VEGF secretion by tumour cells. We demonstrated HUVEC proliferation was reduced following treatment with conditioned medium from HCT116 cells that were previously treated with A-170634, but it did not inhibit HUVEC cell growth directly. This suggests that A-170634 may affect endothelial growth indirectly by inhibiting tumour cell secretion of VEGF. VEGF has been shown to not only stimulate endothelial cell growth *in vivo* but it is also required for their survival [33]. This may involve induction of several survival genes by VEGF such as members of the Bcl-2 family [17], and may lead to programmed cell death when VEGF is suppressed. Thus treatment with

FTI *in vivo* may result in a decrease in VEGF secretion by tumour cells which can lead to the decrease of pre-existing blood vessels by apoptosis in addition to inhibiting the formation of new ones in the tumour.

The decreased VEGF secretion *in vitro* may reflect a reduction in VEGF expression. Rak and colleagues [34] have demonstrated previously that mutant *ras* plays a role in regulating the expression of VEGF in murine and human *ras*-mutated cell lines *in vitro*. In addition to regulating VEGF expression, oncogenic *ras* is also known to regulate the transcription of other potential pro-angiogenic factors such as TGF- β and TGF- α [9]. It seems reasonable to postulate that suppression of oncogenic *ras* activity with FTIs may suppress tumour growth *in vivo* by suppressing factors important for angiogenesis. It is unclear how *ras* genes regulate the expression of VEGF and the precise mechanisms of action of A-170634 on VEGF expression are also unknown. It is conceivable that oncogenic *ras* could lead to an increase in expression of c-Jun and c-Fos, resulting in increased VEGF

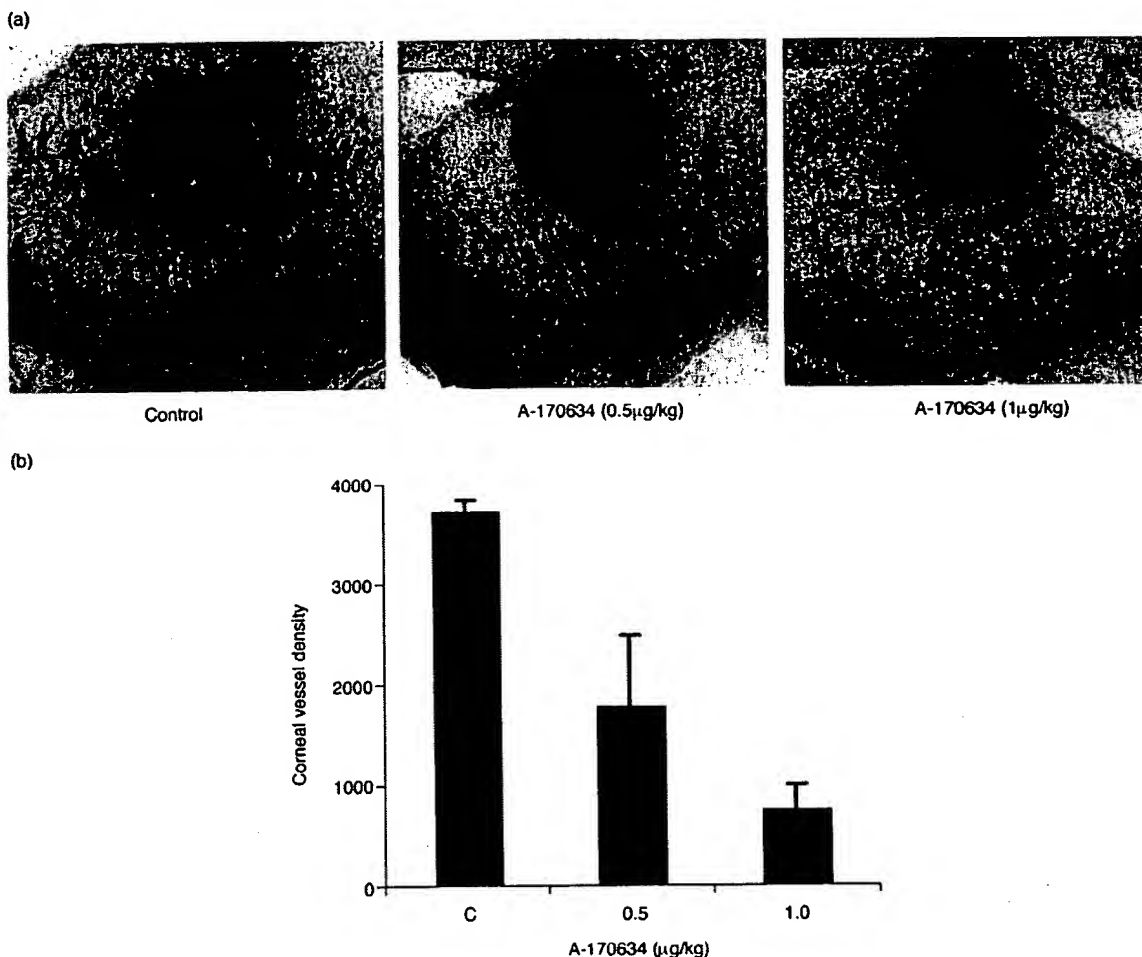


Figure 6. Reduction of corneal angiogenesis in rats by A-170634. (a) After 7 day, corneal neovascularisation was reduced following A-170634 treatments as compared with controls. (b) Corneal neovessel density from each eye was analysed using the image system. Vessel density decreased following A-170634 treatment of 0.5 and 1.0 µg/kg, respectively as compared with controls ($P < 0.05$ and $P < 0.00001$, respectively). Data represents the average (\pm standard deviation, S.D.)

transcription at the four AP1 binding sites in the VEGF promoter [18, 34]. Although we do not know the exact mechanism by which A-170634 suppresses VEGF secretion, it is important to note that VEGF expression may not be solely controlled by oncogenic *ras*, since others [9] have shown that *v-src* may also play a role in the regulation of VEGF. Furthermore, most colon carcinoma express VEGF, but only 50% have a *K-ras* mutation [35, 36]. Since HUVEC differentiation was suppressed by direct treatment with A-170634 *in vitro*, it may also have a direct effect on endothelial cell differentiation *in vivo*. However, the intracellular mechanisms of A-170634 on endothelial differentiation remains unclear.

Although the intracellular mechanisms of action of A-170634 on tumour and endothelial cells is unclear, studies have shown FTIs to inhibit tumour growth *in vivo* with little or no systemic toxicity [37]. This is remarkable despite the fact that Ras has been shown to be essential for normal cell growth and differentiation, endothelial cell migration, and embryogenesis in mice [38, 39]. Other mechanisms of FTI have been proposed recently that may account for their biological activity. For example, FTIs may affect tumour growth by *ras* independent mechanism such as Rho [37, 40], which plays an important role in the organisation of the cytoskeleton.

Others have demonstrated that K-Ras can be geranylgeranylated in the presence of FTI although the biological significance of geranylgeranylated K-Ras is unclear [37, 41]. It is also clear from the literature that the potency of an FTI in cell culture and animal models does not correlate with the *ras* mutational status [15, 37]. Since more than 50 proteins are now known to be farnesylated [41] the true targets of FTI remains uncertain. Despite the uncertainty of whether FTI inhibit tumour growth through the inhibition of Ras function, it has been shown repeatedly that FTI can reduce tumour growth *in vivo* with little or no systemic toxicity [37]. We speculate that the mechanisms involved are likely to be multifactorial and tumour model dependent. For example, in our HCT116 xenograft model, we did not know how much contribution *ras* mutation has on the tumour growth in the context of its other genetic alterations such as overexpressed *mdm2*.

In conclusion, the data presented here demonstrated that A-170634 is a potent and selective peptidomimetic CAAX FTI that may exert its effects on tumour growth *in vivo* by more than one mechanism such as (a) direct and indirect suppression of tumour cell proliferation, (b) inhibition of endothelial proliferation and differentiation and (c) inhibition

of VEGF release and/or expression from tumour cells. These results open the possibility for the development of new therapeutic indications of FTIs specifically targeting angiogenesis.

- Barbacid M. Ras genes. *Ann Rev Biochem* 1987, 56, 779-827.
- Medema RH, Bos JL. The role of p21 Ras in receptor tyrosine kinase signaling. *Crit Rev Oncol* 1993, 4, 615-661.
- McCormick F. How receptors turn Ras on. *Nature* 1993, 363, 15-16.
- James GL, Goldstein JL, Brown MS, et al. Benzodiazepine peptidomimetics: potent inhibitors of Ras farnesylation in animal cells. *Science* 1993, 260, 1937-1942.
- Bollag G, McCormick F. Regulators and effectors of Ras proteins. *Ann Rev Cell Biol* 1991, 7, 601-632.
- Lowy DR, Willumsen BM. Function and regulation of Ras. *Ann Rev Biochem* 1993, 62, 851-891.
- Conn G, Bayne ML, Soderman DD, et al. Amino acid and cDNA sequences of a vascular endothelial cell mitogen that is homologous to platelet-derived growth factor. *Proc Natl Acad Sci* 1990, 87, 2628-2632.
- Rak JN, St Croix B, Kerbel RS. Consequences of angiogenesis for tumor progression, metastasis and cancer therapy. *Anti-Cancer Drugs* 1995, 6, 3-18.
- Rak J, Filmus J, Finkenzeller G, Grugel S, Marmé D, Kerbel RS. Oncogenes as inducers of tumor angiogenesis. *Cancer Metas Rev* 1995, 14, 263-277.
- Hancock JF, Paterson H, Marshall CJ. A polybasic domain or palmitoylation is required in addition to the CAAX motif to localize p21 ras to the plasma membrane. *Cell* 1990, 63, 133-139.
- Kato K, Cox AD, Hisaka MM, et al. Isoprenoid addition to Ras protein is the critical modification for its membrane association and transforming activity. *Proc Natl Acad Sci* 1992, 89, 6403-6407.
- Willumsen BM, Christensen A, Hubbert NC, Papagerge AC, Lowy DR. The p21 ras C-terminus is required for transformation and membrane association. *Nature* 1984, 310, 583-586.
- Qian YM, Blaskovich MA, Saleem M, et al. Design and structural requirements of potent peptidomimetic inhibitors of p21^{ras} farnesyltransferase. *J Biol Chem* 1994, 269, 12410-12413.
- Hancock JF. Anti-Ras drugs come of age. *Curr Biol* 1993, 3, 770-772.
- Sepp-Lorenzino L, Ma Z, Rands E, et al. A peptidomimetic inhibitor of farnesyl: protein transferase blocks the anchorage-dependent and -independent growth of human tumor cell lines. *Cancer Res* 1995, 55, 5302-5309.
- Claffey KP, Brown LF, Aguila LF, et al. Expression of vascular permeability factor/vascular endothelial growth factor by melanoma cells increases tumor growth, angiogenesis, and experimental metastasis. *Cancer Res* 1996, 56, 172-182.
- Rak J, Kerbel RS. Treating cancer by inhibiting angiogenesis: new hopes and potential pitfalls. *Cancer Metas Rev* 1996, 15, 231-236.
- Grugel S, Finkenzeller G, Weindel K, Barleon B, Marmé D. Both v-Ha-ras and v-raf stimulate expression of the vascular endothelial growth factor in NIH 3T3 cells. *J Biol Chem* 1995, 270, 25915-25919.
- Dvorak HF, Brown L, Detmar M, Dvorak A. Vascular permeability factor/vascular endothelial growth factor, microvascular hyperpermeability, and angiogenesis. *Am J Pathol* 1995, 146, 1029-1038.
- D'Amore PA, Shima DT. Tumor angiogenesis: a physiological process or genetically determined? *Cancer Metas Rev* 1996, 15, 205-212.
- Folkman J. Anti-angiogenesis: new concept for therapy of solid tumors. *Ann Surg* 1972, 175, 409-416.
- Kim KJ, Li B, Winer J, et al. Inhibition of vascular endothelial growth factor-induced angiogenesis suppresses tumor growth in vivo. *Nature* 1993, 362, 841-844.
- Millauer B, Shawver LK, Risau W, Ullrich A. Glioblastoma growth inhibited in vivo by a dominant-negative Flk-1 mutant. *Nature* 1994, 367, 576-579.
- Lerner EC, Qian Y, Blaskovich MA, et al. Ras CAAX peptidomimetic FTI-277 selectively blocks oncogenic Ras signaling by inducing cytoplasmic accumulation of inactive ras-raf complexes. *J Biol Chem* 1995, 270, 26802-26806.
- Schnaper HW, Grant DS, Stetler-Stevenson WG, et al. Type IV collagenases and TIMPs modulate endothelial cell morphogenesis in vitro. *J Cell Physiol* 1993, 156, 235-246.
- Polverini PJ, Bouck NP, Rastinejad F. Assay and purification of naturally occurring inhibitor of angiogenesis. In Barnes D, Mather JP, Sato GH. *Methods in Enzymology*. San Diego Academic Press, 1991, 440-450.
- Kenyon BM, Voest EE, Chen CC, Flynn E, Folkman J, D'Amato RJ. A model of angiogenesis in the mouse cornea. *Invest Ophthalmol Vis Sci* 1996, 37, 1625-1632.
- White FC, Carroll SM, Kamps MP. VEGF mRNA is reversibly stabilized by hypoxia and persistently stabilized in VEGF-overexpressing human tumor cell lines. *Growth Factors* 1995, 12, 289-301.
- Rak J, Mitsuhashi Y, Erdos V, Huang SN, Filmus J, Kerbel RS. Massive programmed cell death in intestinal epithelial cells induced by three-dimensional growth conditions: suppression by mutant c-H-ras oncogene expression. *J Cell Biol* 1995, 131, 1587-1598.
- Lebowitz PF, Sakamuro D, Prendergast GC. Farnesyl transferase inhibitors induce apoptosis of ras-transformed cells denied substratum attachment. *Cancer Res* 1997, 57, 708-713.
- Barrington RE, Subler MA, Rands E, et al. A farnesyltransferase inhibitor induces tumor regression in transgenic mice harboring multiple oncogenic mutations by mediating alterations in both cell cycle control and apoptosis. *Mol Cell Biol* 1998, 18, 85-92.
- D'Amato RJ, Loughnan MS, Flynn E, Folkman J. Thalidomide is an inhibitor of angiogenesis. *Proc Natl Acad Sci* 1994, 91, 4082-4085.
- Alon T, Hemo I, Itin A, Pe'er J, Stone J, Keshet E. Vascular endothelial growth factor acts as a survival factor for newly formed retinal vessels and has implications for retinopathy of prematurity. *Nature Medicine* 1995, 1, 1024-1028.
- Rak J, Mitsuhashi Y, Bayko L, Filmus J, Sasazuki T, Kerbel RS. Mutant ras oncogenes upregulate VEGF/VPF expression: implications for induction and inhibition of tumor angiogenesis. *Cancer Res* 1995, 55, 4575-4580.
- Warren RS, Yuan H, Mati MR, Gillett NA, Ferrara N. Regulation by vascular endothelial growth factor of human colon cancer tumorigenesis in a mouse model of experimental liver metastasis. *J Clin Invest* 1995, 95, 1789-1797.
- Brown LF, Berse B, Jackman RW, et al. Expression of vascular permeability factor (vascular endothelial growth factor) and its receptors in adenocarcinomas of the gastrointestinal tract. *Cancer Res* 1993, 53, 4727-4735.
- Lebowitz PF, Prendergast GC. Non-Ras targets of farnesyltransferase inhibitors: focus on Rho. *Oncogene* 1998, 17, 1439-1445.
- Johnson L, Greenbaum D, Cichowski K, et al. K-ras is an essential gene in the mouse with partial functional overlap with N-ras. *Genes Develop* 1997, 11, 2468-2481.
- Fox PL, Sa G, Dobrowolski SF. The regulation of endothelial cell motility by p21 ras. *Oncogene* 1994, 9, 3519-3526.
- Du W, Lebowitz PF, Prendergast GC. Cell growth inhibition by farnesyltransferase inhibitors is mediated by gain of geranylgeranylated RhoB. *Mol Cell Biol* 1999, 19, 1831-1840.
- Cox AD, Der CJ. Farnesyltransferase inhibitors and cancer treatment: targeting simply Ras? *Biochim Biophys Acta* 1997, 1333, F51-71.

Acknowledgements—We thank Jerome Cohen for technical assistance, Jeff Alder and Jang Lee for providing in vivo facilities.

2

A

THE AMERICAN HERITAGE® COLLEGE DICTIONARY

THIRD EDITION



HOUGHTON MIFFLIN COMPANY
Boston • New York



millinery



millipede

mil·li·ll·tre (mil'ə-lē'tar) *n.* Chiefly British. Var. of milliliter.
mil·llme (mil'lm, -ēm) *n.* See table at currency. [Fr. *millième*, thousandth < OFr. *millisme* < Lat. *millēsimus*, thousandth < *millē*, thousand. See gheslo-*.]
mil·ll·me·ter (mil'ə-mē'tar) *n.* A unit of length equal to one thousandth (10⁻³) of a meter, or 0.0394 inch. See table at measurement.
mil·ll·me·tre (mil'ə-mē'tar) *n.* Chiefly British. Var. of millimeter.
mil·ll·mil·cron (mil'ə-mil'krōn) *n.* A unit of length equal to one thousandth (10⁻³) of a micrometer or one billionth (10⁻⁹) of a meter.
mil·llne (mil'lin) *n.* 1. A unit of advertising copy equal to one agate line one column wide printed in one million copies of a publication. 2. The cost of a unit of advertising copy.
mil·ll·ner (mil'ə-nar) *n.* One that makes, trims, designs, or sells hats. [Prob. alteration of ME *Milener*, native of Milan < Milan, the source of goods such as bonnets and lace.]
mil·ll·ner·y (mil'ə-nēr'ē) *n., pl. -les*. 1. Articles, esp. women's hats, sold by a milliner. 2. The profession or business of a milliner.
mil·llng (mil'lng) *n.* 1. The act or process of grinding, esp. grinding grain into flour or meal. 2. The operation of cutting, shaping, finishing, or working products manufactured in a mill. 3. The ridges cut on the edges of coins.
Mill·llng·ton (mil'lng-ton) A city of SW TN N of Memphis. Pop. 17,866.
mil·llon (mil'yan) *n., pl. million or -lions*. 1. The cardinal number equal to 10⁶. 2. A million monetary units, such as dollars. 3. An indefinitely large number. Often used in the plural. 4. The common people; the masses. Often used in the plural. [ME < OFr. *million*, prob. < OItal. *milione*, aug. of *milite*, thousand < Lat. *millē*. See gheslo-*.] — **mil'lon** *adj.*
mil·llon·aire (mil'ya-nār') *n.* A person whose wealth amounts to at least a million dollars, pounds, or the equivalent in other currency. [Fr. *millionnaire* < *million*, million < OFr. *million*. See million-*.]
mil·llonth (mil'yanth) *n.* 1. The ordinal number matching the number million in a series. 2. One of a million equal parts. — **mil'llonth** *adv. & adj.*
mil·ll·pede or **mil·ll·pede** (mil'ə-pēd') *n.* Any of various crawling myriapods of the class Diplopoda, having a cylindrical segmented body with two pairs of legs attached to all segments except for the first four in the thoracic region. [Lat. *millipeda*, a kind of insect; *millē*, thousand; see gheslo-*. + *pēs*, ped-, foot; see ped-*.]
mil·ll·sec·ond (mil'ī-sēk'and) *n.* One thousandth (10⁻³) of a second.
mil·ll·volt (mil'ə-vōlt') *n.* A unit of potential difference equal to one thousandth (10⁻³) of a volt.
mil·ll·watt (mil'ə-wōt') *n.* A unit of power equal to one thousandth (10⁻³) of a watt.
mill·pond (mil'pōnd') *n.* A pond formed by a milldam.
mill·race (mil'rās') *n.* 1. The fast-moving stream of water that drives a mill wheel. 2. The channel for the water that drives a mill wheel.
mill·run (mil'rūn') *n.* 1. See millrace. 2. The output of a sawmill. 3. A test of the mineral quality or content of an ore by milling. 4. The mineral yielded by this test.
mill·run (mil'rūn') *adj.* Being in the state in which a product leaves a mill; unsorted and uninspected: *mill-run fabric*.
mill·stone (mil'stōn') *n.* 1. One of a pair of cylindrical stones used in a mill for grinding grain. 2. A heavy weight; a burden.
mill·stream (mil'strēm') *n.* The rapid stream of water flowing in a millrace.
Mill·ville (mil'vil'). A city of S NJ W of Atlantic City; settled in the 18th cent. Pop. 25,992.
mill wheel *n.* A wheel, typically driven by water, that powers a mill.
mill·work (mil'wōrk') *n.* Woodwork, such as doors, window casings, and baseboards, ready-made by a lumber mill.
mill·wright (mil'wīt') *n.* One that designs, builds, or repairs mills or mill machinery.
Millne (miln), A(lan) A(lexander). 1882–1956. British writer best known for *Winnie-the-Pooh* (1926).
mil·lo (mil'lō) *n., pl. -los*. An early-growing, usu. drought-resistant grain sorghum that resembles millet. (Poss. < Afr. *mealie*, corn, prob. < Port. *milho* < Lat. *millium*, millet. See millet-*.]
mil·lord (mil-lōrd') *n.* 1. An English nobleman or gentleman. 2. Used as a form of address for such a man. [Fr. < E. *my lord*.]
Mil·los also **Me·los** (mē'lōs) or **Mi·lo** (mē'lō, mī'-). An island of SE Greece in the Cyclades Is. of the Aegean Sea. The *Venus* de Milo was found here in 1820.
Mil·losz (mē'lōsh', -wōsh'), Czesław. b. 1911. Polish-born writer who won the 1980 Nobel Prize for literature.
Mil·pi·tas (mil-pē'tas). A city of W CA N of San Jose. Pop. 50,686.
milque·toast (mil'k-tōst') *n.* One who has a meek timid nature. [After Caspar *Milquetoast*, comic-strip character by H.T. Webster (1885–1952).] — **milque'toast'y** *adj.*

mlt (mlt) *n.* 1. a. Fish sperm, including the second polar body. b. The reproductive glands of male fishes when filled with fluid. 2. The spleen of certain vertebrate animals, such as cows or pigs. — *tr.v.* **mlt·ed**, **mlt·ing**, **mlts**. To milt (fish roe) with milt. [ME, roe, spleen, partly < OE *mltan*, and partly < OE *mlt*, spleen; see mel-1-*.]
mlt·er (ml'tar) *n.* A male fish that is ready to breed.
Mil·ti·a·des (mil-tī'ə-dēs) (mil-tī'ə-dēs'). 540?–489? a.c. Athenian general who defeated the Persians at Marathon (490 a.c.).
Mil·ton (mil'ton). 1. A town of SE Ontario WSW of Toronto. Pop. 28,067. 2. A town of E MA, a suburb of Boston. Pop. 25,725.
Milton, John. 1608–74. English poet and scholar who is best known for the epic poem *Paradise Lost* (1667).
Milton Keynes (kēnz). A town of S-central England. Oxford; designated as a new town in 1967. Pop. 124,000.
Mil·wau·kee (mil-wō'kē). A city of SE WI on Lake Michigan. estab. as a fur-trading post in 1795. Pop. 628,088.
Mil·wau·kle (mil-wō'kē). A city of NW OR, a suburb of Portland on the Willamette R. Pop. 18,692.
Mi·mas (mī'mās, mē'-) *n.* A satellite of Saturn. [After *Mimas*, one of the Giants slain by Hercules.]
mlm (mlm) *n.* 1. a. A form of ancient Greek and Roman theater in which the familiar was farcically portrayed on stage. b. A performance of or dialogue for such an entertainment. c. A performer in a mime. 2. A modern performer who specializes in comic mimicry. 3. a. The art of portraying characters and acting out situations or a narrative by gesture and body movement without the use of words; pantomime. b. A performance of pantomime. c. An actor skilled in pantomime. — *v.* **mlm·ed**, **mlm·ing**, **mlms**. — *tr.* 1. To ridicule by imitation; mimic. 2. To act out with gestures and body movement. — *intr.* 1. To act as a mimic. 2. To portray characters and situations by gesture and body movement. [Lat. *mimus*, Gk. *mimos*.] — **mlm'er** *n.*
mlm·e·o (mīm'ē-ō') *Informal.* — *n., pl. -os*. A mimeograph. — *tr.v.* **-eod**, **-o·ing**, **-os**. To mimeograph.
mlm·e·o·graph (mīm'ē-ō-grāf') *n.* 1. A duplicator that makes copies of written, drawn, or typed material from a stencil fitted around an inked drum. 2. A copy made by this method of duplication. [Originally a trademark.] — **mlm'e·o·graph'y** *v.*
ml·me·sis (mī-mē'sis, mī-) *n.* 1. The imitation or representation of aspects of the sensible world, esp. human action, literature and art. 2. Biol. Mimicry. 3. Med. The appearance of symptoms of a disease not actually present. [Gk. *mimēsthai*, to imitate < *mimos*, imitator, mime.]
ml·met·ic (mī-mēt'ik, mī-) *adj.* 1. Relating to, characteristic of, or exhibiting mimicry. 2. a. Of or relating to an imitative, or exhibiting mimicry. 2. a. Of or relating to an imitative, or exhibiting mimicry. b. Using imitative means of representation: *a mimetic dance*. — **ml·met'ic·ly** *adv.*
mlm·ic (mīm'ik) *tr.v.* **-icked**, **-ick·ing**, **-ics**. 1. To copy or imitate closely, esp. in speech, expression, and gesture. 2. To copy or imitate so as to ridicule; mock. See *synonyms*. 3. To resemble closely; simulate. 4. To take on the appearance of. — *n.* 1. One who imitates, esp. a. An actor or a mime. b. One who practices the art of mime. c. One who copies or mimics others. 2. A copy or an imitation. — *adj.* 1. Relating to, acting as, resembling, or characteristic of: *mimic or mimicry*. 2. a. Tending to imitate; imitative. b. Make-believe; mock. [< Lat. *mimicus*, mimic < Gk. *mimos* < *mimos*, imitator, mime.] — **mlm'ic·er** *n.*
mlm·ic·ry (mīm'ik-rē) *n., pl. -ries*. 1. a. The act, practice, or art of mimicking. b. An instance of mimicking. 2. Biol. The resemblance of one organism to another or to an object in its surroundings for concealment and protection from predators.
Mi·mlr (mē'mīr') *n.* Myth. A Norse giant who lived by the roots of Yggdrasil, where he guarded the well of wisdom. [ON. See (s)mer-1-*.]
ml·mō·sa (mī-mō'sə, -zə) *n.* 1. Any of various mostly tropical herbs, shrubs, and trees of the genus *Mimosa*, having globular heads of small flowers and usu. bipinnate leaves that are often sensitive to touch or light. 2. See silk tree. 3. A drink consisting of champagne and orange juice. [NLat. *Mimosa*, name < Lat. *mimus*, mime < Gk. *mimos*.]
mln. *abbr.* 1. a. Mineralogical. b. Mineralogy. 2. *Miles*. 3. Minimum. 4. Mining. 5. Minister. 6. Minor. 7. Also *min*.
ml·na·t (mī'nā) *n., pl. -nas or -nae* (-nē). A varying weight or money used in ancient Greece and Asia. [Lat. < Gk. *mina* < Akkadian *manū*, a unit of weight.]
ml·na·t (mī'nā) *n.* Var. of myna.
ml·na·ble or **ml·na·ble** (mī'nā-bəl) *adj.* That can be mimed or mimed.
ml·na·cloud (mī'nā-shəs) *adj.* Of a menacing or threatening nature; minatory. [Lat. *minax*, *minax* (< *minari*, to threaten < *minare*, threaten; see men-2-*) + *-ious*.] — **ml·na'cloud'y** *adv.* — **ml·na'cloud·ness**, **ml·nac'ity** (mī'nās'ī-tē) *n.*
Min·a·ma·ta disease (mī'nā-mā'ta) *n.* A degenerative neurological disorder caused by poisoning with a mercury compound found in seafood from contaminated waters. [After *Minamata*, a town of W Kyushu, Japan.]
mln·a·ret (mī'nā-rēt') *n.* A tower on a mosque, from which

sermons are
 Ac. *mandrah*,
 Basin (mī'nās),
 Central Nova S
 Channel.
 to·ry (mī'nā-
 to·ry, -tōr', -tōr'
 minacious. [Fr.
 p-part. of
 to·r'ly *adv.*
 dière (mē'nō-d
 ornamental ca
 items. [Fr. < i
 to simpler, si
 prob. < Brete
 v. mlined.
 into very sm
 into minute
 with refine
 sake of politene
 short steps or with
 way. — *n.*
 Ofr. m
 smallness. See m
 meat (mī'nās) mē
 raisins, spices,
 esp. as a pie fill
 mince meat of
 (mī'nā) sing
 ing·ly *adv.*
 mind) *n.* 1. The h
 train and is manife
 will, memory, an
 and unconscious
 and influence
 philosophies, a pr
 reality; the
 of reality. b. In
 in contrast to the
 wing, and apply
 ability. 6. a. Indi
 section. b. A person
 c. The thought
 group; psychologi
 his mind. 8.
 ught; attention. 10.
 mind·ing. m
 to mind; rememb
 Upper Southern U.S.
 mind. 3. To heed in
 about. 6. a. To
 to dislike. 7. To
 tend? — *intr.*
 v. obediently. 3. To
 cautious or carefu
 mind'er *n.*
 and-al·ter·ing (mīn
 ages or distorted pe
 da·na·o (mī'nā-n
 NE of Borneo
 and-bend·ing (mīn'
 v. the mind, esp.
 — mind'·bend'e
 and-blow·ing (mīn'
 calculatory effects: m
 the mind or emotio
 and-bog·gling (mīn'
 emotionally overwhe
 and·ed (mīn'did) *adj.*
 kind of mīn
 ed; evil-minded. 3
 specified. Often
 -er·minded. — mind
 den (mīn'dən). A c
 Bremen; founded
 and-ex·pand·ing (mīn
 v. and distorted p
 increased percepti
 ful (mīn'd'ful) *adj.*
 — mind'·ful·ly *adv.*
 ful·less (mīn'd'lis) *ad
 v. foolish. b. Havin
 section. 2. Giving or
 — mind'·less·ly *adv.*
 do·ro (mīn-dōr'ō,
 Philippines S of Luzon:
 rough reading *n.* The fa
 through extrasensory
 — mind reader *n.*
 and-set or mind-set (i
 the or disposition that
 and interpretations of s*

Steady-State Kinetic Mechanism of Ras Farnesyl:Protein Transferase

David L. Pompliano,^{*,1} Elaine Rands,² Michael D. Schaber,¹ Scott D. Mosser,² Neville J. Anthony,¹ and Jackson B. Gibbs²¹Departments of Cancer Research and Medicinal Chemistry, Merck Research Laboratories, West Point, Pennsylvania 19486

Received October 3, 1991; Revised Manuscript Received January 16, 1992

ABSTRACT: The steady-state kinetic mechanism of bovine brain farnesyl:protein transferase (FPTase) has been determined using a series of initial velocity studies, including both dead-end substrate and product inhibitor experiments. Reciprocal plots of the initial velocity data intersected on the $1/[S]$ axis, indicating that a ternary complex forms (sequential mechanism) and suggesting that the binding of one substrate does not affect the binding of the other. The order of substrate addition was probed by determining the patterns of dead-end substrate and product inhibition. Two nonhydrolyzable analogues of farnesyl diphosphate, (α -hydroxyfarnesyl)phosphonic acid (1) and [(farnesylmethyl)hydroxyphosphinyl]methyl]phosphonic acid (2), were both shown to be competitive inhibitors of farnesyl diphosphate and noncompetitive inhibitors of Ras-CVLS. Four nonsubstrate tetrapeptides, CV(D-L)S, CVLS-NH₂, N-acetyl-L-penicillamine-VIM, and CIFM, were all shown to be noncompetitive inhibitors of farnesyl diphosphate and competitive inhibitors of Ras-CVLS. These data are consistent with random order of substrate addition. Product inhibition patterns corroborated the results found with the dead-end substrate inhibitors. We conclude that bovine brain FPTase proceeds through a random order sequential mechanism. Determination of steady-state parameters for several physiological Ras-CaaX variants showed that amino acid changes affected the values of K_M , but not those of k_{cat} , suggesting that the catalytic efficiencies (k_{cat}/K_M) of Ras-CaaX substrates depend largely upon their relative binding affinity for FPTase.

Site-specific farnesylation is the first step in a series of posttranslational modifications leading to the biological activation of a variety of cellular polypeptides [reviewed in Glomset et al. (1990) and Maltese (1990)]. In a reaction catalyzed by farnesyl:protein transferase (FPTase),¹ the farnesyl moiety of the cholesterol biosynthetic intermediate, farnesyl diphosphate, is linked through a thioether bond to a conserved cysteine residue positioned four amino acids from the C-terminus of the protein acceptor substrate (Scheme 1). Following farnesylation, the three C-terminal amino acids are proteolytically removed, and the newly formed farnesylated cysteine residue is methyl esterified. Proteins that can be farnesylated (or otherwise prenylated by other transferases) have a consensus C-terminal amino acid sequence Ca_1a_2X .¹ The acronym codes for a cysteine residue (C), followed (generally) by two aliphatic amino acid residues (a_1a_2), and ending with another amino acid (X). Exceptions to this Ca_1a_2X mnemonic abound, however. Although the cysteine residue is essential, many proteins with non-glycine residues in the a_1 position are farnesylation substrates. On the other hand, not all proteins with Ca_1a_2X -like sequences are prenylated (e.g., the G α subunit has the Ca_1a_2X sequence CGLF but is not modified; Mumby et al., 1990). Fungal mating factors, nuclear lamins, the γ subunit of retinal transducin, and the cell-transforming GTPase protein Ras all must be farnesylated prior to membrane association, which, in turn, is required for *in vivo* protein activity (Fukada et al., 1990; Glomset et al., 1990; Goldstein & Brown, 1990; Lai et al., 1990; Maltese, 1990; Mumby et al., 1990; Rine & Kim, 1990; Gibbs, 1991). That Ras requires this modification is of particular interest, since activated forms of Ras are found in

20% of human cancers and >50% of colon and pancreatic carcinomas (Bos, 1990). Interference of Ras membrane localization by inhibition of the enzyme-mediated farnesylation reaction is thus a possible anticancer strategy (Goldstein & Brown, 1990; Gibbs, 1991).

FPTase purified to homogeneity from either rat (Reiss et al., 1990) or bovine brain (Moores et al., 1991) is an α/β heterodimer, with its subunits having molecular masses of 47 kDa (α) and 45 kDa (β). A cDNA encoding the β subunit from rat brain (Chen et al., 1991) has been cloned and found to be homologous to the yeast *RAM1* gene. A partial cDNA encoding the C-terminal 329 amino acid residues of the α subunit cloned from bovine brain is homologous to the yeast *RAM2* gene (Kohl et al., 1991). Transfection of the rat α subunit cDNA together with a cDNA encoding part of the rat β subunit yields FPTase activity in human kidney cells (Chen et al., 1991). Since mutations in either *RAM1* or *RAM2* disrupt FPTase activity in yeast, it now appears that the β and α subunits are the mammalian counterparts of the yeast *RAM1* and *RAM2* genes, respectively (Kohl et al., 1991).

The enzymology of FPTase has focused on its isoprenoid diphosphate and protein substrate specificity (Reiss et al., 1990, 1991a,b; Schaber et al., 1990; Moores et al., 1991). FPTase is particular about its isoprenoid substrate, but is quite promiscuous with regard to its protein substrate. Although geranylgeranyl diphosphate and farnesyl diphosphate bind to FPTase with roughly the same affinity (Schaber et al., 1990),

¹ Abbreviations: Ca_1a_2X , Cys (C), an aliphatic amino acid (a_1), any amino acid (X); FPTase, farnesyl:protein transferase; GGP, geranylgeranyl:protein transferase; Ras-CaaX, [(farnesylmethyl)hydroxyphosphinyl]methyl]phosphonic acid; DTT, dithiothreitol; SDS, sodium dodecyl sulfate; HPLC, high-performance liquid chromatography; HPLC, high-performance liquid chromatography.

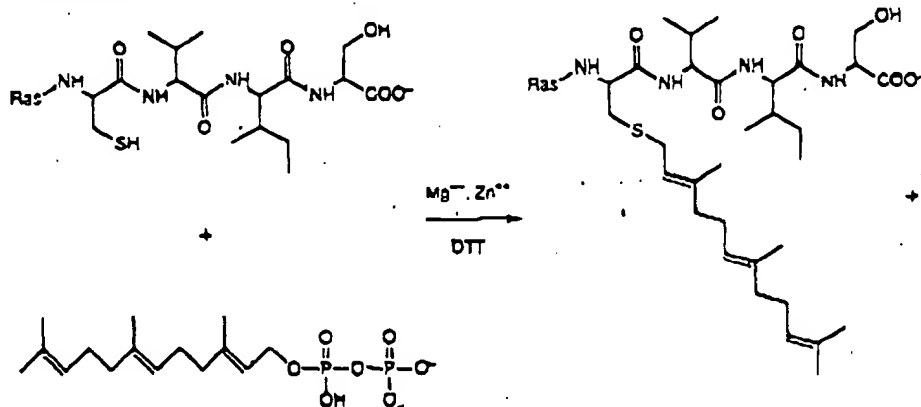
* To whom correspondence should be addressed.

¹ Department of Cancer Research.

² Department of Medicinal Chemistry.

Kinetic Mechanism of FPTase

Scheme 1: Reaction Catalyzed by Farnesyl:Protein Transferase



only farnesyl diphosphate is a kinetically competent substrate in the reaction, while geranylgeranyl diphosphate behaves as a nonreactive inhibitor, using Harvey-Ras as the acceptor protein (Yamane et al., 1990; Moores et al., 1991; Seabra et al., 1991). There are other classes of prenyltransferases (GGPTases) that utilize geranylgeranyl diphosphate as the donor substrate (Casey et al., 1991; Horiguchi et al., 1991; Joly et al., 1991; Moores et al., 1991; Seabra et al., 1991; Yokoyama et al., 1991). Interaction between FPTase and its protein substrates appears to depend only upon the amino acid sequence of the $\text{Ca}_1\text{a}_2\text{X}$ box, on the basis of the observation that cognate tetrapeptides can competitively inhibit the binding of protein substrates (Reiss et al., 1990, 1991a; Schaber et al., 1990; Moores et al., 1991). Within the $\text{Ca}_1\text{a}_2\text{X}$ sequence, substitutions are better tolerated in the a_1 position than in the a_2 position (Stimmel et al., 1990). The best farnesylation substrates contain aliphatic or aromatic residues in the a_2 position. Changes in the X position, however, severely affect the efficiency of farnesylation. In fact, it appears that the terminal residue of $\text{Ca}_1\text{a}_2\text{X}$ proteins determines to which type of transferase the protein will bind, with Ala, Cys, Gln, Ser, and Met favoring binding to FPTase and Leu preferring binding to GGPTase-I (Moores et al., 1991; Reiss et al., 1991a). While an understanding of the substrate specificity is a useful first step, the design of novel compounds that will inhibit the action of FPTase requires a detailed knowledge of the chemical mechanism through which the enzyme-catalyzed reaction proceeds. Thus far, few mechanistic details of the reaction catalyzed by FPTase have been reported. With a two substrate/two product (Bi Bi) system, the logical first question is whether a ternary complex, consisting of FPTase, farnesyl diphosphate, and protein, is formed (sequential mechanism), whether the first product leaves the active site before the second substrate is bound (ping-pong mechanism). In this paper, steady-state enzyme kinetics, including nonreactive substrate and product inhibitor studies, were used to distinguish between these two mechanistic possibilities and to determine the relative binding order of the two substrates.

EXPERIMENTAL PROCEDURES

Materials

FPTase was purified to homogeneity from bovine brain as described in Moores et al. (1991). The *ras* construct [Leu-RAS1(ter)-SLKCVLS, whose gene product is referred to as Ras-CVLS, has been described previously (Temelcofsky et al., 1985; Gibbs et al., 1989). Ras-CaaX proteins were purified as described previously (Moores et al., 1991). [^3H]Farnesyl diphosphate (20 Ci/mmol) was purchased from Du Pont-NEN (Boston, MA). The farnesyl diphosphate analogue,

[[[(farnesylmethyl)hydroxyphosphinyl)methyl]phosphonic acid (2; McClard et al., 1987; Biller et al., 1988), was synthesized by T. J. Lee and W. J. Holtz (Merck Research Laboratories). Peptides and peptide derivatives were synthesized by V. M. Garsky (Merck Research Laboratories) using an Applied Biosystems Model 430A synthesizer, purified by reverse-phase HPLC, and characterized by amino acid analysis and fast atom bombardment mass spectrometry. All other chemicals and reagents were from Sigma, Aldrich, or Fisher and were used without further purification.

Methods

Polyacrylamide gel electrophoresis in the presence of sodium dodecyl sulfate was carried out as described by Laemmli (1970). Gels were stained either with Coomassie Blue or with silver (Daichi Silver Stain, Emprotech, Hyde Park, MA). Protein concentrations were determined using the Bradford (1976) method or were estimated by densitometry on gels. Bovine serum albumin (affinity purified, Pierce, Rockford, IL) was used as the protein standard. Protein solutions were concentrated by ultrafiltration with Amicon PM-30 membranes or by centrifugation in an Amicon Centricon-30 ultrafiltration apparatus.

Transferase Assays. FPTase activity was assayed in the biosynthetically forward direction at 30 °C. Reactions were never allowed to proceed to more than 10% completion based on the limiting substrate. Each velocity data point shown is the average of at least three determinations. For calculations, the molecular mass of the transferase was assumed to be 90 kDa and that of the Ras-CVLS to be 21 kDa. A typical reaction contained the following: [^3H]farnesyl diphosphate (10–500 nM), Ras-CVLS (0.2–8 μM), 50 mM HEPES, pH 7.5, 5 mM MgCl_2 , 20 μM ZnCl_2 , 5 mM dithiothreitol, 0.1% PEG 20000, and pure FPTase (0.2–2 nM). After thermally preequilibrating the assay mixture in the absence of enzyme, reaction was initiated by adding the transferase. Aliquots (250–500 μL) were withdrawn and diluted into 10% HCl in ethanol (1–2 mL) at timed intervals. The quenched reactions were allowed to stand at room temperature for 15 min (to hydrolyze unreacted farnesyl diphosphate). After adding 100% ethanol (2 mL), the reactions were vacuum-filtered through Whatman GF/C filters using a Brandel cell harvester (Model MB-24L, Gaithersburg, MD). Filters were washed four times with 100% ethanol (2-mL aliquots), mixed with scintillation fluid (10 mL, ReadySafe, Beckman), and then counted in a Beckman LS3801 scintillation counter.

FPTase was also assayed by quantitating the amount of farnesylated Ras-CVLS product isolated directly from polyacrylamide gels cross-linked with *N,N'*-diallyltartardiamide (DATD, Bio-Rad; Anker, 1970). Transferase kinetic assays

were performed as described above, except that reaction mixtures (120 μ L) were quenched by the addition of 5X sample loading buffer (20 μ L; 100 mM Tris-HCl, pH 6.8, containing 50% glycerol, 10% SDS, 200 μ M DTT, 50 mM EDTA, and 10 μ g/ μ L Ras-CVLS). Ras-CVLS was included in the sample loading buffer to aid in visualizing the product band in the gel after staining. Polyacrylamide (15%) gels were cast using DATD mole for mole in the place of methylene-bis(acrylamide) as the cross-linking agent. Following separation of the quenched samples by electrophoresis, the gel was stained for protein with Coomassie Blue. Product [3 H]-farnesyl-Ras-CVLS (21-kDa band) was cut out of the gel and then incubated with 2% periodic acid in 0.1% H_3PO_4 (2 mL) at 60 $^{\circ}$ C for 3 h to dissolve the gel. Scintillation fluid (10 mL) was added, and the samples were counted.

When peptide CVLS was used as the protein acceptor substrate, product [3 H]farnesyl-CVLS was isolated from the reaction mixture by reverse-phase HPLC and then counted. Solvent A was 30% CH_3CN containing 10 mM sodium phosphate, pH 6.8, and solvent B was 60% CH_3CN containing 10 mM sodium phosphate, pH 6.8. Samples (100 μ L) were injected onto an analytical Vydac C4 column (150 mm) equilibrated in 0% solvent B at a flow rate of 1.5 mL/min. Product farnesyl-CVLS was eluted by running a linear CH_3CN gradient from 0% to 100% solvent B over 7 min. Total analysis time for each sample was 12 min. Farnesyl-CVLS eluted with a retention time of 7 min. Synthetic farnesyl-CVLS (Schaber et al., 1990) was used to calibrate the column before radioactive samples were injected.

For inhibition studies, assays were run as described above, except inhibitors (peptides or farnesyl diphosphate analogues) were included at various concentrations. Product was quantitated using the acidic ethanol precipitation assay.

Steady-state kinetic parameters were determined either from reciprocal plots or from a nonlinear least squares fit to the relevant rate equation of initial velocity data using the Marquardt algorithm (Marquardt, 1963). For the inhibitor studies, the reciprocal plots were drawn to show the general inhibition pattern, but the values of K_i in Table II were calculated from nonlinear least squares fits to the appropriate inhibition model.

(*R,S*)-Dimethyl [1-Hydroxy-(*E,E*)-3,7,11-trimethyl-2,6,10-dodecatrienyl]phosphonate (3). To a stirred solution of farnesal (245 mg, 1.11 mmol) in acetonitrile (1.1 mL) under argon at room temperature were added triethylamine (0.31 mL, 2.22 mmol) and dimethyl phosphite (0.153 mL, 1.67 mmol), and the resulting mixture was stirred at room temperature for 24 h. After the reaction mixture was concentrated in vacuo, the residue was chromatographed over silica gel eluted with ethyl acetate to afford a colorless oil (141 mg, 38% yield): 1H NMR ($CDCl_3$) δ 1.60 (6 H, s), 1.68 (3 H, s), 1.71 (3 H, d, J = 3.1 Hz), 1.80–2.30 (9 H, m), 3.80 (6 H, m), 4.69 (1 H, dt, J = 9 and 5.4 Hz), 5.00–5.20 (2 H, m), 5.34 (1 H, m).

(*R,S*)-[1-Hydroxy-(*E,E*)-3,7,11-trimethyl-2,6,10-dodecatrienyl]phosphonic Acid (1). Trimethylsilyl bromide (0.107 mL, 0.81 mmol) was added to a stirred solution of 3 (67 mg, 0.203 mmol) and 2,4,6-collidine (0.107 mL, 0.81 mmol) in dichloromethane (3 mL) under argon at 0 $^{\circ}$ C, and the mixture was stirred at 0 $^{\circ}$ C for 30 min and then at room temperature for 5 h. After first diluting the white suspension with toluene (10 mL) and then evaporating the solvent in vacuo, the resulting white solid was dissolved in ethyl acetate and water and the pH was adjusted to pH 3 by the addition of 1 M HCl. The organic layer was separated, dried (over $MgSO_4$), and concentrated in vacuo to afford a pale yellow solid. The solid

PURIFIED BRAIN FPTase

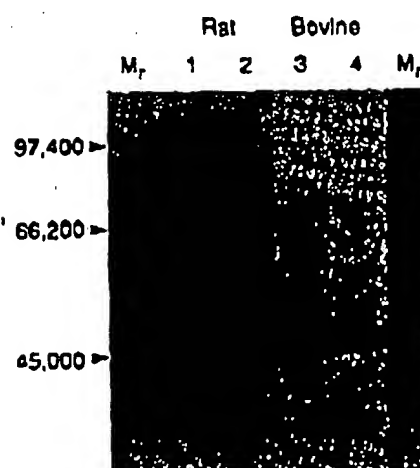


FIGURE 1: SDS-polyacrylamide gel electrophoresis of FPTase isolated from rat and bovine brain. Lanes 1 and 2: 20- and 2-ng samples of purified rat brain FPTase, respectively. Lanes 3 and 4: 2- and 20-ng samples of purified bovine brain FPTase, respectively. Electrophoresis through 7.5% acrylamide gels (160 \times 180 \times 0.75 mm) was carried out at constant current (40 mA) for 1.5 h. Protein was visualized after silver staining. The protein molecular weight standards flank the FPTase lanes.

was washed with dichloromethane (2 \times 5 mL) and then dried in vacuo to yield a white solid (40 mg, 65% yield): 1H NMR ($DMSO$) δ 1.55 (3 H, s), 1.56 (3 H, s), 1.60 (3 H, d, J = 2.0 Hz), 1.80–2.20 (9 H, m), 4.24 (1 H, dd, J = 9.5 and 10.5 Hz), 5.00–5.30 (3 H, m). Anal. Calcd for $C_{13}H_{27}O_4P \cdot 0.25H_2O$: C, 58.71; H, 9.03. Found: C, 58.72; H, 8.94.

RESULTS

FPTase Activity Assay. A filter binding assay was developed to improve the sample to sample reproducibility, lower the background signal, and allow the process to be semi-automated (Moore et al., 1991). By quenching the reaction with acidic ethanol, which precipitates the radioactive product farnesyl-Ras-CVLS and hydrolyzes the remaining substrate farnesyl diphosphate, and by using ethanol to wash the filter, only two solutions were required, which made automating the procedure simple (using a cell harvester to do the washes). Washing the filter with ethanol helped to lower the observed background radioactivity, probably by better solubilizing the hydrolyzed, unreacted radioactive portion of the substrate ([3 H]farnesol). With this assay, we were able to collect statistically relevant initial rate data. Except where noted, all of the results presented below were collected using this acidic ethanol precipitation assay.

Steady-State Kinetics. Pure enzyme, free from competing phosphatase or other prenyltransferase activities, is essential for measuring true initial rates. Like the enzyme from rat brain (Reiss et al., 1990), FPTase isolated from bovine brain (Moore et al., 1991) is an α/β heterodimer, comprised of subunits having molecular masses of approximately 47 (α) and 45 (β) kDa. Figure 1 shows a silver-stained denaturing polyacrylamide gel comparing the rat and bovine brain enzymes. Both enzymes have similar specific activities, 40 and 200 $min^{-1} mg^{-1}$ for the rat (Reiss et al., 1990) and the bovine enzymes, respectively, using Harvey-Ras as protein substrate. Bovine brain FPTase of the purity represented in Figure 1 was better used exclusively in the steady-state kinetic studies.

A double-reciprocal plot of initial velocity against concentration of farnesyl diphosphate at a series of concentrations of Ras-CVLS is presented in Figure 2.

FIGURE 1: diphosphatase activity of 0.1, (●) Second concentration

Table 1: Different

sub

farnesyl diphosphate, Ras-CVLS, Ras-CVLS, Ras-CVLS, Ras-CVLS, Ras-CVLS

intersect

in which

product i

against U

farnesyl

cross-over

intersect

measure

farnesyl

shown; s

are deter

ary rec

inset).

data to th

paramete

Am for fa

0.07 μ M,

reaction v

ence the

[S] axis

value.

We pre

0.1 μ M (2

work

the w

which wa

expos

C-term

purif

CVLS

phosph

phos w

phospho

phos of

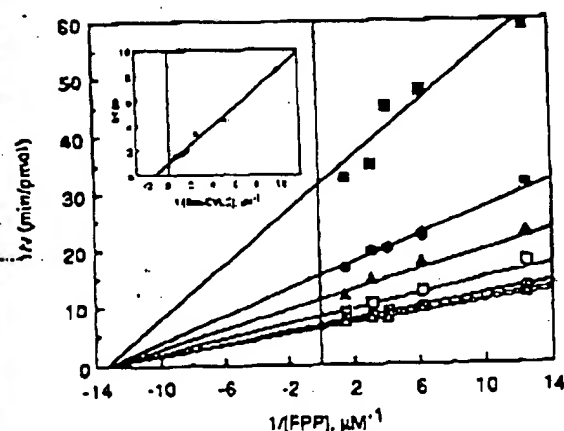


FIGURE 2: Double-reciprocal plot of initial velocity versus farnesyl diphosphate (FPP) concentration at variable fixed Ras-CVLS concentrations. The concentrations of Ras-CVLS were as follows: (■) 0.1, (●) 0.2, (▲) 0.4, (◊) 0.6, (○) 0.8, and (△) 1.6 μM . Inset: Secondary plot of the slopes against the reciprocals of Ras-CVLS concentration.

Table 1: Comparison of Steady-State Kinetic Parameters for Different Substrates

substrate	K_M (μM)	k_{cat} (s^{-1})	k_{cat}/K_M ($M^{-1} s^{-1}$)	rel. k_{cat}/K_M
farnesyl diphosphate	0.04 ± 0.01	0.09	2×10^6	
Ras-CVLS	0.63 ± 0.05	0.093	1.5×10^5	1.0
Ras-CVIM	0.13 ± 0.03	0.023	1.8×10^5	1.2
Ras-CAIM	0.13 ± 0.03	0.028	2.2×10^5	1.5
Ras-CAIL	20 ± 3	0.028	0.014×10^5	0.0096
Ras-CNIQ	0.20 ± 0.02	0.016	1.1×10^5	0.75

Intersecting pattern is consistent with a sequential mechanism, in which both substrates must add to the enzyme before either product is released. The inverse reciprocal plot—initial velocity against the concentration of Ras-CVLS at fixed concentrations of farnesyl diphosphate—was also intersecting and, at the crossover point, gave the same value of $1/v$ (not shown). The intersecting pattern was observed again when initial velocity measurements were determined by quantitating the product farnesyl-Ras-CVLS isolated from polyacrylamide gels (not shown; see Experimental Procedures). Kinetic parameters were determined from slope and intercept replots of the primary reciprocal plots (for a sample slope replot, see Figure 2 inset) as well as from a nonlinear least squares fit of the data to the appropriate rate equation. The values of the kinetic parameters are tabulated in Table 1. Note that the value of K_M for farnesyl diphosphate ($0.04 \mu\text{M}$) varied from 0.02 to $0.07 \mu\text{M}$, due to difficulties inherent in the measurement of reaction velocities at low farnesyl diphosphate concentrations. Since the point of intersection of the reciprocal plots is on the $1/v$ axis, the value of the Michaelis constant (K_M) equals the value of the dissociation constant (K_d) for each substrate. We previously reported the value of K_M (Ras-CVLS) to be $0.63 \mu\text{M}$ (Moore et al., 1991), whereas the value obtained in this work is $0.63 \mu\text{M}$. One possibility for this discrepancy is that the unmodified recombinant Ras-CVLS protein substrate, which was expressed in and isolated from *Escherichia coli*, was exposed to adventitious carboxypeptidases that degraded the C-terminus of the Ras-CVLS substrate during the growth and purification procedures. Since truncated versions of Ras-CVLS are not substrates (nor are they particularly good inhibitors), the presence of these nonsubstrate Ras-CVLS proteins would lead to overestimation of the concentration of substrate-quality Ras-CVLS in the preparation. In turn, the values of parameters which depend on the accurate deter-

mination of substrate concentration, such as the value of K_M , would likewise be overestimated. We looked for an independent method to determine the value of K_M for the protein substrate. Since only the four C-terminal residues of Ras-CVLS appear to interact with the transferase (Moore et al., 1991; Reiss et al., 1991a), we reasoned that the cognate tetrapeptide CVLS should have a value of K_M very similar to that for the actual protein substrate. Using an HPLC-based assay to measure FPTase activity with tetrapeptide CVLS as the varied substrate in the presence of saturating farnesyl diphosphate, the value of K_M (CVLS) was determined to be $0.77 \mu\text{M}$, which agrees closely with the value of K_M for the protein substrate. It thus appears that the current value of $0.63 \mu\text{M}$ for the value of K_M (Ras-CVLS) is the most reliable figure to date.

With pure FPTase, it was possible to extend the findings on the sequence dependence of prenylation (Moore et al., 1991), since the values of both k_{cat} and K_M for each protein substrate could be determined. The second-order rate constant, k_{cat}/K_M , and not K_M alone, is the true measure of the specificity of a substrate for an enzyme. To evaluate the specificity of certain Ras-CaaX substrates for FPTase and to highlight further the importance of the C-terminal residue in determining prenylation specificity, the values of k_{cat}/K_M were determined for five Ras-CaaX variants and are presented in Table 1. Four of the five naturally occurring sequences (CVLS, Ha-Ras; CVIM, Ki-Ras; CAIM, nuclear lamin B; CNIQ, Rap2) were approximately equally specific substrates for FPTase. The Ras-CAIL substrate (γ -6 subunit), which is a known geranylgeranylation substrate (Mumby et al., 1990; Yamane et al., 1990), had a k_{cat}/K_M value 100–200-fold lower than the other protein substrates, indicating that it was a considerably poorer substrate. The value of K_M for farnesyl diphosphate was the same in the presence of all the protein substrates ($0.04 \mu\text{M}$, data not shown), suggesting that there is no interaction between the farnesyl diphosphate and protein binding sites. The values of k_{cat} for these protein substrates were all roughly equal, making the K_M term, which reflects the relative binding affinities, dominant in the measure of catalytic efficiency. Thus, though we previously only classified the suitability of Ras-CaaX variants to act as FPTase substrates on the basis of their relative K_M values (Moore et al., 1991), that ranking also likely reflects the relative catalytic efficiencies (k_{cat}/K_M values) of the various protein substrates.

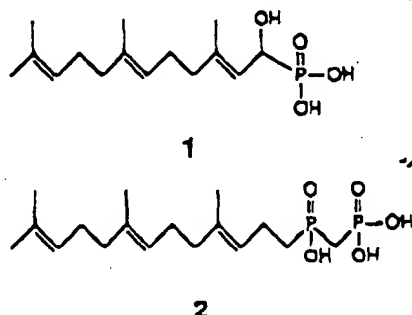
Dead-End Substrate and Product Inhibitor Studies. While the initial velocity studies described above show that both substrates must be on the enzyme at the same time, they cannot be used to determine whether there is an obligatory order of addition or release of reactants, or whether binding in random order occurs. Dead-end substrate and/or product inhibition studies can be used to distinguish between a random order and an obligatory order sequential mechanism (Fromm, 1975). The limitation of the substrate analogue inhibition studies is that a nonsubstrate competitive inhibitor of each substrate (i.e., of farnesyl diphosphate and of Ras-CVLS) must be found. Two nonhydrolyzable analogues of farnesyl diphosphate that cannot participate in the transferase reaction were synthesized (Chart 1): (α -hydroxyfarnesyl)phosphonic acid (1, hydroxy phosphonic acid), a novel compound, and [(farnesylmethyl)hydroxyphosphinyl]methylphosphonic acid (2, farnesyl PMP; McClard et al., 1987; Biller et al., 1988), a known inhibitor of other farnesyl diphosphate handling enzymes, squalene synthetase, and farnesyl diphosphate synthase. Both of these molecules were expected to be competitive inhibitors of farnesyl diphosphate binding. To find nonsubstrate

Table II: Inhibition Patterns and Constants for Substrate Analogue and Product Inhibitors of FPTase*

inhibitor	with respect to FPP		with respect to Ras-CVLS	
	type of inhibition	K_i (μ M)	type of inhibition	K_i (μ M)
hydroxy phosphonate (1)	competitive	0.0052 ± 0.0007	noncompetitive	0.0047 ± 0.0003
farnesyl FMP (2)	competitive	0.83 ± 0.08	noncompetitive	1.3 ± 0.2
CVLS-NH ₂	noncompetitive	32 ± 4	competitive	11 ± 2
Ac-L-penicillamine-VIM	noncompetitive	4.3 ± 0.6	competitive	4.0 ± 1
CV(D-L)S	noncompetitive	8.1 ± 0.5	competitive	13 ± 2
CIFM	noncompetitive	0.034 ± 0.004	competitive	0.0079 ± 0.0007
farnesyl-CVLS	competitive	5.3 ± 1	competitive	8.2 ± 4
FPP	noncompetitive	1400 ± 300	competitive	1400 ± 400

*The K_i value is derived from a nonlinear least squares fit of the initial velocity data to either a purely competitive or purely noncompetitive inhibition model. FPP, farnesyl diphosphate; FMP, inorganic pyrophosphate; Ac, *N*-acetyl.

Chart I: Structures of Farnesyl Diphosphate Analogues



inhibitors of Ras-CVLS, tetrapeptides were incubated with [³H]farnesyl diphosphate in the presence of FPTase, and the reactions were quenched and then resolved by thin-layer chromatography (Figure 3). In the control reaction (no peptide), only unreacted starting material, farnesyl diphosphate, could be seen, indicating that the purified enzyme preparation does not catalyze the hydrolysis of farnesyl diphosphate. For the positive control reaction, known tetrapeptide substrates (Moores et al., 1991; Reiss et al., 1991a) CVLS and CVIM were used and, as expected, showed radioactive product spots with the predicted R_f values. A negative control peptide having a Cys to Ser substitution was not a substrate. Conversion of the carboxyl terminus to an amide (CVLS-NH₂) abolished the ability of the parent compound CVLS to act as a substrate, but a change of the amino terminus to the *N*-acetyl derivative (Ac-CVLS) had no effect. Inversion of stereochemistry at a single center (CV(D-L)S) or substitution of Phe in the α_2 position rendered the parent compound CVLS inactive as a substrate. Recently, Goldstein et al. (1991) have also identified nonsubstrate inhibitor tetrapeptides of FPTase.

The effects of the two classes of inhibitors on the rates of the enzyme-catalyzed reaction were examined with respect to both their cognate and noncognate substrates under nonsaturating concentrations of the fixed substrate (Table II). Reciprocal plots of initial velocities with respect to the concentration of farnesyl diphosphate in the presence of nonsaturating levels of Ras-CVLS at different fixed concentrations of 1 intersected on the $1/v$ axis, suggesting that 1 behaves as a competitive inhibitor with respect to farnesyl diphosphate. Reciprocal plots of initial velocities with respect to the concentration of Ras-CVLS in the presence of nonsaturating levels of farnesyl diphosphate at different fixed levels of 1 intersected on the $1/[S]$ axis, indicating that 1 is a noncompetitive inhibitor of Ras-CVLS. Compound 2 showed the same competitive and noncompetitive behavior against farnesyl diphosphate and Ras-CVLS, respectively. The reciprocal plot pattern for the inhibition of the protein substrate mimic CV(D-L)S showed noncompetitive inhibition with respect to the noncognate

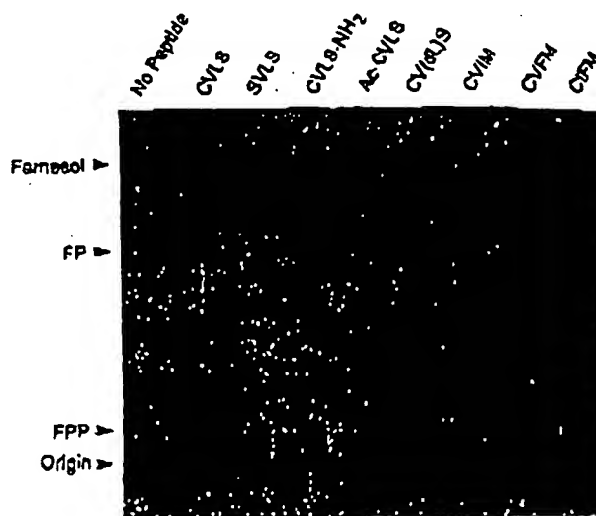


FIGURE 3: Tetrapeptide farnesylation. The indicated peptides (100 μ M) were incubated in the presence of pure bovine FPTase (1.2 nM) and farnesyl diphosphate (0.5 μ M) for 4 h at 30 °C. The TLC plate was eluted with 1-propanol/water (7:3) and visualized by autoradiography after fluorographic enhancement. Exposure time at -70 °C was 48 h. FPP, farnesyl diphosphate; FP, farnesyl monophosphate.

substrate farnesyl diphosphate and showed competitive inhibition with respect to the cognate substrate Ras-CVLS. In addition, at least three other nonsubstrate competitive inhibitors of Ras-CVLS, CVLS-NH₂, *N*-acetyl-L-penicillamine-VIM, and CIFM, showed the same noncompetitive behavior with respect to farnesyl diphosphate. The collection of patterns shown for the dead-end substrate competitive inhibitors is consistent only with the random order sequential mechanism. The inhibitor constants corresponding to the type of inhibition observed for each inhibitor against each substrate are given in Table II.

To confirm the random order of substrate addition, the inhibitory effects of product on the reaction catalyzed by FPTase were next examined. Products should always show inhibition, since they are certainly able to bind to the enzyme. Unfortunately, one of the natural products of the reaction, farnesyl-Ras-CVLS, cannot be readily prepared by synthetic or enzymatic methods. Therefore, we synthesized a truncated (by 182 residues) form of the actual product, the modified peptide farnesyl-CVLS. Since the enzyme recognizes only the four C-terminal amino acid residues of Ras-CVLS, we reasoned that farnesyl-CVLS would act as a product and would bind to the same site as farnesyl-Ras-CVLS. Moreover, because farnesyl-CVLS is made by synthetic chemical methods, its purity and quantity are easily ascertained. When farnesyl-CVLS was examined as an inhibitor of FPTase with respect to each substrate, it was found to be a competitive inhibitor with the same K_i values with respect to each substrate (with

error, T random are form with far access t high far pattern: bled nor reaction of FPTa farnesyl CVLS. 1 mM, l lated (u farnesyl (unexple of incre phospho constant This seri nistent v roborate inhibitors.

DISCUSS FPTa: farnesyl residue (displacin J). This expressio Apart fr has focu substrate proliifera human c perform mediated probe of i is antica inhibitor o through Testing requires a different accuracy products Chromopi reaction iometrica baked th libation of nase, al phosphat is not substrate ed in o: Schaber Ras- Ras- Relatively ti method w cultural e/or pr reprec large

error, Table II). This inhibition pattern is expected for the random order mechanism when no abortive ternary complexes are formed (Fromm, 1975). This pattern is also consistent with farnesyl-CVLS acting as a bisubstrate analogue, blocking access to both the isoprenoid and protein binding sites. At high farnesyl-CVLS concentrations, we observed an inhibition pattern against farnesyl diphosphate that more closely resembled noncompetitive behavior. When the other product of the reaction, inorganic pyrophosphate, was tested for inhibition of FPTase, it was found to be noncompetitive with respect to farnesyl diphosphate and competitive with respect to Ras-CVLS. At concentrations of inorganic pyrophosphate below 1 mM, however, FPTase activity was actually slightly stimulated (up to roughly 2-fold). Squalene synthetase, another farnesyl diphosphate handling enzyme, showed the same (unexplainable) stimulation-inhibition pattern in the presence of increasing concentrations of product inorganic pyrophosphate (Poulter et al., 1989). The patterns and associated constants for product inhibition are summarized in Table II. This series of product inhibition patterns, on its own, is consistent with a random order sequential mechanism and corroborates the results found with the dead-end substrate inhibitors.

DISCUSSION

FPTase catalyzes the transfer of a farnesyl group from farnesyl diphosphate to the thiol of a specific C-terminal Cys residue of a protein substrate, forming a thioether bond and displacing inorganic pyrophosphate in the process (Scheme 1). This posttranslational modification is critical for the full expression of biological activity for many cellular polypeptides. Apart from the great interest of the enzyme itself, attention has focused on FPTase recently because one of its natural substrates, the protein Ras, is a key regulator of cellular proliferation and a potential factor in the development of human cancer. Since Ras must be farnesylated before it can perform its normal cellular tasks, inhibition of the enzyme-mediated farnesyl transfer reaction might be both a useful mode of Ras function *in vivo* as well as an attractive approach to anticancer therapy. The search for a potent, selective inhibitor of FPTase led us first to consider the mechanism through which the enzyme-catalyzed reaction proceeds.

Testing mechanistic possibilities using steady-state kinetics requires a reliable measure of initial rates of reaction. Several different assays of FPTase activity were evaluated for their accuracy and reproducibility. Since none of the substrates or products of the reaction catalyzed by FPTase possess a unique chromophore or fluorophore, the continuous progress of the reaction cannot be easily or directly monitored spectrophotometrically. While we considered using a coupled assay that linked the formation of inorganic pyrophosphate to the oxidation of NADH to NAD⁺ through fructose-6-phosphate phosphatase, aldolase, triosephosphate isomerase, and α -glycerophosphate dehydrogenase (O'Brien, 1976), the assay simply was not sensitive enough to detect turnover at low (V/K) substrate concentrations. The immunoprecipitation assay we used in our initial report of FPTase activity was very sensitive (Chaber et al., 1990), but the response became nonlinear as the Ras-CVLS concentration was increased because the anti-Ras antibody was unable to immunoprecipitate quantitatively the product farnesyl-Ras-CVLS. Another possible method was to separate (by gel electrophoresis, spin-column filtration, or HPLC) and directly quantitate substrate and/or product. While this approach was generally accurate and reproducible, it proved to be too labor-intensive to generate the large number of data points needed for initial rate mea-

surements. The filter binding assay reported by others (Reiss et al., 1990) proved too cumbersome (four different quench and wash solutions) and tended to give high background signals in our hands. We developed a new filter binding assay amenable to automation. The assay we devised requires only two solutions: acidic ethanol to quench the reactions and ethanol to wash the filters. With a cell harvester and an automatic scintillation fluid dispenser, up to 300-400 assays per person per day can be run, processing 24 filters at a time.

Once the validity of the assay was established, we proceeded with the steady-state mechanistic studies of pure FPTase. For a two-substrate/two-product reaction like the one catalyzed by FPTase, there are only two possible kinetic mechanisms: sequential, in which a ternary complex is formed, or ping-pong, which requires two distinct steps and usually involves a modified enzyme intermediate. Enzymes that handle farnesyl diphosphate can use either mechanism. Initial velocity studies of the squalene synthetase reaction point to a ping-pong mechanism involving a farnesyl-enzyme intermediate (Beytia et al., 1973). On the other hand, farnesyl diphosphate synthetase proceeds through an ordered sequential mechanism (Laskovics et al., 1979). When FPTase was considered, initial velocity measurements as a function of either farnesyl diphosphate or Ras concentration in the presence of a series of different fixed concentrations of the nonvaried substrate resulted in reciprocal plots that showed an intersecting pattern representative of a sequential mechanism (Figure 2). From these initial velocity data, the various steady-state kinetic parameters were determined (Table I). The intersection point in the reciprocal plot was on the $1/[S]$ axis, suggesting that one substrate had no effect on the binding of the other. Hence the values of the K_M and the K_i (a pure binding constant) were the same for each substrate. The specificity constant, k_{cat}/K_M , was determined for several naturally occurring Ras-CaaX proteins (Table I). The values of k_{cat} were roughly the same for all of the protein variants tested, indicating that, for FPTase, specificity is determined predominantly by the substrate's binding affinity, and not by any discrimination in the catalytic step(s). Compared to a diffusion-limited, evolutionarily perfected enzyme like triosephosphate isomerase ($k_{cat}/K_M = 4 \times 10^8 \text{ M}^{-1} \text{ s}^{-1}$; Putman et al., 1972), FPTase is a very slow enzyme ($k_{cat}/K_M = 1.3 \times 10^5 \text{ M}^{-1} \text{ s}^{-1}$), although it is similar to another transferase which posttranslationally modifies a protein substrate, myristoyl CoA:protein transferase ($k_{cat}/K_M = 1.3 \times 10^5 \text{ M}^{-1} \text{ s}^{-1}$; Rudnick et al., 1990). We have considered the possibility that allosteric activators of FPTase activity might affect its activity *in vivo*.

To determine whether the ternary complex is formed by successive ordered addition or by random combination of the two substrates, dead-end and competitive substrate and product inhibition studies were carried out. Dead-end inhibitors of substrates show distinctive patterns of inhibition with respect to the two substrates depending on whether the binding of substrates is random or ordered. After identifying nonsubstrate competitive inhibitors of each substrate (Figure 3, Table II), the patterns of inhibition against the noncognate substrate were determined. The farnesyl diphosphate analogue (1) and the protein-CaaX mimic (CV[dL]S) were noncompetitive inhibitors of Ras-CVLS and farnesyl diphosphate, respectively (Table II). The competitive-noncompetitive pattern shown for each inhibitor against the cognate and noncognate substrate is representative of a random order sequential mechanism. These studies were confirmed with at least one other farnesyl diphosphate mimic and three other protein mimics (Table II). If the addition of substrate to the enzyme had been ordered,

The diagram illustrates the transfer of an acyl group from the E-FPP intermediate to the E-Ras intermediate. The E-FPP intermediate is shown on the left, with the acyl group (FPP) being transferred to the E-Ras intermediate. The reaction is reversible, as indicated by the double-headed arrow. The products are E-F-Ras-PPi and E-Ras. The diagram also shows the binding of Ras and FPP to the E-FPP intermediate, and the release of PPi and F-Ras from the E-F-Ras-PPi intermediate.

The most important finding of this work is that the reaction catalyzed by bovine brain FETase follows a random order sequential reaction pathway (Scheme II). This conclusion is based on steady-state initial velocity, dead-end substrate, and product inhibitor studies. Knowledge of the mechanism should

Anker, H. S. (1970) *FEBS Lett.* 7, 293.

Beytia, E., Qureshi, A. A., & Porter, J. W. (1973) *J. Biol. Chem.* 248, 1856-1867.

Billar, S. A., Forster, C., Gordon, E. M., Harrity, T., Scout, W. A., & Closek, C. P., Jr. (1988) *J. Med. Chem.* 31, 1869-1871.

Bos, J. L. (1990) in *Molecular Genetics in Cancer Diagnosis* (Cossman, J., Ed.) pp 273-288, Elsevier Science Publishing Co., New York.

Bradford, M. M. (1976) *Anal. Biochem.* 72, 248-254.

Casey, P. J., Thissen, J. A., & Moomaw, J. F. (1991) *Proc. Natl. Acad. Sci. U.S.A.* (in press).

Chen, W.-J., Andres, D. A., Goldstein, J. L., Russell, D. W., & Brown, M. S. (1991) *Cell* 66, 327-334.

Fromm, H. J. (1975) *Initial Rate Enzyme Kinetics*, Springer-Verlag, New York.

Fukada, Y., Takao, T., Ohguro, H., Yoshizawa, T., Akino, T., & Shimonishi, Y. (1990) *Nature (London)* 346, 658-660.

Gibbs, J. B. (1991) *Cell* 65, 1-4.

Gibbs, J. B., Schaber, M. D., Schofield, T. L., Scolnick, E. M., & Sigal, I. S. (1989) *Proc. Natl. Acad. Sci. U.S.A.* 86, 6630-6634.

Glomset, J. A., Gelb, M. H., & Farnsworth, C. C. (1990) *Trends Biochem. Sci.* 15, 139-142.

Goldstein, J. L., & Brown, M. S. (1990) *Nature (London)* 343, 425-430.

Goldstein, J. L., Brown, M. S., Stradley, S. J., Reiss, Y., & Gierasch, L. M. (1991) *J. Biol. Chem.* 266, 15575-15578.

Horiuchi, H., Kawata, M., Katayama, M., Yoshida, Y., Musha, T., Ando, S., & Takai, Y. (1991) *J. Biol. Chem.* 266, 16981-16984.

Joly, A., Popjak, G., & Edwards, P. A. (1991) *J. Biol. Chem.* 266, 13495-13498.

Kohl, N. E., Djehl, R. E., Schaber, M. D., Rands, E., Selderman, D., He, B., Moores, S. L., Pompliano, D. L., Ferro-Novick, S., Powers, S., Thomas, K. A., & Gibbs, J. B. (1991) *J. Biol. Chem.* 266, 18884-18888.

Laemmli, U. K. (1970) *Nature (London)* 227, 680-685.

Lai, R. K., Perez-Sala, D., Canada, F. J., & Rando, R. F. (1990) *Proc. Natl. Acad. Sci. U.S.A.* 87, 7673-7677.

Laskovics, F. M., Krafcik, J. M., & Poulter, C. D. (1979) *Biol. Chem.* 254, 9458-9463.

Maltese, W. A. (1990) *FASEB J.* 4, 3319-3328.

Marquardt, D. W. (1963) *J. Soc. Ind. Appl. Math.* 11, 431-441.

McClard, R. W., Fujita, T. S., Stremmel, K. E., & Poulter, C. D. (1987) *J. Am. Chem. Soc.* 109, 5544-5545.

Moores, S. L., Schaber, M. D., Mosser, S. D., Rands, E., O'Hara, M. B., Garsky, V. M., Marshall, M. S., Pompliano, D. L., & Gibbs, J. B. (1991) *J. Biol. Chem.* 266, 14603-14610.

Mumby, S. M., Casey, P. J., Gilman, A., Gutowski, S., Sternweis, J. L. (1990) *Proc. Natl. Acad. Sci. U.S.A.* 87, 5873-5877.

O'Brien, W. E. (1976) *Anal. Biochem.* 76, 423-429.

ABSTRACT:
spectroscopic
carboxylic
and 4-
of the
of luciferase
from the
complex
found
within
pseudo-
high level
time course
Estimated
various

This work was supported by the National Science Foundation and the Texas A&M University System.

- Poulter, C. D. (1990) in *The Biochemistry of Cell Walls and Membranes in Fungi* (Kuhn, P. J., Trinci, A. P. J., Jung, M. J., Goosey, M. W., & Copping, L. G., Eds.) Chapter 12, Springer-Verlag, Berlin.
- Poulter, C. D., & Satterwhite, D. M. (1977) *Biochemistry* 16, 5470-5478.
- Poulter, C. D., Argylé, J. C., & Mash, E. A. (1978) *J. Biol. Chem.* 253, 7227-7233.
- Poulter, C. D., Wiggins, P. L., & Le, A. T. (1981) *J. Am. Chem. Soc.* 103, 3926-3927.
- Poulter, C. D., Capson, T. L., Thompson, M. D., & Bard, R. S. (1989) *J. Am. Chem. Soc.* 111, 3734-3739.
- Putman, S. J., Coulson, A. F. W., Farley, I. R. T., Riddleston, B., & Knowles, J. R. (1972) *Biochem. J.* 129, 301-310.
- Reiss, Y., Goldstein, J. L., Seabra, M. C., Casey, P. J., & Brown, M. S. (1990) *Cell* 62, 81-88.
- Reiss, Y., Stradley, S. J., Gierasch, L. M., Brown, M. S., & Goldstein, J. L. (1991a) *Proc. Natl. Acad. Sci. U.S.A.* 88, 732-736.
- Reiss, Y., Seabra, M. C., Armstrong, S. A., Slaughter, C. A., Goldstein, J. L., & Brown, M. S. (1991b) *J. Biol. Chem.* 266, 10672-10677.
- Rine, J., & Kim, S.-H. (1990) *New Biol.* 2, 219-226.
- Rudnick, D. A., McWherter, C. A., Adams, S. P., Ropson, I. J., Duronio, R. J., & Gordon, J. I. (1990) *J. Biol. Chem.* 265, 13370-13378.
- Sandifer, R. M., Thompson, M. D., Gaughan, R. G., & Poulter, C. D. (1982) *J. Am. Chem. Soc.* 104, 7376-7378.
- Schaber, M. D., O'Hara, M. B., Garaky, V. M., Mosser, S. D., Bergstrom, J. D., Moores, S. L., Marshall, M. S., Friedman, P. A., Dixon, R. A. F., & Gibbs, J. B. (1990) *J. Biol. Chem.* 265, 14701-14704.
- Seabra, M. C., Reiss, Y., Casey, P. J., Brown, M. S., & Goldstein, J. L. (1991) *Cell* 66, 429-434.
- Stimmel, J. B., Deschenes, R. J., Volker, C., Stock, J., & Clarke, S. (1990) *Biochemistry* 29, 9651-9659.
- Temeles, G. L., Gibbs, J. B., D'Alonzo, J. S., Sigal, I. S., & Scolnick, E. M. (1985) *Nature (London)* 313, 700-703.
- Yamane, H. K., Farnsworth, C. C., Xie, H., Howald, W., Fung, B. K.-K., Clarke, S., Gelb, M. H., & Glomset, J. A. (1990) *Proc. Natl. Acad. Sci. U.S.A.* 87, 5868-5872.
- Yokoyama, K., Goodwin, G. W., Ghomashchi, F., Glomset, J. A., & Gelb, M. H. (1991) *Proc. Natl. Acad. Sci. U.S.A.* 88, 5302-5306.

Stopped-Flow Kinetic Analysis of the Bacterial Luciferase Reaction[†]

Husam Abu-Soud, Leisha S. Mullins, Thomas O. Baldwin,* and Frank M. Raushel[‡]

Department of Chemistry, Department of Biochemistry and Biophysics, and Center for Macromolecular Design, Texas A&M University, College Station, Texas 77843

Received July 24, 1991; Revised Manuscript Received February 4, 1992

ABSTRACT: The kinetics of the reaction catalyzed by bacterial luciferase have been measured by stopped-flow spectrophotometry at pH 7 and 25 °C. Luciferase catalyzes the formation of visible light, FMN, and a carboxylic acid from FMNH₂, O₂, and the corresponding aldehyde. The time courses for the formation and decay of the various intermediates have been followed by monitoring the absorbance changes at 380 and 445 nm along with the emission of visible light using *n*-decanal as the alkyl aldehyde. The synthesis of the 4a-hydroperoxyflavin intermediate (FMNOOH) was monitored at 380 nm after various concentrations of luciferase, O₂, and FMNH₂ were mixed. The second-order rate constant for the formation of FMNOOH from the luciferase-FMNH₂ complex was found to be $2.4 \times 10^6 \text{ M}^{-1} \text{ s}^{-1}$. In the absence of *n*-decanal, this complex decays to FMN and H₂O₂ with a rate constant of 0.10 s^{-1} . The enzyme-FMNH₂ complex was found to isomerize prior to reaction with oxygen. The production of visible light reaches a maximum intensity within 1 s and then decays exponentially over the next 10 s. The formation of FMN from the intermediate pseudobase (FMNOH) was monitored at 445 nm. This step of the reaction mechanism was inhibited by high levels of *n*-decanal which indicated that a dead-end luciferase-FMNOH-decanal could form. The time courses for the these optical changes have been incorporated into a comprehensive kinetic model. Estimates for 15 individual rate constants have been obtained for this model by numeric simulations of the various time courses.

Bacterial luciferase is a flavin hydroxylase which catalyzes the reaction of FMNH₂, O₂, and an aliphatic aldehyde to yield a carboxylic acid, FMN, and blue-green light ($\lambda_{\text{max}} = 490 \text{ nm}$). The enzyme is a heterodimer consisting of homologous α and β subunits, with molecular weights of 40 108 (Cohn, 1985) and 36 349 (Johnston et al., 1986), respectively. The active center resides primarily, if not exclusively, on the

α subunit; the role of the β subunit remains unclear, but it is required for the efficient generation of light (Baldwin & Ziegler, 1991). The enzyme is commonly assayed by monitoring light emission following injection of FMNH₂ into a vial containing enzyme, an aliphatic aldehyde (e.g., *n*-decanal), and O₂ dissolved in a buffered solution (Hastings et al., 1978). The light intensity rises to a maximum, which is proportional to the amount of enzyme, and then decays exponentially with a rate constant characteristic of the enzyme and the alkyl chain length of the aldehyde (Hastings et al., 1966). This format comprises a single-turnover assay since free (excess) FMNH₂ is quickly depleted by the nonenzymatic autoxidation pathway

This work was supported by the National Institutes of Health (GM 38072) and the National Science Foundation (DMB 87-16262). Correspondence to this author at the Department of Chemistry, Texas A&M University.